Zeitschrift: IABSE reports = Rapports AIPC = IVBH Berichte
Band: 60 (1990)

Rubrik: Theme 2. Mixed steel-concrete structural systems

THEME 2

Mixed Steel-Concrete Structural Systems

Systèmes structuraux mixtes acier-béton

Stahl-Beton — Mischbauweisen

Leere Seite
Blank page
Page vide

Construction Stability of Composite Frames

Stabilité des cadres mixtes acier-béton

Stabilität von Verbundrahmen im Bauzustand

Reidar BJORHOVDE
Professor
Univ. of Pittsburgh
Pittsburgh, PA, USA

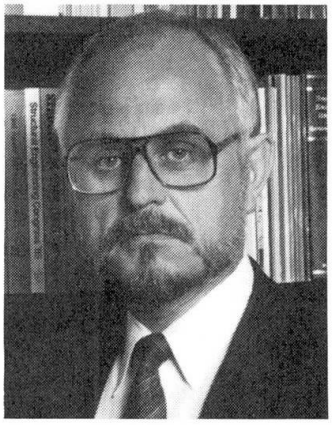

Reidar Bjorhovde, born 1941, received degrees in civil engineering from the Norwegian Institute of Technology in Trondheim, Norway, and Lehigh University, Bethlehem, PA. He has been involved in research and development of steel and composite structures throughout his professional career in the US, Canada, and Norway.

SUMMARY

The past several years have seen the development of composite frames, where the advantages of steel and concrete are combined to provide structural systems of significant strength and stiffness. Their design and construction are very complex, in particular because the designer must also consider the construction method very carefully to ensure satisfactory performance. The unique design considerations that must be made are discussed, including modeling of the frame, assessment of loads, and the effects of construction sequence on overall stability and strength.

RÉSUMÉ

Le développement de la construction de cadres mixtes acier-béton, dans un passé récent, permet maintenant de tirer parti des propriétés des deux matériaux pour réaliser des structures performantes, tant vis-à-vis de la résistance que de la rigidité. La conception, le calcul et la réalisation sont très complexes, car les différentes phases d'exécution doivent être examinées soigneusement. La modélisation de la structure, les hypothèses sur les actions, et les conséquences des différentes étapes de l'exécution sur la stabilité d'ensemble et la résistance sont présentées.

ZUSAMMENFASSUNG

In den letzten Jahren wurden Rahmen in Verbundbauweise entwickelt, welche die Vorteile des Stahles und des Betons kombinieren und beachtliche Tragfähigkeiten und Steifigkeiten aufweisen. Bemessung und Herstellung sind relativ komplex, muss der Planer doch den Bauvorgang bei der Bemessung berücksichtigen, um ein befriedigendes Verhalten sicherstellen zu können. Die Bemessungsannahmen werden besprochen, ebenso die Modellbildung und der Einfluss des Bauablaufs.

1. INTRODUCTION

Composite frames for buildings utilize the interaction of steel and concrete components to resist gravity loads and external environmental forces. In general, these include frames that use isolated composite members such as beams and columns, or the entire frame may perform as a composite assembly.

Methods of analysis and design rules appropriate for composite construction in buildings have not yet been fully developed, in particular as far as the design of the frame as a whole is concerned. It is the purpose of this paper to examine some of the most important considerations that must be made in the design of such structures, including the checks for the governing limit states. The latter present novel problems, to the effect that composite structures are governed by additional limit states that are unique to such systems. The response of the structure during the construction phase, for example, needs to be developed through further analytical and experimental investigations.

2. COMPOSITE FRAMING SYSTEMS

Composite framing systems for high-rise buildings have gained acceptance as viable alternatives to pure structural steel and reinforced concrete systems. The stiffness and economy of the concrete is used along with the strength, speed of construction, and low weight of structural steel, to produce economical structural systems. However, their use requires that additional considerations be given to the contribution of each composite member to the overall behavior of the structure. In particular, the behavior during the construction phase is important.

Further, the stability of the frame is directly related to overall, as well as to bending and shear stiffnesses. For composite structures, the final stability and the resistance to lateral loads are typically not achieved until the concrete has been placed and cured. Depending on the type of concrete, this may mean that anywhere from eight to fifteen stories of bare steel frame have been erected ahead of the placement of the concrete.

Four basic types of composite building systems are currently in use, although modifications are easily made and continue to reflect the attention of the designer to the performance requirements of the structure. These are composite tubular systems, concrete core-braced systems, systems involving composite cladding of the exterior of the building, and concrete-encased steel frames. Sabnis [1] has given a discussion of each of these, and other studies have summarized the evolution of composite building systems [2].

3. CONSTRUCTION CONSIDERATIONS FOR COMPOSITE FRAMES

As one of the primary forms of composite frames, tubular systems combine an exterior structure of closely spaced composite columns with simply connected steel members that frame into the interior. The exterior frame resists all of the lateral loads due to wind and earthquake. The steel floor framing consists of composite steel beams, all simply supported for shear, and designed only for gravity loads. The frame requires that the erection of the steel frame can advance only to a predetermined number of stories ahead of the placement of the concrete. The wind-resisting elements are then encased, as illustrated in Fig. 1.

For large buildings, computer programs have been developed to analyze the behavior of the structure through equivalent plane frames. However, it is preferable to use

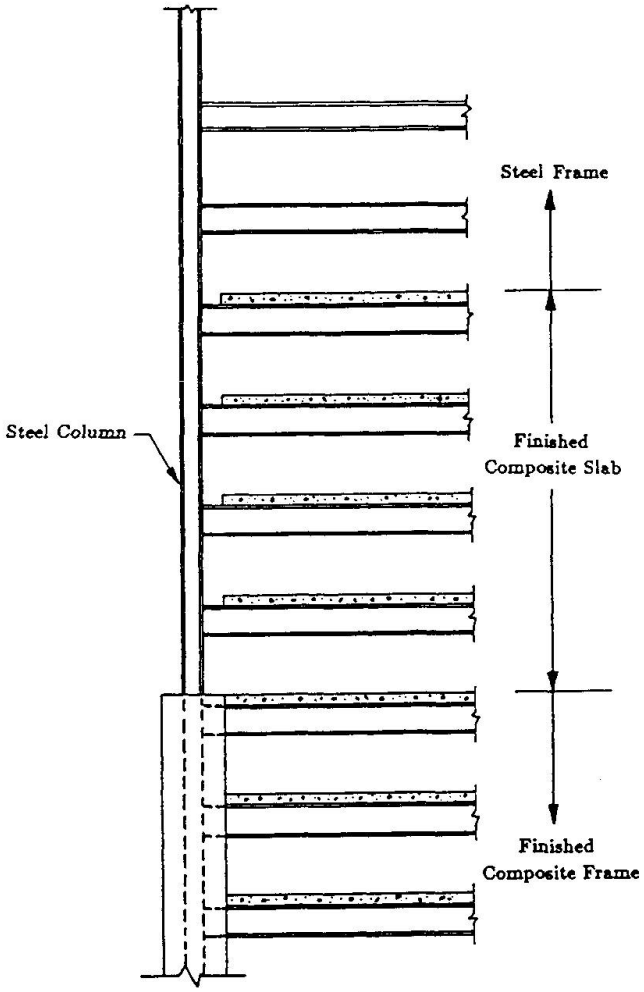

Figure 1 Construction Sequence of a Composite Frame

a three-dimensional structural analysis which includes the characteristics of all members and joints, as well as second order effects. The solution generally requires major computer capacity: whether a planar or a three-dimensional solution is sought, the fact that the construction sequence must be incorporated into the numerical procedure demands mainframe computer capacity.

For the other forms of composite frames, the construction process basically follows the same steps as outlined above, with some modifications that reflect the unique characteristics of each system. Any further discussion will therefore not be provided here; detailed data have been given by Moore and Gosain [3], Griffis [4], and Vallenilla [5].

4. DESIGN FOR CONSTRUCTION

4.1 General Comments

In the design of composite framing systems, the general criteria that need to be taken into account by the design engineer and the contractor are the behavior and strength of the structure during the construction phase. Thus, the structural engineer must address the question of erection stability, to ensure the safety of

the structure and the workers. The erector has to evaluate the influence of a bare steel frame that is light, since it may have been designed only to resist gravity loads during the construction.

The use of the proper construction sequence is basic to achieving the above goals. As pointed out by Griffis [4], there is an optimum construction sequence and spread in timing between the various construction activities that need to be met, if problems such as frame stability and member overstress are to be avoided. Stability problems may occur if too many stories of bare steel are erected ahead of the placement of concrete for slabs and columns, thus possibly overstressing the lower steel members: These are usually designed to resist a limited number of floors during construction.

4.2 Composite Frame Example

To illustrate the behavior of a composite framing system during construction, an existing 52 story building was analyzed. The structure had a floor plan that satisfied the basic requirements of the method of analysis that was used in this study. A construction load of 2.4 kPa was applied, in addition to the self weight of the members. The wind load was based on results from a wind tunnel test, in addition to criteria given for loads on open grid works.

The procedure that was used for the introduction of the combined load effects on the frame in the construction phase was as follows: First, the gravity and lateral loads were applied, and the frame response was evaluated by means of a first order analysis. Then the original load vector was scaled with respect to the magnitude that caused first yielding in any member in the frame, as given by the first order analysis. Small load step increments of the scaled load vector were applied to trace the response of the structure due to the second order terms.

4.3 Construction Sequence

A construction sequence such as indicated in Fig. 1 is very cumbersome to analyze. A simplified method was therefore developed which incorporated the effects of the various construction stages. These include the behavior of the finished composite frame and of the bare steel frame additions above the composite columns at different frame levels.

For the composite frame that was investigated, levels 10, 20, 30 and 40 were analyzed as composite construction stages. For this case, at any level of completed composite framing, four floors of concrete slabs were already poured, and a number of stories of bare steel framing had been erected.

4.4 Composite Frame Behavior Characteristics

As the construction proceeds, the frame is subjected to larger P-Delta-effects. It is important to recognize the second order displacement increases for the composite frame during this phase. The analysis of the composite frame is therefore not complete without an overall stability check. For such a non-linear system, the distribution of the stress resultants at the service loads will not be an adequate index for structural design, if instability is the actual mode of failure.

4.5 Composite Frame with Bare Steel Frame Additions

Figure 2 illustrates the response of the composite frame due to an increasing number of bare steel stories that have been added beyond 20 stories of composite structure. The lateral deflection increases rapidly as the number of added stories increases. Thus, large sway deflections occur after the number of added stories exceed 12 for levels 10 and 20, and after 10 and 8 stories for levels 30 and 40,

respectively. It is therefore apparent that the construction sequence should take frame elevations into account, such that bare steel can be allowed to move ahead of the composite frame by fewer and fewer stories as the overall height goes up.

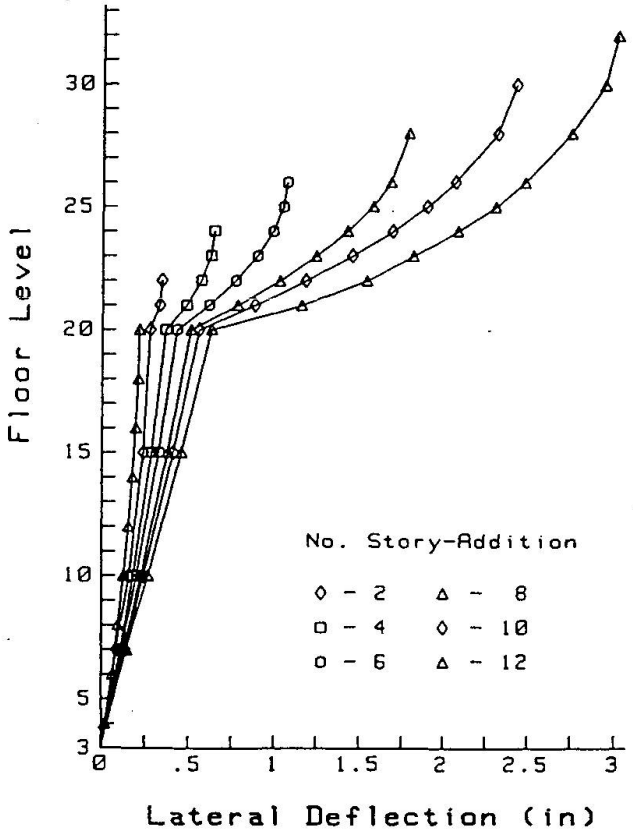

Figure 2 Deflections of Bare Steel Framing Additions to a Composite Frame, and Composite Frame Deflection (1 in = 25.4 mm; 1 kip = 4.45 kN)

The solution for the frame of this study shows that the incremental number of bare steel stories that are erected ahead of the completed composite frame is controlled by either of the following stability criteria: (1) the value of the determinant of the stiffness matrix is equal to zero; or (2) the sidesway displacement of the structure at service load is within a reasonable limit. Although the former is an ultimate and the latter a serviceability limit state, for the case of composite frames during construction, deflections should be treated as ultimate conditions. This led to the concept of the Construction Limit State (CLS) [5].

Another approach to the erection stability is to consider the construction drift and its effects on the frame at different stages. Thus, the magnitude and variation of this drift must be considered for every story that is added. This includes examining the drift of individual frame assemblies, but it is essential to evaluate the drift characteristics of the bare steel frame as it is erected ahead of the concrete placement. The study demonstrated that frame stability should not be of concern for the finished composite frame at any stage.

Frame displacements can be presented in non-dimensional form as Construction Drift Indices (CDI's). The CDI is defined as the horizontal displacement at the top of any story level of the frame, divided by the frame height to that level. When the bare steel framing is considered in the analysis, the height used is that of the

steel itself, measured relative to the composite frame top level.

Drift limitations are set by the individual designer to assure satisfactory structural behavior. For the frame that was analyzed in this study, the drift of the overall frame as well as for the story additions and individual stories were evaluated. Figure 3 shows the drift variation for the finished composite frame and the bare steel story additions for different construction levels. Considering that the frame height-to-width ratios vary during construction, the range of drift indices that were found in the analysis is considered acceptable.

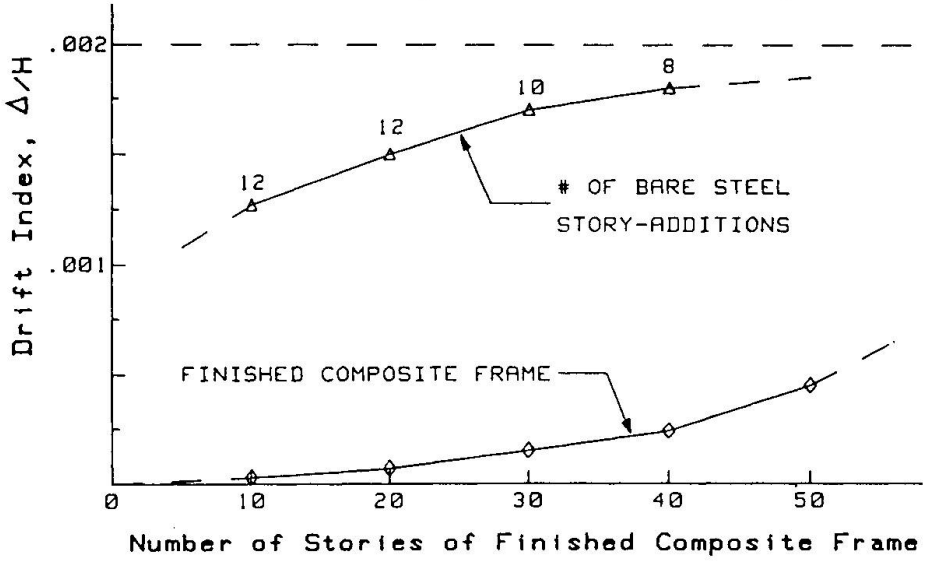

Figure 3 Drift vs. Number of Stories of Finished Composite Frame

5. CONCLUDING REMARKS

The study has shown that certain limitations must be applied to the construction sequence, specifically such that as the building proceeds, a smaller number of stories can be added above the finished composite frame. The construction sequences for a particular composite frame can be determined by developing story addition ranges such as the ones arrived at for the frame of this study.

6. REFERENCES

1. Sabnis, G. M.,"Handbook of Composite Construction Engineering", Van Nostrand-Reinhold Company, New York, NY, 1979.

2. Iyengar, H. S.,"State-of-the-Art Report on Composite or Mixed Steel-Concrete Construction for Buildings", ASCE Special Publication, New York, NY, 1977.

3. Moore, W. P., and Gosain, N., "Mixed Systems: Past Practices, Recent Experience and Future Directions", US-Japan Joint Colloquium on Composite Construction, ASCE Special Publication, ASCE, New York, NY, 1985.

4. Griffis, L. G.,"Some Design Considerations for Composite Frame Structures", Engineering Journal, AISC, Vol. 23, No. 2, 1986 (pp. 59-64).

5. Vallenilla, C. R., "Strength and Behavior of Composite Framing Systems", Ph. D. Dissertation, University of Arizona, Tucson, Arizona, April, 1987.

Structural Properties and Constructability of Composite Members

Caractéristiques structurales et aptitude à la construction de membrures mixtes

Tragwerkseigenschaften und Betonierungsfähigkeit von Verbundbauteilen

T. SHIOYA
Senior Res. Engineer
Shimizu Corporation
Tokyo, Japan

Toshiyuki Shioya, born in 1950, received his degree of Dr. of Engineering from the University of Tokyo. His main fields of research are shear problems of reinforced concrete and composite structures.

H. OOUCHIDA
Manager
Shimizu Corporation
Tokyo, Japan

Hiroki Oouchida, born in 1947, received his B.Sc. and M.Sc. degrees in Civil Engineering from Kyushu University. He has been working on design of offshore structures.

T. HASEGAWA
Research Engineer
Shimizu Corporation
Tokyo, Japan

Toshiaki Hasegawa, born in 1958, received his B.Sc. and M.Sc. degrees in Civil Engineering from Waseda University. His main research interest is fracture mechanics of concrete.

F. OHNO
Civil Engineer
Shimizu Coporation
Tokyo, Japan

Fumiyoshi Ohno, born in 1957, received a degree in Civil Engineering from the Science University of Tokyo and another in Computer and Information Science from the Univ. of Oregon, USA. He is working on offshore engineering.

SUMMARY

Presented are the results of structural and constructability tests of a composite steel/concrete structure using a steel sandwiched concrete system for the purpose of establishing the design and construction methods. It was confirmed by flexure and shear tests that the composite members have high ductility when compared with reinforced concrete members. Sufficient infilling and effectiveness of a continuous concreting system were confirmed in mock-up tests.

RÉSUMÉ

Cet article décrit les résultats d'essais structuraux et d'aptitude à la construction d'une construction mixte acier/béton qui utilise un système de béton armé type sandwich avec le but d'établir des méthodes de conception et de construction. On a pu confirmer à l'aide d'essais de flexion et de cisaillement que les membrures mixtes possèdent une ductilité élevée, comparées aux membrures en béton armé. En outre, des essais de maquette ont confirmé un remplissage et une efficacité adéquats d'un système de bétonnage continu.

ZUSAMMENFASSUNG

Die Ergebnisse von Tragfähigkeits- und Betonierungsfähigkeitsprüfungen an einem Verbundtragwerk werden vorgestellt. Diese Prüfungen wurden durchgeführt, damit die Entwurfs- und Betonierungsmethoden entwickelt werden können. Bei den Biegungs- und Schubprüfungen zeigte sich, daß die zusammengesetzten Bauteile im Vergleich zu normalen Stahlbetonbauteilen eine höhere Duktilität haben. Durch Betonierungsfähigkeitsprüfungen wurden Füllgrad und die Wirksamkeit des Systems bestätigt.

1. INTRODUCTION

Arctic offshore structures are subjected to severe ice loads. A composite member in which concrete is injected into a steel encasement is remarkably well suited for use in such conditions because of its excellent ductility and high strength[1][2]. It can facilitate the potential to improve the constructability of the structure, resulting in the reduction of construction costs and time needed. However, practical methods for construction and design of such a composite member have not been fully established yet. Therefore extensive research work was carried out to verify the strength characteristics and to develop an applicable construction procedure.

2. FLEXURE TEST

2.1 Outline of test

To investigate the buckling behavior of compression plates under flexural loading, 13 flexural tests were performed. Dimensions and basic configurations are shown in Fig. 1. The parameters in the flexure tests are as follows:

(A) Height of stiffeners : h_f
(B) Spacing of stiffeners : l_f
(C) Direction of stiffeners ;
A-type : stiffeners were set longitudinally
B-type : stiffeners were set transversely

In addition, a reinforced concrete model, having the same steel ratio as the composite test model, was tested. The target compressive strength of the concrete was approximately 45MPa. Mix proportions are shown in Table 2. Steel properties are shown in Table 1. The tests were carried out using a 4-point bending configuration as illustrated in Fig. 1.

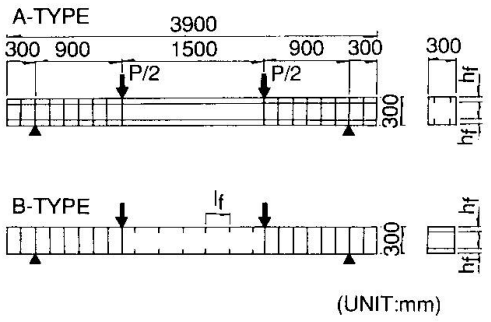

Fig. 1 Flexure test models and loading configurations

2.2 Result of flexure tests

(1) Load deflection relation curves

The deflections measured at midspan under flexural loading are shown in Fig. 2. For the composite models, unless elastic buckling of the compression plate took place, failure occurred due to plastic buckling of the compression plate after 8 to 10 times the deflection at yield. For the reinforced concrete model, compared with the composite models, it failed with the crushing of the concrete at smaller deflection. In short, the composite members had a higher ductile capacity under flexural loading.

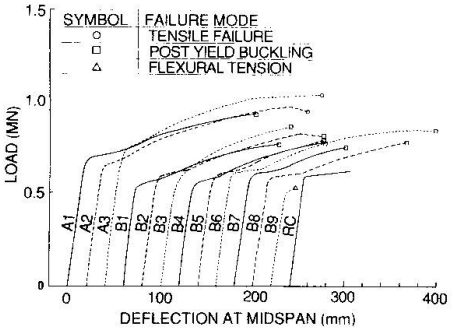

Fig. 2 Load - deflection curves

(2) Flexural failure strength

Figure 3 shows the ratios between the experimental yield moment and the calculated value based on conventional RC (Reinforced Concrete) beam theory. It turns out that the experimental yield moment agreed well with that calculated by the RC theory. It was observed, up to the yield load, that at the section in constant moment span the "plane sections before bending remain plane after bending" assumption can be made for the composite members. The composite member showed a higher

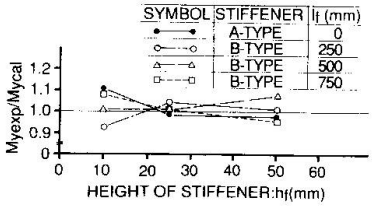

Fig. 3 Experimental/calculated yield moment

Table 1 Varieties of models and principal test results

Test	Test model	Dimension of model				Concrete			Steel				Inner stiffener			Test results						Failure mode
		Length L (mm)	Loading span l (mm)	Effective depth d (mm)	Breadth b (mm)	Mix	Comp. strength f'_c (MPa)	Splitting tensile strength f'_t (MPa)	Thickness t (mm)	Yield strength f_{sy} (MPa)	Tensile strength f_{st} (MPa)	Main steel ratio p (%)	Type	Height h_f (mm)	Spacing l_f (mm)	Yield load P_y (MN)	Buckling load P_b (MN)	Maximum load P_{max} (MN)	Maximum moment M_{max} (MN m)	Maximum shear strength (MPa)		
Flexure	A1	3900	3300	296	300	M1	41.5	2.78	9	324	520	3.05	A	10	-	0.667	0.937	0.937	0.422	-		Post yield buckling
	A2	3900	3300	296	300	M1	43.3	2.91	9	324	520	3.05	A	25	-	0.647	-	0.981	0.441	-		Discontinuance due
	A3	3900	3300	296	300	M1	43.7	2.93	9	324	520	3.05	A	50	-	0.745	-	1.06	0.477	-		to support-slip
	B1	3900	3300	296	300	M1	44.0	2.96	9	324	520	3.05	B	10	250	0.549	0.780	0.780	0.351	-		Post yield buckling
	B2	3900	3300	296	300	M1	45.5	3.07	9	324	520	3.05	B	25	250	0.588	0.814	0.843	0.380	-		Post yield buckling
	B3	3900	3300	296	300	M1	46.1	3.11	9	324	520	3.05	B	50	250	0.569	0.863	0.873	0.393	-		Post yield buckling
	B4	3900	3300	296	300	M1	46.3	3.13	9	324	520	3.05	B	10	500	0.569	0.789	0.789	0.355	-		Post yield buckling
	B5	3900	3300	296	300	M1	46.8	3.18	9	324	520	3.05	B	25	500	0.588	0.794	0.804	0.362	-		Post yield buckling
	B6	3900	3300	296	300	M1	46.9	3.20	9	324	520	3.05	B	50	500	0.608	0.873	0.873	0.393	-		Post yield buckling
	B7	3900	3300	296	300	M1	47.3	3.23	9	324	520	3.05	B	10	750	0.608	0.760	0.760	0.342	-		Post yield buckling
	B8	3900	3300	296	300	M1	47.4	3.25	9	324	520	3.05	B	25	750	0.588	0.809	0.809	0.364	-		Post yield buckling
	B9	3900	3300	296	300	M1	47.9	3.30	9	324	520	3.05	B	50	750	0.539	0.294	0.539	0.243	-		Flexural tension
	RC	3950	3300	300	300	M1	46.3	3.48	#6x10*	343	520	3.19	-	-	-	0.569	-	0.642	0.289	-		Flexural tension
Shear	CBR	4000	1800	618	590	M2	59.4	2.59	12	304	441	1.94	RIB	550	350	-	-	2.17	-	5.95		Shear compression
	CBF	4000	1800	618	590	M2	56.8	3.11	12	304	441	1.94	FB	100	200	-	-	3.23	-	8.86		Shear compression
	CSR	4000	1800	618	1190	M2	59.4	3.05	12	304	441	1.94	RIB	550	350	-	-	5.80	-	7.88		Shear compression
	CSF	4000	1800	618	1190	M2	56.8	3.00	12	304	441	1.94	FB	100	200	-	-	6.67	-	9.11		Shear compression
	RCB	4000	1800	600	600	M2	55.3	2.74	#10x9*	343	549	1.99	-	-	-	-	-	2.73	-	7.58		Shear compression
	CBFS	2012	900	309	300	M2	56.7	3.72	6	358	409	1.94	FB	50	100	-	-	1.20	-	12.8		Shear compression
	A	3000	2400	296	300	M1	40.3	2.70	9	324	520	3.05	A	50	-	-	-	0.361	-	4.04		Tied-arch
	B	3000	2400	296	300	M1	40.7	2.73	9	324	520	3.05	B	50	300	-	-	0.108	-	1.20		Diagonal tension

(Note) *:Deformed reinforcing bars

Table 2 Mix proportions of concrete

Mix	Target comp. strength f'_c (MPa)	Maximum size of coarse aggregate G_{max} (mm)	Range of slump (cm)	Range of air content (%)	Water-cement ratio W/C (%)	Sand-agg. ratio s/a (%)	Unit content(kg/m^3)				
							Water W	Cement C	Silica fume SF	Sand S	Gravel G
M1	45	25*	24±2	5±2	35	39	157	450	-	646	1042
M2	50	15**	>25	7±2	29	38	146	502	50	589	598

(Note) * :Normal weight coarse aggregate
**:Light weight coarse aggregate

increase of strength from yield strength to ultimate strength in comparison with the corresponding reinforced concrete member. For the estimation of ultimate strength, we may take into account the effect of strain hardening state of steel, and the effect of enhanced concrete strength due to multiaxial confinement.

3. SHEAR TEST

3.1 Outline of test

To evaluate shear strength of composite beams and slabs with different inner configurations, 7 shear tests were performed. The dimensions and basic configurations are shown in Fig. 4. Four types of stiffener configurations were considered, they were as follows:
(A) FB-type: Lattice shaped flat bars were set.
(B) RIB-type: L-shaped stiffeners were set transversely.
(C) A-type: Stiffeners were set longitudinally.
(D) B-type: Stiffeners were set transversely.
Furthermore, a RCB (Reinforced Concrete Beam) model, having the same steel ratio as the RIB type models, was tested to compare the shear strength. The target compressive strength of concrete was 45 to 50 MPa. Mix proportions are shown in Table 2. Steel properties are shown in Table 1. The tests were carried out using simply supported configurations with two or four point concentrated loadings as illustrated in Fig. 4.

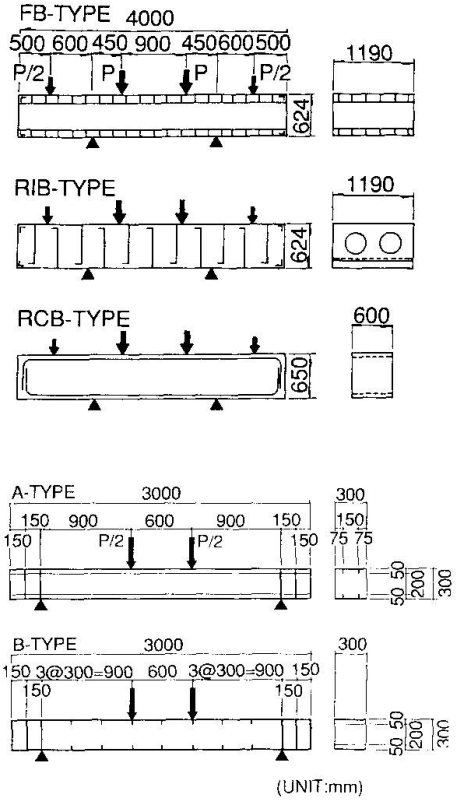

Fig. 4 Shear test models and loading configurations

3.2 Result of shear test

(1) Shear stress deflection relation of FB, RIB, RCB-type models

The deflections of FB, RIB, RCB-type models measured at mid-span under shear loading are shown in Fig. 5. It was confirmed that the composite members are superior in resisting earthquake loads by the fact that the energy absorbing capacity for the CBR model is 5 times greater than for the RCB model, and for other models is more than 20 times greater than that for the RCB model.

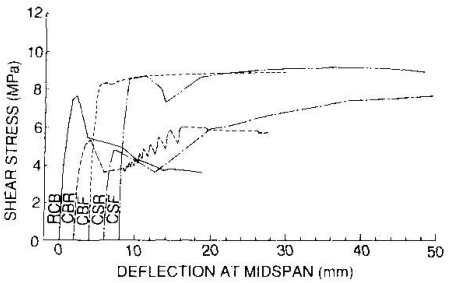

Fig. 5 Shear stress - deflection curves

(2) Ultimate shear strength of FB, RIB, RCB-type models

Figure 6 shows ratios between the experimental shear strengths and values calculated by the JSCE (Japan Society of Civil Engineers) equation[3] for deep beams and by the ACI equation[4]. The calculation by the JSCE equation showed a good agreement with the experimental results, and calculation by the ACI equation gave relatively conservative results. The JSCE equation is expressed as;

$$\tau_D=3.0\,(d/100)^{-1/4}\,(100p_w)^{1/3}\,f'_c{}^{1/2}/[1+(a_v/d)^2], \quad (1)$$

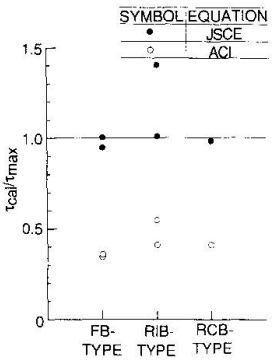

Fig. 6 Experimental/calculated shear strength

where, τ_D: shear strength of deep beam (kgf/cm^2), d: effective depth (cm), p_w: longitudinal tension reinforcement ratio, a_v:shear span length less half of the support plate width (cm), f'_c: compressive strength of concrete (kgf/cm^2)

(3) The effect of stiffener direction on shear strength
Figure 7 shows the ratio between experimental shear strengths of A-type and B-type beams and calculations by the JSCE equation for slender beams. Stiffeners were set longitudinally in the A-type beam and transversely in the B-type beam. The B-type beam failed in shear. Although the A-type beam failed in flexure, the maximum shear stress of the A-type beam was three times larger than that of the B-type beam. It was observed that transversal stiffeners became the trigger of diagonal tension cracks. Therefore, there are some cases where beams with no transversal stiffener have larger shear strength. The JSCE equation is expressed as ;

$$\tau_c=0.94f'_c{}^{1/3}\beta_p\beta_d[0.75+1.4/(a/d)], \quad (2)$$
$$p_w=100A_s/(b_w d), \beta_p=p_w{}^{1/3}<1.5,$$
$$\beta_d=d^{-1/4}<1.5, d[m]$$

where, τ_c: ultimate shear strength (kgf/cm^2), f'_c: compressive strength of concrete (kgf/cm^2), a: shear span, d: effective depth, b_w: breadth of web, A_s: cross-sectional area of tension reinforcing bars.

(4) Size effect on shear strength of composite beam.
The deflections of CBF and CBFS models measured at midspan under shear loading are shown in Fig. 8. The CBFS model is a half scale of the CBF model. The nominal shear strength decreased as the beam size increased. Therefore, when designing large composite members, it is necessary to consider the size effect on shear strength. Figure 9 shows the ratios of the values calculated by JSCE equation for deep beam to the experimental shear strength. The JSCE equation showed a good agreement with the experimental shear strengths.

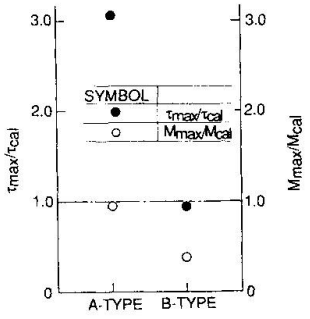

Fig. 7 Calculated/experimental shear strength

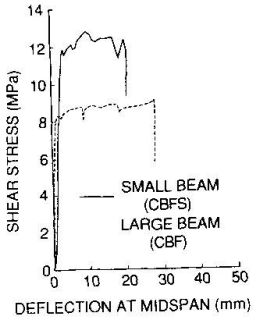

Fig. 8 Shear stress - deflection curves

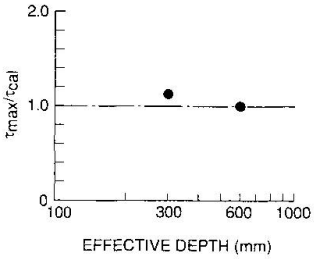

Fig. 9 Experimental/calculated shear strength

4. CONSTRUCTABILITY TEST

4.1 Outline of test

To aid in the development of a practical construction procedure, 18 injection tests were carried out. Details of the injection tests are described in Ref. 1. After the injection tests, in order to confirm the applicability of the concrete placing system achieved through the injection tests the large constructability test was performed. The test models are shown in Fig. 10, acrylic plates were used

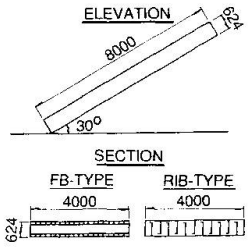

Fig. 10 Large constructability test models

on the surface of the models to allow visual inspection. The concrete injecting system is shown in Fig. 11, the system employs valve controlled multiple outlets using flexible tremie pipes which are continuously inserted and elevated. The pipes are equipped with vibrators for consolidation.

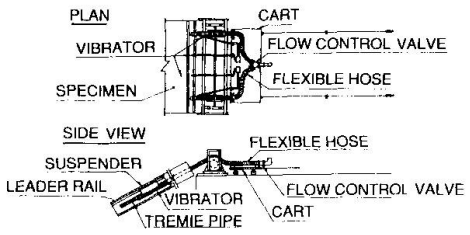

Fig. 11 Concrete injecting system

4.2 Result of constructability test

The results are summarized as follows;

(1) Perfect injection was observed.

(2) Although the maximum temperature rise of concrete was 68°C, no cracks on the concrete surface were observed.

(3) The injection equipment operated well. The result confirmed that it can be applicable in the actual construction. From the test, the placing rate is estimated to be approximately $40m^3/hr$.

5. CONCLUSION

(1) Flexural tests confirmed that the yield moment of composite members can be calculated using the conventional theory for reinforced concrete. The composite beams showed a high ductility. Failure occurred when deflection reached 10 times the yield deflection. The failure modes of the composite beams were compression plate buckling and concrete crushing. As for the reinforced concrete beam, failure occurred, prior to such large deflection, due to crushing of concrete in the compression region.

(2) The shear strength of the composite members is almost the same as that of reinforced concrete members as long as an appropriate inner stiffener configuration is employed. It is observed that calculation by the JSCE (JSCE: Japan Society of Civil Engineers) equation agreed well with the experimental results, and the calculation by the ACI equation showed relatively conservative results. In addition, the composite member showed extremely large energy absorption capacity, 20 times larger than that of a reinforced concrete beam. However, inner stiffeners induced the shear failure of the beam. Without inner transverse stiffeners, shear strength of the beam becomes larger.

(3) The shear strength of the composite beam decreased as the depth of the beam increases (size effect on shear strength). Therefore, when designing composite beams, it is necessary to consider the size effect on shear strength.

(4) A concrete placing system that enables continuous placement of highly plastic and segregation-free concrete into intricate steel encasements was developed. Sufficient infilling of concrete and the effectiveness of the system were confirmed in mock-up tests.

REFERENCES

1. SHIOYA T., MATSUMOTO G. et al., Development of Composite Members for Arctic Offshore Structures. Proc. of POLARTECH '86, Vol.2, Oct. 1986, pp.660-677.
2. OHNO F., SHIOYA T. et al., Experimental Studies on Composite Members for Arctic Offshore Structures. POAC '87 (to appear).
3. JSCE, Standard Specification for Design and Construction of Concrete Structures- 1986, part 1 (Design). 1986.
4. ACI, Building Code for Reinforced Concrete(318-83). 1983.

Ouvrage mixte à hourdis préfabriqué et précontraint

Verbundplatte mit vorfabrizierten Elementen und Vorspannung

Composite Construction with Prefabricated Prestressed Concrete Elements

J. BUFFA
Ingénieur
SCETAUROUTE
Fréjus, France

Mr COLOMBERO
Ingénieur ETP
Entreprise Colombero
Digne, France

Mr DEMARET
Ingénieur
Chargé d'Études
Digne, France

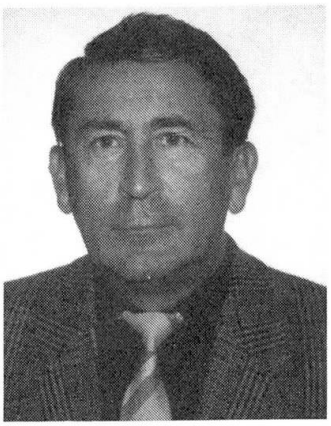

RÉSUMÉ

L'article relate un mode particulier de réalisation d'un hourdis en béton préfabriqué et précontraint sur une structure métallique. Le processus retenu avait trois objectifs: innovation, raccourcissement du délai d'exécution, et réduction du coût des travaux. La nouveauté du procédé ainsi que le court délai imparti aux études n'ont pas permis d'en tirer tous les avantages techniques et financiers.

ZUSAMMENFASSUNG

Der Artikel beschreibt die besondere Herstellung einer Platte aus Fertig- und Vorspannbeton auf einer Stahlkonstruktion. Der gewählte Bauvorgang sollte drei Ziele erreichen: die Innovation, kürzere Bauzeit und geringere Erstellungskosten. Wegen der Neuheit dieses Herstellungsverfahrens und der zeitlichen Einschränkungen konnten die finanziellen und technischen Vorteile der Herstellungsmethode noch nicht vollkommen ausgenutzt werden.

SUMMARY

This article concerns a special method for a prefabricated and prestressed concrete construction on a steel structure. The chosen process had three purposes: innovation, reducing execution time and work cost reduction. The newness of this process and the short time allowed for research have not yet permitted achieving all the technical and financial advantages possible.

1 - DESCRIPTION

L'ouvrage est le passage inférieur n°901 de l'autoroute A.51 du Val de Durance, construit au dessus de la voie ferrée Grenoble / Marseille, sur la section Manosque - Sisteron mise en service fin 1989. Il comporte deux tabliers séparés, de longueurs hors tout 188,86m pour le tablier Ouest et 213,23m pour le tablier Est. Ces tabliers sont constitués de 4 travées continues :

- Ouest : 36,16 + 63,27 + 55,24 + 32,14
- Est : 35,84 + 62,73 + 62,73 + 49,78.

Les piles de type marteau sont fondées sur des puits uniques forés Ø 2,50m. Une culée est classique, l'autre est constituée d'un chevêtre reposant sur des puits Ø 0,80m forés à travers les remblais de la plateforme.

Les tabliers sont du type ouvrage mixte à 2 poutres métalliques sous chaussée, supportant un hourdis préfabriqué et précontraint longitudinalement d'épaisseur variable de 0,25m à 0,34m au droit des poutres. D'une largeur utile de 8,50m comptée entre barrières métalliques BN4 et glissières, ils présentent en plan un rayon unique de 1200m et en travers un devers constant de 3,5 %.

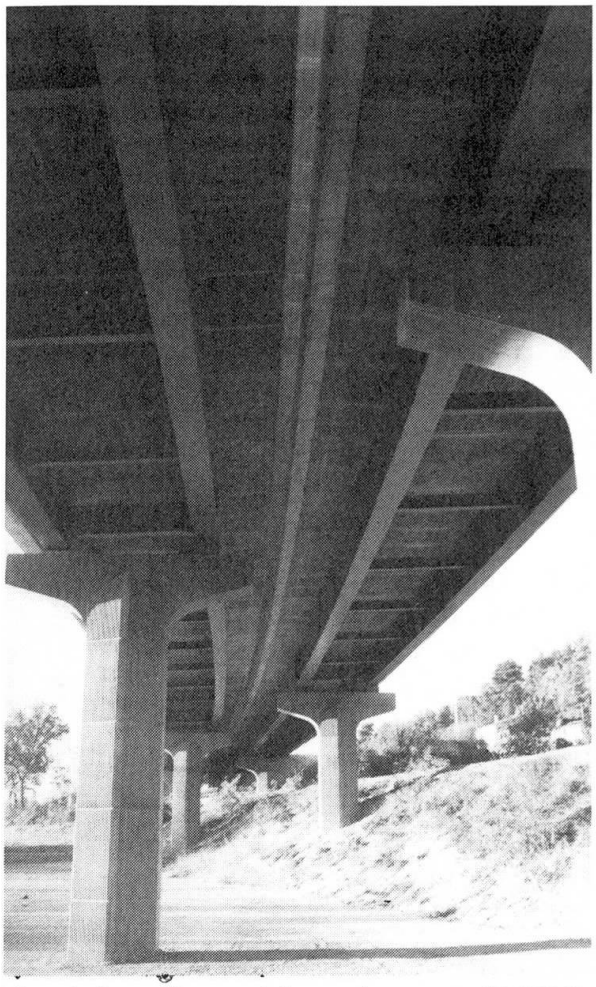

Fig.1-Vue d'ensemble prise par dessous

2 - RAISONS DU CHOIX

L'ouvrage a été dévolu avec un hourdis en béton armé construit après lancement des ossatures métalliques au moyen d'un coffrage roulant sur les poutres. La durée d'exécution de chaque hourdis estimée à 3 mois ne permettait pas de respecter les délais de mise à disposition des tabliers au terrassier en raison d'un retard dans le démarrage de travaux.

L'entreprise adjudicataire de l'ouvrage, spécialisée dans la préfabrication de pièces en béton pour les bâtiments industriels et d'habitation, proposa alors de préfabriquer le hourdis pour réduire la durée d'exécution. L'examen de la variante montrait un gain de temps et également une réduction sensible du coût : la dépense de précontrainte était compensée par une diminution d'une part du ferraillage passif et d'autre part de l'ossature métallique, par suite de la prise en compte du béton non fissuré sur appuis.

Dans ces conditions, le Maître d'Oeuvre accepta la proposition de l'entreprise, et associa aux études le Service Technique des Routes et Autoroutes (SETRA).

Le contre-calcul scientifique établi par ses soins a pris en compte les déformations différées du béton (fluage et retrait), les pertes de précontrainte en résultant, ainsi que le transfert d'une partie des efforts de compression dans le béton vers la charpente métallique.

En outre, ce contre-calcul scientifique a permis de vérifier le calcul classique de l'Entreprise, fait à partir des résultats du programme OMC du SETRA.

3 - EXECUTION

3-1 Le hourdis se compose essentiellement d'éléments préfabriqués de longueur 2,50 m et de quelques parties bétonnées en place (abouts et clavages).
La préfabrication a été faite sur le chantier dans 2 moules métalliques, équipés de vibrateurs pneumatiques.
Le coffrage des éléments préfabriqués comprenait :
. dans l'axe une clé et un défoncé correspondant sur l'autre face,
. des réservations pour le logement des connecteurs.

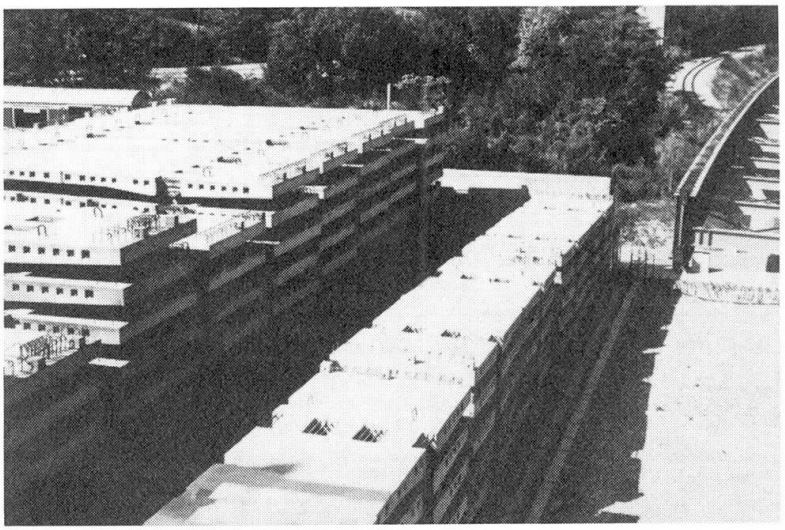

Fig. 2
Stockage
des éléments
préfabriqués

3-2 La mise en oeuvre des éléments préfabriqués a été faite suivant une méthode similaire à celle utilisée dans les tabliers construits en encorbellement, à savoir
a/ Construction des 3 "fléaux" relatifs aux 3 piles comprenant la pose des éléments préfabriqués, le collage et la mise en précontrainte de câbles 4K15 assurant la solidarisation de paires d'éléments disposés symétriquement.
b/ Pose des éléments préfabriqués intermédiaires et collage : le serrage nécessaire (environ 1 bar) était assuré par des petits vérins prenant appui sur les connecteurs.
c/ Bétonnage en place des abouts des hourdis et des clavages prévus dans les 2 travées centrales.
d/ Mise en oeuvre de la précontrainte de continuité constituée de câbles filants 12K15 ancrés dans les abouts.
e/ Bétonnage des réservations.

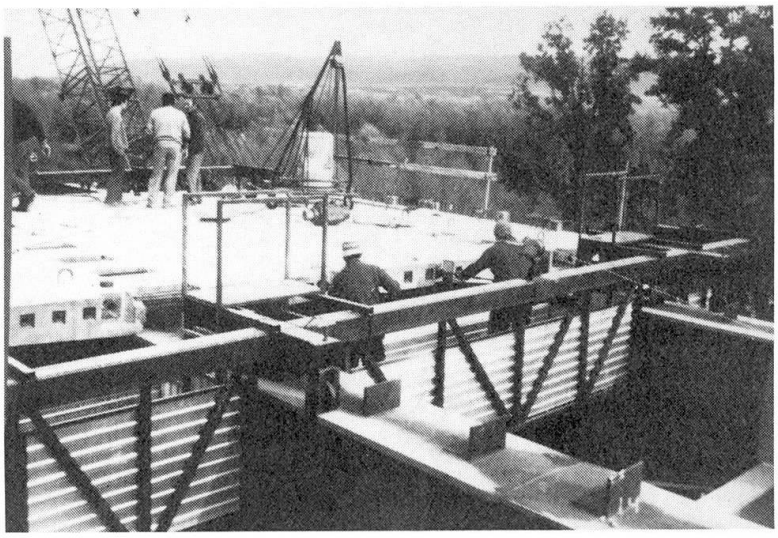

Fig.3- Assemblage des éléments préfabriqués.

3-3 Matériel utilisé :
- Grue à tour POTAIN 8 520 appurant la préfabrication, le stockage (à proximité) et le chargement des éléments.
- Semi-remorque pour le transport des éléments, 1 élément d'environ 17 T par rotation.
- Grue Manitowac 3900 sur le site pour le déchargement du semi-remorque et la pose des éléments sur l'ossature.

4 - INTERET DE LA SOLUTION

4-1 Réduction du délai de moitié : à savoir 6 semaines calendaires au lieu des 12 prévues initialement, par tablier.

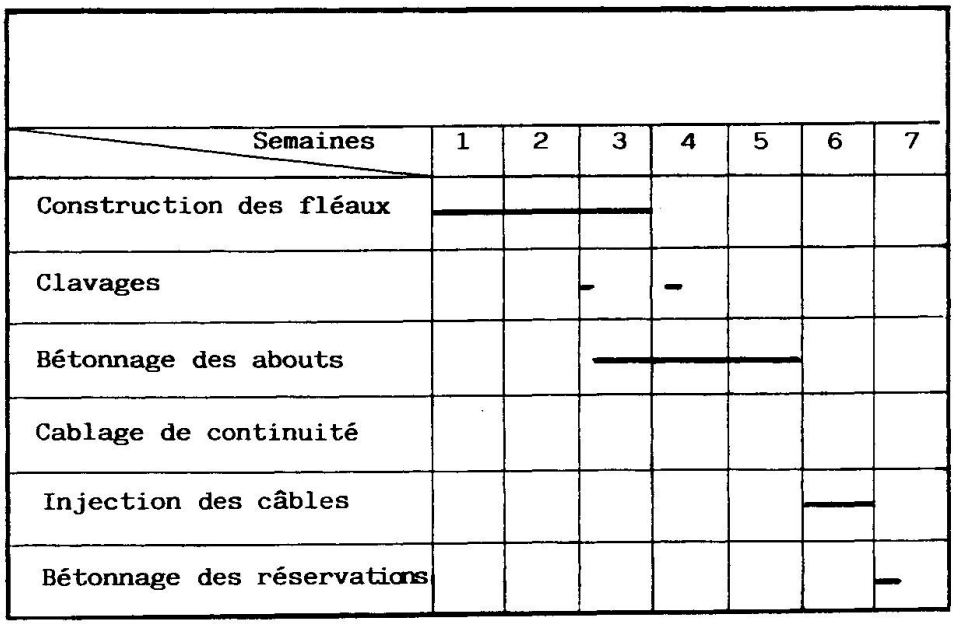

Planning d'exécution des hourdis

4-2 Réduction du coût des tabliers : 5 % du coût Marché des tabliers non équipés suivant détails ci-après.

- Volume béton hourdis inchangé	=	1 145 m3
- Gain en armatures passives	=	113 kg/m3
- Gain en ossature métallique 87 T sur les 700 T prévues au marché soit un gain ramené au m3 de béton du hourdis	=	76 kg/m3
- Dépense de précontrainte	=	40 kg/m3
- Bilan établi : avec les prix du Marché de base Mai 1988 (-113x5,60-76x8,931+40x19) 1145	=	631 000 Frs HT

5 - DEFAUTS ET AMELIORATIONS

5-1 Défauts

Les coffrages métalliques ont subi des déformations qui ont entrainé des défauts géométriques sensibles sur les faces de contact.

5-2 Améliorations

- Phasage : la durée d'exécution peut être réduite à 4 semaines calendaires en démarrant l'exécution des abouts en même temps que les fléaux moyennant une section de clavage dans les travées de rive.

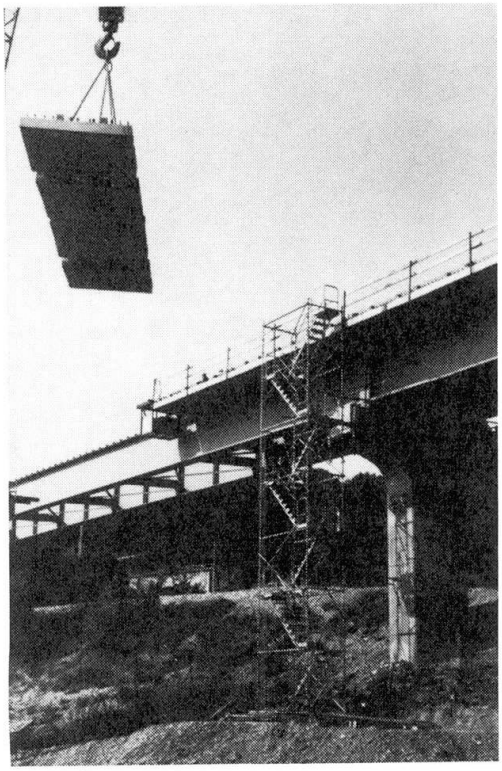

Fig.4-Pose d'un élément préfabriqué

- Coffrage du hourdis : les défauts de contact peuvent être réduits par la technique des joints conjugués.
En outre, en observant l'importance relative du poids du hourdis par rapport à l'ossature métallique (environ 80 %), il apparait qu'un gain notable sur l'ossature métallique pourrait être obtenu en réduisant le volume de ce hourdis.
- Ossature métallique : il convient en outre d'affiner le calcul OMC, le bilan présenté plus haut en aurait été notablement amélioré.
Une analyse plus poussée des hypothèses de calcul et un délai d'études plus conséquent doivent permettre d'améliorer sensiblement le bilan.

6 - CONCLUSION

L'expérience relatée a été positive. La rapidité d'exécution est l'élément prépondérant de l'innovation : on peut raisonnablement envisager de construire un tablier de type Ouvrage Mixte de longueur 200 m en 6 semaines calendaires, hors équipements.
Par contre, l'exécution est plus délicate que la solution classique et le calcul plus compliqué. Aussi pour des ouvrages moyens pour lesquels les délais ne sont pas prépondérants, la solution classique reste valable.

Leere Seite
Blank page
Page vide

Design of Beam-Column Connections for Composite-Framed Structures

Conception des assemblages entre poutre et poteau pour des structures à ossature mixte

Entwurf von Rahmenknoten in Verbundbauweise

Gregory G. DEIERLEIN
Assist. Professor
Cornell University
Ithaca, NY, USA

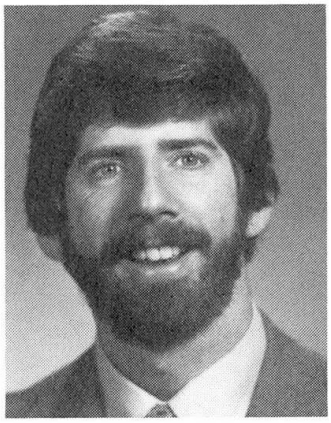

Deierlein joined the faculty at Cornell in 1988 after completing his Ph.D. at the University of Texas. He also holds a MS from the University of California at Berkeley and a BS from Cornell University. He is a registered engineer and has experience in the design of steel, concrete and composite building structures.

Co-Authors
Tauquir M. **SHEIKH**, Associate, CBM Engineers Inc., Houston, TX, USA
Joseph A. **YURA**, Professor, University of Texas, Austin, TX, USA
James O. **JIRSA**, Professor, University of Texas, Austin, TX, USA

SUMMARY

This paper addresses the design of composite beam-column joints which have been used in tall buildings with perimeter frames consisting of structural steel beams and reinforced concrete (or composite) columns. The connection behavior is described based on an experimental research program in which specimens were tested to failure under monotonic and cyclic loads. Mechanisms for evaluating the joint shear strength are proposed which consider interaction of the structural steel and reinforced concrete joint panels.

RÉSUMÉ

Cet article décrit la conception des assemblages entre poutres en acier et poteaux en béton armé (ou mixtes), qui sont utilisés dans des bâtiments élevés avec portiques extérieurs. La description du comportement de ce système est décrite sur la base d'un programme de recherche expérimentale dans lequel des échantillons furent soumis à rupture sous l'action de forces monotones et cycliques. Des mécanismes sont proposées pour calculer la résistance au cisaillement des assemblages, avec prise en considération des interactions entre l'ossature en acier et les dalles en béton armé.

ZUSAMMENFASSUNG

Dieser Artikel behandelt den Entwurf und die detaillierte Bemessung von Rahmenknoten in Verbundbauweise. Seite einigen Jahren werden solche Verbindungen in hohen Gebäuden mit Aussenrahmen, die aus Stahlriegeln und Stahlbeton- oder Verbundstützen bestehen, eingesetzt. Das Verbindungsverhalten wurde in einem Forschungsprogramm untersucht, in dem Versuchsstücke unter monotoner und zyklischer Belastung bis zum Versagen getestet wurden. Bemessungsgrundlagen wurden entwickelt für die Berechnung der Gesamttragfähigkeit unter Einschluss der Wechselwirkung zwischen den Stahlträgern und den Stahlbetonverbindugsscheiben.

1. INTRODUCTION

Increasingly, composite and mixed steel-concrete construction is being used to build more efficient structures than either material alone could provide. However, due to the traditional separation of structural steel and reinforced concrete design, there are pressing research needs to develop design guidelines for composite components and systems. One such need is in the design and behavior of connections which are an integral part of composite-framed structures.

As used herein, the term "composite frame" describes a moment resisting frame consisting of steel beams and reinforced concrete (or composite columns). To date, such frames have been employed for lateral load resisting perimeter tube systems for buildings in the 40 to 70 story height range. Typically, such structures are built by first erecting a frame of light steel erection columns and deep steel beams. The steel columns are later encased by reinforced concrete to create the composite frame [1].

In this paper, the behavior of composite beam-column joints is presented based on recent research in which seventeen large-scale specimens were tested under monotonic and cyclic loads. The internal force mechanisms are described using familiar concepts from current design standards for structural steel and reinforced concrete joints. A more detailed discussion of the research and recommendations for design are presented by Sheikh et.al. [2] and Deierlein et.al. [3].

2. JOINT BEHAVIOR AND DETAILING

In a frame subjected to lateral loading, the moments and shears imposed on the beam-column joint are shown in Figs. 1(a-b). In composite frames, typically the steel beam is continuous through the joint, and where used the steel erection column is interrupted by the beam. As shown in Figs. 1(a-b), joint behavior is characterized by two primary modes of failure. Panel shear failure is similar to that usually associated with structural steel or reinforced concrete joints, but in composite joints the relative contribution from each material should be considered. Vertical bearing failure occurs in regions of high compressive stresses and permits rigid body rotation of the steel beam within the concrete column. Vertical joint reinforcement, as shown in Fig. 1(b), is one means of strengthening for bearing failure.

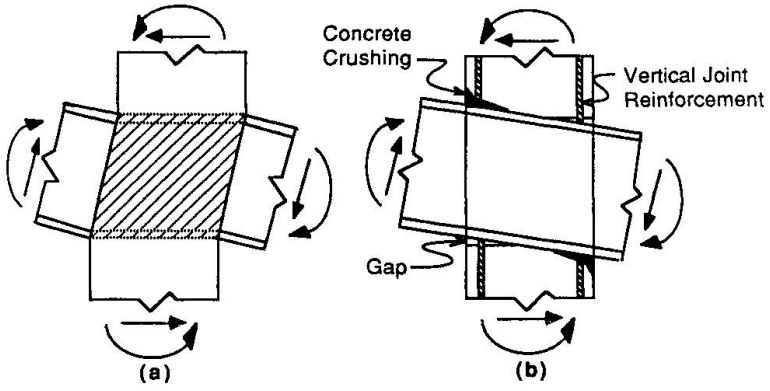

Fig. 1. Primary Failure Modes: (a) Panel Shear, (b) Vertical Bearing

Three mechanisms for joint shear resistance are shown in Figs. 2(a-c). In these figures, beam and column moments are shown as horizontal and vertical force couples, respectively. The joint shear mechanisms can be visualized by considering how they resist the beam flange forces and thus prevent horizontal movement of the beam flanges through the joint.

The steel web panel, shown in Fig. 2a, acts similarly in composite and structural steel joints. The web is idealized as carrying pure shear stress over an effective panel length, jh, which is dependent on the location and distribution of vertical bearing stresses.

The concrete compression strut, shown in Fig. 2b, is similar to the mechanism used in U.S. practice to model the shear strength in reinforced concrete joints [4]. In composite joints, the concrete strut is mobilized by vertical stiffener plates attached to the beam that bear against the concrete. The location and width of the stiffener plates determine how effectively the inner region of concrete is mobilized in resisting joint shear.

The concrete compression field, shown in Fig. 2c, consists of multiple struts that act together with horizontal reinforcement to form a truss mechanism similar to that used for modeling shear in reinforced concrete beams. The compression field is developed in the region outside the steel beam. As shown in Fig. 3, shear is transferred into the compression field by horizontal struts which form through bearing against either: embedded steel columns, stiffener plates extended above and below the beam, and shear studs or other attachments welded to the beam flanges.

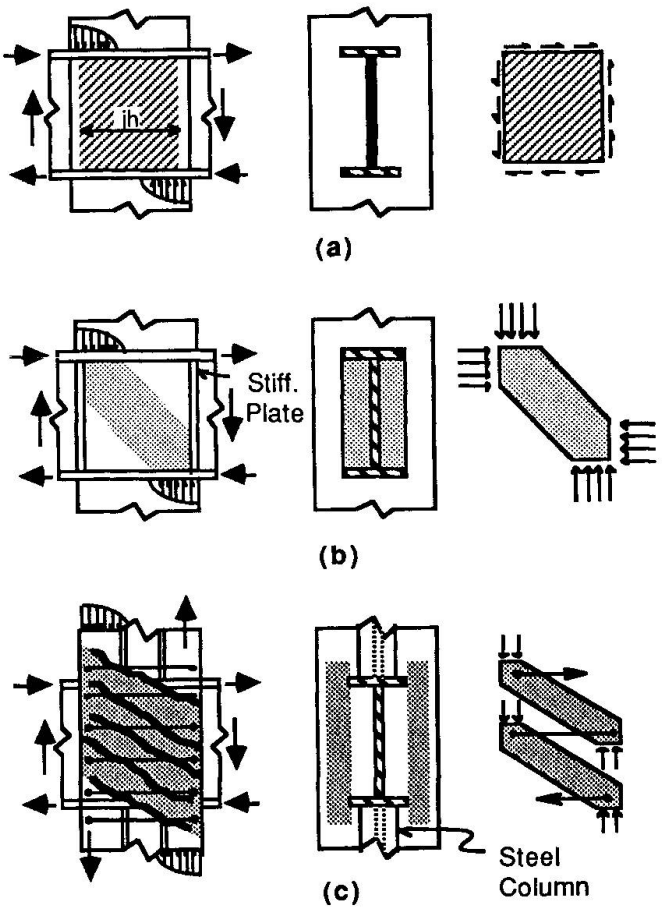

Fig. 2: Joint Shear Mechanisms: (a) Steel Web Panel, (b) Concrete Compression Strut, (c) Concrete Compression Field

3. EXPERIMENTAL RESEARCH PROGRAM

To evaluate the effectiveness of various joint details in mobilizing the internal force mechanisms, an experimental program was undertaken where seventeen beam-column joint specimens were built and tested [2,3]. In this paper, results from five tests are presented to illustrate the relative effectiveness of various details in mobilizing internal joint mechanisms.

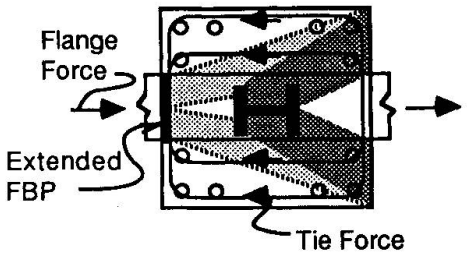

Fig. 3 Horizontal Force Transfer

3.1 Specimen Description: The cruciform shaped joint specimens consisted of 510 mm square concrete columns and built-up steel beams 460 mm deep which were continuous through the joint. The connections were loaded to replicate in-plane joint forces from lateral loading as shown previously in Figs. 1(a-b). For experimental purposes, both the steel beams and concrete columns were overdesigned in shear and flexure to force failure in the joint, however, in actual design the members should be proportioned so that yielding occurs in the beams before the joint or column strength is reached.

corners to allow clear passage of the steel beams through the column. Horizontal ties were provided within the beam depth to confine concrete in the joint and carry tension forces associated with the compression field mechanism. These ties were U-shaped stirrups which passed through holes drilled in the beam web. Above and below the beam, three layers of closed rectangular hoops confined the concrete in the region where high bearing stresses developed and where there were tension forces associated with the strut and tie mechanism shown in Fig. 3. Concrete compressive strengths ranged between 24.8 to 34.5 MPa (3.6 to 5.0 ksi). As described below, various attachments to the steel beam were used to investigate the strength of the joint shear mechanisms of Fig. 2.

3.2 Load-deformation response:

The response for a test which is representative of the cyclic behavior is shown in Fig. 4. The vertical axis indicates the applied beam load which is proportional to the beam moments adjacent to the connection. The total joint distortion on the horizontal axis is a measure of the relative angular rotation between the steel beam and column.

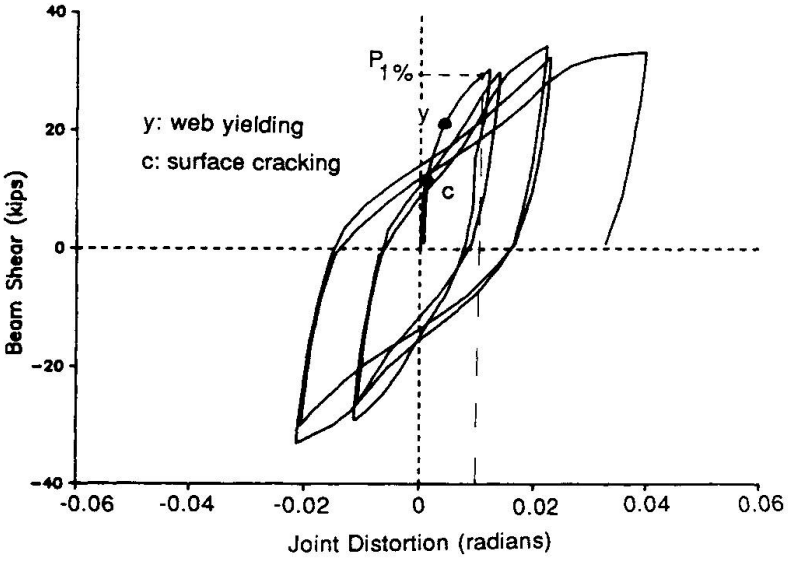

Fig. 4 Typical Load-Deformation Response

The load-deformation curve indicates that the joints failed in a "ductile" manner and displayed a fair degree of toughness under cyclic loading. In the figure, the points, *c* and *y*, indicate when cracks were first observed on the column face and when the steel web inside the joint yielded in shear. Web yielding was detected through electronic strain gages attached to the web. The joint continued to carry increasing load beyond web yielding, thus demonstrating participation of the concrete shear mechanisms. As indicated in the figure, the joint capacity measured at 0.01 radians distortion was chosen as the strength for comparison between tests and represents a reasonable measure of the nominal strength for use in design.

3.3 Visual Damage:

The typical surface cracking and concrete crushing is shown in Fig. 5. Diagonal cracks on the column face indicated the formation of compression field struts which carried joint shear. In specimens where plain beams were used without attachments, the concrete panel was not mobilized and these cracks did not form. Cracks on the side of the column revealed the dissipation of compression forces beneath both the top and bottom beam flanges. Bearing was concentrated directly below the beam flanges, and at high loads

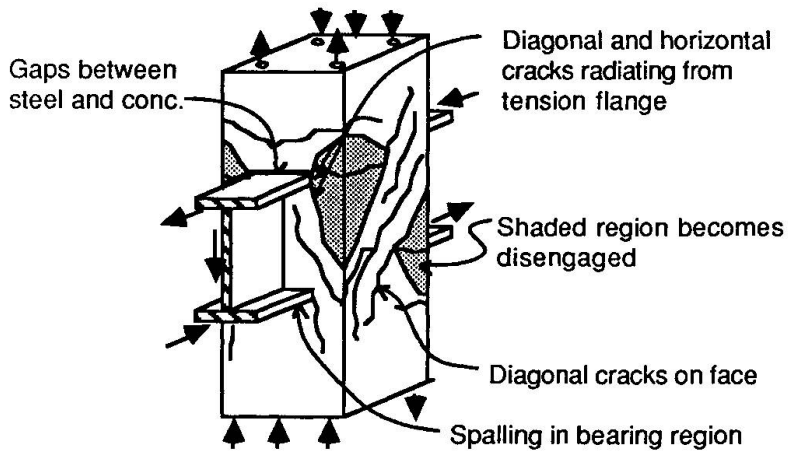

Fig. 5 Visible Damage and Cracking Pattern

concrete spalling was observed in this area. Once joint cracking progressed to a certain point, the concrete regions shown shaded became disengaged from the joint core. This decreased the transfer of vertical force to the longitudinal column bars through the joint region since the bars were located in the corners of the column.

3.4 Comparison of nominal joint strengths: In Fig. 6, the relative strengths are summarized for five test specimens with the details shown in Fig. 7. The results reveal how effectively each detail mobilized shear resistance in the steel web, concrete compression strut, and concrete compression field. The reported joint strengths were all measured at deformations of 0.01 radians and are normalized with respect to specimen 1.

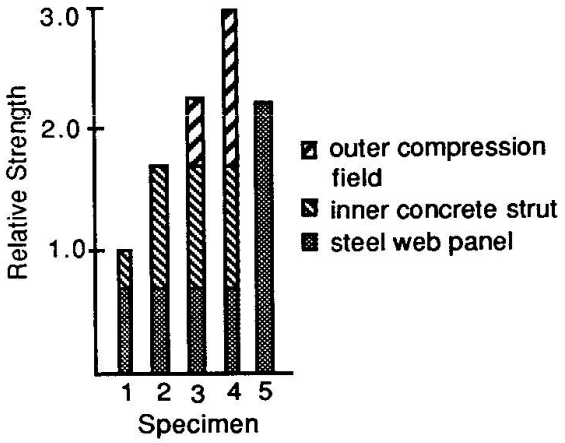

Fig. 6 Comparison of Joint Strengths

The strength of specimens 1 to 4 was limited by the shear capacity of the joint. In specimen 1, which consisted of a plain steel beam, most of the shear was carried by the steel web with only a small contribution from the concrete that was developed through adhesion and friction between the steel and concrete. In specimen 2, the face bearing (stiffener) plates mobilized the diagonal compression strut directly and the additional concrete contribution increased the total strength to 1.67 times that of specimen 1. In specimen 3, the addition of a W5 (130 mm) steel column increased the total strength to 2.25 times that of specimen 1 by mobilization of the outer panel through the strut mechanism of Fig. 3. Similarly, in specimen 4 which had a strength of almost 3 times specimen 1, the extended face bearing plates mobilized the outer concrete panel to an even greater degree. As shown in Fig. 3, the bearing plates at the face of the column result in a more effective transfer mechanism than with the steel column due to the shallower compression strut angles. In specimen 5, thick doubler plates were welded to the steel web in the joint to preclude yielding and thereby eliminate the shear failure mode. In this case, failure occurred by vertical bearing which provided a measure of the crushing strength for concrete bearing against the flanges. This test showed that for design the maximum concrete bearing stress above and below the flanges may be taken as $2\,F'_c$ [3]. It is interesting to note that where the outer compression field was mobilized (specimens 3 & 4), concrete crushing did not control the strength even though the applied load was larger than in specimen 5. Presumably, this was due to the fact that when the concrete compression field was mobilized the total effective joint width (and bearing zone width) was increased.

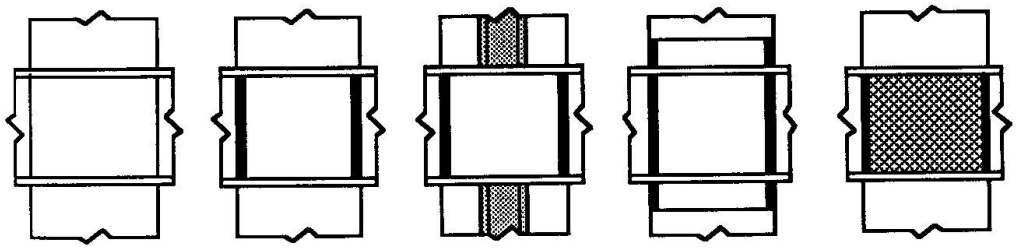

Fig. 7 Specimen Details

4. SUMMARY

Test results have shown that composite beam-column connections are reliable details which provide adequate stiffness at service loads, fail in a ductile manner at ultimate limit loads, and exhibit reasonable toughness under cyclic loading. Further, the strength of such connections can be increased significantly by simple details which mobilize the concrete panel in resisting joint shear. Such details can be designed using models derived from basic mechanics which are similar to those used for structural steel and reinforced concrete joints. These tests demonstrate the potential for composite joints as an attractive design alternative to structural steel or reinforced concrete.

ACKNOWLEDGMENTS

The material presented herein is based on research supported primarily by the National Science Foundation under Grant No. MSM-8412111. Additional funding was provided by the University of Texas, the American Institute of Steel Construction, and CBM Engineers of Houston, Texas.

REFERENCES

1. Griffis, L., "Some Design Considerations for Composite-Frame Structures." AISC Engrg. J., 2nd Quarter, 1986.

2. Sheikh, T.M., Deierlein, G.G., Yura, J.A., and Jirsa, J.O., "Part 1: Beam-Column Moment Connections for Composite Frames," J. Struct. Engrg., ASCE, 115(11), Nov. 1989, pp.2858-2876.

3. Deierlein, G.G., Sheikh, T.M., Yura, J.A., and Jirsa, J.O., "Part 2: Beam-Column Moment Connections for Composite Frames," J. Struct. Engrg., ASCE, 115(11), Nov. 1989, pp. 2877-2896.

4. ACI-ASCE Committee 352, "Recommendations for Design of Beam-Column Joints in Monolithic Reinforced Concrete Structures," Report ACI 352 R-85, 1985.

The Twin Cable-Stayed Composite Bridge at Baytown, Texas

Pont jumelé mixte à haubans de Baytown au Texas

Schrägkabelbrücke mit Verbundträgern in Baytown, Texas

H. S. SVENSSON
Manager
Leonhardt, Andrä & Partner
Stuttgart, FR Germany

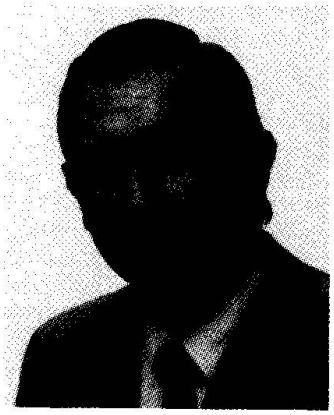

Holger S. Svensson, born in 1945, received his Dipl.-Ing. (M.Sc.) from Stuttgart University in 1969, his US registration as professional engineer (P.E.) in 1985, and his Canadian registration (P.Eng.) in 1988. He has extensive experience in the design of long-span, cable-stayed bridges all over the world.

Thomas G. LOVETT
Assoc. Vice Pres.
Greiner, Inc.
Tampa, FL, USA

Thomas G. Lovett, born in 1953, received his Bachelor of Science degree in Civil Engineering from the University of Maryland in 1975 and is a U.S. registered professional engineer (P.E.). He has participated in the design of several long span cable stayed bridges in the United States.

SUMMARY

This cable-stayed bridge with a main span of 381 m has two independent composite beams. The twin diamond shaped concrete towers rise about 130 metres above ground. Each beam comprises a steel grid from exterior main girders and cross-girders with a concrete roadway slab on top which was designed for composite action under dead and live load. The stay cables consist of strands within a poly-ethylene pipe and cement grout.

RÉSUMÉ

Ce pont haubané, d'une portée centrale de 381 m, présente deux tabliers indépendants à construction mixte. Chaque tablier est composé de poutres principales en treillis métallique reliées par des entretoises métalliques et surmontées d'une dalle en béton servant de chaussée; l'ensemble agissant comme construction mixte pour le poids propre et pour les surcharges. Les pylônes jumelés sont formés d'un Y renversé et atteignent une hauteur de 130 m. Les haubans sont composés de torons parallèles entourés d'une gaine en polyéthylène et protégés d'un coulis de ciment.

ZUSAMMENFASSUNG

Diese Schrägkabelbrücke mit einer Hauptspannweite von 381 m besitzt zwei Verbundträger, die aus einem Stahlträgerrost und Querträgern bestehen. Die Betonfahrbahnplatte wurde für Verbundwirkung unter ständigen Lasten und Verkehrslast bemessen. Die rhombusförmigen Doppelpylone erreichen 130 m Höhe. Die parallelen Litzen der Schrägkabel werden durch Polyaethylen-Rohren mit Zementinjektion geschützt.

1 INTRODUCTION

The bridge crosses the Houston Ship Channel 20 miles east of Houston between the cities Baytown and LaPorte in the State of Texas, USA, where it replaces the severely restrictive two-lane Baytown tunnel by an eight-lane high level crossing. It is the first cable-stayed bridge with two superstructures, and its total deck area of about 32 800 m² makes it one of the largest cable-stayed bridges to date.
In accordance with current US requirements alternate steel and concrete designs were prepared. In 1987 four bids ranging from 91.3 to 126.5 million dollars were received for the total project including the approach bridges, with all bidders selecting the steel-composite main bridge.
Construction started in 1987, and the bridge will be opened in 1991.

2 OVERALL SYSTEM

The cable-stayed bridge is continuous over its length of 675 m, see Fig. 1. The beam is supported by stay cables in a semi-fan arrangement at about 15 m intervals.

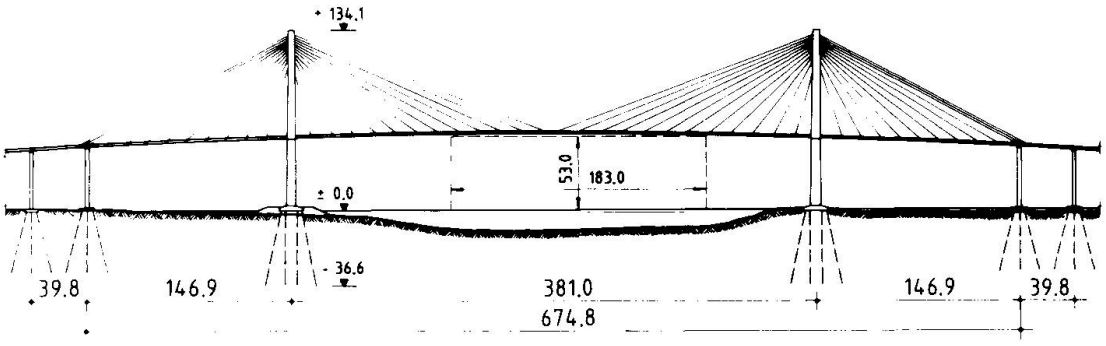

Fig. 1 General Layout

The support conditions render a completely symmetric structure. The beams are connected to each tower with flexible neoprene bearings, 250 mm high, which follow the temperature movements by shear deformation and distribute longitudinal forces equally to both towers. The anchorpiers are connected to the beams by rotational bearings. They are slender enough to follow the temperature movements of the beam by deflection. The vertical beam rotations are taken by strip seals above the anchor piers, the longitudinal movements are accommodated by expansion joints above the next piers. Transverse wind loads are taken by bumpers at the towers, and at the anchor piers.
The bridge is located in a hurricane prone area near the Gulf of Mexico. The basic design wind speed for a 100 year return period was determined as 50 m/sec at 10 m height with a duration of 10 minutes. Wind tunnel tests were performed on a section model (scale 1:96, [1]) and a full bridge model (scale 1:250, [2]). The test results and an independent analytical investigation showed that the bridge is aerodynamically stable for laminar wind with a speed in excess of 67 m/sec. For a turbulence intensity of 12% the peak-to-peak deflection at midspan comes to 1.65 m.
The structural design was done in accordance with the AASHTO Bridge Specification, amended as required by other US and international codes.

3 COMPOSITE BEAM

3.1 Structural Details

The four lanes with full shoulders require a roadway width of 22 m for each direction of travel. Two, three and four cable planes for supporting the roadway transversely were investigated. It was found that two independent beams - each supported by two outer cable planes, see Fig. 6, - are most economic. The cross-section of an individual beam is shown in Fig. 2. It consists of a steel grid composite with a concrete roadway slab.
The outside main girders have one continuous longitudinal stiffener, see Fig. 3. The vertical stiffeners at 5.2 m intervals are welded to the main girders, except for the regions of high moments near the center and the ends of the bridge where they are bolted to the bottom flanges due to fatigue. All floor beams are field bolted to the vertical stiffeners, see Figs. 2 and 3.

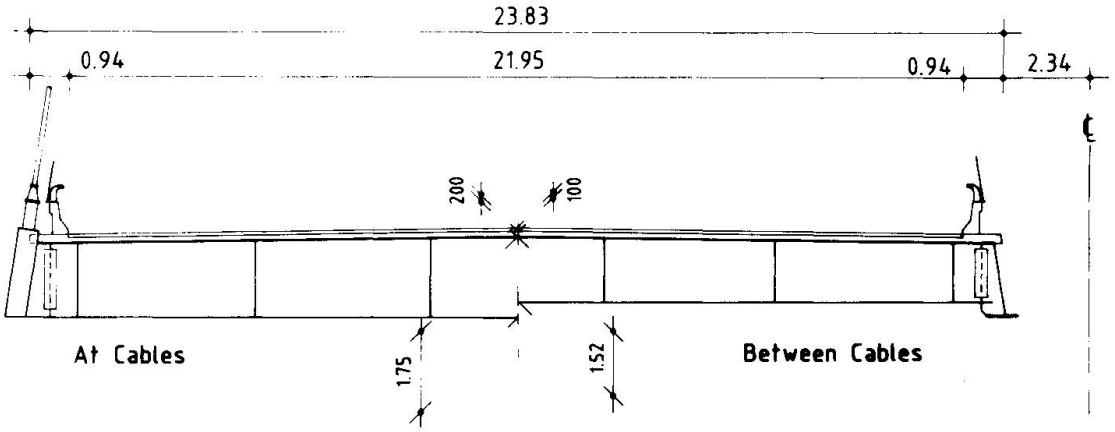

Fig.2 Individual Beam Cross-Section

The concrete deck is 200 mm thick and has a 100 mm reinforced concrete wearing surface. Longitudinal and transverse composite action is achieved by conventional shear studs. On the main girder top flange they are arranged in rows of three with a constant longitudinal spacing of 115 mm.
Crack control is achieved by a substantial amount of reinforcement with close spacing. At midspan where the compression is smallest diam. 18 mm bars at 115 mm spacing top and bottom (2,2%) were used longitudinally and transversely.
The cables are anchored in welded boxes bolted to the main girders, see Fig. 4. The eccentricity moment is carried by a force couple in compression to the roadway slab and in tension to the bottom flange of the full-depth main floor beams.

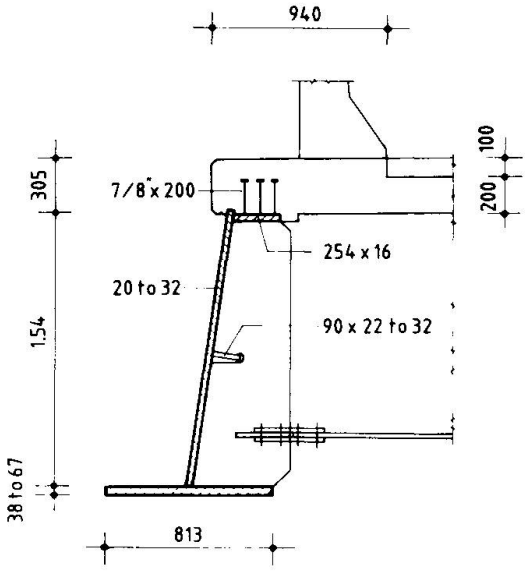

Fig.3 Edge Girder Detail

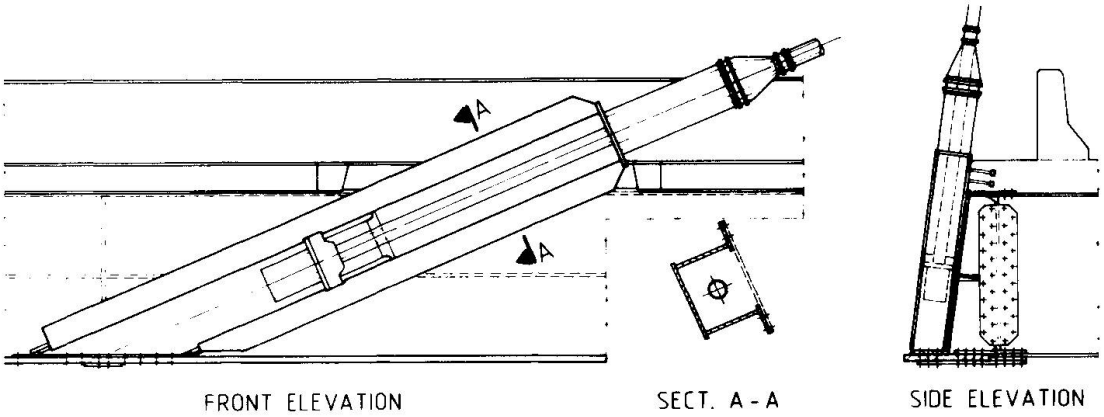

Fig.4 Stay Cable Anchorage at Beam

3.2 Design

The overall beam forces under permanent loads were chosen similar to those for a beam rigidly supported at the cable anchorpoints, except for the midspan and end regions where a positive camber is introduced to provide additional compression in the roadway slab. Composite action for dead load was to be achieved by casting the roadway slab onto a continuously supported steel grid on ground . The deck was thus under compression in transverse direction also as top flange of a simply supported girder under dead load.
The shrinkage and creep values were calculated in accordance with the CEB-FIP Model Code [3], which resulted in approximately the following ratios of moduli of elasticity for permanent loads:

n_0 = 6.0 initially and for transient loads
n_1 = 12.5 at opening for traffic
n_∞ = 18.0 after creep has taken place

(W/C = 0.35, relat. humidity 75%, age of deck at installation 1 month).

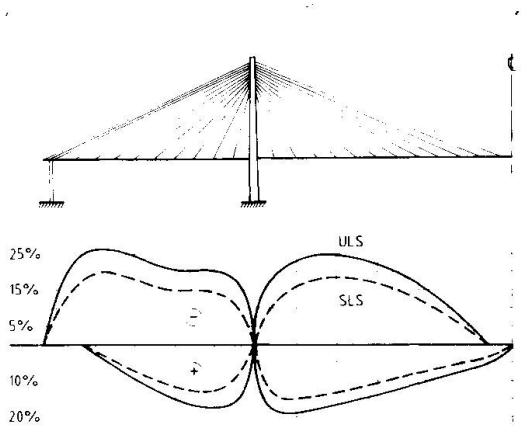

Fig.5 Non-linear increase of Live Load Moments

The overall girder moments due to live load increased by up to 26% in the ultimate limit state due to non-linear effects of the rather slender deck with a main span to depth ratio of about 1 in 200, compare Fig. 4 and [4]. The main girder shear studs are designed for the combined action of local and overall shear, and cable force introduction. An assumed limited amount of slip and plastic deformation of the studs in the ultimate limit state led to the uniform arrangement of shear studs over the length of the beam. The introduction of the shear force from the 300 mm thick concrete edge beam into the regular 200 mm thick slab (see Fig. 3) proved to be critical.

The sizing of the slab was governed by ultimate strength and crack control under service conditions. The plate girder stability was calculated in accordance with [5].

3.3 Contractor's Option

Instead of the proposed continuous roadway slab the contractor opted to use precast slabs connected by cast-in-place joints on top of the floor beams.Due to the resulting loss of composite action for dead load this required additional 640 t of structural steel, or an increase of 17% from 121 kg/m² to 141 kg/m².

4 STAY CABLES

The stay cables were sized in accordance with the PTI-Recommendations [6]. They were specified as shop-fabricated parallel strand HiAm cables in PE-pipes with cement grout and a wrapping with a laminated Tedlar tape, see [4] and [7] for further details.
The structure was designed to permit the exchange of any stay cable in conjunction with a reduction of live load to two lanes and reduced safety factors. Additionally, any stay cable can be accidentally severed under full live load without structural instability.
The contractor opted for in-situ fabricated parallel strand cables with wedge anchorages in PE-pipes and cement grout.

5 TOWERS

The towers are shown in Fig. 5. Their legs and the tie beams underneath the decks have box sections with a minimum wall thickness of 305 mm.

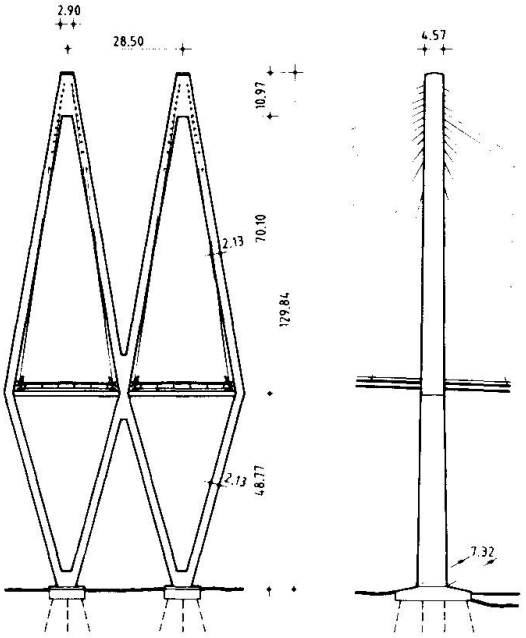

Fig.6 Tower Layout

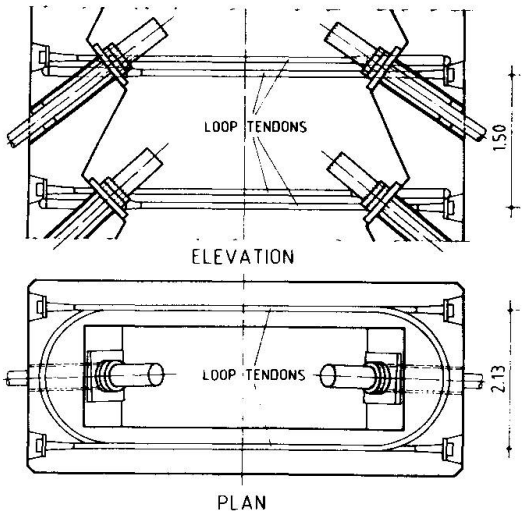

Fig.7 Tower Cable Anchorage

The double diamond shape is a natural progression from the twin decks. The A-frames on top of the decks reduce the torsional rotations of the beam significantly by forming a triangular space frame, compare [4]. By joining the two lower A-frames at deck level, a truss is created which carries the transverse wind loads in tension and compression to the two foundations. The transverse width of the towerlegs can thus be small. In longitudinal direction the tower legs act as cantilevers in bending, especially during construction. Those widths

have thus to be significantly greater. The tie beams act as direct tension members and are fully post-tensioned against the outward thrust from the tower legs.
At the towerhead the stay cables pass through steel pipes embedded in the tower walls, see Fig. 7. They are individually anchored inside on steel bearing plates resting on concrete corbels. The horizontal cable components are tied back with alternating loop tendons so that each cable anchorage region is confined by the radial forces from the loops.

6 CONSTRUCTION

From the four foundation alternates shown on the bid drawings th contractor opted to use 500 mm square precast prestressed concrete piles. They were driven from the artificial island on the LaPorte side and the existing levee on the Baytown side, see Fig. 1. 3.60 m thick CIP pile caps formed the basis for the towerlegs.
The towers were built in 4.5 m sections with jumping forms. For the first tower all four legs were built in parallel. For the second tower the two inner lower legs were built first, and then the outer legs were tied back to them.
The beams are constructed by free cantilevering from the towers outwards. The contractor opted to build the two beams in parallel with auxiliary tie-downs. The steel grids for each pair of cables are lifted up and connected in place. The precast slabs are then positioned and the cast-in-place joints poured before proceeding to the next section.

7 ACKNOWLEDGEMENT

Owner is the Texas State Department of Highways and Transportation. The cable-stayed main bridge was designed by Greiner, Inc., Tampa, Florida in association with Leonhardt, Andrä and Partners, GmbH, Stuttgart, Germany. Dr. Robert H. Scanlan served as consultant for wind. Williams Brothers Construction Co., Inc., and Traylor Bros., Inc. (a joint venture), are the contractors. The stay cables are supplied by the VSL Corporation.

REFERENCES

[1] SCANLAN, R.H.: Dynamic Wind Effects on the Houston Ship Channel Bridge Crossing (Steel Alternative). Report dated 1986.

[2] REINHOLD, T.A.: Wind Tunnel Aeroelastic Model Study of the Baytown Bridge Steel Alternative, Applied Research Engineering Services, Inc. Report 5101-1, May 29, 1986.

[3] International Recommendations for the Design and Construction of Concrete Structures, CEB-FIP (1978) Appendix E: "Time Dependent Behavior of Concrete Creep and Shrinkage".

[4] SVENSSON, H., CHRISTOPHER, B.G. and SAUL, R.: Design of a Cable-Stayed Steel-Composite Bridge. Journal of Structural Engineering, ASCE, Vol.112, No.3, March, 1986, pp. 489-504.

[5] Proposed Design Specifications for Steel Box Girder Bridges, Federal Highway Administration Report No. FHWA-TS-80-205, January, 1980.

[6] Recommendations for Stay Cable Design and Testing, by Post Tensioning Institute Ad Hoc Committee on Cable-Stayed Bridges, USA, Jan. 1986.

[7] SAUL, R. and SVENSSON, H.: On the Corrosion Protection of Stay Cables. Der Stahlbau 4/5, 1990.

Double Skin Construction

Construction en sandwich

Doppelhaut-Konstruktionen

Howard WRIGHT
Lecturer
Univ. of Wales
Cardiff, Wales, UK

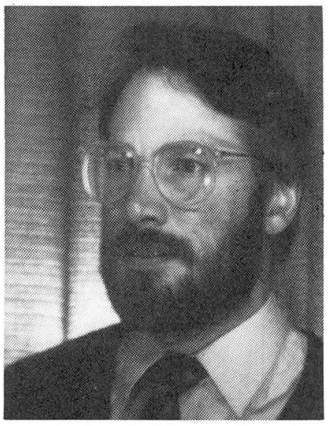

Howard Wright, born 1952 graduated from Sheffield University and has spent 9 years in practice before joining the staff at Cardiff. He has published extensively on composite construction including his Ph.D. on the subject in 1988.

Taiwo ODUYEMI
Res. Assist.
Univ. of Wales
Cardiff, Wales, UK

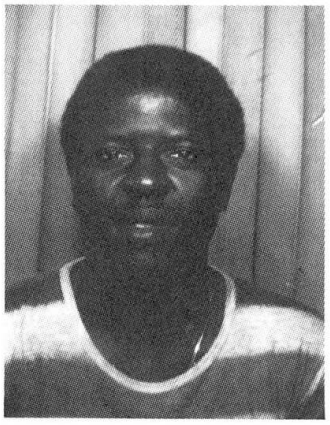

Taiwo Oduyemi graduated from the University of Birmingham in 1983 where he also obtained a Ph.D. in 1987. He has spent three years in Cardiff.

SUMMARY

Double skin composite elements are formed from two skins of steel plate and an infill of concrete. The sandwich acts compositely by means of welded stud shear connectors on the internal faces of the steel. This paper describes model tests on beam, column and beam column double skin elements. Comparisons are made with reinforced concrete design methods and guidance is given to allow engineers to dimension typical elements.

RÉSUMÉ

Les éléments mixtes en sandwich sont constitués d'un noyau de béton délimité par deux plaques métalliques. L'effet «sandwich» est réalisé au moyen de goujons soudés aux faces intérieures des plaques métalliques. Le présent article décrit des essais effectués sur des poutres, des poteaux et des éléments d'assemblage poutres-poteaux en sandwich. Une comparaison est faite avec les méthodes de dimensionnement du béton armé et un guide est fourni en vue de permettre aux ingénieurs de dimensionner des éléments typiques.

ZUSAMMENFASSUNG

Doppelhaut-Verbund-Elemente werden duch Verbindung zweier Stahlplatten mit einer Betonfüllung hergestellt. Die Schichtung wird durch geschweisste Beschlagnägel als Scherverbindungen auf den Innenseiten der Stahlplatten zusammengehalten. Hier werden Modellversuche an Trägern und Stützen aus Doppelhautelementen beschrieben. Vergleiche mit Entwürfen aus Stahlbeton und Ratschläge für die Bemessung werden gegeben.

1 INTRODUCTION

Double skin or dual skin construction is the term used to describe steel-concrete-steel sandwich elements where the steel skins are connected to the concrete core with welded stud shear connectors. Large structural elements may be fabricated in this way using the steel skins as both permanent formwork and reinforcement. Fig. 1 shows a typical section through a double skin element along with the possible failure modes that may occur. The system was developed primarily for use in submerged tube tunnel construction [1] but it has potential applications in nuclear containment and blast resistant structures.

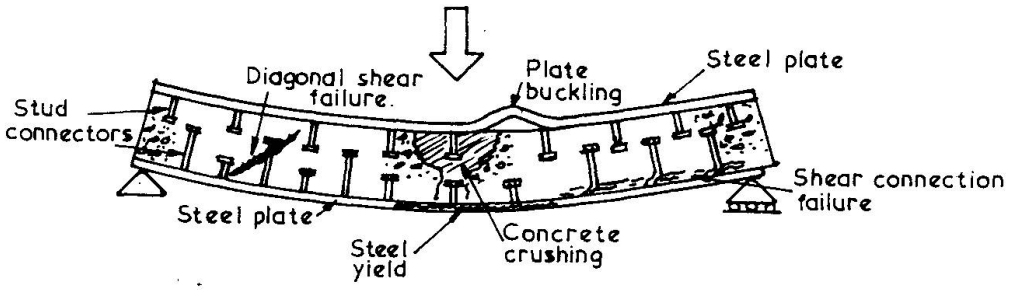

Fig. 1 Double skin composite construction

The failure modes are more various and more complex than those normally associated with reinforced concrete structures.

1) The steel skins may yield in tension and in compression although it is more likely that buckling will dictate the latter.

2) The concrete may crush in the compression zone and diagonal tension cracks may cause failure in areas of high shear.

3) The connection between the concrete and steel may fail and the flexibility of the studs is likely to precipitate alternative modes of failure.

These failure modes have been investigated by the authors in a programme of experimental and theoretical studies. The experimental programme invoved 53 scale model tests on beam, column and beam-column specimens. The theoretical studies have included classical modelling along with design oriented approaches. The results of this work have been correlated into a series of guidance notes for designers.

2 BEAM BEHAVIOUR

Eighteen model scale double skin beams have been tested by the authors. A typical test specimen in shown in fig. 2 along with the loading pattern applied in all cases. The parameters investigated in the tests were steel sheet thicknesses, concrete

strengths, connector spacing and connector lengths. The interaction of these parameters is complex and has been presented elsewhere [2]. The major criteria for design appear to be the size, number, position and length of the shear connectors.

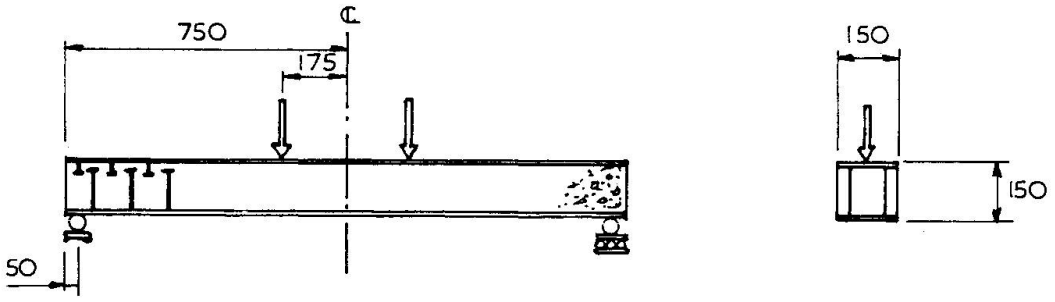

Fig. 2 Test set up

The connectors fulfil several roles. Firstly they transmit shear stresses between steel and concrete. Secondly they act to prevent diagonal tension in the areas of high shear in much the same way as links in reinforced concrete beams. Finally they act as stiffeners to the compression skin of steel and prevent buckling.

Unfortunately they also have a slight detrimental effect on the concrete in the tension zone as they act as crack inducers. The connector strength and stiffness is adversely affected when it is placed in cracked concrete.

The ultimate strength of the section in bending can be reliably predicted using a stress block approach similar to that used in reinforced concrete design [3]. It is also possible to predict the ultimate strength of sections that have fewer connectors than are required to transmit the potential force that can be generated in the steel. This partial connection design is similar to that used in composite beam design [4].

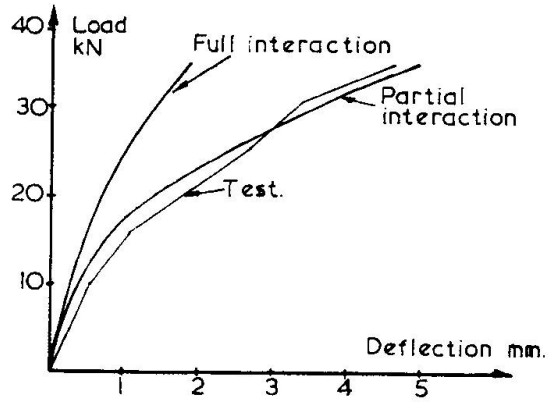

Fig. 3 Load deflection

The successful analytical modelling of the stiffness of the system is dependent upon the correct prediction of the concrete and connection behaviour. Fig. 3 shows two attempts to model the behaviour of one of the beam tests.

Initially a simple fully composite beam analysis was carried out by assuming that the full connection existed between each layer in the system. This approach can be seen to considerably overestimate the stiffness of a beam that had only partial

connection and a method was therefore developed to include connector flexibility. Governing differential equations were derived using the partial interaction theory of Newmark [4]. This approach included a piecewise linearisation technique to model the non-linear connection between the various layers. The results show close agreement with the experimental work but the method is restricted to simple boundary condition problems. It should be noted, however, that the stiffness and strength of a double skin element that has been provided with sufficient well placed and adequately long connectors will be very close to that of the fully composite section.

Consequently for design purposes the engineer may analyse the section as a fully composite element and assume that the stiffness will be that derived from a cracked section analysis. This procedure will be valid as long as the following conditions are met.

a) The spacing of connectors on the steel skin in compression must be close enough to ensure buckling does not take place. This may be achieved if the centres of the studs to plate thickness ratio does not exceed 33.

b) The capacity of the shear connectors joining the steel skin in compression to the concrete should be taken as 80% of their characteristic value. This is in accord with British codes dealing with conventional composite beams [4].

c) The capacity of the shear connectors joining the steel skin in tension to the concrete should be taken as 50% of their characteristic value. This is due to the loss of strength found in connectors sited in cracked tension concrete.

d) Sufficient long studs should be provided to act as links to prevent shear failure. These may be designed using the same rules quoted in concrete codes of practice [3] although the head of the stud should normally be situated in the compression area of concrete.

3. COLUMN BEHAVIOUR

Twenty three columns of similar proportions to the beam specimens were tested to investigate the behaviour of double skin elements under axial load. Ten of the specimens were tested under a concentric load and the remaining thirteen under eccentric loads. Again the major parameters under investigation were; steel area, concrete strength and connector spacing and length. The results of this work have been presented in a report [6] and are not reproduced here. The steel skins are generally in compression in axially loaded columns and this dominates the behaviour.

The steel skins are more prone to lateral instability than the reinforcement in a conventional reinforced concrete column. The connector spacing to steel thickness ratio is therefore

important. The concrete core of the double skin element needs to be confined by the steel skins in a similar way to concrete filled rolled hollow section columns. Consequently the stud pull out resistance is also critical.

However with an adequately designed section the full squash load can be achieved. It is, therefore, recommended that double skin columns can be designed using conventional reinforced concrete methods of section analysis. Once again certain restrictions are necessary.

a) The stud spacing to steel plate thickness ratio should not exceed 33 if buckling of the plate is to be avoided.

b) The length of the studs must be greater than ten times their diameter in order to avoid pull out failure.

c) For concentrically loaded columns the strength of the shear connectors should be taken as 80% of their characteristic value. This reduction is the same as that used for the connectors in the compression area of the beam elements.

d) For eccentrically loaded columns the strength of the shear connectors should be taken as 60% of their characteristic value. This reduction takes account of the possibility that some tensile strain is possible on one face of the column.

4. BEAM COLUMNS

Concentric and eccentrically loaded columns are subject to mainly compression. In order to obtain the full spectrum of behaviour between pure compression and pure bending it is necessary to test beam columns. 12 specimens of similar size and proportions to the beam and column specimens were tested with a combination of axial and lateral loads. Again steel plate thickness, concrete grade and stud spacing was varied. The detailed results of these tests are presented in a report [7].

From these tests it has been established that a ductile flexural failure may be achieved if the conditions stated above for beams and columns are met. However for beam columns where bending failure is likely then the shear connectors should be assumed to have only half of their characteristic strength in the tensile area of the section.

5. CONCLUSIONS

This paper has described an experimental programme that has invstigated the behaviour of double skin composite elements. It has been found possible to predict their strength using conventional reinforced concrete design methods as long as the shear connectors have been designed to resist shear and pull-out and are spaced closely enough to prevent steel plate buckling.

The stiffness of double skin beam elements can be analysed using partial interaction methods, although if full or nearly full connection is provided then the stiffness will be close to that determined using a conventional cracked section analysis.

6 ACKNOWLEDGEMENTS

This work has been carried out under a contract with the Science and Engineering Research Council in Britain. The authors would like to thank the sponsors for their support.

7 REFERENCES

1. NARAYANAN R., WRIGHT HD., EVANS HR., & FRANCIS RW., Double skin Composite Construction for Submerged Tube Tunnels. Steel Construction Today 1(1987)185-189.

2. ODUYEMI T O W., & WRIGHT H D., The Behaviour of Double Skin Composite Beams. Report DS1, University of Wales College of Cardiff, 1988.

3. B.S.8110: Structural use of Concrete, Part 1: Code of Practice for Design and Construction, British Standards Institution, London 1985.

4. NEWMARK, N M., SIESS, C P., & VIEST, I M., Tests and Analysis of Composite beams with incomplete Interaction, Proc. Society for Experimental Stress Analysis, 9(1), 1951, pp75-95.

5. B.S.5950: Structural use of Steelwork in Building, Part 3.1: Code of Practice for the Design of Composite Beams, British Standards Institution, London 1988 (draft for public comment)

6. ODUYEMI T O W., & WRIGHT H D., The Behaviour of Double Skin Composite Columns, Report DS2, University of Wales College of Cardiff 1989.

7. ODUYEMI T O W., & WRIGHT H D., The Behaviour of Double Skin Composite Beam-columns, Report DS3, University of Wales College of Cardiff 1990.

Continuous Composite Decks

Planchers mixtes continus

Durchlaufende Verbundplatten

Howard WRIGHT
Lecturer
Univ. of Wales
Cardiff, Wales, UK

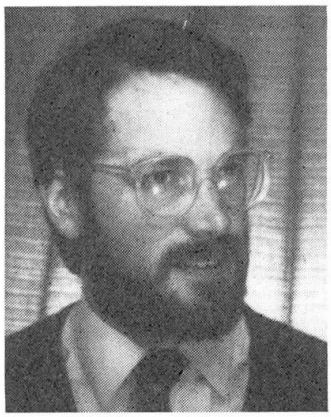

Howard Wright, born 1952 graduated from Sheffield University and has spent 9 years in practice before joining the staff at Cardiff. He has published extensively on composite construction.

Robert FRANCIS
Struct. Engineer
Sir A. Gibb & Partners
Cardiff, Wales, UK

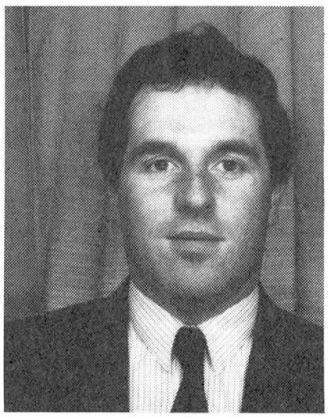

Robert Francis graduated from Cardiff in 1985 and has spent three years working for a Ph.D. He is now employed as an Engineer in an international practice.

Saad RAKIB
Res. Student,
Univ. of Wales
Cardiff, Wales, UK

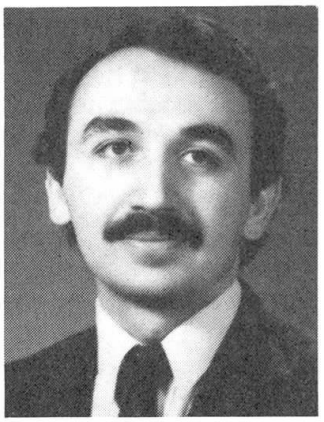

Saad Rakib graduated in 1986 and completed an M.Sc. in 1988. He is currently working for a Ph.D.

SUMMARY

Composite floor decks comprising composite slabs acting with steel sections to provide composite beams are a common form of construction. This paper investigates the variation in behaviour brought about by changes in the support condition and continuity between beams. Comparisons are made between simply supported beam tests carried out using roller and web cleat supports and between continuous beam tests with minimal and optimal slab reinforcement.

RÉSUMÉ

Les planchers mixtes, constituées d'une couche de béton interagissant avec des sections métalliques afin d'obtenir des poutres mixtes, sont couramment utilisés en construction. Le présent article étudie l'effet des conditions d'appui et de continuité sur le comportement de la dite structure. On y fait des comparaisons entre des poutres d'essai sur appuis simples avec supports à rouleau et à méplat, ainsi qu'entre des poutres d'essai continues avec armatures minimale et optimale de la dalle.

ZUSAMMENFASSUNG

Aus Plattenelementen und Stahlträgern zusammengesetzte Verbundböden sind eine verbreitete Konstruktionsart. Hier werden Streuungen im Verhalten solcher Teile unter wechselnden Stützenlagen und Durchlaufwirkung untersucht. Einfeldplatten auf Rollenlagern werden mit Durchlaufplatten und Minimal- und Optimalbewehrung verglichen.

1. INTRODUCTION

Composite decks are a common form of flooring system in America and Europe [1]. They are formed by using profiled steel sheeting as permanent formwork and tension reinforcement to the concrete slab. Welded shear connectors may be used to connect the slab to the supporting steel sections to form a composite beam.

In Britain these beams are often designed and detailed as simply supported spans as the steel connection is then uncomplicated and inexpensive. The profiled steel sheeting is normally laid continuously over several spans along with a light mesh which serves as shrinkage and fire reinforcement. It is common for whole floors to be cast in a single uninterrupted operation.

Although the design is for simple connections there exists some scope for the beam to transfer moment to adjacent spans and act as a continuous element. The slab reinforcement will carry some tension and the corresponding compression may then be transferred through the lower part of the connection.

The authors have carried out a series of full scale tests to study the effect of partial shear connection on stiffness and strength [2]. During the tests they have been able to observe the effect of end connection on beam behaviour. Six beams have been tested, four single spans and two single spans with adjacent cantilevers. Fig. 1 shows a typical test specimen and loading arrangement. Table 1 gives the main test parameters.

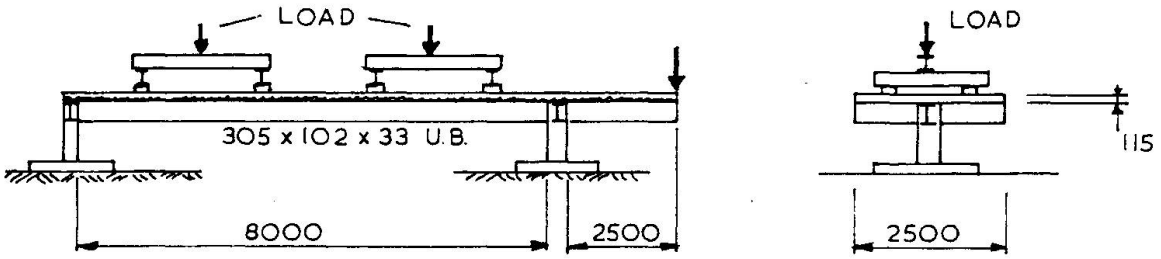

Fig. 1 Test arrangement

Beam	Span type	nominal% connection	Concrete strength N/mm^2	Steel Yield N/mm^2	Reinforcement over support %
1	S/S	50%	42	297	-
2	S/S	30%	44	325	-
3	S/S	40%	40	307	-
4	S/S	20%	40	317	-
5	C	50%	33	319	0.1%
6	C	50%	40	309	1.0%

Table 1 Test parameters

2. SINGLE SPAN BEAM TESTS

The construction of unpropped composite beams gives rise to deformations in the steel section due to the weight of wet concrete. All of the beams tested were cast unpropped with end cleats securely bolted to the stub columns. The web cleats were then removed for initial static tests on roller supports. Each bolt in the connection had to be "hammered out" and there was a definite horizontal movement recorded as the steel section relaxed and rotated at each end. Clearly the web cleats had offered some form of restraint.

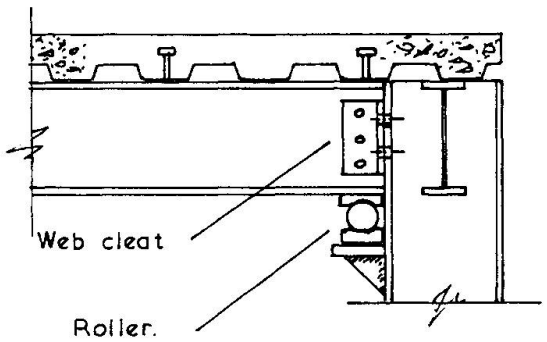

Fig. 2. Support details

The beams were loaded to working load with the ends resting on the roller supports shown in fig. 2. They were then off-loaded, the web cleats replaced and then reloaded to failure. The deflections at mid-span were recorded in each test and this allowed comparison between the stiffness of the roller supported and web cleated end conditions. In addition comparisons were made with stiffnesses predicted using simple beam theory with the assumption that 100% interaction occurred.

The comparisons are shown in the interaction diagram, fig. 3 which is a plot of test stiffness over theoretical stiffness against degree of interaction. This figure records approximately 20% difference between the roller supported and web cleated condition. It is apparent that the assumption that the web cleats give rise to an idealised pin support is conservative. It can also be seen that the analysis is less than conservative, especially for the beams with low interaction levels.

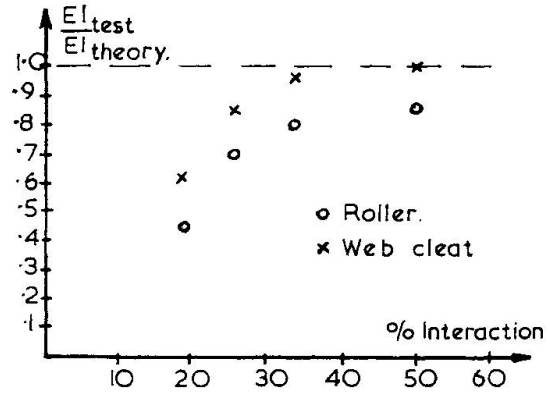

Fig.3. Effective stiffness for varying interaction

The beams were designed for partial interaction levels below 50% and consequently as the beams were loaded to failure the slabs moved in relation to the steel section. This movement or slip is shown in fig. 4 and it can be seen that the maximum end slip generated is in the order of 1.0mm. This slip may not occur if the slab was continuous between spans as each adjacent span would give rise to opposing movement in the slab.

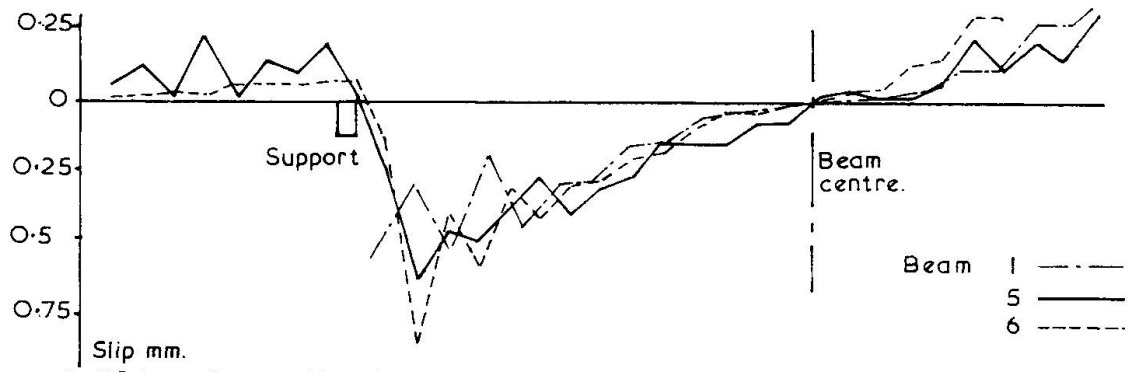

Fig. 4 Slip along the beams

3. CONTINUOUS BEAM TESTS

The simple span tests had shown that web cleat connections offer some moment restraint between the beam and column. The continuous span tests were devised to investigate the increase in this restraint once the slab continued over the support. The first of the two beams tested (beam 5) used web cleat connections and light mesh reinforcement as before so simulating a beam detailed for idealised pin connections. The second beam (beam 6) used a full end plate and substantial slab reinforcement over the connection area. This enabled a comparison of the moment transfer generated in a beam designed and detailed as simply supported and a beam designed to provide maximum continuity but using the same steel section and slab geometry.

Initially each beam was loaded with a point load on the cantilever alone. This was to investigate the transfer of moment and rotation between loaded and unloaded spans. The concrete slab over the support cracked early during the loading of the beam with simple end connections. Despite this cracking it was possible to achieve over 40kNm. support moment in a beam that was designed as simply supported. During this test it was noted that almost no moment transfer or deformation occurred between spans and it was assumed that the moment generated was resisted by the very stiff column support. Far fewer and smaller cracks were noted in the test on the beam full slab reinforcement. This connection carried a support moment of 185kNm which was almost equal to the value expected from the design. Fig. 5 shows a comparison of the moment rotation characteristics for both beams.

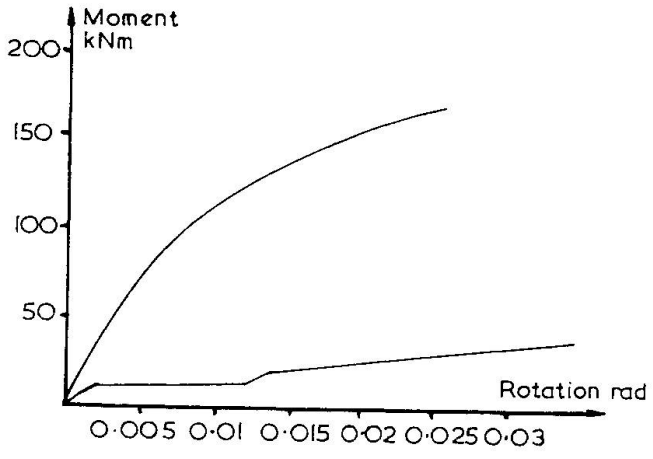

Fig. 5 Moment rotation

Each beam was then loaded on the main span with an eight point load system as used in the single span tests and with a point load at the end of the cantilever. The loads were applied to ensure that the rotation of the beam and the cantilever remained the same over the support throughout the test. This simulated an internal support for beams loaded uniformly on each span and provided further information on the moment capacity and moment rotation characteristics for this joint. In addition it was possible to investigate the stiffness of the beams and the longitudinal slip between slab and steel section.

Table 2 gives a resume of the loads achieved in each of the tests and it can be seen that the effects of continuity on the load carrying capacity of the beams is marginal. For simple connections the continuity of the concrete makes little difference to the maximum load achieved. The provision of full end connection and substantial reinforcement achieved an increased load capacity of 23%.

Beam	Maximum Test Load kN	Design Load kN
1	196	184
2	158	158
3	174	169
4	128	134
5	195	186
6	240	212

Table 2 Test Results

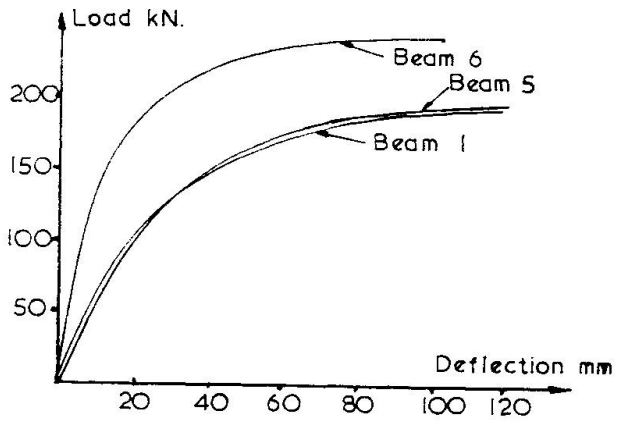

Fig. 6 Load deflection curves

Fig. 6 shows the relationship between the mid-span deflection, recorded for the main span, and the load applied for tests 1, 5 and 6. It can be seen that there is no difference in behaviour between the two tests that have simple end connections. This may show that the continuity of the concrete slab has little effect on the beam stiffness. The test carried out with a designed continuous connection was considerably more stiff than the other beams.

It is interesting to note the distribution of slip between the slab and steel section and to make comparisons with the slip distribution found in the simply supported beam. Fig. 4 shows the slip distribution for beams 1, 5 and 6. For both the continuous beams tested there is no slip present at the support point. However the slip recorded only 300mm away is similar for each of the three beams. This is possibly explained by the

slip strain close to the support matching and cancelling the strain generated due to the hogging moment in the concrete.

4. CONCLUSIONS

This paper has described results from a series of composite beam tests. The comparisons made between simple span beams, continuous beams with simple connections and continuous beams have given the following conclusions:-

a) Simple span beams with web cleat connections are approximately 20% stiffer than simple span beams with roller supports.

b) The ultimate loads obtained in the tests for simple beams and continuous beams with simple connections did not vary by a large amount.

c) The stiffness of beams with simple end connections are similar for both simple spans and for the condition where the concrete slab is continuous.

d) The stiffness and strength of continuous beams that have been designed to transfer moment is substantially greater than for beams with simple end connections.

5. ACKNOWLEGEMENTS

This work has been carried out under the sponsorship of the Steel Construction Institute and the authors would like to thank their sponsors for the help and encouragement provided during the programme.

6. REFERENCES

1. WRIGHT H.D., EVANS H.R., & HARDING P.W., The use of Profiled Steel Sheeting in Floor Construction. Journal of Constructional Steel Research. Vol 7 No.4 1987 279-295.

2. WRIGHT H.D. & FRANCIS R.W., Tests on Composite beams with Low Levels of Shear Connection. Paper to be Submitted for publication 1990.

3. COMMISSION OF THE EUROPEAN COMMUNITIES., Eurocode 4. Common Unified Rules for Composite Steel and Concrete Structures. Report EUR 9886 EN, 1985.

Composite Beam Finite Element Method Considering Shear-Lag Effect

Méthode des éléments finis de la poutre mixte considérant l'effet de traînage de cisaillement

Finite Elemente für Verbundträger unter Berücksichtigung der Schubverschiebung

Haifan XIANG
Professor
Tongji Univ.
Shanghai, China

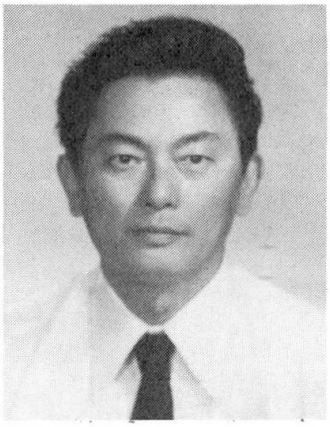

Haifan Xiang, born in 1935, graduated from Tongji University in 1955, and completed his postgraduate study in 1958, he is now the Director of Bridge Engineering Department.

Guoping LI
Lecturer
Shanghai College of Eng.
Shanghai, China

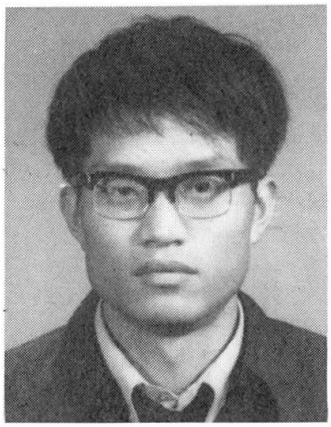

Guoping Li, born in 1958, graduated from Tongji University in 1983, and received Master of Engineering in 1989.

SUMMARY

In the design of cable-stayed bridges with composite deck, the shear-lag effect in a reinforced concrete slab should be carefully considered. In order to analyze correctly the shear-lag effect in the composite beam, a special finite element of T-type girder is developed on the basis of Reissner's theory. The stress distribution in the deck slab of Huangpu River cable-stayed bridge in Shanghai, China, are calculated, and the results are verified by a conventional finite element analysis program, as well as compared with that from British Standards Code.

RÉSUMÉ

Dans le projet de pont à haubans avec tablier mixte, l'effet de traînage de cisaillement dans la dalle en béton armé doit être attentivement prise en considération. En vue d'analyser correctement cet effet dans la poutre mixte, un élément fini spécial a été développé sur la base de la théorie de Reissner. La distribution des contraintes a été calculée dans le tablier du pont à haubans sur la rivière Huangpu à Shanghai en Chine. Le résultat a été vérifié par le programme conventionel de la méthode des éléments finis puis comparé avec celui des normes britanniques.

ZUSAMMENFASSUNG

Im Entwurf der Schrägseilbrücken mit Verbundträgern sollte die Schubverschiebungswirkung (Shear-lag Effect) in der Stahlbetonplatte vorsichtig berücksichtigt werden. Um die Schubverschiebungswirkung richtig zu analisieren, wird in diesem Bericht ein besonderes finites Elementes für Verbundträger auf der Grundlage der Reissner-Theorie entwickelt. Die Spannungsverteilung in der Platte des Verbundträgers der Schrägseilbrücke über den Fluss Huangpu in Shanghai, China, wurde berechnet. Die Ergebnisse wurden durch ein übliches Finite-Element-Programm bestätigt und auch mit den englischen Normen verglichen.

1. INTRODUCTION

Since the Annacis Bridge in Vancouver, Canada with a record-breaking main span length of 465 m was completed in 1984, the composite design with a very simple, economical and easy-to-erect girder/deck framing system shows an outstanding advantage in some competition of long-span cable-stayed bridge. In the design of Huangpu River cable-stayed bridge in Shanghai with the main span of 423 m, the composite alternative beat an all-concrete design due to its lower weight, fewer cables, less massive towers, fewer foundation piles and shorter construction period required.

About half a century ago von Karman first studied the shear-lag effect in T-type girder, and established a basic theory of calculating the effective width of slab for design purpose. In after years many authors have made contributions towards this problem in simple-supported or continuous beam bridges, in which the Reissner's theory for analyzing the shear-lag in box girder by the principle of minimum potential energy is more effective and noticeable. But very few attention has been paid to the composite deck of cable-stayed bridges.

In order to analyze correctly the shear-lag effect in the composite beam, a special finite element of composite T-girder is developed in this paper on the basis of Reissner's theory. As an in-plane composite beam element, a new displacement parameter u_r reflecting the shear-lag effect of the flange slab, namely the relative longitudinal displacement between the root and end of the cantilever flange, is added in each end of the element. The stiffness matrix and loading matrix of this special beam element can be derived by the variational principle.

2. FORMULATION AND SOLUTION OF PROBLEM

The differential equations of displacement function reflecting shear-lag effect can be established by the variational principle for elastic structures. Let us consider a section of T-type composite beam as shown in Fig. 1.

2.1 Assumption for displacement functions

The displacement functions varying longitudinally in the composite beam are assumed as:

$w(x)$, vertical displacement of composite beam;
$u_{st}(x)$, axial displacement of steel girder;
$u_r(x)$, relative longitudinal displacement between the root and end of cantilever flange reflecting the shear-lag effect.

The displacement function varying transverly in the slab can be described as:

$$\tilde{u}_r(y)=1-(y/b)^i \quad (i=2,3,4) \qquad (1)$$

in which, b is the width of slab on each side, and the coordinate system is shown in Fig. 1.

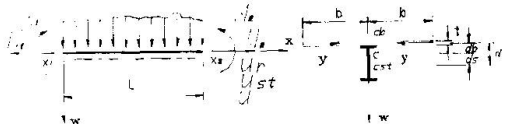

Fig. 1 Analysis model and Coordinate System

2.2 assumption for stress and strain

The cross sections of steel girder remain plane. As a result, the longitudinal displacement of slab at various points can be written as:

$$u_b(x,y) = w'(x)d + u_{st}(x) + u_r(x)\,\tilde{u}_r(y) \qquad (2)$$

in which, d is a vertical distance between the middle surface of slab and the cross section centroid of steel girder.

The curvature of R.C. slab and of steel girder are identical in vertical bending.

The stress and strain in slab are regarded as a plane stress problem.

2.3 Differential equations of displacement functions

According to the assumptions mentioned above, the total potential energy of composite beam can be determined, and it may be written in the form as:

$$\pi = \pi(w'', u'_{st}, u'_r, u_r, x) \tag{3}$$

By means of the calculus of variation, we obtain

$$\delta\pi = \int_{x_1}^{x_2} \{ \frac{\partial\pi}{\partial w''}\delta w'' + \frac{\partial\pi}{\partial u'_{st}}\delta u'_{st} + [\frac{\partial\pi}{\partial u_r} - \frac{d}{dx}(\frac{\partial\pi}{\partial u'_r})]\delta u_r \} dx + \frac{\partial\pi}{\partial u'_r}\delta u_r \Big|_{x_1}^{x_2} \tag{4}$$

The differential equations and boundary condition can then be established by making $\delta\pi=0$, and finally we obtain:

$$w'' + \frac{d_b}{I_c} F_b u'_r = -\frac{M_p}{E_{st} I_c} \tag{5}$$

$$u' + \frac{F_b}{A_c} u'_r = \frac{N_p}{E_{st} A_c} \tag{6}$$

$$u''_r - \tilde{k}^2 u_r = \frac{\tilde{k} M'_p d_b}{E_{st} I_c} - \frac{\tilde{k} N'_p}{E_{st} A_c} \tag{7}$$

$$[E_{st} \bar{F} u'_r + (\frac{N_p}{A_c} - \frac{M_p d_b}{I_c}) F_b] \delta u_r \Big|_{x_1}^{x_2} = 0 \tag{8}$$

In which, M_p, N_p are the bending moment and axial force in composite beam;
$u=u_{st}+d_s w'$, is the axial displacement of composite beam;
A_c, I_c are the cross section area and moment of inertia of composite beam; E_{st} is the modulus of steel girder;
d_b is a vertical distance from the middle surface of slab to the cross section centroid of composite beam;
where, $F_b = t/n \int_b \tilde{u}_r dy$; $\tilde{k}=F_b/\bar{F}$; $\tilde{k}^2=\hat{F}'/(2+2\mu)$; $\bar{F}=\hat{F}-F_b^2(1/A_c+d_b^2/I_c)$, d_s is a distance from the cross section centroid of steel girder to that of the composite beam; μ is Poisson's ratio;
$\hat{F}=t/n \int_b (\tilde{u}_r)^2 dy$; $\hat{F}'=t/n \int_b (u'_r)^2 dy$; $n=E_{st}/E_b$, E_b—the modulus of slab.

3. COMPOSITE BEAM FINITE ELEMENT METHOD CONSIDERING SHEAR-LAG EFFECT

The composite beam finite element can be established by using the differential equations of displacement functions and the boundary condition derived above. It can be seen from equations (5) to (8) that three displacement functions of w, u, and u_r are fundamental for determining the displacements and internal forces of composite beam. If we take an extra parameter u_r in addition to the conven-

tional three displacement of in-plane beam element u, v, θ, as the basic displacement parameters of a special composite beam element, namely(see Fig. 2)

$$\{\delta\}^e = [\ \theta_i\ ,\ u_i\ ,\ v_i\ ,\ u_{ri}\ ,\ \theta_j\ ,\ u_j\ ,\ v_j\ ,\ u_{rj}\ ]^T \tag{9}$$

which will determine solely the stress state of composite beam element.

The stiffness matrix of composite beam element $[k]^e_{8\times8}$ can be obtain by using the solutions of Eqs. (5) to (7) under boundary conditions related to determining elements of stiffness matrix. It should be pointed out that the elements k_{ij} (i=4,8;j=1,2,...8) in the matrix are related to the additional displacement u_{ri} and u_{rj} .

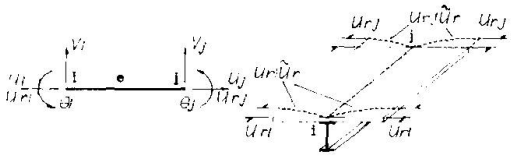

Fig. 2 Displacement Parameters

The elements of loading matrix $\{P\}^e$ can be calculated by using Eqs. (5) to (7), making influence lines of reactions M, R and R at beam ends, and loading on lines, which are carried out by computer program.

Finally, the equilibrium equation of composite beam element can be written as:

$$[k]^e\{\delta\}^e - \{P\}^e = 0\ , \tag{10}$$

in which,

$$\{P\}^e = [\ M_i\ ,\ R_{ix}\ ,\ R_{iy}\ ,\ N_{ui}\ ,\ M_j\ ,\ R_{jx}\ ,\ R_{jy}\ ,\ N_{uj}\ ]^T \tag{11}$$

N_{ui} , N_{uj} are a generalized elastic resistance corresponding to the displacement $\tilde{u}_r$ and may be defined as work done by normal stress in slab at ends of element caused by M, R_x and R_y on the displacement $\tilde{u}_r$.

It can be proved that the equilibrium equation relative to N_{ui} or N_{uj} in Eq.(10) is the another form of Eq.(8). So that when an element is in equilibrium, it must satisfy the boundary condition from the variation of the total potential energy.

As a verification of the composite beam finite element method developed in this paper, a simple-supported composite beam subjected to a concentrated load or a fully uniform load is taken, and the results of effective width ratio in different cases are obtained. Compared with the BS 5400 code, under the uniform loading, the results are in good agreement with the BS code; under the concentrated loading, the results in range of width-span ratio b/L < 0.5 are close to that in the BS code. The best choice of i in equation (1) is 4.

4.APPLICATION TO HUANGPU RIVER BRIDGE

The Huangpu River Bridge is a T-type composite beam cable - stayed bridge with a main span of 423 m (Fig. 3) in construction.

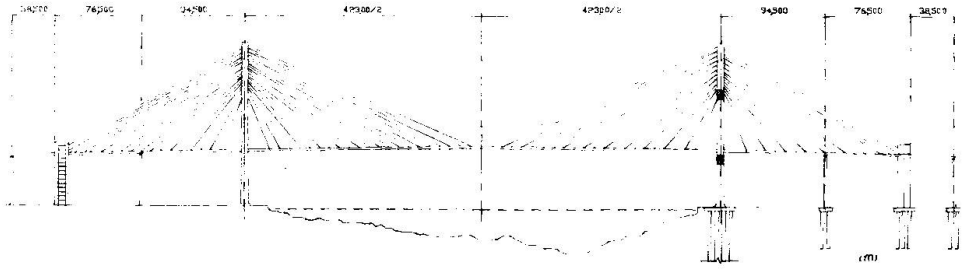

Fig. 3 Huangpu River Bridge in Shanghai

4.1 Effective width ratio of slab and internal forces in the composite beam under dead load

The conventional FEM is used for calculating three cases:
Case (a), (b) and (c) express that the effective width ratio (E.W.R.) of slab ϕ=1.0, 0.05-0.25 and 0.1-0.5 are taken respectively in determining the bending stiffness of composite beam, and ϕ =1.0 in axial stiffness for three cases. In which case(b) withϕ=0.05-0.25 is obtained according to the BS code when the composite beam is regarded as a continuous beam supported rigidly on the cables.

By using the special FEM considering shear-lag effect, the internal forces, the variation of effective width ratio along the span,and the normal stress distribution in slab in the middle of span are also given, which is named as case (d) as shown in Fig. 4 and Fig. 5.

It can be seen that under dead load a little difference of internal forces exists among four cases except the region near the tower. Compared with case (d), the biggest difference appears in case (a), and the least in case (c).In fact, the amount of axial force in deck is much larger than under live loads, and the bending moment is relatively small. So it may be accepted that the bending and axial stiffness are determined by ϕ =1.0, however a better result of normal stress in slab from case (b) or (c) is more close to the reality.

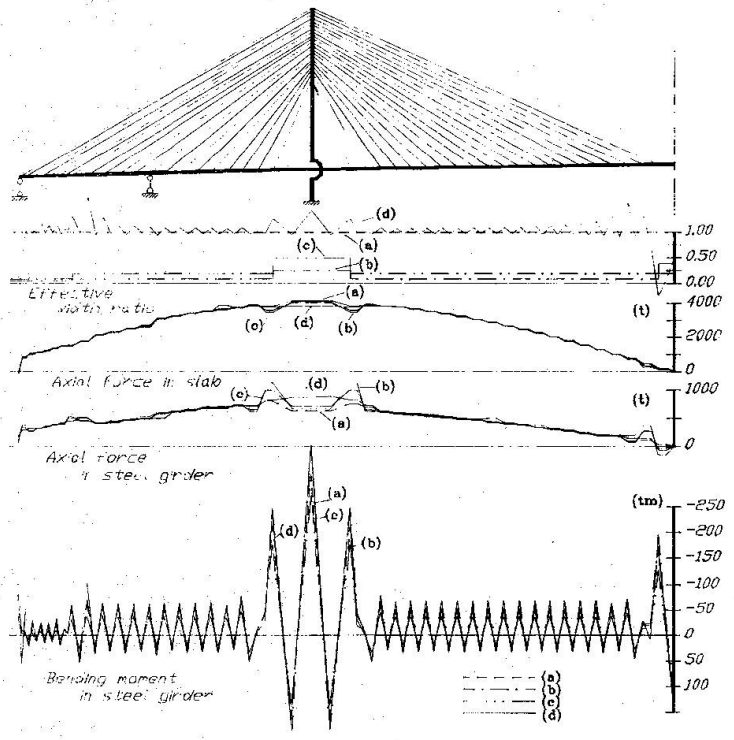

Fig. 4 E.W.R. Curves and Internal Forces

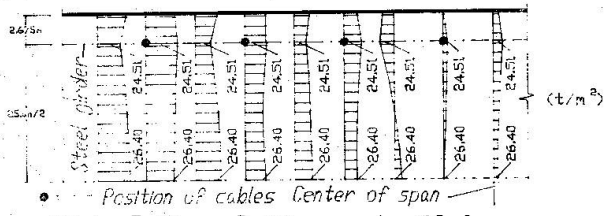

Fig. 5 Normal Stress in Slab

4.2 Effective width ratio of slab and internal forces in the composite beam under live loads

The truck loads are taken as live loads, and the sections 1,2,3 and 4 are chosen for calculating the internal forces. In Table 1 the bending moments of four sections obtained by FEM are listed with the effective width ratioϕ=0.4 to 1.0. The results obtained from special FEM considering shear-lag effect are also shown.

It can be seen in the Table that from ϕ =0.4 to 1.0, the bending moments change little and about ϕ=0.5 the results approach the values by FEM considering shear-lag effect. It should be noticed that if we take a length of an influence line (same symbol) of a section concerned as the span of an equivalent continuous beam, we may obtain an effective width

Table 1 Moments and effective width ratios

section	1	2	3	4
E.W.R.ϕ		moments (tm)		
1.0	-696.02	763.70	-246.72	668.62
0.6	-676.20	745.41	-244.03	651.83
0.5	-667.36	737.08	-242.50	642.66
0.4	-655.20	725.57	-240.60	630.05
FEM considering shear-lag effect				
moments	-671.62	739.87	-242.37	633.97
E.W.R.ϕ	0.914	0.852	0.750	0.805

ratioϕ=0.5 from the BS code.

According to the position of live loads, under which the bending moment of the section 3 or 4 arrives its most unfavourable value,the variation of effective width ratio obtained from FEM considering shear-lag effect are shown in Fig. 6.

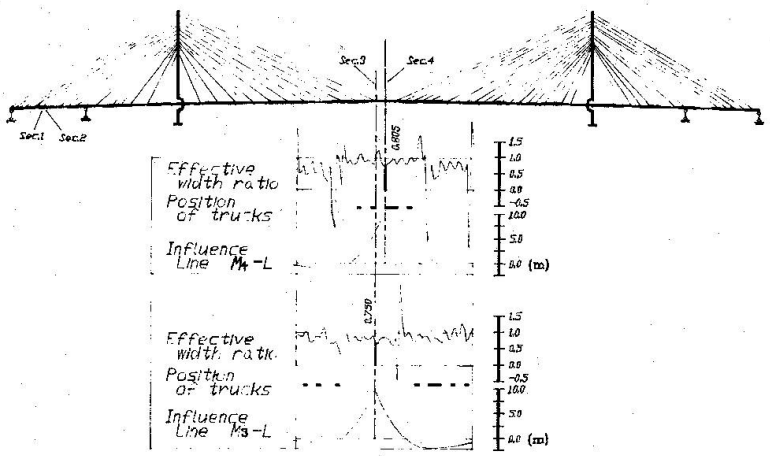

Fig. 6 E.W.R. Curves (Loading on M_3-L, M_4-L)

Because of the interaction caused by the wheel loads, vertical and horizontal componets of cables, the curves wave along the span. We are much interested in the normal stress in slab at the sections 3 and 4, where the effective width ratios show ϕ =0.805 and 0.75. So it makes clear that the normal stress distribution in slab is also uniform enough, just as shown in Fig. 7.

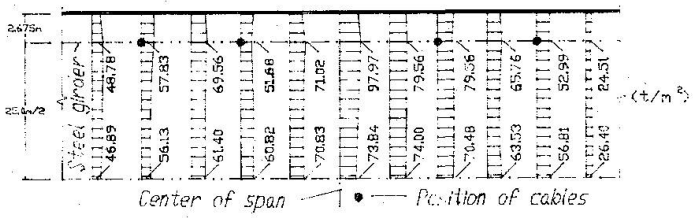

Fig. 7 Normal Stress in Slab (Loading on M_4-L)

5.CONCLUSIONS

In the composite deck of cable-stayed bridges, the effective width related to the normal stress in slab is very complicated. For dead or live loads, axial force or bending memont, the effective width should be different theoretically, and varies along the span.

A special FEM considering shear-lag in slab of a T-type composite beam is established on the basis of Reissner's theory. An additional displacement parameter reflecting the shear-lag is included in the beam element.

Under dead load, the normal stress in slab due to axial force can be calculated as distributed uniformly on the full width of slab, but the normal stress due to bending moment should be considered by using effective width corresponding to a rigidly-supported continuous beam.

In determining the internal forces under live loads, the different value of effective width is not sensitive, and the full width can be taken for making the inflnence lines,but care must be taken in determining the stress. An equiavalent continuous beam with a span equals to the length of influence line concerned can be used for calculating the effective width on the safe side.

REFERENCES

1. Shanghai Municipal Engineering Design Institute(SMEDI): Design materials of Huangpu River Bridge in Shanghai.
2. Zhang, Dr. S.D.: Theory of Bridge Design (in chinese) 1984.
3. Reissner, E.: Analysis of Shear-lag in Box Beams by the Principle of Minimum Potential Energy. Quarterly of Applied Mathematics, Vol. 4 Oct. 1946.
4. Moffatt, K.R. and Dowling P.J.: British Shear-lag Rules for Composite Girders. ASCE. No. ST7. July 1978.
5. BS 5400. Steel, Concrete and Composite Bridges. 1978-1983.

Strength of Concrete Slab at Composite Beam-to-Column Connection

Résistance de la dalle en béton armé à la jonction poutre-poteau mixte

Die Festigkeit der Stahlbetonplatte über den zusammengesetzen Balken an der Verbundträger-Stützen-Verbindung

S. IGARASHI
Professor
Osaka Univ.
Osaka, Japan

Sadayoshi Igarashi, born 1927, received his doctor's degree from Kuoto Univ. He has worked at Osaka Univ. since 1968 and has been a professor since that time. His researches have been concerned with strength and behavior of steel members and connections.

Kazuo INOUE
Assoc. Prof.
Osaka Univ.
Osaka, Japan

Kazuo Inoue, born 1946, received his doctor's degree from Osaka University in 1982. He has been involved mainly in research into the plastic strength and inelastic behavior of steel and composite structures.

S. TSUJIOKA
Lecturer
Hukui Inst. of Techn.
Hukui, Japan

Shizuo Tsujioka, born 1948, received his doctor's degree from Osaka University in 1987. His researches have been concerned with strength and elastic-plastic behaviour of connections.

Tsutomu ARAI
Struct. Engineer
Ohbayashi Corp.
Osaka, Japan

Tsutomu Arai, born 1964, received his master's degree from Osaka University in 1990.

SUMMARY

To calculate the positive bending strength of composite beams at the beam-to-column connection under earthquake load, it is necessary to evaluate the compressive force in the concrete slab. The ultimate compressive force in the slab is limited by the bearing strength at the column face and the shear strength at the column sides. Theoretical expressions are developed for both bearing and shear strength of concrete slabs, and are checked by experimental investigations.

RÉSUMÉ

Afin de calculer la résistance positive à la flexion des poutres mixtes à la jonction poutre-poteau sous charge sismique, il est nécessaire d'évaluer la force de compression dans la dalle en béton armé. La force de compression ultime s'exerçant dans la dalle est limitée par la force portante en tête du poteau et par la résistance au cisaillement des faces latérales du poteau. Les expression théoriques sont développées pour les deux types de sollicitation, puis elles sont vérifiées par des recherches expérimentales.

ZUSAMMENFASSUNG

Zur Ermittlung des Biegewiderstandes von Verbundträgern bei Rahmenknoten unter Erdbebenbeanspruchung ist die Druckkraft in der Betonplatte abzuschätzen. Diese wird beschränkt durch die Druckspannung an der Stützenfront und die Schubspannung an den Seiten der Stütze. Für beide Spannungen wurden theoretische Ansätze entwickelt und durch Versuche abgesichert.

1. INTRODUCTION

When the framed structures are subjected to earthquake loading, both positive and negative bending moment act on composite beams as shown in Fig. 1. The positive bending strength of composite beams is mainly affected by the compressive force in the slab. For the simple composite beams, compressive force in the slab is determined by the effective width of slab which depends on the beam span. However, at the beam-to-column connection, the compressive force in the slab is kept in equilibrium with the bearing stress (C_B) and shear stress (C_S) as illustrated in Fig. 2. So that the ultimate compressive force is limited by the bearing strength at the column face and the shear strength at the column sides. In the case of the square tube column, only the bearing stress is balanced with the slab compressive force.

Empirical value of bearing strength of concrete slab based on push out tests has been suggested by B. Kato et al[1]. In the present paper, theoretical expressions are developed for both bearing and shear strength of concrete slab. Theory of the concrete plasticity based on the *modified Mohr-Coulomb* criterion is used in the analysis. To examine the theoretical expressions, two series of experimental investigations were intended. One is the push out test to confirm the bearing and shear strength of the slab. In the other series, the composite beam-to-column subassemblages were tested to ensure the positive bending strength of composite beams.

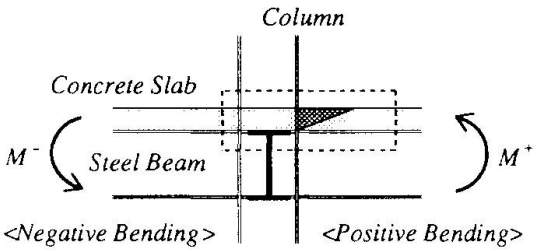

Fig. 1

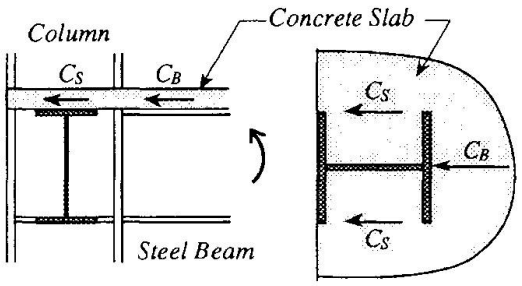

Fig. 2 Transmission of compressive force in the concrete slab

2. THEORETICAL SOLUTIONS OF BEARING AND SHEAR STRENGTH

2.1 Assumptions

To calculate the positive bending strength of composite beams at the beam-to-column connection under the earthquake load, it is necessary to evaluate the compressive force in the concrete slab. Fig. 3 shows the failure model to obtain the ultimate compressive force in the slab. Due to the spreading of the crack resulting from negative bending, no forces can be transmitted on the left side of the column in this figure. Yield lines are developed along the either side of the column, and the wedge of concrete is pushed out from the face of the flange plate of steel column. This model is assumed according to the failure modes observed in the tests. The ultimate compressive force in the slab is limited by the bearing strength at column face and the shear strength along the column sides. Theoretical expressions are developed for both bearing and shear strength of concrete slab based on the following assumptions:

1) Steel and concrete are the rigid-plastic material, and concrete obeys the *modified Mohr-Coulomb* criterion.
2) The dowel effect of the reinforcement is neglected.
3) Friction between concrete slab and the steel column is neglected.
4) The drawing strength of headed studs is neglected.

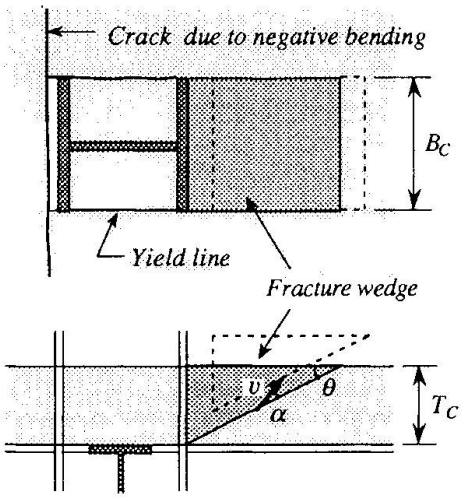

Fig. 3 Failure mode

2.2 The Ultimate Compressive Force in the Slab

The solution of the shear strength of reinforced concrete slabs with load in their plane is obtained by B. C. Jensen[2] and is explained in Ref.[3,4]. The relative displacement which is perpendicular to the yield line along the column side will be

prevented by the cross beam and the bending rigidity of slab in its plane. So that the ultimate shear stress along the column side is given by the following equation.

$$\frac{\tau_u}{F_C} = \frac{1}{2}\nu \tag{1}$$

where, F_C is cylinder strength, and ν is efficiency factor of concrete strength. The ultimate value of C_S in Fig. 2 is obtained from multiplying τ_u by the area of the column side A_S, that is

$$C_{SU} = \frac{1}{2}\nu F_C A_S \quad (\nu = \frac{2}{3}) \tag{2}$$

Next, the bearing strength at the column face is derived from the following. Fig. 4 shows the forces act on the failure wedge. Assuming that the vertical load does not act on the wedge, the maximum principal stress (σ_1) and the minimum principal stress (σ_3) take the direction shown in Fig. 4. The direction of σ_1 coincides with the longitudinal axis of the composite beam. σ_3 is perpendicular to the plane of slab and equals to 0. Clearly, the intermediate principal stress (σ_2) perpendicular to σ_1-σ_3 plane is compressive; then it has no influence on the failure. Mohr's circles corresponding to the stress field of the sliding plane are drawn in Fig. 5 together with the *modified Mohr-Coulomb* criterion. From this figure, it is evident that the sliding plane forms the angle $\theta = 45° - \phi/2$ with the slab surface. The angle of friction ϕ takes the value of 37° [3,4]. The normal stress σ and the shear stress τ lie on the point P in Fig. 5, and are given by

$$\sigma = \frac{F_C}{2}(1 - \sin\phi) \ , \ \tau = \frac{F_C}{2}\cos\phi \tag{3}$$

The ultimate shear stress on the triangular shear planes of either side of the failure wedge is given by eq.(1). For the equilibrium of the failure wedge shown in Fig. 4 including the yield axial force of reinforcement bar, the average bearing stress (F_B) can be expressed as:

$$\frac{F_B}{F_C} = 1 + \frac{\nu T_C}{2 B_C \tan\theta} + \frac{{}_r a \cdot {}_r\sigma_y}{F_C T_C B_C} \tag{4}$$

in which, B_C is the width of column, T_C is the thickness of slab, ${}_r a$ and ${}_r\sigma_y$ are the total area and the yield stress of reinforcement bar, respectively. The resultant bearing strength C_{BU} is obtained from multiplying F_B by the area of the column face, and the location of C_{BU} is determined by the equilibrium condition, as follows:

$$C_{BU} = F_B T_C B_C \ , \ d_C = \frac{F_C}{F_B}\left(\frac{T_C}{2} + \frac{\nu T_C^2}{6 B_C \tan\theta} + \frac{d_r \cdot {}_r a \cdot {}_r\sigma_y}{F_C T_C B_C}\right) \tag{5}$$

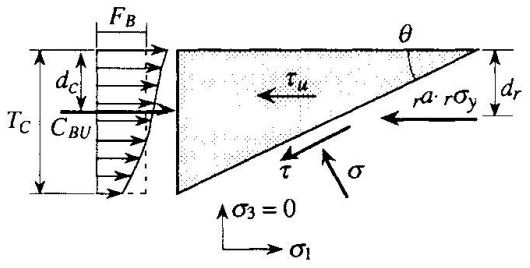

Fig. 4 Forces on failure wedge

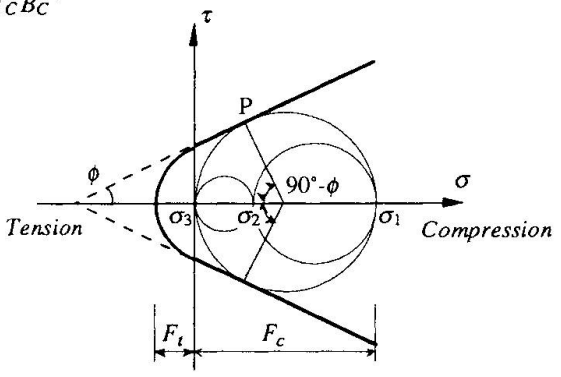

Fig. 5 Fracture criteria and Mohr's circle

3. PUSH OUT TEST OF CONCRETE SLAB

Three types of push out test specimens of concrete slab were considered : bearing tests, shear tests, and the tests combining bearing and shear. Fig. 6 (a) and (b) show the bearing and shear test specimens, respectively. For the bearing specimens (B-type), slits of the slab are made on either side of H-shaped column to avoid the effect of shear, and for the shear specimens (S-type), a slit is made on the face of the column so as not to cause the bearing force. BS-type specimens have no slits, and are subjected to bearing and shear force simultaneously. The principle variables are the thickness of slab. The list of specimens and the test results are summarized in Table 1. For each kind, the two same specimens were used. The mechanical properties of materials are also shown beside Table 1.

Specimen	T_C (mm)	P_{max} (kN)	ε_B (x10^{-6})	$P_{max}/A_C F_C$		Test / Analysis
				Test	Analysis	
B1-1	100	789	1790	1.44	1.31	1.10
B1-2		791	1700	1.45		1.10
B2-1	145	1093	2210	1.38	1.45	0.95
B2-2		1097	2380	1.39		0.96
S1-1	100	432	1770	0.79	0.58	1.36
S1-2		434	1740	0.79		1.36
S2-1	145	596	2160	0.75	0.58	1.29
S2-2		530	1830	0.67		1.16
BS1-1	100	1098	1960	2.01	1.90	1.06
BS1-2		1100	2150	2.01		1.06
BS2-1	145	1615	2160	2.04	2.03	1.00
BS2-2		1656	2750	2.09		1.03

$A_C = B_C T_C$: Bearing area

Mechanical Properties

Concrete : F_C = 21.9MPa
F_t = 2.61MPa

Reinforcement : σ_y = 356MPa
σ_B = 510Mpa

Table 1 Summary of specimens and Test Results

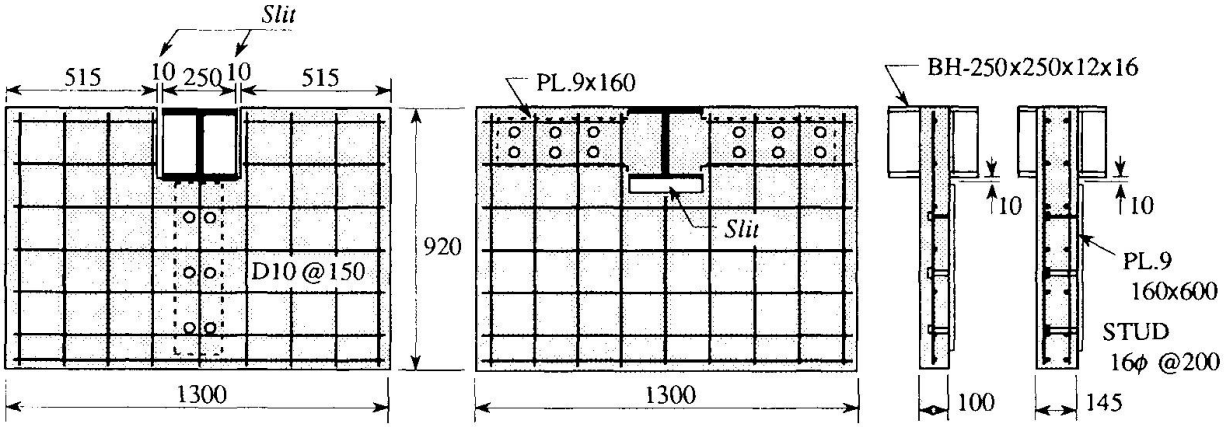

(a) B-typy Specimen (b) S-type Specimen

Fig. 6 Push out test specimens

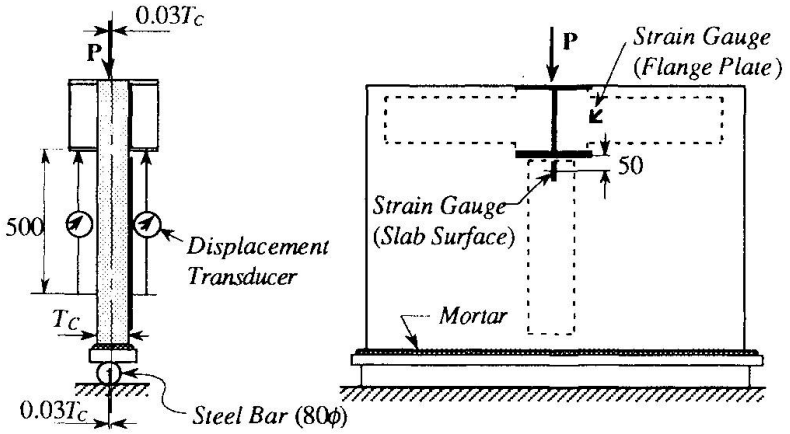

Fig. 7 Test setup

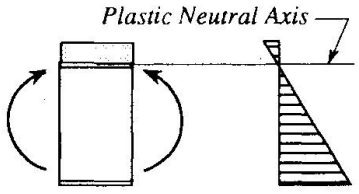

Fig.8 Strain distribution of composite beam

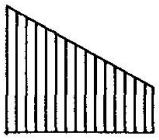

B1-1

Fig.9 Strain distribution of B1-1 specimen

An outline of the test procedure is shown in Fig. 7. To give the strain inclination along the section of slab which occurs in the actual composite beam (see Fig. 8), load is applied on all specimens with eccentricity 3% of the slab thickness as shown in Fig. 7. As an example, the distribution of strain along the section of B1-1 specimen at the maximum load is shown in Fig. 9. Hereafter, an average strain of the middle surface of the slab determined by the measured values of displacement transducers located on both sides of the slab is taken as the representative value. In Table 1, P_{max} is the maximum load, and ε_B is the average strain of the middle surface corresponding to P_{max}.

As shown in Fig. 6, thin steel plates corresponding to the upper flange of the steel beam, on which the headed studs are welded, are placed on one side of the concrete slab. The vertical steel plate of B-type specimens is placed with the column and the plate kept 10 *mm* apart so as to prevent supporting the load. Next, the horizontal steel plates in S-type specimens, which correspond to the upper flange of the cross beam, support part of load. This load is calculated from the data measured by strain gauges, and is subracted from the test results such as P_{max}.

The relations between load (P) and the average strain (ε) of concrete slab are summarized in Fig. 10 in which load P is nondimensionarized by $A_C F_C$. All these relations indicate the average of the two same specimens. Horizontal lines show the theoretical ultimate load levels obtained from eq.(2) and eq.(5). P-ε relations of BS-type are compared with the superposed P-ε relations of B-type and S-type specimens (indicated by dashed line).

Table 1 and Fig. 10 lead to the following: The strain ε_B, at which the maximum load is reached, takes the approximate value of 0.002 for all specimens. Consequently, the bearing strength and the shear strength can be simply superposed.

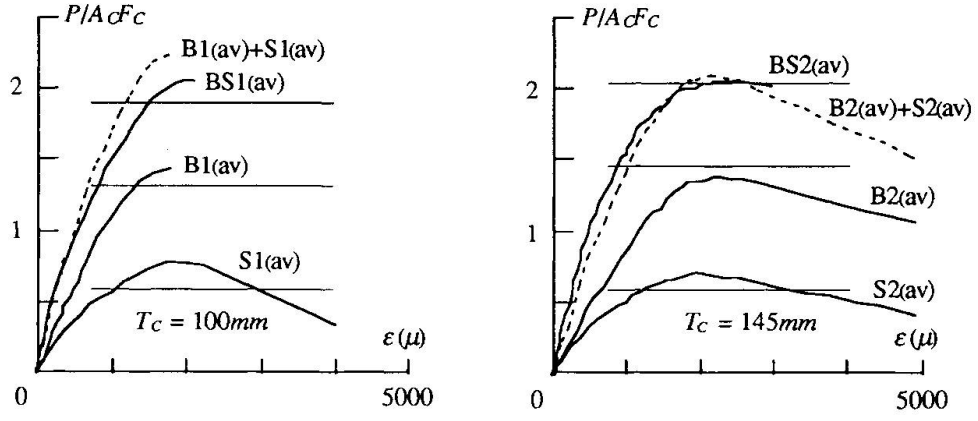

Fig.10 Load-to-average strain relations of push out test specimens

4. TEST RESULTS OF COMPOSITE BEAM-TO-COLUMN SUBASSEMBLAGE

The dimensions and member sizes of composite beam-to-column subassemblage are shown in Fig. 11. Both H-shaped and square tube section were used for the steel column. To ensure the effect of the beam span on positive bending strength, two kinds of beam length were selected. The specimen with bare steel beam is also tested to confirm the composite effect.

The earthquake type of force were repeatedly applied to all specimens. Only the initial part of the beam end moment (M)-to-beam rotation (θ) relations are shown in Fig. 11. Fig. 12 shows the failure mode of concrete slab connected to H-shaped column, which verifies the validity of the assumed failure model shown in Fig. 3.

By calculating the compressive force in the slab from eq.(2) and eq.(5), the positive bending strength of composite beams is easily obtained[5]. Horizontal lines in Fig. 11 indicate the theoretical positive bending strength. The theory proposed here proves that positive bending strength depends only on the boundary condition of the beam-to-column connection. The strength of composite beam connected to a H-shaped column is greater than that of composite beam connected to a square tube column as predicted theoretically. This is due to the additional shear resistance of H-shaped column sides. The fact that the

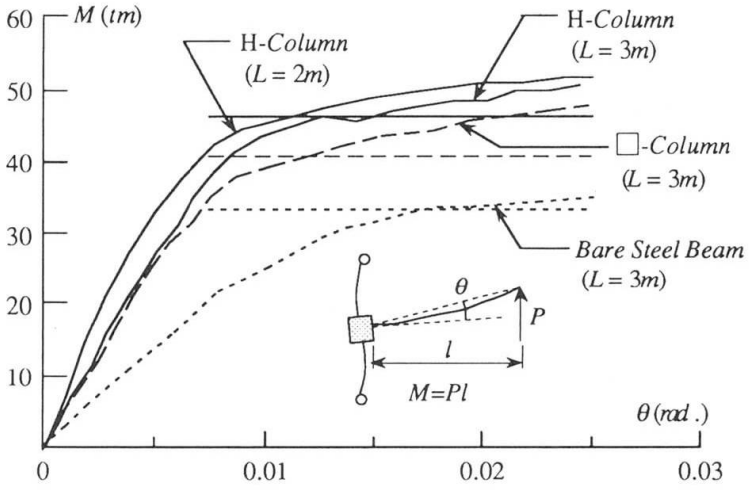

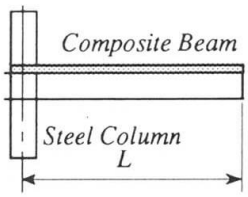

Steel Beam : H-350x150x9x12
Steel Column : H-300x300x16x16, □-300x300x12
Concrete Slab : *Thickness* = 70, *Width* = 1500
Reinforcing Bar : D10 @100, Single
Stud : 13ϕ *L*=55, *Double*

Fig. 11 Moment-rotation curves of composite beams and test specimens

difference of beam span does not affect the positive bending strength is also confirmed by comparing the test results from beams of different length.

5. CONCLUSION

The ultimate compressive force in the slab is limited by the bearing strength at column face and the shear strength at the column sides. So that the positive bending strength of composite beams is affected by the boundary condition of the beam-to-column connection under the earthquake type of loading. Theoretical expressions based on the concrete plasticity are developed for both bearing and shear strength of concrete slabs. The validity of the theory was confirmed through the push out tests of reinforced concrete slabs and the tests of composite beam-to-column subassemblages.

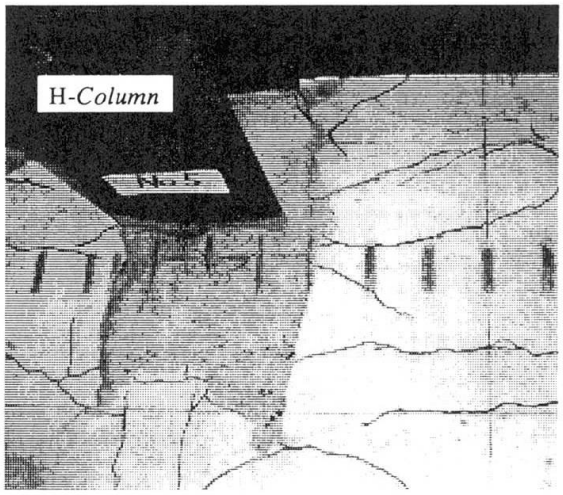

Fig. 12 Failure mode of concrete slab

ACKNOWLEDGMENTS

The authors are grateful to Lecturer Eiji Tateyama of Kinki University for his help in the tests of the composite beam-to-column subassemblage.

REFERENCES

1. KATO B. and TAGAWA Y., Strength of Composite Beams under Seismic Loading. The Second US-Japan Joint Seminar on Composite and Mixed Construction, Univ. of Washington, pp.42-49, July 1984.
2. JENSEN B. C., Lines of Discontinuity for Displacements in the Theory of Plasticity of Plane and Reinforced Concrete. Magazine of Concrete Research, Vol.27, No.92, pp.143-150, September 1975.
3. CHEN W.F., Plasticity in Reinforced Concrete. McGraw-Hill, 1982.
4. NIELSEN M.P., Limit Analysis and Concrete Plasticity. Prentice-Hall, Inc., 1984.
5. HANSELL W.C. and GALAMBOS T.V. et al, Composite Beam Criteria in LRFD. Proc. of ASCE, ST9, pp.1409-1441, September 1978.

Partially Anchored Composite Cable-Stayed Bridge

Pont haubané mixte à ancrage partiel

Teilweise verankerte Schrägkabelbrücke mit Verbundträgern

H. OTSUKA
Assoc. Prof.
Kyushu Univ.
Fukuoka, Japan

H. TANAKA
Assist. Manager
Hitachi Zosen
Osaka, Japan

J. NOGUCHI
Section Mgr
Sogo Eng. Inc.
Osaka, Japan

T. ETOH
Assist. Chief
Mitsui Co. Ltd.
Osaka, Japan

I. SAKAI
Section Mgr
Sumitomo Co. Ltd.
Osaka, Japan

Hisanori Otsuka, born 1948, got his Dr. Eng. degree at Kyushu Univ. His research interests include structural analysis of bridges.

Hiroshi Tanaka, born 1949, got his M.Sc. degree at Kyoto Univ. He has been engaged in designing and research of steel bridges.

Jiro Noguchi, born 1951, got his M.Sc. degree at Osaka City Univ. He has been engaged in design of steel bridges.

Tetsuroh Etoh, born 1949, got his B.Sc. degree at Kyushu Univ. He has been engaged in design and erection of steel bridges.

Itsurou Sakai, born 1948, got his B.Sc. degree at Kyoto Univ. He has been engaged in design & research of concrete bridges.

SUMMARY

Compared to the self-anchored type, partially anchored cable-stayed bridges are more efficient for long span bridges because the axial forces in the main girders are decreased. Mixed girders are suitable in partially anchored systems because either axial compression or axial tension acts in the main girders depending on girder location along the bridge length. This paper treats one design example of a composite cable-stayed bridge with a 900 m center span and 300 m side spans.

RÉSUMÉ

En comparaison du type à auto-ancrage, l'ancrage partiel s'avère plus efficace pour les ponts haubanés à grande portée, car les forces axiales s'exerçant dans les poutres maîtresses diminuent. Les poutres mixtes sont mieux indiquées dans le système à ancrage partiel, étant donné que les efforts axiaux de compression ou de tension dans les poutres maîtresses dépendent de leur disposition le long du pont. Cet article présente un exemple de calcul de pont haubané à ancrage partiel, ayant une travée centrale de 900 m de portée et des travées latérales de 300 m de portée.

ZUSAMMENFASSUNG

Die teilweise verankertern Schrägkabelbrücken weisen gegenüber den voll verankerten Vorteile auf, da die Normalkräfte im Hauptträger kleiner sind. Verbundträger eignen sich speziell für teilweise verankerte Systeme, da die Längszug- (oder -druck)kräfte in den Hauptträgern wirken. Dieser Beitrag beschreibt eine Schrägkabelbrücke mit Verbundträgern mit 900 m Haupt- und 300 m Nebenspannweiten.

1. INTRODUCTION

Cable-stayed bridges are classified into three types according to the degree of anchoring used. These are self, fully, and partially anchored cable-stayed bridges. Using simple structural models for cable-stayed bridges (each anchorage type) and suspension bridges, cost comparisons show that partially anchored cable-stayed bridges are most efficient for span lengths up to about 2000 m (Refs. 1-3).

Partially anchored systems may be constructed either by using hinges which can not transmit axial forces into center or side spans, or by introducing pulling forces to the continuous main girders from the ends of the side spans. Anchorages are necessary in both types of partially anchored systems.

In partially anchored systems, the main girders in the vicinity of towers are in axial compression, while axial tension acts in the main girders in the middle parts of the center span and at the end parts of the side spans. From a material standpoint, composite main girders made of a steel member and a PC member may therefore be more efficient compared to conventional steel main girders or prestressed concrete main girders. Further investigations on partially anchored composite cable-stayed bridges are necessary for determining the validity of this hypothesis (Ref. 5).

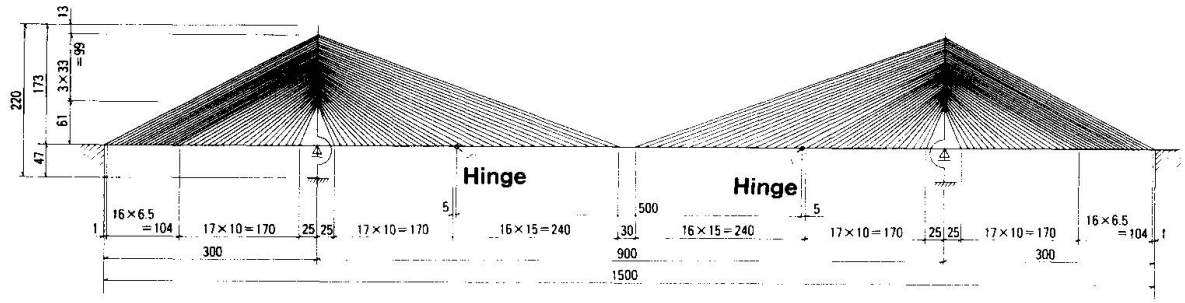

Fig.1 General View of Model Bridge

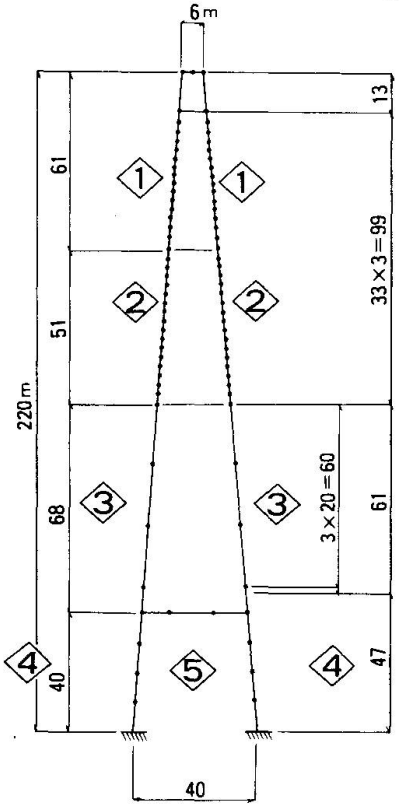

Fig.2 Tower

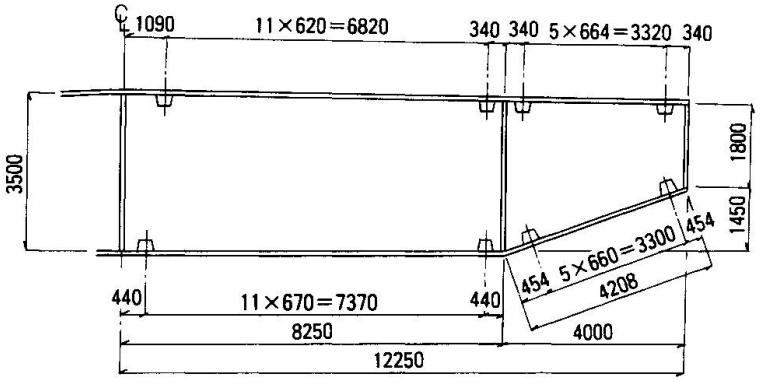

(a) Metal Girder

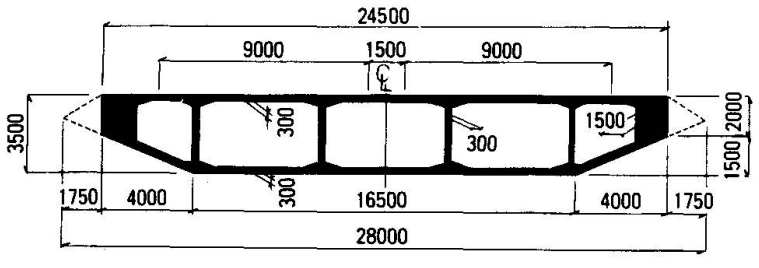

(b) PC Girder

Fig.3 Cross Sections

This paper shows one design example of a composite cable-stayed bridge with a 900 m center span and 300 m side spans. These numerical results are compared to those of a self anchored cable-stayed bridge. The two types of partially anchored cable-stayed bridges considered here (i.e. hinge type and continuous girder type) are compared from the viewpoint of constructing method.

2. STRUCTURAL MODEL

Figs. 1, 2, and 3 show a general view of the hinge type bridge, towers, and cross sections, respectively, of the composite cable-stayed bridge treated in this paper. Typical cross-section properties and load values are listed in Table 1. Steel main girders are used between two hinges. The cable-stayed bridges are idealized as plane structures and analyzed using matrix structural theory.

3. ANALYSIS RESULTS

Fig.4 shows bending moments and axial forces in the main girders for the self and partially anchored systems caused by both dead loads and prestressing forces in cables. Bending moments are almost same for both anchoring systems but axial compression in the partially anchored system is about 53 % less than that of the self anchored system. Variations of bending moments from D+L(-) to D+L(+) in the partially anchored system are smaller than those of the self anchored system as shown in Fig.5. On the other hand, the corresponding variation of axial force in the partially and self anchored systems is almost same and small as shown in Fig.6.

Table 2 shows internal forces and longitudinal movements at the hinges. To dampen the longitudinal movements produced by earthquakes, oil dampers will be inserted at the hinge locations. Axial forces at hinges are caused by the special links inserted for analysis in this example, but in actual structures these values are almost zero. Hinge design for partially anchored systems is relatively easy.

Reacting forces at the anchorages are shown in Table 3. By optimizing the shape of anchorages constructed for partially anchored cable-stayed bridges, the cost of anchorages may be decreased compared to the conventional type used for suspension bridges.

Table 1 Characteristics of Cross Sections & Dead Load

Members		A(m^2)	Iz(m^4)	Iy(m^4)	D(tf/m)
Main Girders	Steel	1.13	2.52	62.2	18
	PC	20.0	30.0	800.0	60
Towers	1	1.32	9.1*	2.9**	22
	2	2.08	15.9*	4.6**	34
	3	2.24	18.8*	5.0**	34
	4	2.58	23.3*	5.8**	42
	5	0.70	2.9	2.9	21
Cables	I	0.024	—	—	0.019
	II	0.022	—	—	0.017
	III	0.020	—	—	0.016

A : Area of cross section
Iz, Iy : Moment of Inertia in and out of plane, respectively
* for two columns, ** for one column, 1 tf = 9.81 kN

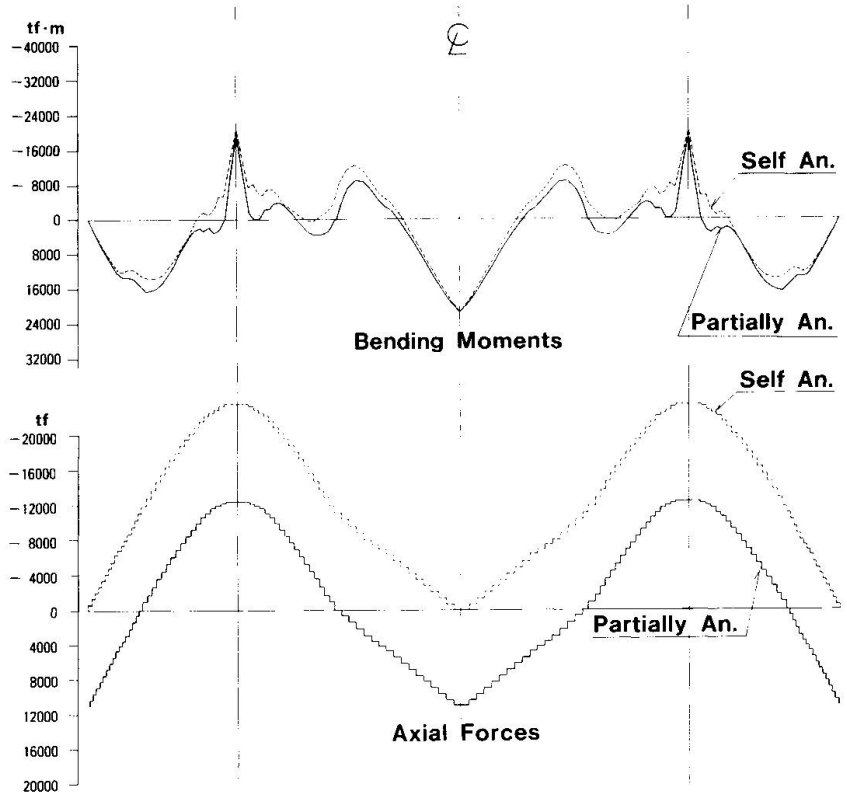

Fig.4 Bending Moments and Axial Forces (1 tf·m = 9.81 kN.m)

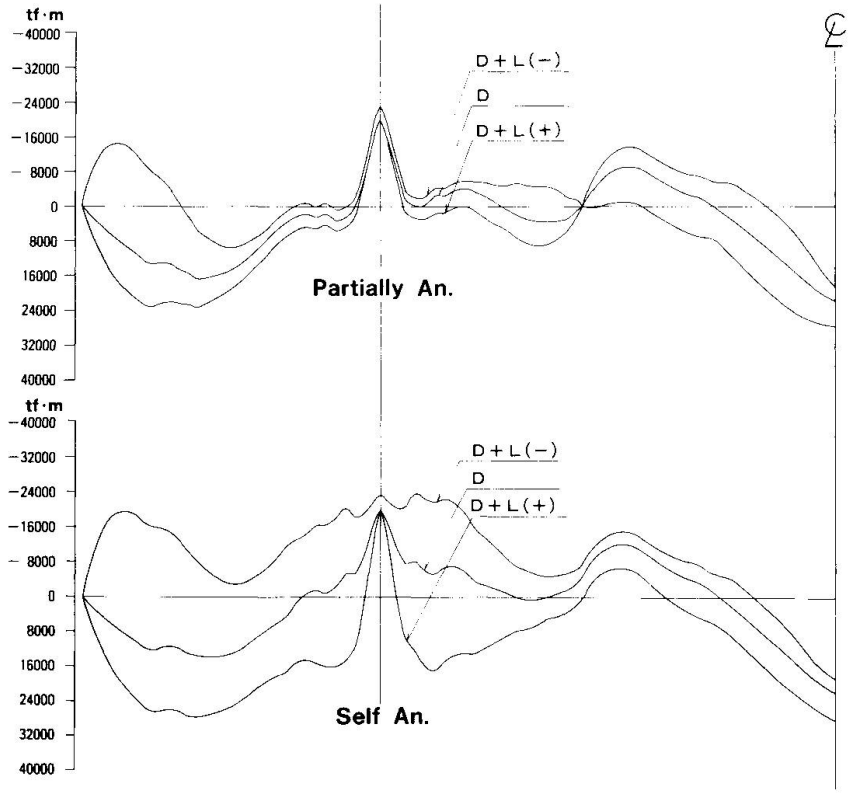

Fig.5 Variations of Bending Moments (1 tf·m = 9.81 kN·m)

Table 3 Reacting Forces at Anchorages

Load Case	Reacting Forces
Dead Load + Prestressing	Rx = 10998 tf, Ry = 174 tf
Temperture(±35℃)	Rx = ±466 tf, Ry = ±13 tf
Live Load	Rx = 2107 tf(max), 519 tf(min) Ry = 519 tf(max), -1032 tf(min)
Wind Load (Trans.)	Rz = -256 tf, Mx = -2641 tf·m My = 43747 tf·m
Earthquake (Trans.)	Rz = -2501 tf, Mx = -17588 tf·m My = 260428 tf·m
Earthquake (Longi.)	Rx = ±4932 tf, Ry = ± 948 tf

x : longitudinal direction, z : transverse direction
y : vertical direction, 1 tf = 9.81 kN

4. ALTERNATIVE DESIGN

The hinges inserted in partially anchored systems would be rather expensive and would disturb the smooth driving of vehicles. Furthermore, from the viewpoint of constructing the girder, it may be difficult to expand the main girders beyond the hinges.

Partially anchored cable-stayed bridges without hinges can be accomplished by pulling the main girders from anchorage side after completing the continuous main girders. According to the Specifications for Japanese Highway Bridges, allowable stresses can be increased 25 % during the construction stages. Furthermore, it is easy to change prestressing values in PC main girders. Therefore , this type of partially anchored system becomes an attractive alternative design plan. After pulling main girders , total system behaves like a self anchored system due to the continuity of main girders. However, since bending stresses due to live loads are small compared to axial stresses , the advantages of the partially anchored system are realized in this system.

REFERENCES

1) GIMSING , N.J. , Cable Systems for Bridges, Proc. of 11th Congress of the IABSE , Vienna , Austria , 1980 , pp.727-732.
2) GILSANZ , R.E. , Cable Stayed Bridges: Degrees of Anchoring, Proc. of ASCE, Journal of Stru. Eng., Vol.109. , No.1, January, 1983, pp.200-220.
3) OTSUKA , H. , et.al., Optimum Anchoring for Long Span Cable-Stayed Bridges , Proc. of JSCE , Struc.Eng.& Earthq. Eng., Vol.1, No.2, Oct., 1984, pp.201s-209s.
4) OTSUKA , H. , et.al. , Static and Dynamic Characteristics of Partially Anchored Cable-Stayed Bridges, Proc. of the Recent Advances in Stru. Eng., Bangkok, Thailand, 1985, pp.335-351.
5) OTSUKA , H. , et.al. , Optimization of Girder Supporting Systems and Materials in Composite Cable-Stayed Bridges , Composite Construction in Steel and Concrete, ASCE, 1988, pp.226-239.

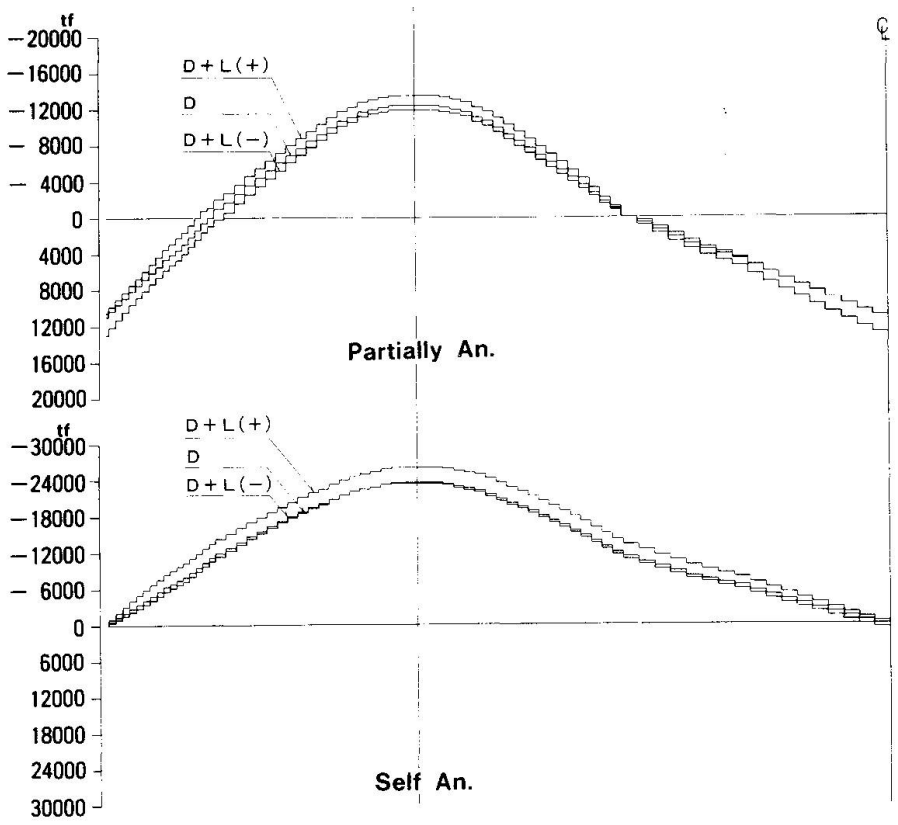

Fig.6 Variations of Axial Forces (1 tf = 9.81 kN)

Table 2 Internal Forces & Longitudinal Movements at Hinges

Load Case	Internal Forces	Movements (mm)
Dead Load + Prestressing	S = 267 tf	22
Temperture(±35℃)	S = 231 tf	±308
Live Load	S = 95 tf	±273
Wind Load (Transverse Direction)	S = 530 tf T = 1887 tf·m M = -781 tf·m	0
Earthquake (Trans.)	S = 2755 tf T = -3746 tf·m M = -24632 tf·m	0
Earthquake (Longi.)	N = ±771 tf	±1024

S = Shearing Force, T = Torque, M = Bending Moments,
N = Axial Forces, 1 tf = 9.81 kN

Design and Construction of a Cable-Stayed Bridge with Mixed Structure

Conception et construction d'une structure mixte pour un pont à haubans

Bemessung und Bau eines Verbundträges für eine Schrägkabelbrücke

J. TAJIMA
Professor
Saitama University
Tokyo, Japan

M. OHASHI
Director
Honshu-Shikoku B.A.
Tokyo, Japan

K. TADA
Head of office
Mukaijima Constr.
Hiroshima, Japan

K. YAMAGISHI
Chief of Construction
Mukaijima Constr.
Hiroshima, Japan

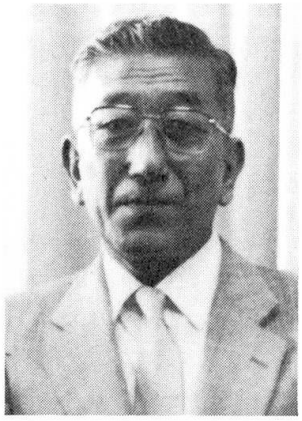

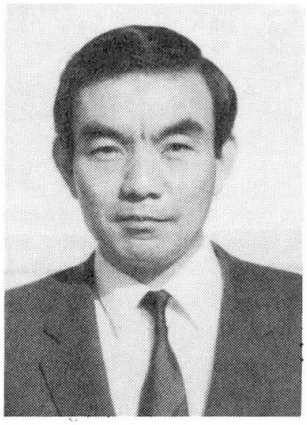
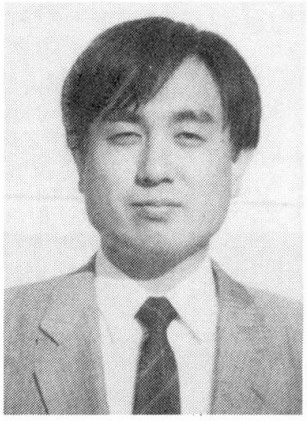

SUMMARY

Ikuchi Bridge is a cable-stayed bridge with a 490 m main span. The main girder of this bridge is a steel concrete mixed structure consisting of a steel girder for the center span, and prestressed concrete girders for both side spans. The connected parts between them were designed by taking account of the transmission mechanism of the stress, steel fabrication, actual construction methods etc. This report deals mainly with the design and construction of the connected parts between two types of girders.

RÉSUMÉ

Le Ikuchi Bridge est un pont à haubans avec une travée principale de 490 m. La poutre principale de ce pont est une structure mixte acier-béton, comportant une poutre en acier pour la travée centrale et des poutres en béton précontraint pour les deux travées latérales. Les éléments de jonction entre les deux types de poutres ont été conçues en tenant compte de la mécanique de transmission de la charge, de la fabrication en usine, des méthodes actuelles de construction, etc. Ce rapport traite essentiellement de la conception et de la construction des éléments de jonction entre les deux types de poutres.

ZUSAMMENFASSUNG

Die Ikuchi Brücke ist eine Schrägkabelbrücke mit einer Hauptspannweite von 490 m. Der Hauptträger dieser Brücke ist eine Verbundkonstruktion aus Stahl und Beton, die aus einem Stahlträger für den mittleren und aus Spannbetonträgern für die beiden Seitenspannweiten besteht. Die Verbindungsteile zwischen ihnen wurden unter Berücksichtigung der Belastungsübertragung, der Stahlherstellung, der aktuellen Bauverfahren, usw. entworfen. Dieser Bericht behandelt in erster Reihe den Entwurf der Verbindungsteile zwischen den zwei Trägertypen.

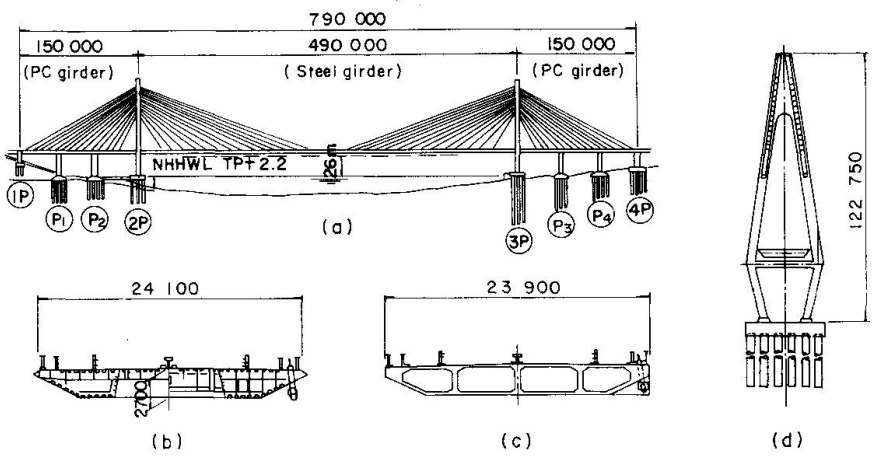

Fig. 1 Ikuchi Bridge : (a) Side view (b) Steel girder section, (c) Concrete girder section, (d) Side view of tower (2P)

1. OUTLINE OF IKUCHI BRIDGE

The Ikuchi Bridge is a cable-stayed bridge, connecting Innoshima island and Ikuchi island, on the Onomichi-Imabari, west side route of the Honshu-Shikoku Bridge Project in Japan.

Characteristics of this cable-stayed bridge are that the main girder is a steel-concrete mixed structure which consists of steel girder for the center span and prestressed concrete (PC) girders for both side spans.

This type is adopted, because as the side span length is short in comparison with the center span length from the condition of horizontal road alignment, it is favorable that the dead load of side spans is heavy in order to eliminate the negative reaction force. For this reason the main girder in the side spans is made of concrete, which is supported by the two middle piers as shown in Fig. 1.

2. DESIGN OF CONNECTION

2.1 OUTLINE

The steel girder is firmly jointed to PC girder over an entire section at the point out of the support on the lateral beam of the tower to the center slightly. On the connection between the steel girder and PC girders, where the structural and material characters change. It was necessary to fully investigate the mechanism of load transmission and design to be safe and rational.

For the structure type of connection, after studies about different kinds of types through large scale experiments, the type transmitting load from the steel cells to the PC girder through the filled concrete in the cells was adopted ([1], [2]).

Perspective of the connection and the typical crosssection are shown in Fig. 2 and Fig. 3 respectively.

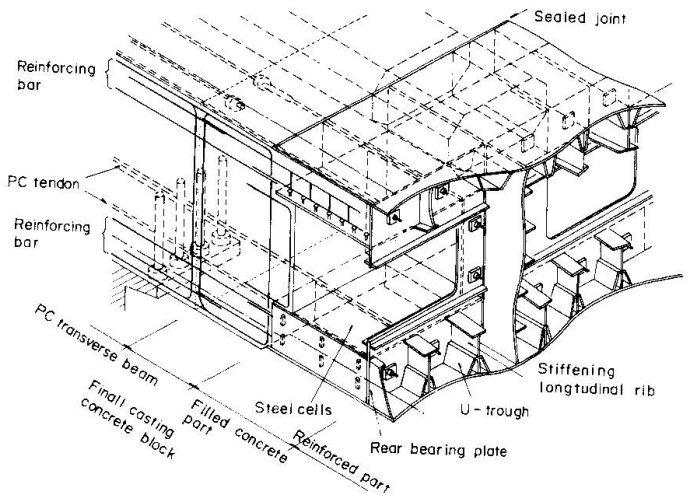

Fig. 2 Perspective of connected part

2.2 DESIGN PROCEDURE

The connected part was designed by the following procedure.
(a) Determined the shape and general proportions of the connection considering the mechanism of the stress transmission and the ease of fabrication and erection.
(b) Determined the design section forces at the connected part.
(c) Proportioned the sections of the main girder : PC section, steel section and composite section.
(d) Designed the elements of the stress transmission part : shear connectors, rear bearing plate and checked the stress in the filled concrete.
(e) Designed the structual detailes : the reinforced part in the steel girder, the tip of the steel plate and the arrangement of the reinforcing bars in the filled concrete.

2.3 DETAILS OF CONNECTION

The details of the connection was decided as follows.
(1) Steel cells
The width of the steel cells equals to the distance of the U-shaped ribs and the height was decided considering ease of fabrication of the steel cells, arrangement of the prestressing tendons and reinforcing bars, casting the filled concrete and required area across the filled concrete to distribute the load to the PC girder.
The length of them was decided considering how to transmit the load from the steel cells into the filled concrete smoothly and to arrange the required shear connectors.
(2) Reinforced part in the steel girder
In the reinforced part longitudinal stiffening ribs were welded to the deck in order to distribute the load smoothly from the deck plate, inclined flange and lower flange into the filled concrete part. This stiffening ribs were inserted in the the U-shaped ribs of the deck plate.
The length of the reinforced part was determined by consideration of the stress distribution characteristics and the distance of cross beams.

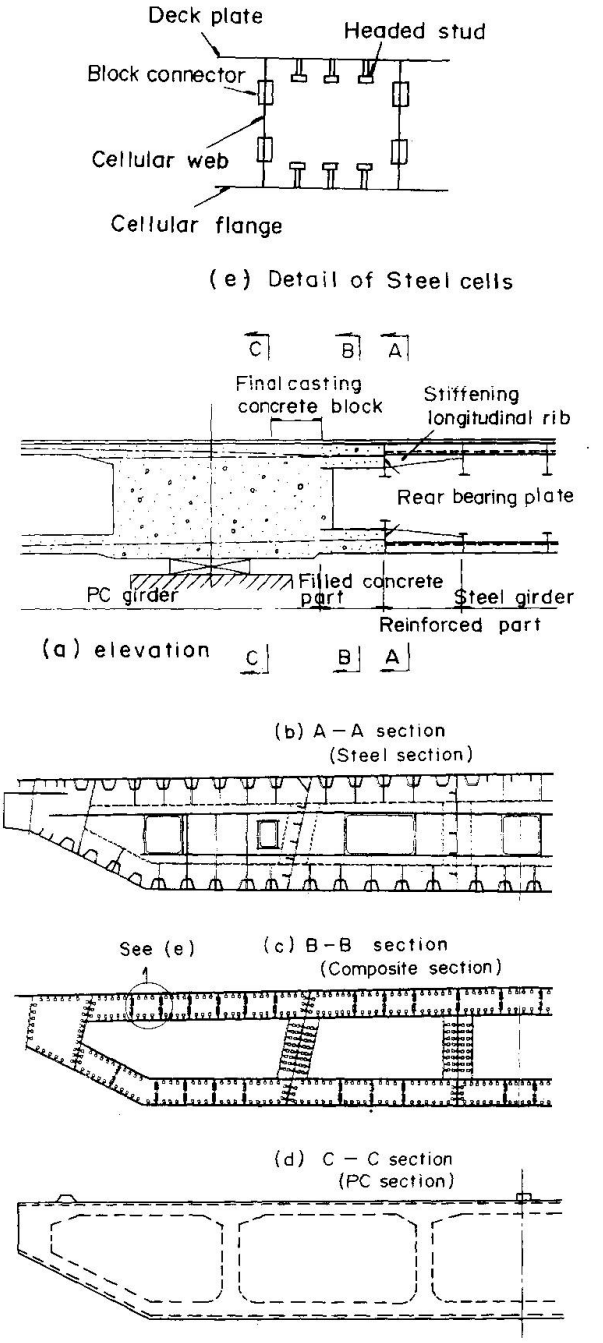

Fig. 3 Cross-section of connected part

(3) Selection of shear connector
Headed studs were adopted for shear connectors welded to deck plates, inclined flanges, lower flanges, flanges in the steel celles and webs, which resist the tensile stress as well as the shearing stress and protect to separate the fillled concrete from the steel cells. However the rectangular blocks were welded to the webs of the steel cells between the filled concrete, for there is no problem of the separation and headed studs disturb the assembly of this part.

2.4 DESIGN SECTION FORCES

An example of the design diagrams for the section forces acting on the main girder

under service loading conditions is shown in Fig. 4. The bending moments distribution in the center span are relatively smooth, whereas those for both side spans distribute with some peaks at the supports of the middle piers and towers.

These bending moments were adjusted mainly by varying the tensile force of stay cables in center span, because the flexural stiffness of steel girder is smaller than that for the prestressed concrete girder.

The maximum axial forces in the girder occur at the location of each tower due to the type of cable-stayed girder. The shearing forces for side spans are extremely larger than those for center span.

The typical values for section forces which have been used for design of the connected part of main girder are shown in Table 1.

2.5 TRANSMISSION PROCESS OF INTERNAL FORCES

Table 2 shows the working stresses acting on the section of steel-concrete connected part under service loading conditions. The tensile stresses in the composite section at the filled concrete part does not occur due to the action of large axial compressive force.

The transmission mechanism of axial forces at the connected part between steel beam and prestressed concrete girder, was considered that the stresses acting on the standard portion of steel beam are dispersed at the reinforced part of the beam and transferred to filled concrete part.

At the filled concrete part, the stress acting on the steel multi-cells will be transferred to the filled concrete by the following mechanism, namely, ① rear bearing plate, ② shear connectors and ③ friction at the interface between steel and concrete. The stresses at the filled concrete are uniformly transmitted to the prestressed concrete transverse beam on the supports at the tower.

As the results of the static loading tests in which the scale model specimens for one steel cellular box were used, it was recognized that the rate of the stresses transferred by the friction was considerably large ([3]). However, the transmission factor by the friction was neglected in designing because of its uncertainties, and this would be considered as a safety margin.

Fig. 5 shows an example of the results of finite element analysis on the model for the filled concrete part with neglecting the friction. Though the stress concentration occurs locally at the welded corner between rear bearing plate and cellular plate, the maximum stress in concrete is less than its allowable bearing stress. It shows that the most of the concentrated axial force induced from steel beam is uniformly dispersed to the filled concrete by rear bearing plate and shear connectors, and the stress concentration does not occur at the tip of steel plate, as shown in Fig. 5 (a).

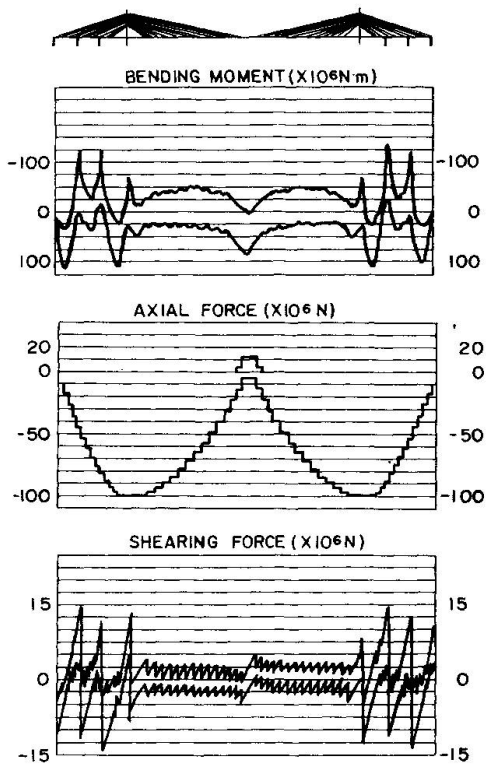

Fig. 4 Section forces

Category	Mzmin (X10⁶N m)	N (X10⁶ N)	Sy (X10⁶N)
2P side	−72.8	−90.3	− 8.2
3P side	−69.7	−90.6	8.1

Table 1 Section forces at the connected part (At service loading condition)

(MPa)

Category			Top fiver	Bottom fiver
PC section	2P side		− 0.7	−7.0
	3P side		− 0.9	−8.8
Steel section	2P side		13.0	-155.8
	3P side		8.3	-152.0
Composite section	Steel plate	2P side	− 1.9	−38.5
		3P side	− 2.8	−37.2
	Filled concrete	2P side	− 0.3	−5.6
		3P side	− 0.4	−5.4

(Compressive stress: negative)

Table 2 Working stress at the connection part

Also, it is seen that the forces resisted by shear connectors reduce step by step according to a part from the bearing plate as shown in Fig. 5 (b). From these results, the transmission rate by headed studs was assumed to be 35 % and in the same manner that by block connectors was obtained to be 50 % by another result.

As the compressive forces are locally transferred to the prestressed concrete transverse beam through the filled concrete of the top and bottom flanges, the stress condition in concrete at connected part was examined in detail by finite element analysis. The following stresses were under consideration as shown in Fig. 6. ① Bearing stress at the root of the filled concrete ② Bursting stress at that point ③ Tearing stress in the front of the transverse beam. The reinforcing bars were arranged in proportion to the magnitude of these working stresses.

If the concrete of the transverse beam is in contact with the tip of steel plates, it may crush locally due to large stress concentration. Therefore the sealed joints were provided around the external periphery of steel girder.

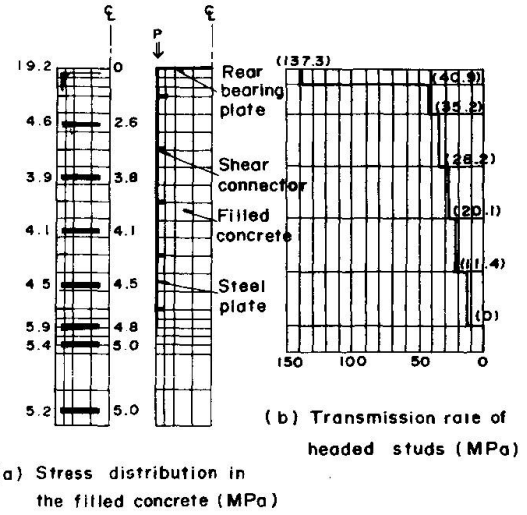

Fig. 5 Transmission mechanism of the filled concrete

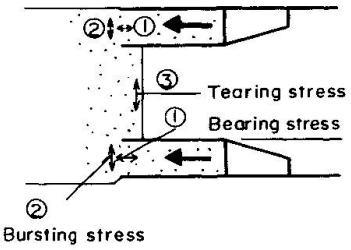

Fig. 6 Local stress at the connected part

3. CONSTRUCTION OF THE CONNECTION

Prestressed concrete girder was constructed by a cantilever erection with traveling forms and cast-in-place construction on false works, to complete 3-span continuous girders. The connection segment of the steel girder was temporarily fixed on the inclined bent as the construction of the prestressed concrete girder approaches the completion, after which the connection concrete was placed so as to minimize, if any, the effect of the construction errors of the prestressed concrete girder. Erection procedure is shown in Fig. 7.

The filled concrete inside the connection segment of the steel girder was placed in advance at the manufacturing of the girder. Non-shrinkage concrete was used considering the restraint condition of the concrete by the steel cells, and to reduce the effect on shear connectors due to bleeding.

Furthermore, the concrete was placed in such a way that the bearing area of the studs faces upward so as to avoid relative or residual slippages due to bleeding which otherwise may develop on the bearing area, and to facilitate the concrete placement.

4. STAY CABLE ANCHORAGES OF THE PRESTRESSED CONCRETE GIRDER

Each cable anchorage of the prestressed concrete girder in the side span consists of a thick steel bearing plate and a steel casing pipe. In the anchorage zone anchoring of a stay cable with the maximum design force of 5800 KN as well as transverse prestressing tendons with that of 4200 KN induces, in the concrete, considerable stresses due to bearing, bursting and tearing, which requires congested arrangement of reinforcing bars. The form of the reinforcing bars to be arranged behind a bearing plate was, to facilitate construction, a grid instead of a spiral which has been commonly used. Grid type of reinforcing bars improves the bearing capacity of the concrete by dispersion of the bearing pressure whereas spiral type of reinforcing bars does so by triaxially confining the concrete.

A static loading test, conducted using 1/3 scale model of the anchorage zone, showed no specific difference of properties in the stresses, deformations or cracks between the grid type and the spiral type.

5. CREEP AND SHRINKAGE

Changes in resultant forces due to creep and shrinkage of the concrete induced as the progress of construction of the prestressed concrete girder and following cantilever erection of the steel girder after its completion were calculated by a plane-frame analysis, allocating appropriate values of coefficients of creep and shrinkage to each construction segment.

The most remarkable result shown by the analysis was 50 mm of toppling of the tower toward the center span and 70 mm of downward deflection of the steel girder resulting from axial shortening, which is also 50 mm, of the prestressed concrete girder in the side span due to the creep and shrinkage.

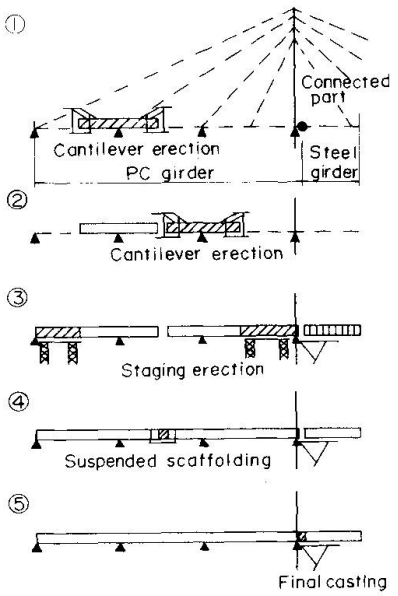

Fig. 7 Constructing sequence of the connected part

6. AERODYNAMIC STABILITY DURING CONSTRUCTION

The aerodynamic stability during construction was investigated by wind tunnel tests using an elastic model of 1/65 scale. Not only free-standing of the tower but also just before the girder closure was examined. The test results are as follows :

(1) It was determined that the liquid-type damper, so-called Tuned Sloshing Damper, would be installed at the top of the tower while free-standing to suppress vortex-induced oscillation at the wind speed of about 10 m/s. The sloshing phenomena of water is applied using a rectangular tank by the size of 5m x 0.8m x 1.4m (length, width and height, respectively) with the water depth about 0.8m.

(2) It was observed that there was no oscillation in a smooth flow, however a buffeting oscillation was evoked in a turbulent flow during the erection of the center span girder. This vertical bending oscillation was judged to be not harmful to the structural safety, because the maximum amplitude at design wind speed (i. e., 41m/s) was only 120mm.

7. CONCLUDING REMARK

The construction of both PC girders in side spans has been already finished, and now the erection of steel girder in center span is under construction by the cantilever method. The design of Ikuchi Bridge has been proceeded under the guidance of the Technical Committee and the Mixed Structure Committee of Honshu-Shikoku Bridge Authority.

REFERENCES

1. OHASHI, TAJIMA, YAMASHITA, MORI, Design of complex cable-stayed bridge. International conference on cable-stayed bridge Bangkok, November 1987.

2. Third Construction Bureau, Honshu-Shikoku Bridge Authority. The Research and Investigation Report with regard to Main Girder Complex Structure of Ikuchi Bridge, May (1986 - 1989) (in Japanese).

3. Mori, Hoashi, Kimura, Report on two Experiments for the Design of Transition Elements of the Superstructure on Ikuchi Bridge, HONSHI TECHNICAL REPORT, Vol. 13 No. 49 (in Japanese).

Composite Semi-Rigid Frame Analysis and Erection Procedures

Dispositifs de montage d'un portique à connecteurs souples

Verbundrahmen mit nachgiebigen Rahmenknoten bei der Montage

Jindřich PAŘÍK
Assist. Prof. of Civil Eng.
Czech Techn. University
Prague, Czechoslovakia

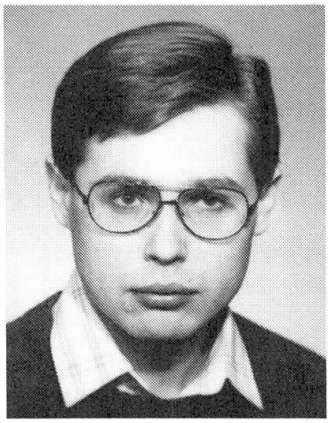

Jindřich Pařík, born 1959, got his civil eng. degree at Czech Techn. University. For four years he was a structural engineer with Consulting engineering Co. in Prague (PPÚ). He has been actively engaged in research on composite structures.

František WALD
Assist. Prof. of Civil Eng.
Czech Techn. University
Prague, Czechoslovakia

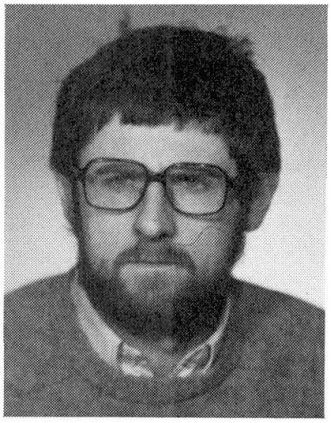

František Wald, born 1953, received his civil eng. degree and Ph.D. degrees from the Czech Technical University. He has studied at Lyngby, Denmark, Berkeley and Purdue, USA Universities. He has been actively engaged in research and testing of steel structures.

Jiří PECHAR
Prof. of Civil Eng.
Czech Techn. University
Prague, Czechoslovakia

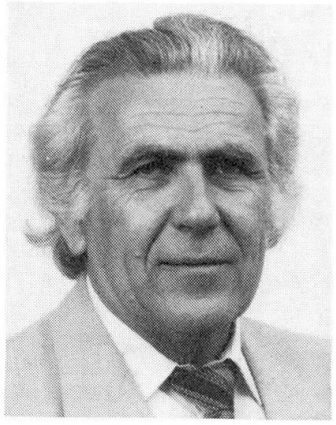

Jiři Pechar, born 1930, professor for steel structures, since 1986 director of Building Research Institute in Prague.

SUMMARY

A numerical nonlinear model of composite steel-concrete frame with semi-rigid connections, slip in connectors and nonlinear material behavior has been developed. The result of a study taking account of different erection procedures is presented.

RÉSUMÉ

Pour le calcul des portiques mixtes acier-béton à connecteurs souples, on a créé un modèle numérique en admettant le glissement dans les connecteurs et le comportement non linéaire du matériau. Cette étude présente l'influence des séquences de montage sur l'état de contrainte de la construction.

ZUSAMMENFASSUNG

Im Programm für die Berechnung von Verbundrahmen wurden nachgiebige Rahmenknoten, Dübelverschiebung und das elastisch-plastische Verhalten des Materials berücksichtigt. Konkrete Beispiele des Einflusses auf den Montageablauf werden dargestellt.

1. INTRODUCTION

The widespread use of the composite steel-concrete construction in steel building frames has drawn the attention to semi-rigid composite connections which seemes to be an economically attractive solution for moments redistribution and for resistance to moderate horizontal forces. The major obstacle to the use of composite frames with semi-rigid connections is the lack of experimental verification and of analytical models both for the moment-rotation interaction in connections and for concrete-steel composite action. Joint and frame behaviour is very sensitive on erection procedures in steel-concrete composite structure.

The physical model consists of an I-shaped steel girder, concrete slab, steel reinforcement and steel shear studs. For each of these components a nonlinear material behaviour for monotonic loading is known. Therefore the method of analysis can be based on the calculation of moment-rotation behaviour of the cross-section and on the finite difference numerical integration along the span of the girder. The initial stress method is used for iteration on each load step in the frame analysis.

We use a simplified analytical spring prediction model to be compatible with the used frame in a plane design which would take full advantage of composite action in practice. A three-parameter power model is formed using the initial connection stiffness affected by slip in connectors, steel connection and contact between the concrete slab and the column and the ultimate moment carrying capacity. It is then the purpose of this paper to show erection problems when the semi-rigid steel frame connection changes from hinged model.

2. MATERIAL ASSUMPTION

Numerical model takes into account arbitrary nonlinear stress-strain interaction curve for concrete, steel and reinforcement. Steel-concrete connection is made by studs, slip is introduced in form of a function expressing the q - longitudinal shear force, u_c - slip). For practical calculation the corresponding values given in EC 4 were used.

3. COMPOSITE ACTION

Due to nonlinear behavior, mainly due to cracks in concrete in negative moment region the distribution of internal forces along a beam can be changed. This fact is taken into the account by such a computation procedure, in which the beam is divided in elements of finite length L and of the ideal stiffness EI corresponding to the curvature Φ . This curvature is taken from the interaction curve $M - \Phi$, $M - N - \Phi$ respectively. Equivalent stiffness of each element is computed in every iteration step repeatedly, since it must correspond anytime to adequate acting forces. The iteration is closed when proposed small difference of stiffness in two consequent iteration steps is reached.

3.1 Moment-curvature

Accepting the Navier´s hypothesis, the strain ε_z in the distance z from the neutral axis is

$$\varepsilon_z = \Phi \cdot Z \qquad (1)$$

where Φ is the angle of curvature.

The slip strain ε_d [5] can be introduced as

$$\varepsilon_d = \varepsilon_s - \varepsilon_c \qquad (2)$$

where ε_s is strain in top fibers of steel girder flange
ε_c is strain in bottom fibers of concrete slab.

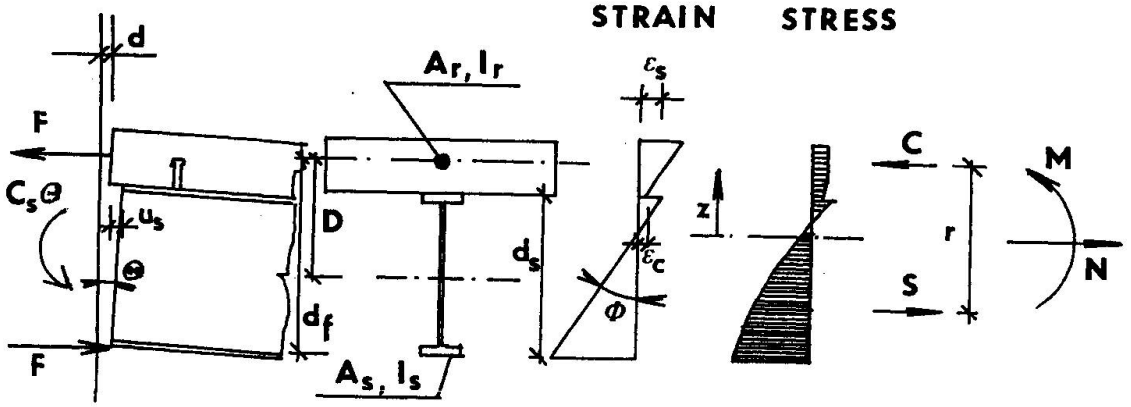

Fig. 1 The Composite Beam Element Model

Then the steel girder strain is $\varepsilon_{z,s} = \Phi \cdot Z$ (3)

and that one in concrete slab is $\varepsilon_{z,c} = \Phi \cdot Z - \varepsilon_d$ (3a)

The external load produces in concrete slab a force C, which can be calculated by integration over concrete slab area

$$C = \int \sigma_c \cdot dA_c \qquad (4)$$

Similarly, the force S in steel section and R in concrete reinforcement has to be calculated.

Normal stress in all sections is

$$\sigma = f(\varepsilon) \qquad (5)$$

Of course, the equilibrium condition for inter nal and external forces in the form

$$C + S + R + N = 0$$
$$C \cdot r = S \cdot r = M \qquad (6)$$

must be fulfilled.

If the length L of an element is small enough, the uniform distribution of longitudinal shear force along the element can be assumed

$$q = - C/L \qquad (7)$$

from $q = f(u_c)$ (8)

where u_c - slip

and from slip strain correlation $\varepsilon_d = u_c/L$ (9)

the formula (10) can be derived

$$C = - L \cdot f(u_c) \qquad (10)$$

Introducing (3), (3a) and (5) in (4), using numerical integration and iteration for searching the actual position of neutral axis (with help of eq. (6))it is possible to find out for the given value of slip u_c and that of curvature Φ the correspondent value of bending moment M. By numerical solution of eq. (10) for the known value C the unknown value of slip u_c for following iteration step can be calculated.

4. COMPOSITE JOINT BEHAVIOR

4.1 The Moment-rotation Relationship

The moment-rotation relationship of a composite joint is the end product of a complex interaction between the composite beam and the concrete slab. Using the initial connection stiffness C_i and the ultimate moment carrying capacity

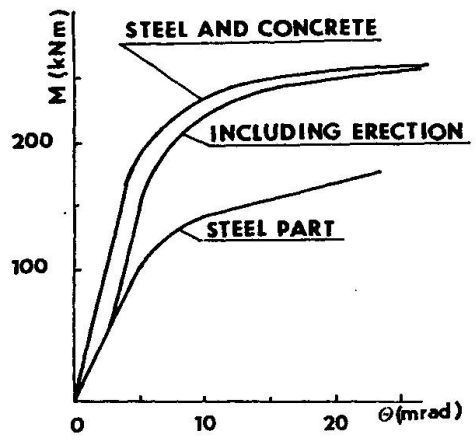

M_u a three parameter power model is found to be adequate for representing the moment-rotation stiffness. Therefore we adopt this model for the presented composite connections.

The moment-rotation relationship can be represented adequately by the power model in the form

$$M = C_i.\Theta(1+(\Theta/(M_u/C_i))^n)^{-1/n} \qquad (11)$$

in which is n the shape parameter.

Fig. 2 Moment-rotation Behavior Prediction Model of Flush End Plate Connection

4.2 Modeling of Steel Connection Behavior

Several analytical prediction models have been developed to represent steel connection flexibility. These models are generally either sophisticated numerical simulation or an approximation based on test data. We used prediction models, which are determined by using simple analytical procedures |3|, |6|.

4.3 Initial Stiffness

The initial stiffness of cracked composite connection is influenced by the concrete slab action, steel part connection and slab-column action. The interface slip substantially affects the response of the connection.

For the simple composite joint shown in Fig. 1. the equilibrium and compatibility conditions at the column face are

$$M = F \cdot h_F + C_s \cdot \Theta \qquad (12)$$

$$\Theta \cdot h_s = (d_1 + d_2).h_s/h_F + u_s \qquad (13)$$

C is the secant stiffness of the steel part of connection.

For the slab-column action we divide the deflection in steel bars of the slab d_1 and in the connection d_2 . The deflection d_1 we can determine

$$d_2 = F(1+(M - M_2)/M)/C_r \qquad (14)$$

for C_r as secant stiffness of steel bar connection to the column and M_2 a moment on the opposite side of the column.

The contribution of slip action is accepted from composite beam behavior on each load step.

4.4 The Ultimate Capacity of the Composite Joint

The ultimate moment capacity of the joint can be determined simply by adding up the moment capacity of the steel connection M_s to the moment of resistance given by the yield strenth of the bars |3|

$$M_u = M_s + A_r \cdot f_r \cdot d_f \qquad (15)$$

5. THE DISCUSSION OF ERECTION PROBLEM

The frame in Fig. 3 was analyzed using the composite girder and steel columns for both noncomposite and composite design. Beam-to-column connections were constructed in form of different types of steel connections. The survey of steel connection constants is in Table 1. The ultimate limit was established by limit deformations of beam and collapse load of whole frame. The proportional limit load with real connections to the rigid ones summaries the results of parametrical study in Table 1 (column 3). The same results are for frames with flexible connections with only composite action (column 4).

Connections	1	2	3	4
	C_i |kNmmrad-1|	M_u |kNm|	P_{ul}	P_{ulcom}
1. Double Web-Angle	20	20	0,45	0,70
2. Top and Seat-Angle	25	40	0,48	0,70
3. Top and Seat-Angle with Double Web-Angle	30	80	0,80	0,95
4. Header Plate	50	60	0,45	0,80
5. Flush End-Plate	90	110	0,90	0,98

Table 1

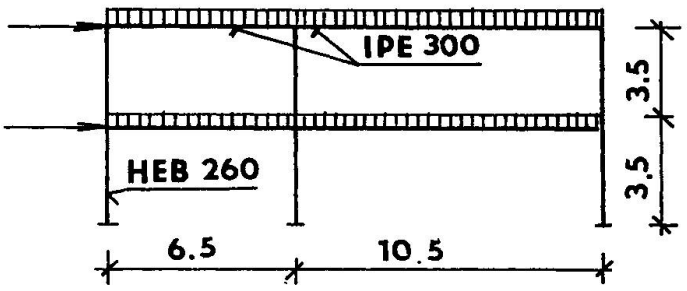

Fig. 3 Frame Configuration

6. CONCLUSIONS

1. The proposed power model is in a good agreement with the available results of cantilever tests. The power model can be implemented in a second-order analysis more easily than a piece-wise linear model.

2. Due to the longitudinal interface slip between the steel beam and concrete slab in composite members the moment-rotation characteristic does not depend solely on joint parameters and it is necessary to take into account the behavior of the whole frame. For a beam element the slip strained calculation and numerical integration along the beam element give reasonable accurate results conform ing with the slip in initial stiffness for some known cantilever tests.

3. The slab-column interaction is of great importance and affects the moment-rotation characteristics, first of all the initial stiffness, when the node is subject to asymmertical loading. Establishing the value of major parameters is the problem of the prepared tests and numerical study.

4. The limited knowledge of the behavioral mechanisms of this type of joints hampers their practical use. There is great need for experimental verification of numerical model.

5. The steel should act as simply supported under dead and constructions loads. The use of semi-rigid steel connections under erection could show reasonable advantages. The reduction of ductility is under required limits.

REFERENCES

1. EUROCODE 3, Design of Steel Structures, Commision of European Communities, Final draft, Dec. 1988, Liason Engineers
2. EUROCODE 4, Composite Steel and Concrete Structures, First Draft, European Economic Community, 1984.
3. JOHNSON R.P., LAW C.L.C., Semi-Rigid Joints for Composite Frames, Joints in Structural Steelwork, Hewlett, J.H. at all ed., John Wiley and Sons, NewYork, 1981, pp. 3.3.-3.19.
4. ZANDONINI R., Semi-Rigid Com posite Joints - Strength and Stability Series, Vol. 8, Connections, Ed. Narayanan, R., Elsevier Applied Science, 1989.
5. ZAREMBA, Ch.J., Strength of Steel Frames using Partial Composite Girder, Journal of Structural Engineering, Vol. 114, No. 8, Aug. 1988, pp. 1741-1759.
6. CHEN W.F., KISHI N., Moment-Rotation Relation of Top and Seat Connections Ing. Col. Bolted and Spec. Struct. Con., Pres. 2., Moscow 1989, pp. 126-130.
7. WALD F., PAŘÍK J., A Semi-Rigid Composite Connection for Beam Element, Acta Polytechnica 4, ČVUT, Prague 1990, in printing.

Composite Action in Steel-Concrete Structures

Interaction spatiale dans un pont mixte acier-béton

Räumliche Wirkungen bei Verbundkonstruktionen von Brücken

Jiří PECHAR
Director
Build. Res. Inst.
Prague, Czechoslovakia

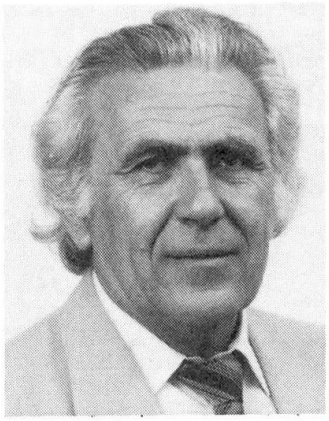

Jiří Pechar, born 1930, received his civil engineering degree from the Czech Technical University of Prague. Profesor in the department of steel structures and bridges, CTU.

Jiří FALTUS
Civil Engineer
State Inst. Transp. Design
Hradec Králové, CSSR

Jiří Faltus, born 1945, received his civil engineering degree from the Czech Technical University of Prague. He has worked in transport as a designer of bridges since 1972.

SUMMARY

The paper deals with the investigation of a composite oblique bridge structure and its behavior in space. The structure consisting of main steel plate I-girders and reinforced concrete slag without any cross and longitudinal bracing. Results of theoretical analysis were compared with results of a loading tests on the real bridge.

RÉSUMÉ

L'article concerne les recherches théoriques relatives aux structures obliques mixtes en acier-béton d'un pont et de leur interaction spatiale. La construction se compose de poutres principales en acier à âme pleine à section en I et d'une dalle de tablier en béton armé sans entretoisement longitudinal et transversal. Les résultats de la solution théorique ont été comparés avec ceux de l'essai de charge effectué sur le pont réel.

ZUSAMMENFASSUNG

Der Beitrag befasst sich mit der Ermittlung von schrägen Verbundkonstruktionen von Brücken. Die Tragkonstruktion besteht aus Stahl-Hauptträgern (I-Profil) und aus einer Stahlbeton-Fahrbahnplatte ohne Längs- und Querversteifung. Die Ergbenisse der teoretischen Lösung werden mit den Resultaten, der auf der aufgebauten Brücke durchgeführten experimentalen Belastungsprobe verglichen.

1. INTRODUCTION

In the construction of bridges (mainly roadway) there are widely used structures which are created from steel plate girders and reinforced concrete slab of bridge floor, assembled as composite structure, number of girders can be various. Transverse load distribution depends on the stiffness of main girders, slab and cross bracing girders respectively.

In Czechoslovakia there are most often used carrier structures with three or more main girders. Concrete slab replaces cross bracing girders. This approach allows to use steel I - shaped profiles for main bridge beams. Such beams are produced in series by automatic welding. This type of structures diminishes the structural depth and improves the aesthetics of the bridges. Utilization of steel of main girders of this type of struktures are better because we can use wide assortment of widths and thicknesses of flanges. Possibility of useing of steel light sheeting is further advantage of this type of structures.

The carrier structure was investigated theoretically. Results were compared with results of experimental loading test. Good agreement of results proved correct choice of calculation model.

2. DESCRIPTION OF THE STRUCTURE (Fig. 1.)

The investigated structure consists of four main lateral steel plate girders without cross bracing and reinforced conrete slab of bridge floor cast in situ. Connection between slab and girders is made by stud connectors, welded on the steel flange. Precambered steel girders were not supported during erection.

Material's data :

steel - yield strength 340 MPa
tensile strength 480 - 630 MPa
modulus of elasticity 210 000 MPa

concrete - compresive strength after 28 days (cubes) 40 MPa
- modulus of elasticity 33 000 MPa

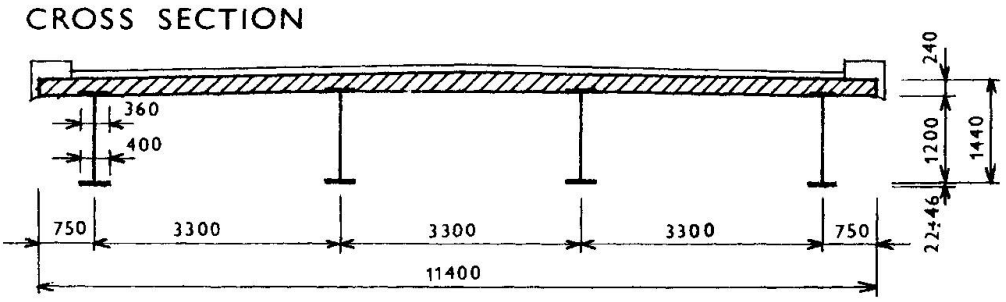

Fig. 1. Sketch of bridge structure

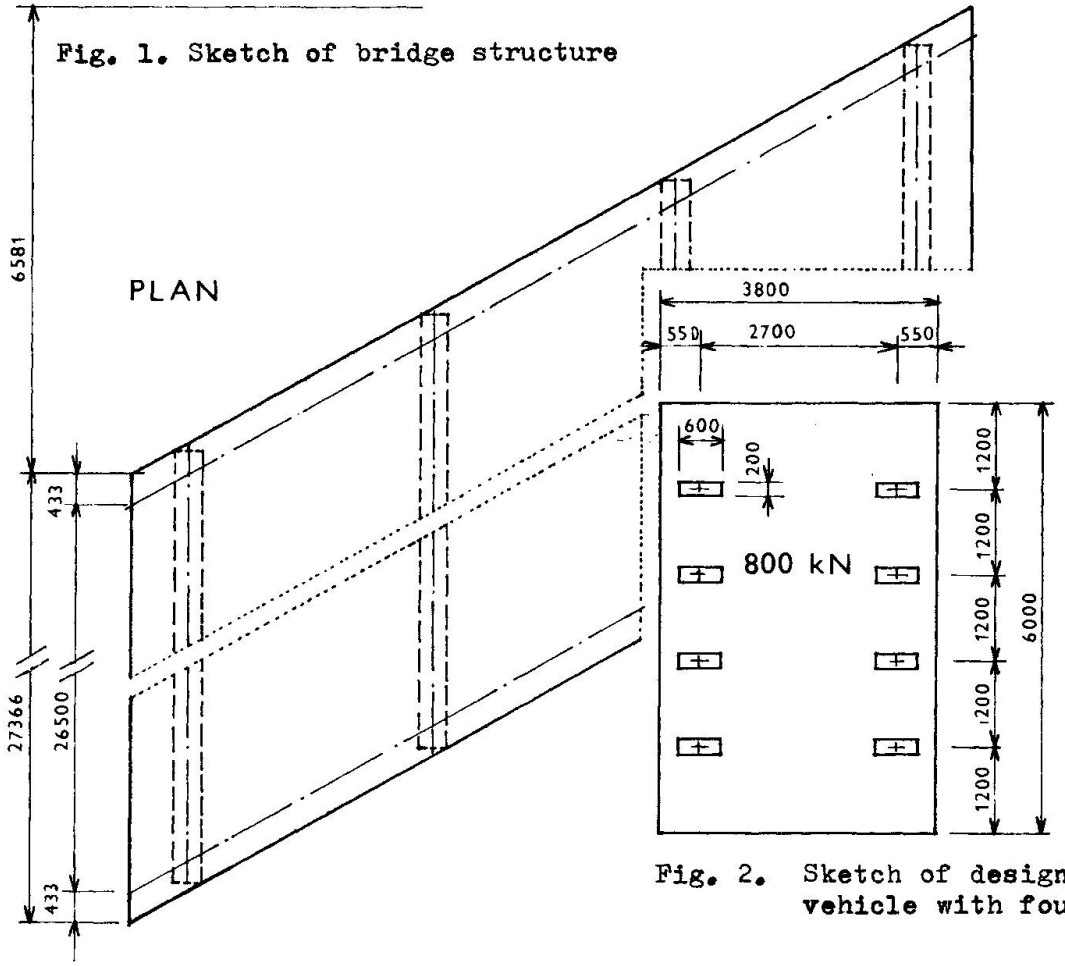

Fig. 2. Sketch of design load vehicle with four axles

3. THEORETICAL ANALYSIS

3.1 Design load

During theoretical investigation we considered all required kinds of load. For the investigation of transverse load distribution both uniform surface load and load by design vehicle with four axles were used. Weight of vehicle is 800 kN (Fig. 2.). Creep: $\varepsilon_d(t) = \varphi(t)\frac{\sigma}{E_b}$ Shrinkage: $\varepsilon_z(t) = \frac{\varepsilon_{z\infty}}{\varphi_\infty}\varphi(t)$

Coefficients for thermal prolongation :

For steel $d = 1{,}2 \cdot 10^{-5}$ for concrete $= 1{,}0 \cdot 10^{-5}$

3.2 Calculation model

Calculation model for theoretical investigation by finite element method was assembled to respect real common work of concrete and steel as a whole in space. We used finite element method for solution of three dimensional problem and we respected the whole shape of the structure and its individual elements. Diferent physical and mechanical properties of materials, of individual elements of structure including shear connectors were considered too. Calculation model alowed to consider skrinkage and creep of concrete, effecte resulting from temperature changes, different coeficients of linear thermal expansion for steel and concrete elements. Model enables to respect real location of design load, working load, test load.

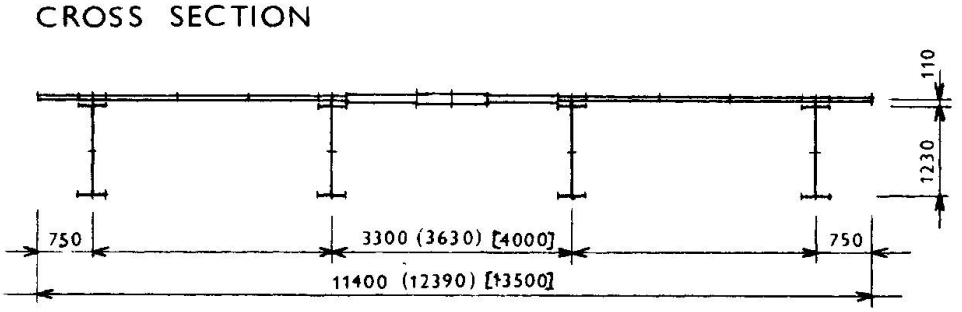

Fig. 3. Sketch of calculation model for FEM

3.3 Survey of theoretical investigation - results

On base of theoretical investigation of real structure in space following conclusions can be derived :

- reinforced concrete slab is a structural element which provides usualy sufficient stiffness for transverse load distribution on the main girders. Even in the case when additional cross section bracing is used the slab plays decisive role in transverse load distribution.
- It is necessary to provide the longitudinal slab reinforcement also at the top surface of the concrete slab because of the bending stresses in slab from transverse load distribution.
- Uplift stresses in studs due to transverse bending of the slab are not as a rule greater then those due to longitudinal bending. The combination of both effects is not particularly important for studs design.

- The change of longitudinal bending stresses in concrete slab due to shear lag is significantly affected by the cross section deformation (i.e. by the distance between bridge neutral axis and concrete slab)
- Top flanges of main girders are stressed by transverse bending due to slab deformation. Therefore the top flange width should be limited as much as possible.
- In skew structures the increase of normal stresses in the slab corners area due to negative bending moments should be considered. This takes place especially under the excentric load at the longitudinal unsupported edge of the slab.
- Midspan vertical deflections from design load are illustrated on fig. 4. Deflections are illustrated for following main girders, spacings : A. 3,3 m (real bridge), B. 3,63 m, C. 4,0 m. The structures were without cross section bracing except the lastly structure (4,0). In this structure were considered in addition with and without rigit cross bracing (cases D, E).

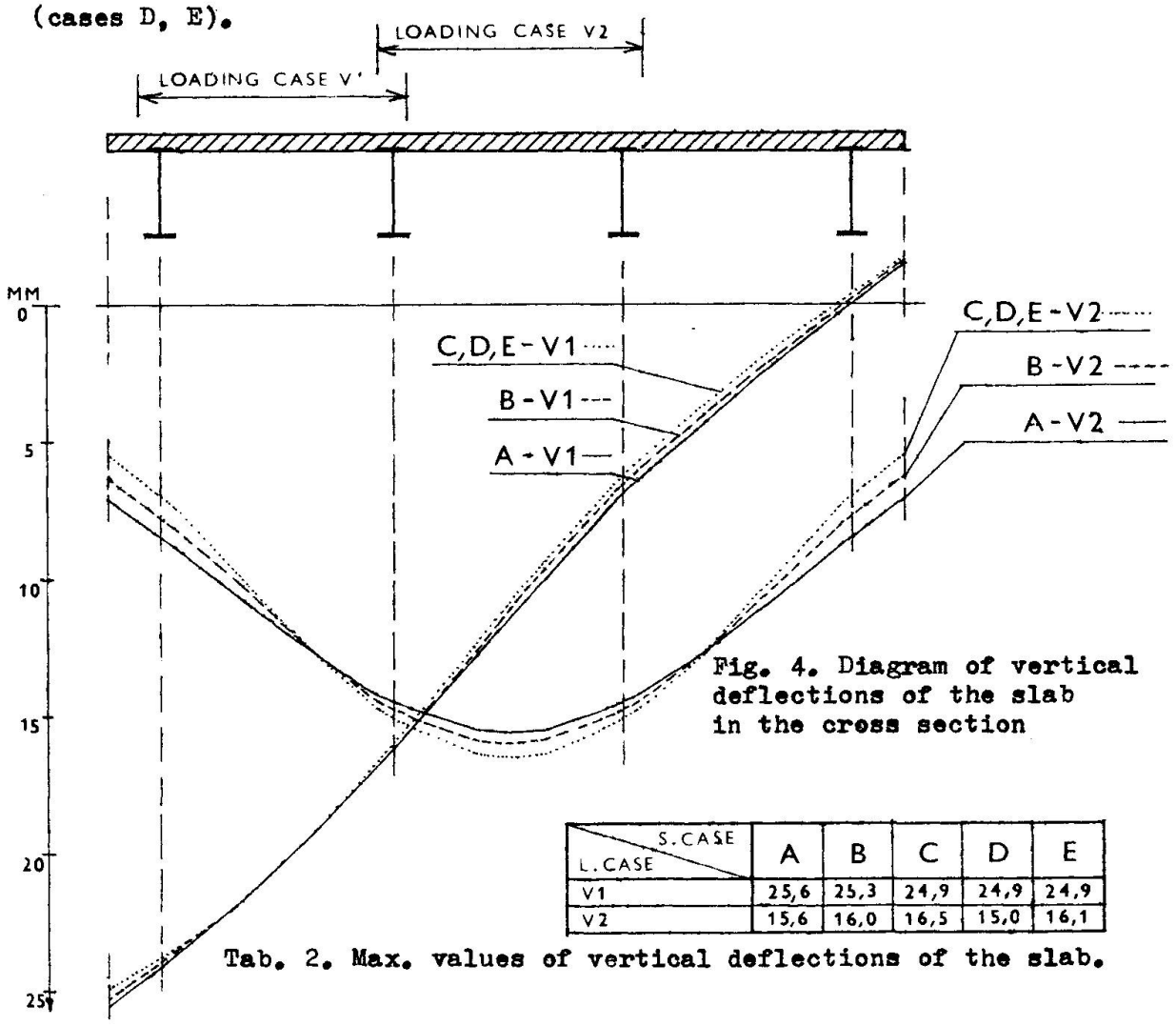

Fig. 4. Diagram of vertical deflections of the slab in the cross section

L.CASE \ S.CASE	A	B	C	D	E
V1	25,6	25,3	24,9	24,9	24,9
V2	15,6	16,0	16,5	15,0	16,1

Tab. 2. Max. values of vertical deflections of the slab.

4. EXPERIMENTAL INVESTIGATION

Prefabricated concrete road panels were used as a load in experimental loading test in situ. The total weight of panels was 540 kN. Panels were placed on wood pads (size 0,2 m x 0,2 m) directly upon the concrete slab of the bridge structure. Structure was investigated in three loading cases.

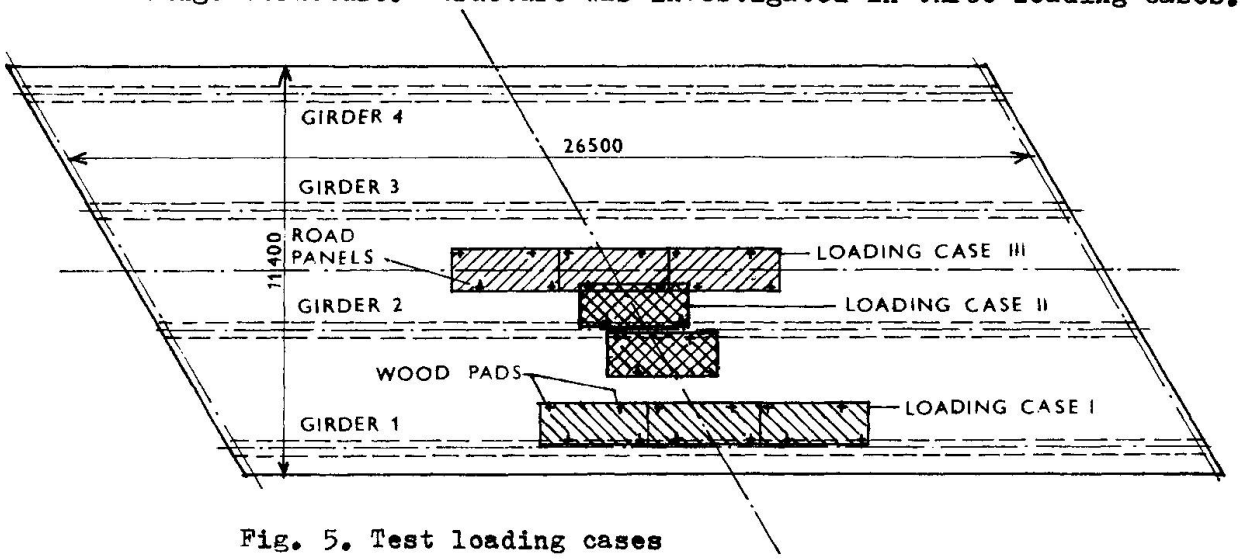

Fig. 5. Test loading cases

Comparison results of theoretical and experimental investigation is done for vertical midspan deflections of main girders (Tab. 1.) and for normal stress in lower flanges of main girders in the middle of span (Tab. 1.)

LOADING CASE			I		II		III	
			THEOR	EXP	THEOR	EXP	THEOR	EXP
σ (MPa) STRESS	GIRDER	1	59,7	54,2	29,0	26,3	14,0	16,0
		2	30,6	29,6	45,6	40,6	32,5	33,5
		3	8,6	9,3	24,0	20,5	32,5	32,8
		4	−2,4	−1,7	6,2	8,1	14,0	17,1
y (MM) VERTICAL DEFLECT.	GIRDER	1	19,2	17,4	10,0	8,9	5,2	4,7
		2	10,0	9,0	11,8	11,2	9,7	9,2
		3	3,0	2,5	7,5	6,8	9,7	9,0
		4	−1,2	−1,3	2,3	1,8	5,2	4,6

Tab. 1. Values of normal stresses and vertical deflections

5. CONCLUSION

Results of theoretical and experimental investigation of composite action in space of the composite bridge structure verify the agreement of theoretical solution which includes all elements of structure into the bearing capacity. Results verify that both for working and design load we can consider the whole funation of structure. Use of modern design procedures is the way how to improve optimalization of design of structure from the point of view of reliability, serviceability and economy.

Verhalten von Kopfbolzen und Kühlrohren zur Linerverankerung

Behaviour of Headed Studs and Cooling Pipes in Liner Anchorage

Comportement de goujons et de tuyaux de refroidissement pour l'ancrage de tôles d'étanchéité

Wieland RAMM
Prof. Dr.-Ing.
Universität Kaiserslautern
Kaiserlautern, BRD

Prof. Ramm, geb. 1937, studierte Bauingenieurwesen an der TH Darmstadt und promovierte ebenda. Nach mehreren Jahren Tätigkeit im Ingenieurbüro und in einer großen Baufirma leitet er nun das Fachgebiet Massivbau und Baukonstruktion an der Univ. Kaiserslautern.

Joachim SCHEELE
Dipl.-Ing.
Universität Kaiserslautern
Kaiserlautern, BRD

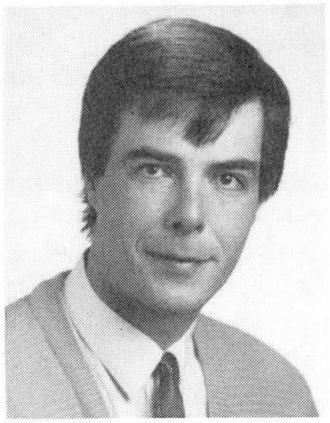

J. Scheele, geb. 1960, studierte Bauingenieurwesen in München und arbeitet zur Zeit als wissenschaftlicher Mitarbeiter im Fachgebiet Massivbau und Baukonstruktion der Universität Kaiserlautern.

ZUSAMMENFASSUNG

In diesem Beitrag wird über Versuche zur Ermittlung von Last-Verformungskennlinien von Verankerungsmitteln unter für Liner spezifischen Bedingungen berichtet. Das duktile Verhalten der untersuchten Verankerungen — einzelne Kopfbolzen, Gruppen von Kopfbolzen und Gruppen von Kopfbolzen und Kühlrohren — macht diese für die Aufnahme der formschlüssigen Beanspruchungen besonders geeignet.

SUMMARY

In this paper the results of experimental studies on the load-deformation-behaviour of liner anchorages under conditions specific for liners are described. The ductile behaviour of the examined anchorages—single headed studs, groups of headed studs and groups of studs and cooling pipes—makes them suitable for deformation controlled loading.

RÉSUMÉ

Cet article décrit les résultats d'essais effectués en vue de déterminer les lignes caractéristiques charge-déformation d'éléments d'ancrage sous des conditions spécifiques aux tôles d'étanchéité. Le comportement ductile des ancrages examinés — des goujons isolés, des groupes de goujons et des groupes de goujons et de tuyaux de refroidissement — les rend aptes à absorber tout particulièrement les sollicitations avec déformation contrôlée.

1. Einführung

Großbehälter, die mit nennenswerten Innendrücken beansprucht werden und die aus Sicherheitsgründen zugleich ein hohes Maß an Zuverlässigkeit und Dichtigkeit aufweisen müssen, lassen sich wirtschaftlich als Spannbetonbehälter ausführen. Beispiele hierfür sind Reaktordruckbehälter und Containments. Zur Gewährleistung der erforderlichen Dichtigkeit werden solche Behälter in der Regel mit einer innenliegenden Dichthaut aus Stahlblech, einem sogenannten Liner, ausgerüstet.
Normalerweise werden Liner über Kopfbolzendübel oder Rippenanker mit der Betonstruktur verbunden. Bei Reaktordruckbehältern sind zusätzlich oft betonseitig Stahlrohre auf den Liner aufgeschweißt, die primär zur Kühlung dienen. Sie können jedoch rechtwinklig zu ihrer Laufrichtung auch Lasten übernehmen, wenn in ihrer Nähe Anker angeordnet sind, die ein Herausziehen der Kühlrohre aus dem Beton verhindern.
Zur Auslegung des Liner-Anker-Systems werden die Last-Verformungskurven der Verankerungsmittel benötigt.
Nachfolgend soll über die beiden an der Universität Kaiserslautern durchgeführten Forschungsprojekte /1, 2/ zur Ermittlung der Last-Verformungskennlinien an einzelnen Kopfbolzendübeln und an Ankergruppen berichtet werden.
In mehr als einhundertfünfzig Versuchen zur Linerverankerung wurden dabei im wesentlichem folgende Punkte untersucht:

1. Das Verhalten von einzelnen Kopfbolzendübeln unter den für Liner spezifischen Bedingungen (Hochfester Beton, Vorspannung, Temperaturbelastung und zyklische Belastungen mit großen Amplituden) bei Belastung auf Abscheren.
2. Der Einfluß der Ankerabstände in einer Gruppe von Kopfbolzen
3. Das Verhalten von Ankergruppen aus Kopfbolzendübeln und Kühlrohren und die Einflüsse von Ankerabstand, Ankermuster und Vorspanngrad bei Belastung auf Abscheren.
4. Das Verhalten von Gruppen aus Kopfbolzendübeln unter kombinierter Schub-Zugbelastung, worüber jedoch an dieser Stelle nicht berichtet werden soll.

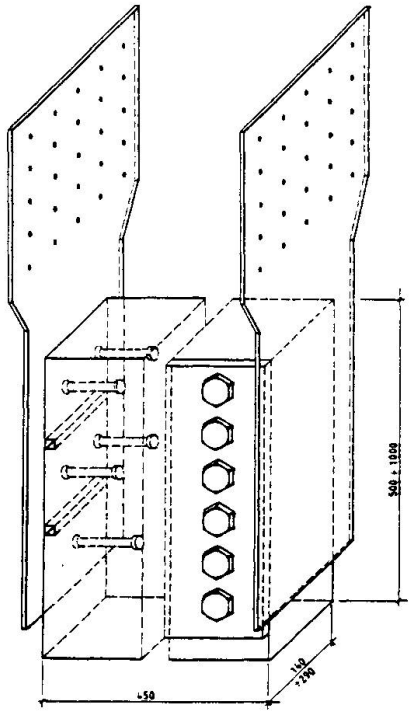

Bild 1: Versuchskörper

2. Versuchsaufbau und Versuchsdurchführung

Die Versuchskörper bestanden aus quaderförmigen Betonteilen, mit denen auf zwei Seiten ein Linerblech mittels der zu untersuchenden Anker verbunden war (Bild 1). Die Betonkörper wurden in beiden zum Linerblech parallelen Richtungen mit 20 N/mm^2 vorgespannt. In den Versuchen, in denen nur Bolzen untersucht wurden, wurde die obere Lasteinleitungsplatte, wie in Bild 2 dargestellt, direkt bis an das Linerblech herangeführt, während bei den Versuchen mit Kühlrohren ein Spalt zwischen Linerblech und Stahlplatte offen blieb, um dadurch den Effekt nachzubilden, den das im Bauwerk an dieser Stelle angeordnete nächste Kühlrohr haben würde.
Nach Aufbringung der Vorspannung wurden die Versuchkörper in einen Versuchsrahmen eingebaut. Durch schrittweises Erzeugen einer Relativverschiebung zwischen Beton und Linerstahl wurden die Anker auf Abscheren bis zum Bruch belastet.

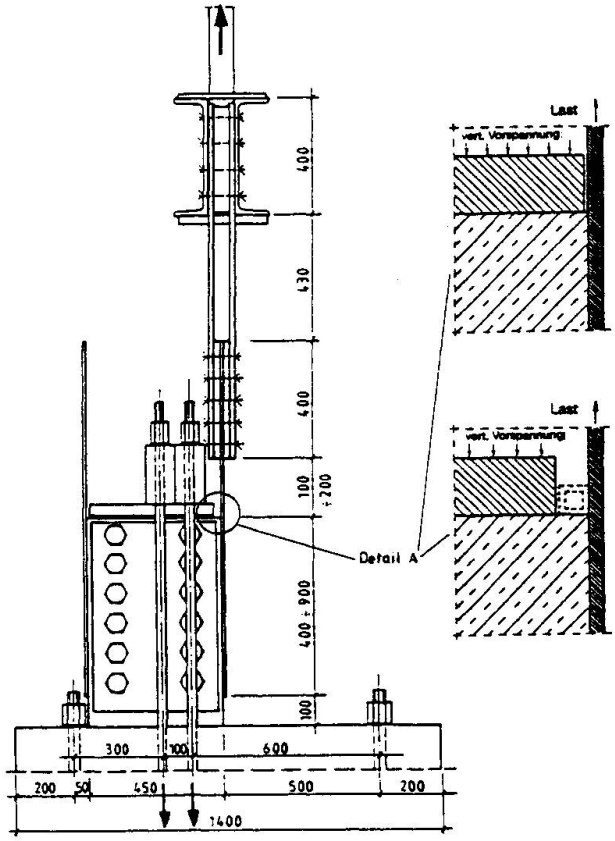

Bild 2: Versuchsaufbau

Die beiden Parameter Betondruckfestigkeit und Vorspanngrad waren schon in einer Serie von Vorversuchen zwischen 45 N/mm^2 und 65 N/mm^2 bzw. zwischen 20 N/mm^2 und Null variiert worden. Wegen der relativ geringen Einflüsse auf das Bolzenverhalten wurde in beiden Versuchsprogrammen durchgehend ein B55 verwendet. Die Vorspannung wurde aus dem gleichen Grunde nur in Verbindung mit der Untersuchung von kombinierten Ankergruppen variiert. Weiterhin wurde auf Grund der hinsichtlich der Bruchverschiebung nicht ganz zufriedenstellenden Ergebnisse der Vorversuche als Bolzenmaterial für alle weiteren Versuche anstatt des üblichen St 37-3 K ein St 37-3 K+N gewählt. Dies hatte bei nur geringen Verlusten in der Bruchlast einen deutlichen Gewinn bei der Bruchverschiebung zur Folge.

3. Ergebnisse der Versuche an einzelnen Kopfbolzen

Einen wesentlichen Bestandteil der Untersuchungen bildeten die Versuche bei erhöhten Temperaturen. Hierbei zeigte sich, daß mit einer Temperaturerhöhung eine Abnahme der Bolzensteifigkeit und der Bruchlast einherging (Bild 3). Entgegen den Erwartungen zeigte sich, insbesondere bei den Versuchen mit T=250^{0}C, eine deutliche Abnahme der Bruchverschiebung mit steigender Temperatur. Der Grund für dieses Verhalten dürfte unter anderem im Einfluß der Temperatur auf das Bolzenmaterial zu suchen sein. Hierzu sind jedoch noch weitere Untersuchungen nötig.

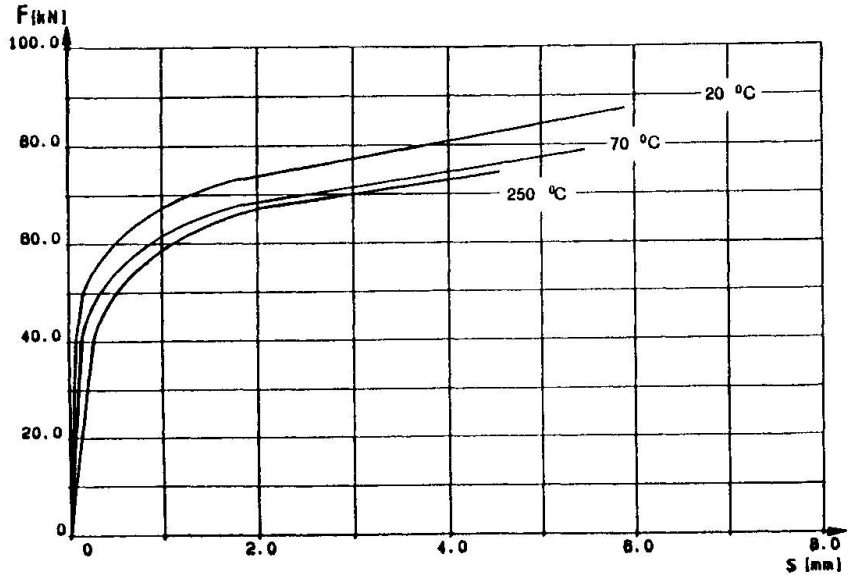

Bild 3: Einfluß der Temperatur auf die Kennlinie eines Bolzens

Weiterhin wurden zyklische Vorbelastungen und deren Einfluß auf das Bolzenverhalten untersucht. Bei den entsprechenden Versuchen wurden die Kopfbolzen zunächst bis zur nach DIN 25459 zulässigen Verschiebung (0.25 s_U) belastet und anschließend einer zyklischen Belastung unterzogen. Dabei wurden sowohl reine Schwellbelastungen als auch Zyklen mit wechseln-

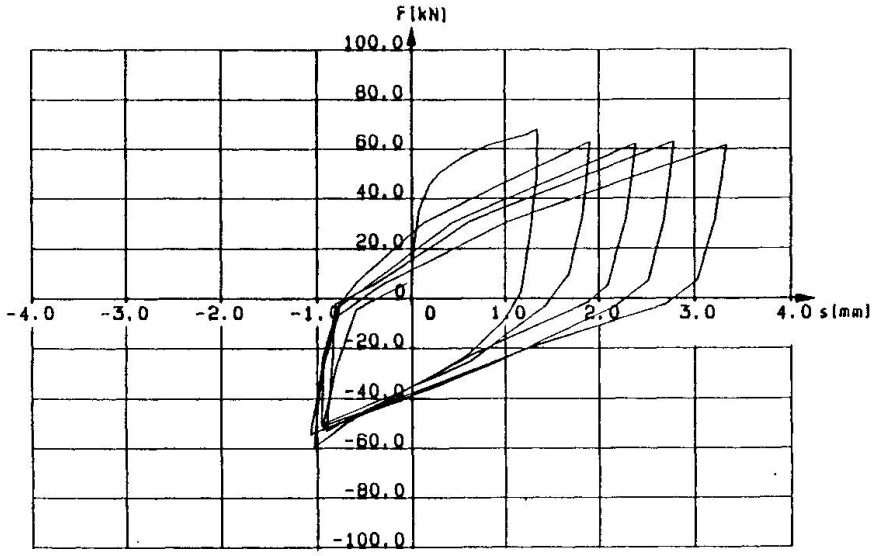

Bild 4: Kennlinie eines 5/8" Kopfbolzens bei zyklischer Belastung mit wechselndem Vorzeichen

dem Vorzeichen gefahren.
Bei der Schwellbelastung wurden bis zu 5000 Lastwechsel mit einer Amplitude von bis zu 75% der Bruchlast gefahren. Anschließend wurden die Versuchskörper kontinuierlich bis zum Bruch belastet. Abgesehen von einer während der zyklischen Belastung aufgetretenen relativ geringfügigen Verformungszunahme waren kaum Einflüsse der Schwellbelastung auf das Tragverhalten der Bolzen festzustellen.

Für die zyklische Belastung mit wechselndem Vorzeichen wurde die Amplitude auf etwa die 1,5fache Bruchlast vergrößert. Bei diesen Versuchen brachen die Bolzen schon nach wenigen Lastzyklen (Bild 4). Der Grund hierfür liegt darin, daß durch die konstant gehaltene Kraftamplitude die plastischen Verformungen des Bolzens sehr schnell zunahmen und so der Bruch eingeleitet wurde. Belastungen mit wechselndem Vorzeichen und derartig großer Amplitude sind daher unbedingt zu vermeiden. Jedoch lassen zyklische Beanspruchungen mit konstanten Verformungsamplituden eine sehr viel größere Anzahl von ertragbaren Lastwechseln erwarten. Dies soll in weiteren Versuchen noch geklärt werden, da konstante Verformungsamplituden auch der wirklichen Belastung eines Liners besser entsprechen.

In einer weiteren Serie von Versuchen wurde der Einfluß einer länger anstehenden Dauerbelastung in Kombination mit einer Temperaturbelastung untersucht. Dazu wurden die Versuchskörper zunächst auf die entsprechende Temperatur (70° C oder 120° C) aufgeheizt und anschließend innerhalb von zwei Wochen in vier Laststufen auf etwa 85% der zu erwartenden Bruchlast belastet. Diese Laststufe wurde ungefähr für weitere zwei Wochen gehalten. Danach wurde die Belastung bis zum Bruch gesteigert. Auch diese Belastungsweise brachte keine wesentlichen Veränderungen im Tragverhalten der Kopfbolzen.

4. Ergebnisse der Versuche an Verankerungsgruppen

In der ersten Serie der Versuche an Verankerungsgruppen wurde der Einfluß der Ankerabstände sowohl parallel als auch rechtwinklig zur Last auf eine Gruppe von Kopfbolzen untersucht. Die untersuchten Bolzenabstände betrugen 70 mm, 100 mm und 130 mm bei einem Bolzendurchmesser von 22 mm. Es zeigte sich, daß das Bolzenverhalten so lange unbeeinflusst blieb, wie sich die vor dem Bolzenfuß liegende Zone der Betonschädigung unbeeinflusst ausbilden konnte. Normalerweise erstreckt sich diese Zone auf etwa den 1,5fachen Bolzendurchmesser oberhalb und seitlich des Bolzens. In den Versuchen mit einem Bolzenabstand von nur 70 mm dehnte sich dieser Bereich

jedoch über den gesamten Bolzenzwischenraum aus, was eine merkbare Reduzierung der Bruchlast zur Folge hatte. Auch bei sehr kleinen Bolzenabständen rechtwinklig zur Lastrichtung ist eine solche Beeinflussung in Form einer Überschneidung der Betonschädigungszonen denkbar. In den durchgeführten Versuchen, die einen minimalen Bolzenabstand von 70 mm aufwiesen, trat dieser Effekt jedoch nicht auf.
Einflüsse auf die Größe der Bruchverformung wurden in den Versuchen nicht festgestellt.

Insgesamt drei Versuchserien befaßten sich mit dem Verhalten von kombinierten Ankergruppen aus Kopfbolzendübeln und Kühlrohren. Obwohl dabei sowohl die Vorspannung variiert wurde als auch Versuche ohne Vorspannung in Lastrichtung gefahren wurden, um einen freien Rand zu simulieren, treffen doch die meisten Ergebnisse für alle drei Versuchserien zu.
Das Verhalten von Ankergruppen, die aus Kopfbolzendübeln und Kühlrohren bestehen, wird von dem Verhalten des in Lastrichtung jeweils vor den Kühlrohren liegenden Betons dominiert. Die Versuche versagen in den meisten Fällen durch Abscheren des Betons in einer zu dem Linerblech parallelen Ebene.

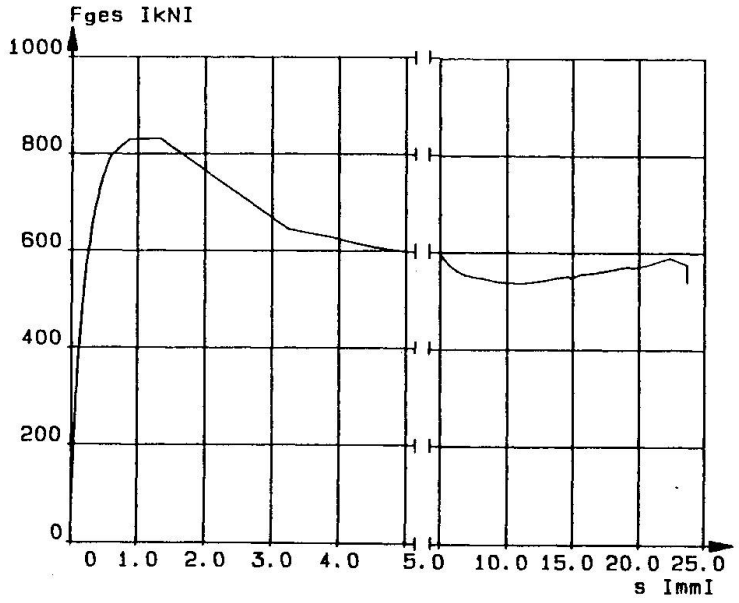

Bild 5: Typische Kennlinie einer kombinierten Verankerung

Die Kennlinie einer solchen kombinierten Ankergruppe (Bild 5) kann in vier Teile unterteilt werden:

1. Bis zu etwa 75% der Maximallast besteht eine nahezu lineare Beziehung zwischen Last und Verformung.
2. Anschließend nimmt die Krümmung mehr und mehr zu, bis die Maximallast erreicht ist.
3. Mit Erreichen der Maximallast versagt der vor den Kühlrohren liegende Beton. Dies geschieht jedoch nicht schlagartig wie bei dem Versagen eines Kopfbolzendübels, sondern spielt sich in einem Zeitraum von mehreren Sekunden ab.
4. Nach weiterer langsamer Lastabnahme stabilisiert sich die Last und die Verformungen nehmen stark zu. Bei Verformungen von bis zu 30 mm wird ein zweites Lastmaximum erreicht, das in seiner Größe vom Verhältnis der Tragfähigkeiten von Bolzen und Betonscherflächen abhängig ist. Kurz darauf versagt der erste Bolzen.

Die Tragfähigkeit einer kombinierten Ankergruppe resultiert aus verschiedenen Lastabtragungsmechanismen. Es konnte festgestellt werden, daß bei Berücksichtigung von drei verschiedenen Lastabtragungsmechanismen eine ausreichende Genauigkeit bei der Vorhersage der Maximallast erreicht werden kann. So reicht es aus, nur den Beton zwischen zwei Kühlrohren, über dem obersten Kühlrohr und die Bolzen zu berücksichtigen, während verschiedene Ankeranordungen, die Position eines Bolzens in einem Ankermuster, der Bolzenabstand und der Kühlrohrabstand nicht berücksichtigt werden müssen.

Zwischen zwei Kühlrohren wurde der Beton in allen Versuchen abgeschert, wobei eine maximale Scherspannung von etwa 5 N/mm^2 erreicht wurde. Waren die Versuchskörper auch in der Richtung parallel zur Last vorgespannt, so trug die Betonscherfläche oberhalb des oberen Kühlrohres die gleiche Spannung. Bei den Versuchen, in denen ein freier Rand simuliert werden sollte, konnte diese Betonscherfläche nur eine reduzierte Scherspannung von etwa 1,5 N/mm^2 übertragen. Die verwendeten Kopfbolzen mit 22 mm und 16 mm Durchmesser trugen beim ersten Lastmaximum Lasten von etwa 115 KN bzw. 68 KN.
Die Verformungen zwischen Beton und Liner lagen an dieser Stelle zwischen etwa 0,8 mm und 1,3mm, was recht gut den Werten entspricht, die in den Versuchen mit einzelnen Kühlrohren an der Ruhr-Universität Bochum /3/ gefunden wurden. Dabei hatten im wesentlichen zwei Parameter einen Einfluß auf die Größe der Verformung:

1. Bei Verwendung von 16 mm Bolzen erreichten die Verformungen beim ersten Lastmaximum nur etwa 80 % der Werte für 22 mm Bolzen.
2. Es liegt eine Tendenz vor, nach der die Verformungen beim ersten Lastmaximum bei einer Verringerung des Kühlrohrabstandes abnehmen.

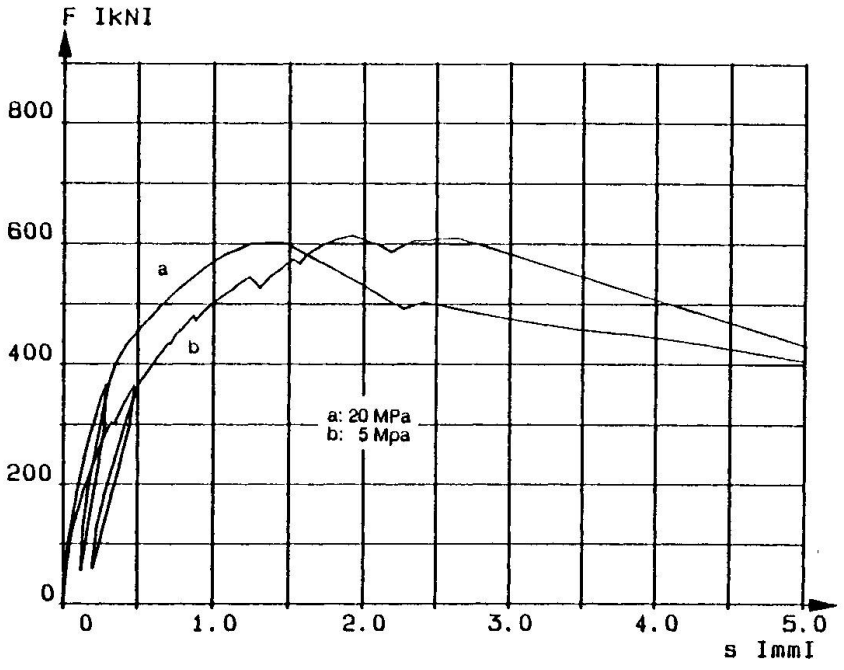

Bild 6: Einfluß der Vorspannung auf eine kombinierte Verankerung

Ein Vergleich von ansonsten identischen Versuchen mit unterschiedlicher Vorspannung, jedoch ohne Simulation eines freien Randes, zeigte, daß die Vorspannung keinen großen Einfluß auf das generelle Verhalten der Versuchskörper hat. Jedoch vergrößerten sich die Verformungen beim ersten Lastmaximum bei einer Reduzierung der Vorspannung von 20 N/mm^2 auf etwa 5 N/mm^2 um bis zu 50 %, während die Steifigkeit im Anfangsbereich auf etwa 50 % der vorherigen Werte abnahm.

5. Literatur

1. RAMM W., SCHEELE J., Ankerkennlinien zur Linerverankerung. Versuchsbericht, Universität Kaiserslautern, Fachgebiet Massivbau und Baukonstruktion, April 1987

2. RAMM W., SCHEELE J., Ankerkennlinien-Gruppenversuche zur Linerverankerung. Versuchsbericht, Universität Kaiserslautern, Fachgebiet Massivbau und Baukonstruktion, Mai 1989

3. STANGENBERG F., BAUSCH S., Versuche an betonverankerten Kühlrohr-Liner-Verbindungen zur Ermittlung von Ankerkennlinien. Versuchsbericht, Ruhr-Universität Bochum, Lehrstuhl für Stahlbeton- und Spannbetonbau, 1987

Application of Composite Members to Marine Structures in Japan

Utilisation d'éléments mixtes dans les structures marines au Japon

Anwendung der Verbundbauweise für Meeresbauten in Japan

Osamu KIYOMIYA
Chief
Port and Harbour Res. Inst.
Yokosuka, Japan

Osamu Kiyomiya, born 1948, received his Dr. Eng. degree at Tokyo Institute of Technology, Tokyo. For seventeen years he was involved in structural problems in port and harbour areas. Osamu Kiyomiya, now chief of structural mechanics laboratory, is conducting research on structural analysis of port and harbour facilities.

Hiroshi YOKOTA
Senior Res. Eng.
Port and Harbour Res. Inst.
Yokosuka, Japan

Hiroshi Yokota, born 1955, received his M.Sc. (Eng.) degree at Tokyo Inst. of Techn., Tokyo. For ten years he was involved in structural problems in port and harbour regions. Hiroshi Yokota, now a senior research engineer of the structural engineering division, is conducting research on design and construction methods of composite port and harbour structures.

SUMMARY

Composite structures combining steel an concrete have been applied to port and harbour facilities in Japan since the early 1980s. Composite structures have such superior merits as high strength, high rigidity, watertightness, light weight, and rapid construction in marine areas. This paper presents the outline of some facilities made of composite structures and their design. The facilities described herein are a floating type breakwater, a gravity type seawall, and an undersea tunnel.

RÉSUMÉ

Depuis le début des années 1980, les éléments mixtes acier-béton ont été introduits au Japon dans les installations portuaires. Les éléments composites possèdent, dans un environnement marin, des caractéristiques remarquables telles que résistance élevée, haute rigidité, étanchéité à l'eau, faible poids et mise en place rapide. Cet article présente les méthodes de conception et les grandes lignes de quelques-unes des installations portuaires réalisées avec des éléments mixtes. Les installations décrites sont un môle flottant, une digue et un tunnel sous-marin.

ZUSAMMENFASSUNG

Seit Anfang der 80-er Jahre sind Verbundelemente aus Stahl und Beton für Hafen- und Meeresbauten in Japan verwendet worden. Verbundelemente haben in Meeresbereichen große Vorteile wie z.B. große Steifheit, Wasserdichtheit, geringes Gewicht und kurze Bauzeit. Dieser Beitrag gibt einen Überblick über einige aus Verbundelementen hergestellte Bauwerke und ihre Entwurfsmethoden. Bei den hier behandelten Bauwerken handelt es sich um einen schwimmenden Wellenbrecher, eine Küstenschutzmauer vom Schwerkrafttyp und einen Untermeerestunnel.

1. INTRODUCTION

Structural members composed of steel and concrete have been widely used in land facilities for many years. Those members exhibit merits of both materials. In marine facilities, structural members composed of steel plates and concrete began to be introduced around the early 1980s in Japan. Some port and harbour facilities have been constructed with those composite members since then. This paper presents the mechanical characteristics of composite structures in marine circumstances and the outline of structures and design methods of actual marine facilities, a floating type breakwater, a gravity type seawall, and an undersea tunnel.

2. STRUCTURAL CHARACTERISTICS

Composite structures of steel plates and (reinforced) concrete are schematically depicted in Figure 1. Two types of structure have considerable potential in marine areas, that is, an open-sandwich structure and a sandwich structure. The open-sandwich structure has both a plated and a concrete surfaces, and the sandwich structure has two plated surfaces. In both types of structures, steel plates carry tensile forces and reinforcing bars, steel plates and concrete carry compressive forces. This load-carrying mechanism is the same as that of an ordinary reinforced concrete structure.

To make sure this mechanism, steel and concrete should be joined tightly by a appropriate method. Natural bond forces between steel and concrete may be expected, but they are rather small. Shear connectors are generally applied to carry shear and pull-off stresses between them. Headed studs are most popular as the shear connector. Besides studs, many kinds of shear connector have been examined, and channels, angles, T-shapes, etc. will be introduced in port and harbour facilities. These make it possible to stiffen the steel plate and to result in reducing form and false work.

Basic mechanical characteristics of a composite structure will be roughly mentioned.

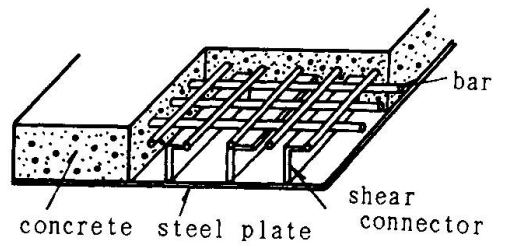

(a) open-sandwich structure

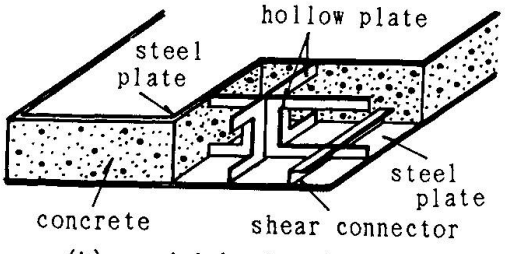

(b) sandwich structure

Figure 1 Composite structures

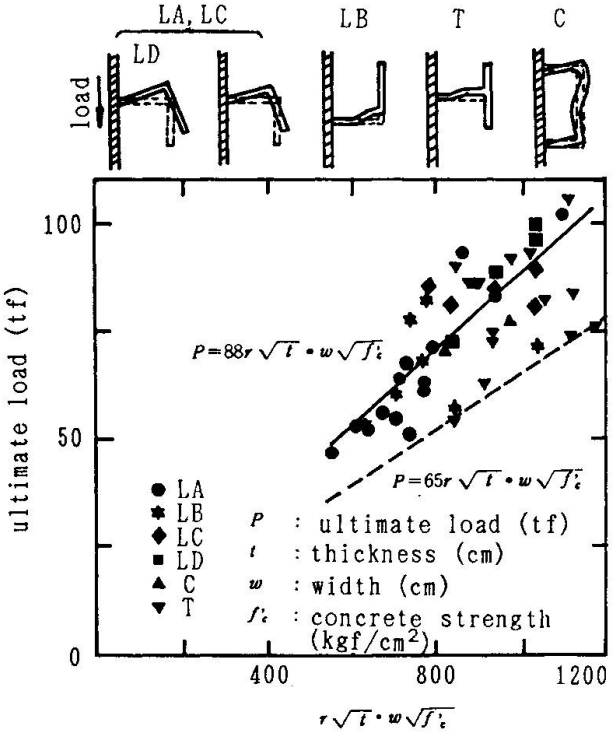

Figure 2 Load-carrying capacity of shear connectors

2.1 Shear connectors

Shear connectors will be designed due to induced shear forces between the two materials. The mode of failure and load-carrying capacity of shape steel shear connectors which have been obtained by push-off tests [1] are shown in Figure 2. Shape and direction of the shear connector and the strength of concrete had great effects on them.

2.2 Flexure and shear strength

The composite structure subjected to flexure may be designed as if it were an ordinary reinforced concrete. That is, the steel plate can be considered to be a reinforcing bar with the same cross sectional area. Loading tests on composite beams [2] showed that cracks concentrate at the tip of shear connectors and their widths become large, as depicted in Figure 3.

Excessive cracks can degrade the durability and the watertightness of the member in marine areas. Furthermore, these cracks may cause shear failure. Stirrups can be applied to the composite structure and they have to be welded the steel plate. Besides stirrups, long J-shaped reinforcement should prevent shear failure. The design for the shear reinforcement can be made on the assumption that the shear resisting mechanism is principally the tied-arch action [2] as shown in Figure 4. On that occasion, adequate shear reinforcement should be supplied and effective depth and shear span length should be modified due to the presence of the shear connectors.

2.3 Buckling

Buckling has to be examined when the steel plate exists on the compression side. If buckling will not occur, a composite structure behaves with excellent

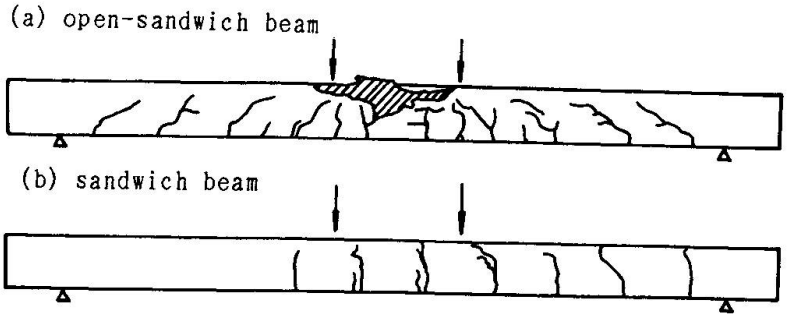

Figure 3 Crack formation

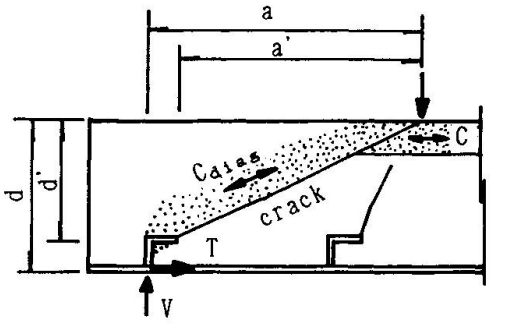

Figure 4 Shear resisting mechanism

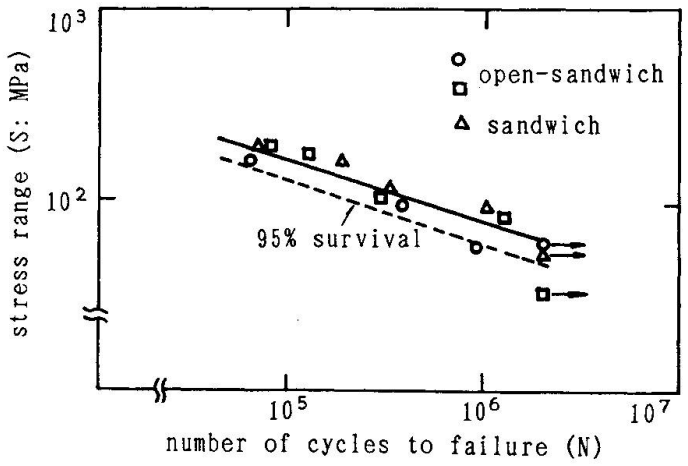

Figure 5 S-N relationship of steel plates

ductility. The interval of the shear connector relates to buckling strength of the compressive steel plate. This may be examined by Euler's formula.

2.4 Fatigue endurance

In the composite structure, many reinforcing bars and shear connectors which are welded to the steel plate may cause fatigue failure. On the basis of the experimental results undertaken by the authors [3], fatigue strength of the composite structure is considerably smaller than that of an ordinary reinforced concrete. Under repeated loads, the tensile steel plate may be broken by its fatigue. An empirical S-N relationship of the steel plate in the composite structure subjected to flexure is shown in Figure 5. Using this relationship and sea waves near Japan, the Miner-sum is calculated to be 0.28, and this indicates that the possibility of fatigue failure could be small.

2.5 Connections

L and T connections of the composite structure have been tested [4]. The yield of the tensile steel plate causes to collapse the open-sandwich structure and the buckling of the hollow diaphragm and the crushing of concrete occur in the sandwich structure. The structural details at these connections are being examined.

3. ADVANTAGES IN MARINE AREAS

The composite structure is expected to have the following splendid performance in marine areas, while its structural mechanism and characteristics are trying to make clear:

- Excellent mechanical behaviours

This structure has high strength and rigidity. Thus, thin section may achieve its required behaviours. This makes it possible to construct a complicated facility and to have many varieties of its size and shape. Furthermore, light weight is advantageous for the structures constructed on soft sea mud.

- Watertightness

The outer steel plate prevents sea water from leaking when cracks form. This contributes to a floating structure and an undersea tunnel element.

- Rapid construction

Bar installment, form work, and false work may be very much reduced. Skilled workers on such works are not essential to fabricate a structure. Furthermore, each structural element can be fabricated in a factory, that is, a prefabricated structure. This can cut down the construction period on the site, often on the sea.

- Total costs

Although material cost is not always low because of high price of steel, total cost can be reduced due to rapid construction, small energy consumption on fabricating, and so on.

A structure which has high potential and performance and is made with reasonable cost is required for future marine development. Two alternatives in composite port and harbour structures are the open-sandwich and the sandwich ones. For the open-sandwich structure, concrete is directly exposed to sea water and the steel plate is not. That is, durability of the structure may not be serious when concrete cover thickness to embedded steel bars and the maximum crack width are paid attention in design as well as for an ordinary reinforced concrete. On the other hand, for the sandwich structure, the steel plate is suffered from sea wave attack. In particular, special attention has to be paid prior to application in

severe circumstances such as in the splash zone. Heavy protection such as cathodic protection is essential. In the circumstances that always submerged in sea water, little oxygen is supplied and less possibility of corrosion.

4. EXAMPLES OF APPLICATION

4.1 Floating breakwater

A floating type breakwater is intended to prevent port and harbour areas from wave invasion by floating bodies which are moored to the sea bed by chains. This type of breakwater is adopted in large depth of water and mild wave condition. Floating type breakwaters have often been constructed in small ports and harbours, particularly fishing ports. The floating breakwater presented herein is constructed at Hiroshima, south-west of Japan, which is against tidal waves as shown in Figure 6. This breakwater consists of six pontoons, which are fabricated by prestressed concrete and the composite structure with steel and concrete. Each pontoon is 60 through 70 m long, 10 m wide, and 3 m high. Prestressing forces also enable to attain watertightness and light weight. Longitudinal prestressing stress is 4.7 MPa. Main forces acting the pontoon are wave forces and water pressures. Ultimate, serviceability, and fatigue limit states are examined using the design wave of 30 years return period. Neoprene rubber coating is applied to the surface of the pontoons for certain water-tightness.

4.2 Gravity seawall

A gravity type seawall to which the open sandwich structure is applied will be

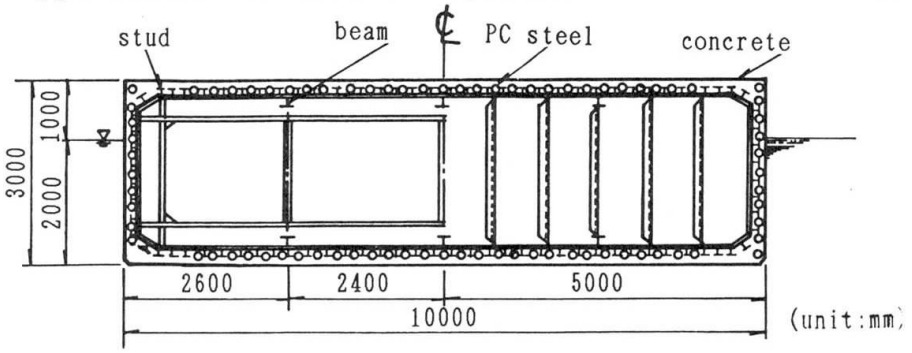

Figure 6 Cross section of the floating body

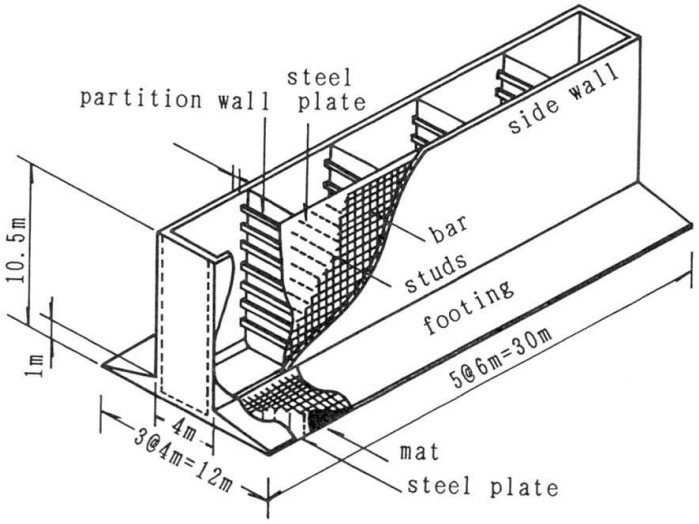

Figure 7 Details of the caisson

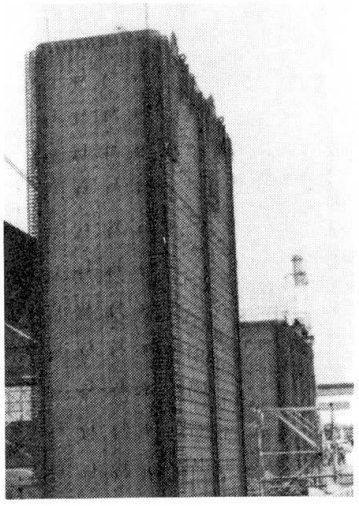

Figure 8 Steel plates and studs

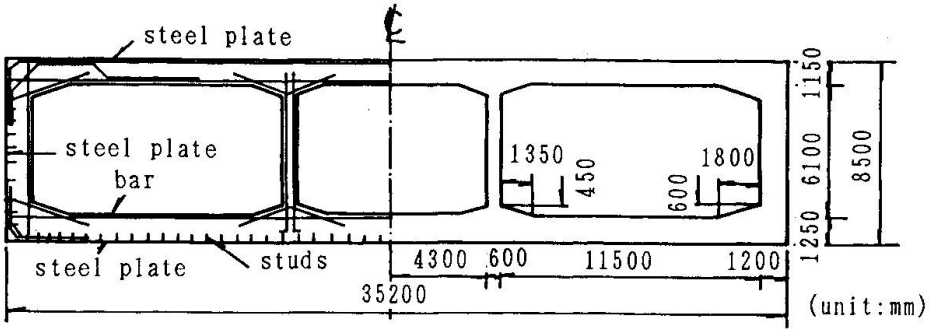

Figure 9 Cross section of the tunnel element

introduced. This seawall is located in front of reclaimed lands at Yokohama, near Tokyo. The schematic view of the breakwater caisson and its sizes are shown in Figure 7. The fundamental size of the caisson is 20 m long, 6 m wide, and 14.9 m high. The bottom slab, 40 cm thick, is made of the open-sandwich structure. The steel plate, 6 mm thick, is used at the bottom surface and composed to surrounding concrete by headed studs. The partition wall is made of a steel plate itself of 8 mm thick with stiffeners. The composite bottom plate makes it possible to enlarge the length of footings, which results in light weight of the whole structure. This caisson is designed according to the present specification which has been applied to an ordinary reinforced concrete seawall. The load-carrying capacities of the footing, L and T connections between walls and the slab have been examined by static loading tests at a laboratory. The caisson at the fabrication in a dock is shown in Figure 8.

4.3 Undersea tunnel

An undersea tunnel will be constructed to link lands separated by a river or a channel in port and harbour areas. They are usually constructed by reinforced concrete and/or steel shells. In Osaka port, the construction of an undersea tunnel is now in progress. This tunnel, 2700 m long, is made by ten composite elements. The walls and slabs are made of open-sandwich structure as shown in Figure 9. In ordinary methods of construction them, outer steel plates are used only for watertightness, that is, they have no structural elements. When outer steel plates are used both for watertightness and structural elements, they have enough strength, and leads to light weight and economical. Here, these steel plates directly touches the sea water action, and should be degraded by corrosion. Thus, cathodic protection and other effective countermeasures may be applied to reduce the danger of corrosion and subsequent failure.

REFERENCES

1. Kiyomiya, O. et al., Strength Properties of Shear Connectors by Shape Steel. Transactions of the Japan Concrete Institute, Vol.8, 1986, pp.345-352.
2. Yokota H. and Kiyomiya O., Effect of Shear Reinforcement on the Ultimate Strength of Steel-Concrete Composite Beams. Transactions of the Japan Concrete Institute, Vol.9, 1987, pp.373-380.
3. Yokota H. and Kiyomiya O., Fatigue Behaviours of Steel-Concrete Hybrid Beams. Transactions of the Japan Concrete Institute, Vol.11, 1989, pp.455-462.
4. Kiyomiya O. and Yokota H., Strength of T-Shaped Connection of Steel-Concrete Hybrid Members. Proceedings of The 2nd Symposium on Research and Application of Composite Constructions, Japan Society of Civil Engineers, Kobe, September 1989, pp.75-80 (in Japanese).

Reliability Prediction for Steel Concrete Composite Bridges

Diagnostic de la fiabilité des ponts mixtes acier-béton

Sicherheitsprognose von Brücken in Verbundbauweise

N. NOVOZHILOVA
Professor
Leningrad, USSR

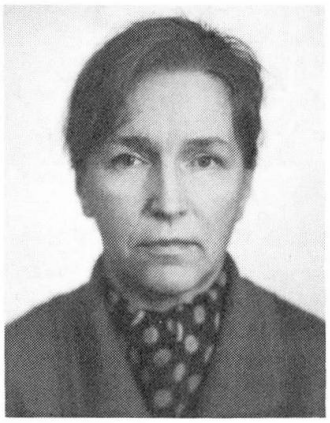

N. Novozhilova, born 1924, graduated from the Novosibirsk transport engineering institute. She was the chief of reliability laboratory at the Leningrad bridge research institute till 1978, then the chief of the bridges section in Leningrad building-engineering institute, since 1989 she is a professor.

V. BISTROV
Cand. Eng. Sc.
Leningrad,. USSR

V. Bistrov, born 1938, graduated from the Leningrad building-engineering institute, then worked as an engineer in the field of bridge construction and tunnels, since 1969 he was involved in problems of improvement of steel concrete bridges and their reliability. In 1989 he was elected the chief of the bridges section in Leningrad building-engineering institute.

SUMMARY

The paper considers the spectrum of unstationary loading by applying live testing and operating loads to steel concrete composite continuous girders of highway bridges. The article interprets theoretically some experimental laws obtained. The analysis of the actual stress-strain state was done and the key details which are responsible for the bridge structures fatigue failure and reliability were established.

RÉSUMÉ

On a examiné les spectres du chargement non stationnaire des travées continues de ponts-routes de type mixte acier-béton, par mise en place des charges de service et des surcharges d'essai. On donne une interprétation de quelques lois expérimentales en découlant. On a présenté l'analyse de l'état réel des contraintes et des déformations; on a en outre établi les données-clés responsables de la fiabilité et de la rupture à la fatigue des structures de pont.

ZUSAMMENFASSUNG

Das Spektrum der beweglichen Lasten auf Durchlaufträger in Verbundbauweise bei Autobahnbrücken wird behandelt. Einige Versuchsresultate werden theoretisch begründet. Die vorhandenen Spannungen und Dehnungen, welche für die Ermüdungssicherheit massgebend sind, werden ermittelt.

A considerable number (morethan 110 units) of operated steel concrete composite bridges with continuous girders and the free beams within span-length range from 33 to 147 metres were tested in field and their stressed-strained state was investigated by using of theoretical-design methods realized by means of electronic computers. It resultedinthe most dangerous members and the "key details" which are responsible for structure's fatigue failure and reliability were established.

Those structure's characteristics depends on the properties of materials, the types of joints, the design standards and the quality of work. Above mentioned bridge structures were designed in according to the USSR normative documents and standard projects which have been applying for 1950-1990 years. Some of them were adapted to the particular local conditions.

The serviseability resources for the bridges can be estimated most completely by assessing of unstationary load effect with dynamic components selected out and studying of operating loading conditions. But this estimation also depends on spatial working of wide bridges either on features of bridge deck constructions.

It has been established in our previous studies [1... 4] that particular attention should be given to the most dangerous parts of construction such as the steel beam lower flange within zones of assembly joints, the upper flange extanded within zones with negative values of bending moments for continuous girders and also the zones with variable signs of efforts (fig.1,e,2-2). The reinforced concrete slab in these zones of composite bridge arouses an especial interest for it's working and for a stressed-state of reinforcement. The efforts in slab members can be increased considerably because of rough carriage way, impact factors of expansion joints and others.

Inspite of the fact that theoretical and experimental data confirming a considerable safety margin for standard reinforced concrete slabs from static loads was obtained recently, it is the slab which often determins the serviceability resources for absolute majority of composite bridges [1,2]. This fact is explained by not only concrete slab working together steel beam, but also by its working under local loading. Besides that the slab is subjected various environmental effects during its lifetime protecting the steel girders from this effect or taking it easer.

The results obtained by testing of two continuous composite girders of big bridge across the river Shelon built in 1963 are shown in diagram of stress probability density. (fig.1...3). She places of installations electric resistance gauges are maked with letter "D" in diagram.

The girders with riveted and welded joints made with R_{yn}=350 MPa steel adjointed the slab made of concrete B 30 exept zones above the piers by means of stiff connectors. The thickness of slab varies from 0,14 to 0,21 metres.

7 heavy trucks "CAMAZ"-5511" weighing from 190 to 192 kN were used as a testing load. They moved in columns in according to the test programm with velocities V=5,56 + 16 m/s. with intervals between them from 30 to 100 metres.

The rough sirface of carriage way was simulated in order to obtain the frequency of stress distribution. Unevenness was created

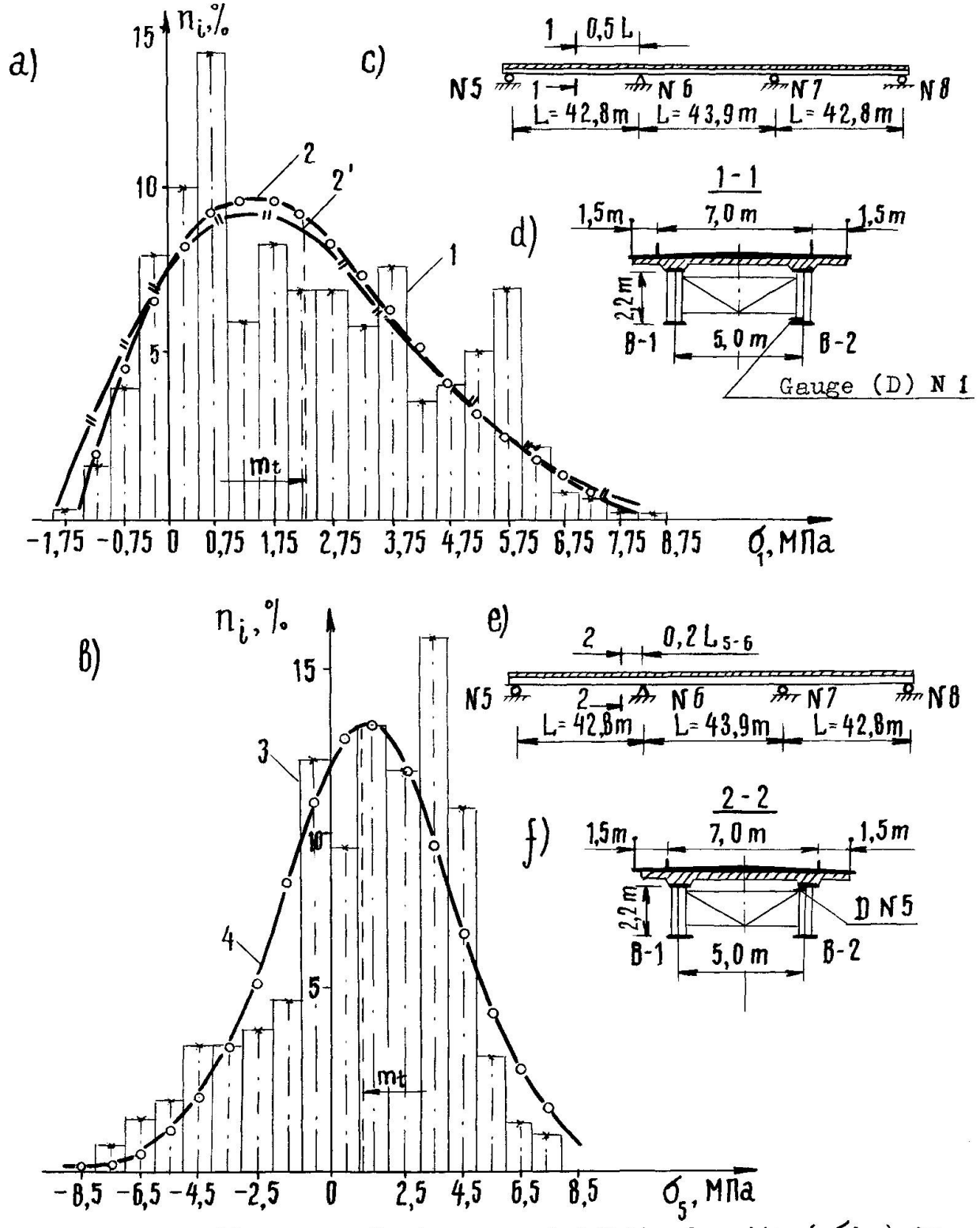

Fig.1. The diagrams of stress probability density (σ_i) in the lower (a, section 1-1) and upper (b, 2-2) flanges of the bridge girder: 1,3 - in according to the experimental data; 2, 2', 4- the theoretical curves for the destribution Vaybull, Relay laws and normal; c,e and d,f - the diagrams and cross-section of structures.

by means of placing wooden planks 150x50 mm. Besides the currents of transit transport passing across the bridge in operating order were used also as a dynamic load.

The live load accounted for 88% for the design load and caused the maximum deflection equal 34 mm (1/1260). The constructive corrections for stresses from static load for considered sections didn't exceed the value equal one.

The oscillograms were treated by means of electronic analyser F-014. The obtained data were storedoncomputer to establish their probability characteristics. The dynamic characteristics of composite girders according to various velocities V(5,56-16 m/s) were established. The dynamic coefficient $(1+\mu)$ varies from 1,26 to 1,80; the free oscillation frequency ω_0 from 2,87 to 3,33 Hz; the repetition time of free oscillation from 0,348 to 0,298 s; the logarithmic decrement of attenuation δ from 0,50 to 0,65.

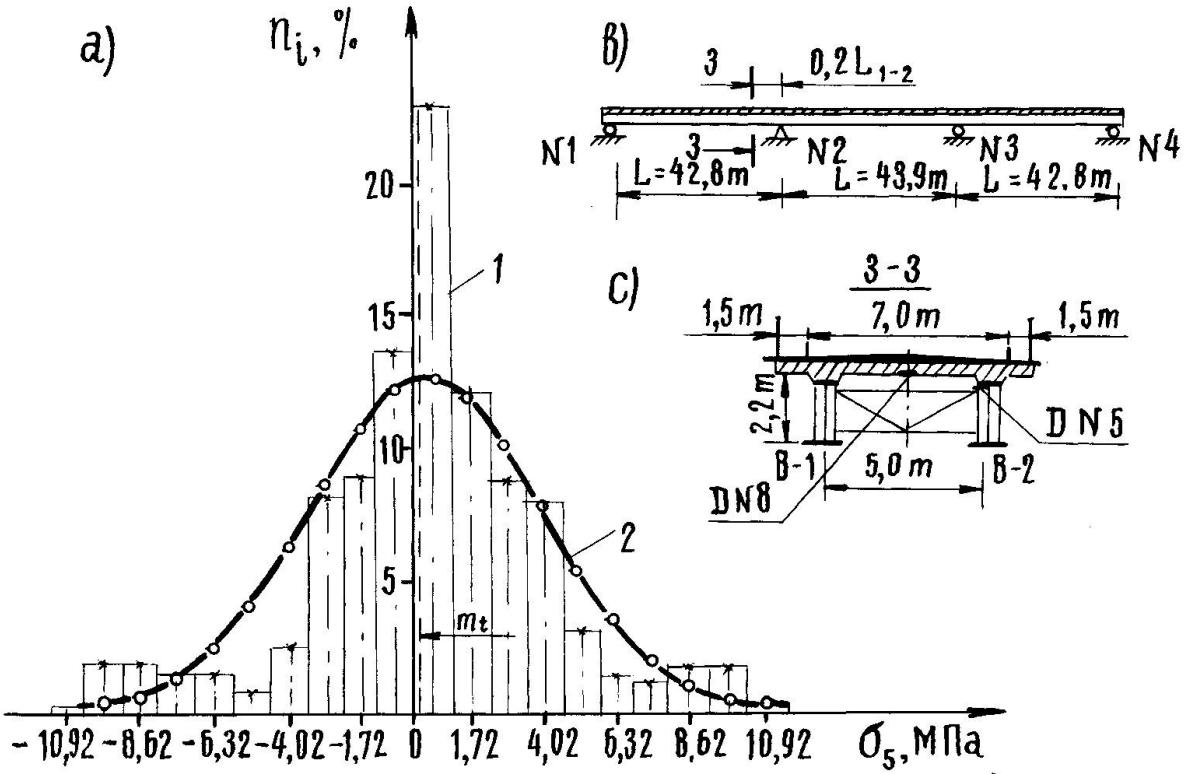

Fig.2. The diagram of stress probability density (δ_i) in the upper flange of the bridge girder B - 2 in the span L_{1-2} (section 3-3): 1 - in according to the experimental data; 2 - the theoretical destribution normal law.

As it was the velocity 5,56 m/s, that caused the maximum stresses, the represented diagrams describes, the truck passage both along the upstream part (fig.1) and along two parts (fig.2) of carriage way with velocity 5,56 m/s mainly. The maximum measured tensile stresses in the lower flange of the girder B-2 in the span L_{5-6} from the testing load (fig.1,a) don't exceed 9 MPa. The mathematical expectation of approximative curve m_t=2,35 MPa; the standard deviation δ_t=2,13 MPa; while the maximum stress from the design static load in this section totals 215,5 MPa. In fact the stresses in that section change from 224 to 214 MPa with the asymmetry cycle coefficient ρ =0,90...0,95.

The upper flange within section 3-3 shown in fig.2B works practically in symmetrical cycle both from the column of testing load (fig.1,b) and from the current of transit traffic loads (fig.2,a). The measured stresses can be approximated by the law of normal distribution, but the stress amplitude from transit traffic was greater and equal ±10,925 MPa. It resulted in the strong asymmetry cycle coefficient equal =-0,40 taking into account the load in the most dangerous case.

It can be derived from the represented studies, that various loading considerably influences the upper flange work in the zone with negative values of bending moments for continuous composite girders especially when the connection between the reinforced concrete slab and the steel girder doesn't work.

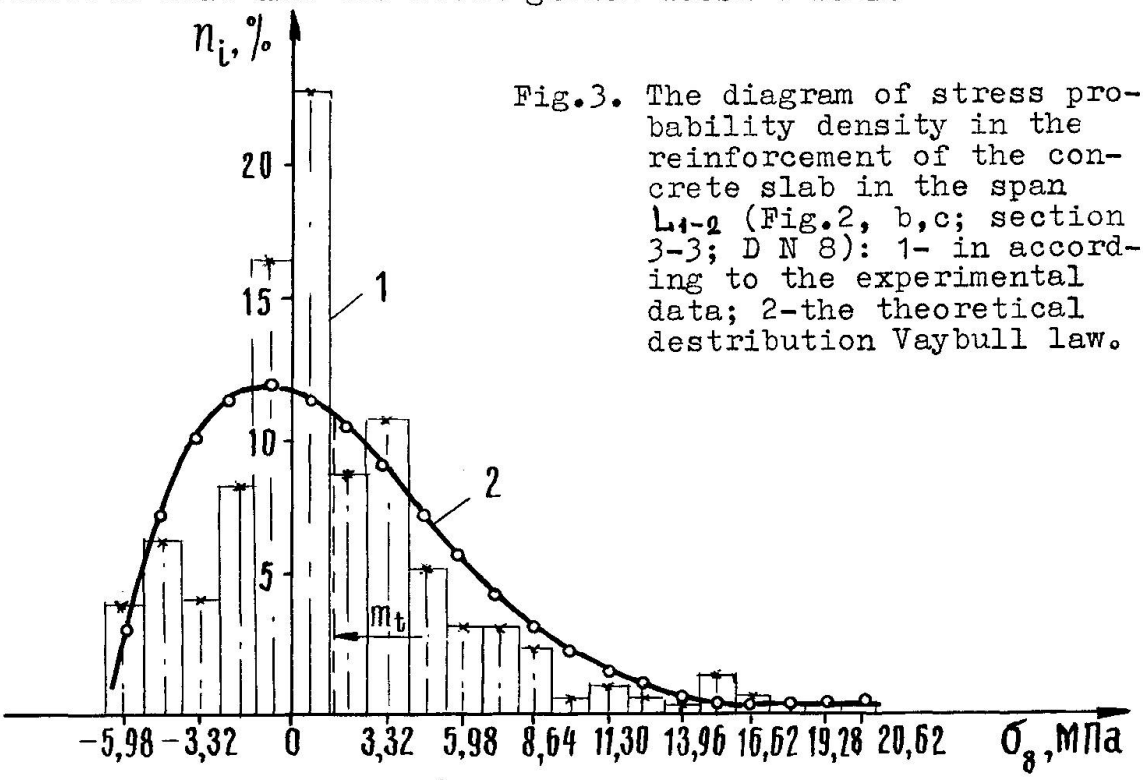

Fig.3. The diagram of stress probability density in the reinforcement of the concrete slab in the span L_{1-2} (Fig.2, b,c; section 3-3; D N 8): 1- in according to the experimental data; 2-the theoretical destribution Vaybull law.

The obtained stress destribution in the extanded slab reinforcement for section 3-3 is shown in fig.3. There was used the same load as for the girder upper flange. The asymmetry experimental diagram is approximated by Vaybull destribution low with the mathematical expextation m_t=1,49 MPa and the standard deviation σ_t=4,61 MPa. It shows high-stressed slab work under dynamic local loading. The tensile stresses in the reinforcement from the permanent load were equal 11,9 MPa while they were changed from 32,5 to 5,9 MPa from live load. The coefficient ρ =0,18 is close to the pulsating cycle wich is unfavourable for the reinforced concrete structure fatique. It is the value of coefficient which causes the most rapid loss of the slab safety margin inspite of the fact that the stresses in the reinforcement don't amount to the fatigue limit.

It can be pointed out that the considered analysis results of composite girders reliability correspond to an average statistical structure and don't take into account both the real values of the stress concentration coefficient β for joints and the possibility of their increasing because of some defects. This correc-

tion was provided by carefull monitoring and surveillance of every individual considered structure.

The serviceability resources estimation for the composite girder can be established by using the formula T/T_e expressed in cycle units [3]. However the approximation law should be corrected as this formula was derived by means of the law of normal stress destribution.

$$\frac{T}{T_e} = \frac{N_o e^{b\sigma_o}}{\sqrt{2\pi}\, b\sigma_t e^{0,5(b\sigma_t)^2}\left[\Phi(\sigma_{max}/\sigma_t - b\sigma_t) + \Phi(b\sigma_t)\right] + 1} \qquad (1)$$

where $\Phi(\sigma) = 1/\sqrt{2\pi}\int_0^{\sigma} e^{-u^2/2}du$ - the Laplas function calculated by the tables;

σ_t - the standard deviation of the stress destribution probability curve;

N_o, b, σ_o - the experimental parameters depending on the joint type and the durability of steel, for example for the assembly joint of the girder flange $N_o = 0,886 \times 10^6$ cycles; $b=0,296$; $\sigma_o = 187,0$MPa;

σ_{max} - the maximum stress, MPa;

T_e - the effective repetition time for the process with the appointed frequency ω is equal $T_e = 2\pi/\omega$.

1. Bistrov V.A. The improvement of the structures and designs of the steel concrete composite bridges.- L.: The Leningrad University publishing house, 1987. -185 p.

2. Novozhylova N.I., Bistrov V.A., Shayckevich V.L. The reliability prediction for the steel and composite bridge structures: the educational texbook. L.:LISI, 1989.-86 p.

3. Novozhylova N.I. The metal fatigue of the bridge structures and the methods of its calculation: the educational texbook. L.: LISI, 1985.-86 p.

4. Bistrov V.A. The loading regimes of the steel concrete composite highway bridges with the aim of estimation of its reliability // The problems of bridge structures reliability: The science works collection. L., 1984. p.16-23.

Stress Transfer from Steel Beams to Reinforced Concrete Columns

Transfert de contraintes des poutres d'acier vers les poteaux en béton armé

Kraftübertragung von Stahlriegeln auf Stahlbetonstützen

Yasushi NISHIMURA
Lecturer
Osaka Inst. of Technology
Osaka, Japan

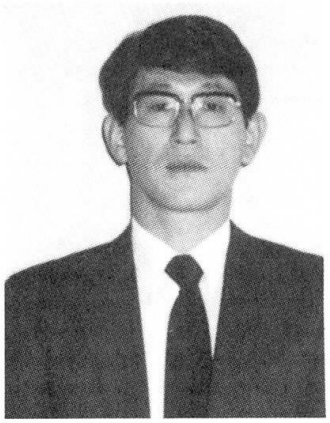

Graduated from Osaka Institute of Technology, Japan, in 1973. Since 1984, he has been Lecturer at Osaka Institute of Technology. His research interests are analysis of beam-column joints, column bases and column joints in composite structures.

Koichi MINAMI
Assoc. Prof.
Osaka Inst. of Technology
Osaka, Japan

Graduated from Osaka Institute of Technology, Japan, in 1964, and received Dr. Eng. from Kyoto Univ. in 1985. Since 1985, he has been Assoc. Prof. of Osaka Inst. of Technology. His research interests are analysis of beams, columns, walls, joints, and frames in RC and composite structures.

SUMMARY

Use of structural system composed of steel beams and reinforced concrete columns has been thought to be more economical and flexible in structural design. This paper describes the mechanism of stress transfer from the steel beams to reinforced concrete columns through the joint. In this mechanism, the principle of prying action of the steel beam embedded in reinforced concrete column was applied to estimate the ultimate strength of joint, because of its simplicity and reasonable accuracy.

RÉSUMÉ

L'emploi de structures composées de poutres d'acier et de poteaux en béton armé s'est avéré nécessaire pour obtenir davantage d'économie et de flexibilité dans les projets de structures. Cet article décrit le mécanisme de transfert de contraintes au niveau des joints, des poutres d'acier vers les poteaux en béton armé. Le principe d'effet de pince à levier a été appliqué, dans ce mécanisme, sur la poutre d'acier noyée dans le béton du poteau, afin d'évaluer la résistance ultime du joint de liaison; ceci pour une raison de simplification et de précision acceptable.

ZUSAMMENFASSUNG

Tragsysteme aus Stahlriegeln und Stahlbetonstützen sind kostengünstiger und erlauben eine flexiblere Projektierung. Dieser Beitrag beschreibt die Kraftübertragung von Stahlriegeln auf die Stahlbetonstützen. Dabei wird die Spaltwirkung des im Beton eingebetteten Bewehrungsstabes zur Abschätzung der Knotentragfähigkeit herangezogen, da dies zu einer einfachen und vernünftig genauen Lösung führt.

1. INTRODUCTION

Recently in Japan, structural system composed of steel beam and reinforced concrete column is proposed. Reinforced concrete columns have excellent axial capacity and steel beams have excellent strength and ductility against bending and shear load. Therefore, it is reasonable to construct a building using reinforced concrete columns and steel beams. However, very little information is available on the stress transfer from the steel beam to the reinforced concrete column through the joint. The object of this study is to make the stress transferring mechanism of the joints clear theoretically and experimentally.

2. STRESS TRANSFERRING MECHANISM

Fig. 1 shows the mechanism of the stress transfer from the embedded steel beam to the reinforced concrete column through the interior composite beam-column joint. The mechanisms are illustrated by the free body diagrams of each members. As shown in Fig. 1, the forces acting in the steel beam consist of the bearing forces $x_b b\lambda F_c$ for below the bottom flange and above the top flange of embedded steel beam, the frictional forces $P_{rc}l/h$ and external load P_{rc}. In this paper, this force system is called the prying mechanism. On the other hand, the system of forces acting in the lower and upper reinforced concrete columns consist of the bearing force, the frictional force $P_{rc}l/h$, tensile force ${}_rT_y$ of the longitudinal bars and external load $P_{rc}l/h$ and N_{rc}. In this mechanism, the longitudinal bars in the joint act for transmitting the bearing forces to the lower and upper columns.

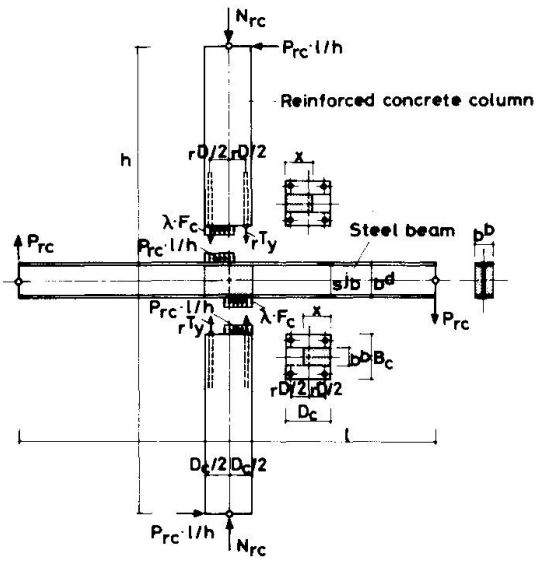

Fig. 1 Stress Transferring Mechanism.

3. ULTIMATE STRENGTH OF INTERIOR BEAM-COLUMN ASSEMBLY

The ultimate strength ${}_tm$ of interior beam-column assembly is given as,

$$ {}_tm = \min.\ ({}_mm,\ {}_pm) \qquad (1) $$

where ${}_mm$ and ${}_pm$ are the flexural capacities of the members and the shear capacity of the joint, respectively. The shear capacity of the joint is not dealt in this paper, because the object of this study is to estimate the mechanism of stress transfer from the steel beam to the reinforced concrete column through the joint.

The flexural capacities ${}_mm$ are estimated as,

$$ {}_mm = \min.\ ({}_bm,\ {}_cm,\ {}_{be}m) \qquad (2) $$

where ${}_bm$ and ${}_cm$ are the resisting moment of the beam and column, respectively. ${}_{be}m$ is the resisting moment for the prying mechanism of the embedded steel beam. ${}_bm$ and ${}_cm$ can be estimated by the superposed strength method easily. Therefore, a method for predicting the resisting moment capacity for the prying mechanism is discussed in this paper.

The steel beam is assumed to be rigid. As shown in Fig. 1, The compressive stress block on the top and bottom flanges of the embedded steel beam has a uniform stress of λF_c, where λF_c is the bearing strength of the concrete. The effective width of the concrete is assumed to be equal to the width of the

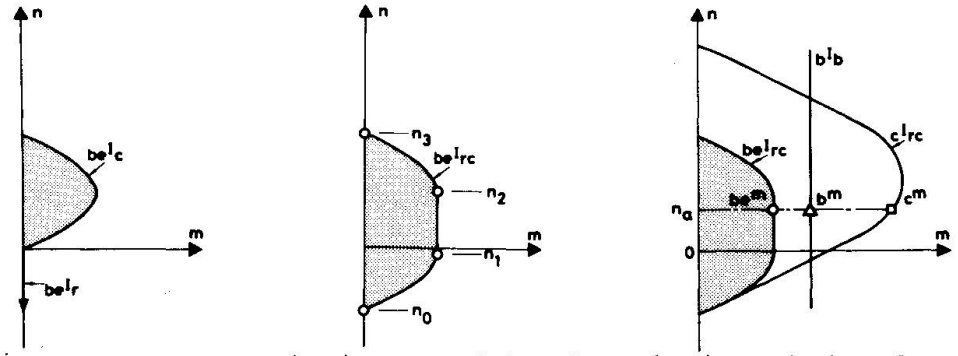

(a) Ultimate strength of each element for prying action.

(b) Superposition of ultimate strength for each element.

(c) Prediction of ultimate strength.

Fig. 2 Prediction of ultimate strength

embedded steel beam. On the base of these assumptions, the relationships between the resisting moment M and axial compression N of the concrete section at the top and bottom flanges of the embedded steel beam are given as,

$$m = n (1 - n / \lambda_1) / 2 \qquad (3)$$

where $m = M/B_c D_c^2 F_c$, $n = N/B_c D_c F_c$, $\lambda_1 = {}_b b\lambda / B_c$. These relationships are shown as N - M interaction curve ${}_{be}I_c$ in Fig. 2 (a). In eq. 3, the effect of frictional strength between the steel beam and concrete is not considered.

Interaction straight line ${}_{be}I_r$ for the longitudinal bars is given as,

$$n = - 2 ({}_r p_t \cdot {}_r\sigma_y / F_c) = - 2 \cdot {}_r\mu_t \qquad (4)$$

where ${}_r p_t$ and ${}_r\sigma_y$ are the tension reinforcement ratio and the yield stress of longitudinal bars, respectively. Interaction line ${}_{be}I_r$ is shown in Fig. 2 (a).

N - M interaction curve ${}_{be}I_{rc}$ for the prying action can be obtained from using superposed method of interaction line ${}_{be}I_r$ on the interaction curve ${}_{be}I_c$. Accordingly, as shown in Fig. 2 (b), the resisting moment capacity is given by the following expressions :

$$n_0 \leqq n \leqq n_1, \quad m = (n + 2 \cdot {}_r\mu_t) \{ 1 - (n + 2 {}_r\mu_t) / \lambda_1 \} / 2 \qquad (5)$$

$$n_1 \leqq n \leqq n_2, \quad m = \lambda_1 / 8 \qquad (6)$$

$$n_2 \leqq n \leqq n_3, \quad m = n (1 - n / \lambda_1) / 2 \qquad (7)$$

where, $n_0 = - 2 \cdot {}_r\mu_t$, $n_1 = \lambda_1 / 2 - 2 \cdot {}_r\mu_t$, $n_2 = \lambda_1 / 2$, $n_3 = \lambda_1$.

As shown in Fig. 2 (c), using interaction curve ${}_{be}I_{rc}$, the resisting moment for prying action of embedded steel beam under axial compression n_a is obtained as ${}_{be}m$. In Fig. 2 (c), ${}_b I_b$ and ${}_c I_{rc}$ denote the interaction curves of the beam and column, respectively. Using these interaction curves, the resisting moment of the beam and the column under axial compression n_a is given as ${}_b m$ and ${}_c m$, respectively.

4. TEST PROGRAM AND TEST RESULTS

Table 2 Test and theoretical results

Specimen	Applied Axial Load N(kN)	Flexural Cracking Load P_{fl}(kN)		Diagonal Tension Cracking Load P_{cr}(kN)		Maximum Load $P_{max.}$(kN)		Theoretical Values $P_{theo.}$(kN)		$P_{max.}/P_{theo.}$
		P.L.	N.L.	P.L.	N.L.	P.L.	N.L.	P.L.	N.L.	
I0N	0	18.8	21.2	26.7	14.6	41.4	39.5	32.8	1.26	1.20
I2N	514	32.4	42.0	32.4	45.5	50.5	48.4	32.8	1.54	1.48

P.L. : Positive Loading. N.L. : Negative Loading.

To verify this proposed mechanism of stress transfer and the method capable of predicting the ultimate strength of the joint, two interior steel beam-reinforced concrete column assemblies were tested under reversed cyclic loading. Details of test specimens are shown in Fig. 3. The dimension of specimen and cross sections are identical for each specimen. Experimental variable was the applied axial load. The applied axial load was 0 and 20 % of the ultimate compressive strength N_o of the column. The mechanical properties of materials are listed in Table 1.

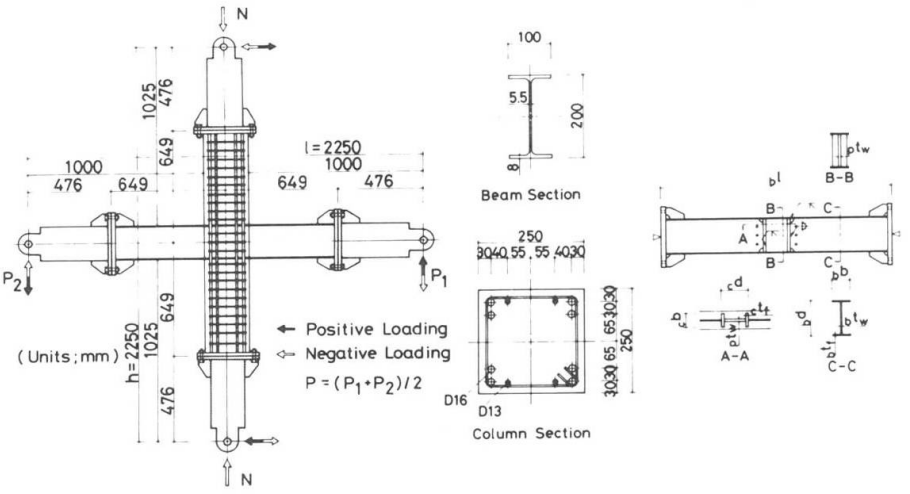

(a) Overall dimensions, loading and cross sections.

(b) Detail of steel beam.

Fig. 3 Details of test specimens.

Fig. 4 shows a hysteresis loop for each specimen. The ordinate represents the applied load at end of beam. The abscissa gives the deflection of the beam relative to the column at the point of application of load. $_bP$ denotes the calculated ultimate flexural strength of steel beam. For each specimen, the hysteresis loop shows the reversed S-shape with very small energy dissipation. After the attainment of the maximum load, the strength reduction due to reversed load for specimen I2N is remarkable. The strength reduction was caused by the crushing of concrete on the top and bottom flanges of the embedded steel beam as shown in Fig. 5. The above situation of concrete failure is similar to failure of concrete block that is tested to investigate the bearing strength.

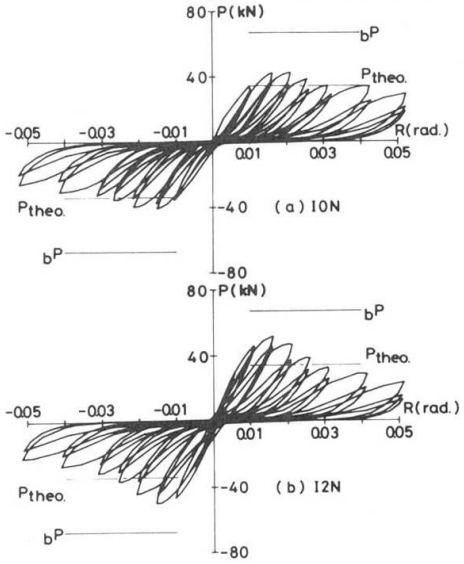

Fig. 4 Hysteresis loops.

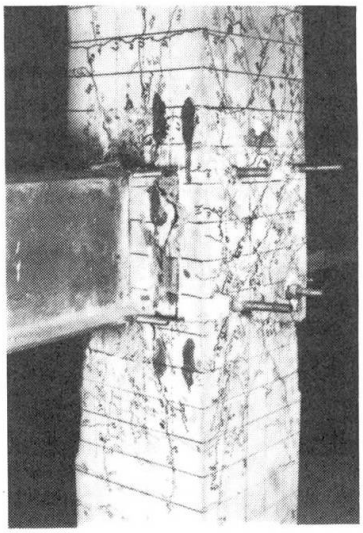

Fig. 5 Failure mode. for Specimen I0N.

5. PREDICTION OF TEST RESULTS

N - M interaction curves according to the present analysis are shown in Fig. 6. The ordinate and abscissa present the axial load n and resisting moment m, respectively. $_{be}I_{rc}$, $_bI_b$ and $_cI_{rc}$ denote the interaction curves for prying mechanism of embedded steel beam, steel beam

Table 1 Properties of materials.

	Steel			Reinforcing Bar			Concrete	
	σ_y	$\sigma_{max.}$	ϵ_u	σ_y	$\sigma_{max.}$	ϵ_u	F_c	F_t
	(N/mm^2)			(N/mm^2)			(N/mm^2)	
ℓ 5.5	367	443	0.201	6φ	181	288	0.290	
ℓ 8	319	424	0.259	D13	360	525	0.148	28.6 2.68
ℓ 16	264	434	0.304	D16	378	554	0.189	

F_c : Compressive Strength. F_t : Splitting Strength
σ_y : Yield Stress. $\sigma_{max.}$: Maximum Stress. ϵ_u : Maximum Elongation

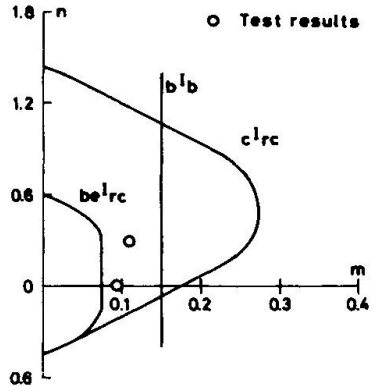

Fig. 6 Predictions of test results.

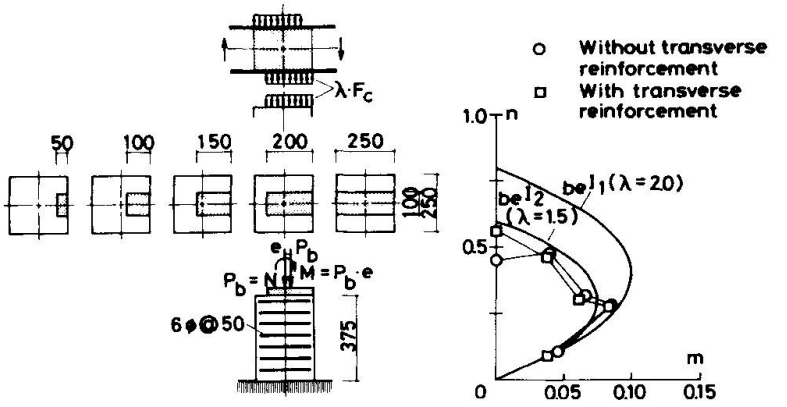

(a) Details of test specimens. (b) Bearing strength.
Fig. 7 Bearing test.

and reinforced concrete column, respectively. The open circle shows experimental values. The coefficient λ of 1.5 was adopted, based on tests to simulate the bearing zone under a steel beam as shown in Fig. 7. The comparisons of predictions with test results are listed in Table 2. The predictions are good agreement with the test results.

6. APPLICATION TO JOINTS WITH ADDITIONAL REINFORCEMENT

This proposed method was applied to estimate the ultimate strength of steel beam - reinforced concrete column joints containing additional reinforcement ; shear studs and reinforcing bars welded to the outside faces of the embedded steel beam, and steel beam - composite column joints. In predicting the ultimate strength of joints with additional reinforcement, the ultimate strength $P_{theo.}$ of the joints was given as,

$$P_{theo.} = P_u + \Delta P_u \qquad (8)$$

where P_u is the ultimate strength obtained by eq. 5 - eq. 7. ΔP_u is an additional strength provided by additional reinforcement.

Figs. 8 (a) compares predictions with the test results of specimens with shear studs or reinforcing bars conducted by author [2]. In this test, shear studs were intended to increase the frictional strength between the steel beam and concrete. On the other hand, reinforcing bars were intended to increase the resisting moment capacity for prying action. In case of these specimens with shear studs, additional strength ΔP_u was given as $n \cdot Q_{st} \cdot {}_b d / l$, where n is the number of the shear stud at the above or bottom flange of embedded steel beam, Q_{st} ($= 0.5 \cdot {}_{st}a \sqrt{E_c \cdot F_c}$) is the strength per shear stud, ${}_{st}a$ is cross-sectional

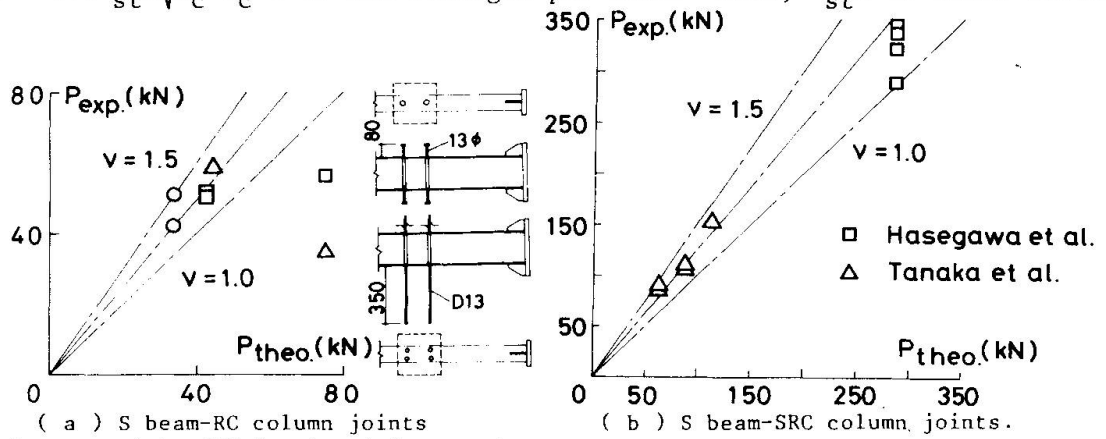

(a) S beam-RC column joints with additional reinforcement.
(b) S beam-SRC column joints.

Fig. 8 Application of proposed method

Table 3 Comparison of predictions with test results

Reference	Specimen	Experimental Value	Theoretical Value			
		$P_{exp.}$(kN)	$P_{theo.}$(kN)*)	P_u(kN)	ΔP_u(kN)	$P_{exp.}/P_{theo.}$
2	WS0002N	49.1	41.8	32.8	9.01	1.18
	WS0000N	50.0	41.8	32.8	9.01	1.20
	WH0002N	58.2	43.2	32.8	10.5	1.35
3	N0-Ms10	86.3	62.3	43.3	18.9	1.38
	N0-Ms25	110.8	86.7	43.3	43.3	1.28
	N40-Ms10	91.2	62.3	43.3	18.9	1.46
	N40-Ms25	105.9	86.7	43.3	43.3	1.22
	N0-Ms50	152.0	111.8	43.3	68.2	1.36
4	A-01	314.8	285.4**)	-	-	1.10
	A-01R	337.3	285.4	-	-	1.18
	A-04	329.5	285.4	-	-	1.15
	A-001	282.4	285.4	-	-	0.989

*) $P_{theo.} = P_u + \Delta P_u$
P_u : Ultimate strength for prying mechanism of embedded steel beam.
ΔP_u : Additional strength obtained by additional reinforcement.
**) Flexural strength of steel beam.

area , E_c and F_c is elastic modulus and compressive strength of concrete, respectively. On the other hand, ΔP_u of specimens with reinforcing bars was given as $2 \cdot {}_{re}a \cdot {}_{re}\sigma_y \cdot {}_{r}d \;/\; l$, where ${}_{re}a$ is cross-sectional area of tension reinforcing bars welded at the above or bottom flange of embedded steel beam, ${}_{re}\sigma_y$ is the yield stress of the reinforcing bar. Figs. 8 (b) compares predictions with the test results of interior steel beam - composite column joints [3, 4]. In this case, N - M interaction curve ${}_{be}I_{src}$ for the prying mechanism of embedded steel beam was obtained by means of superposition of the interaction curve ${}_{c}I_{s}$ for the steel column section on the interaction curve ${}_{be}I_{rc}$ obtained by eq. 5 - eq. 7. In these figures, the ordinate and abscissa represent the test results and predictions, respectively. The comparisons of predictions with test results are listed in Table 3. The predictions were shown to be in good agreement with the test results.

7. CONCLUDING REMARKS

The following remarks can be drawn from the discussion presented above.

1) The mechanism of stress transfer from the steel beam to reinforced concrete column was clarified experimentally and theoretically. In this mechanism, the principle of prying action of the steel beam embedded in reinforced concrete column was applied.

2) On the basis of this mechanism, a method capable of predicting the ultimate strength of joint was developed. The predictions were in good agreement with the test results.

3) This proposed method could be applied to estimate the ultimate strength of steel beam-reinforced concrete column joints containing additional reinforcement and steel beam-composite column joints.

REFERENCES

1. NISHIMURA Y. and MINAMI K., Stress Transferring Mechanism in Interior Steel Beam-Reinforced Concrete Column Joint. Transactions of AIJ, No.401, 1989.7, pp.77-85. (in Japanese)
2. UEOKA T., HUKUDA T., NISHIMURA Y. and MINAMI K., Effects of Reinforcement on Strength of Beam-Column Joints in Mixed Construction. Summaries of Technical Papers of Annual Meeting, AIJ, 1986, pp.1309-1310. (in Japanese)
3. TANAKA T. and NISHIGAKI T., Experimental Studies on Steel Beam-Composite Column Joint. Summaries of Technical Papers of Annual Meeting, AIJ, 1972, pp.1505-1506. (in Japanese)
4. HASEGAWA N., HIJIKATA K. et al., Experimental Study on Steel Beam to SRC Column Connections (part 1) - (part 4). Summaries of Technical Papers of Annual Meeting, AIJ, 1987, pp.1221-1228.(in Japanese)

Computer Model for the Fire Resistance of Composite Structures

Programme de calcul pour l'analyse de la sécurité au feu de structures mixtes

Rechenprogramm für die Feuerwiderstandsbemessung von Verbund-Konstruktionen

L. G. CAJOT
Research Engineer
ARBED-Research
Luxembourg

L. G. Cajot, born in 1963, received his Civil Engineering degree in 1986 at Liège University. Here he has also worked for one year at the Bridge and Structural Engineering Department. He is now research engineer at ARBED-Research Centre.

J. M. FRANSSEN
Research Engineer
Liège University
Liège, Belgium

J. M. Franssen was born in 1959. He graduated in 1982 as a Civil Engineer at the University of Liège. Since this time he has been doing research at this University on the fire behaviour of composite structures and obtained his Ph.D. in 1987.

J. B. SCHLEICH
Department Manager
ARBED-Research
Luxembourg

J. B. Schleich, born in 1942, received his Civil Engineering degree in 1967 at Liège University. Since 1984 he is responsible for the research in steel construction at ARBED-Research Centre. He is chairman of TC5 on CAD/CAM of ECCS.

SUMMARY

The behaviour of buildings during fire is a complex problem. For single elements such as one column or one beam, simplified methods or full scale fire tests in furnaces allow to determine the fire resistance. For complete structures, a numerical method as used by the program "CEFICOSS" enables to predict the fire behaviour. In this contribution the possibilities of this program and simulations of composite steel-concrete frames are described.

RÉSUMÉ

Le comportement des bâtiments lors d'un incendie est un problème complexe. Pour des éléments seuls, tels qu'une colonne ou une poutre, des méthodes simplifiées ou des essais au feu en vrai grandeur dans des fours permettent de déterminer la résistance au feu. Pour des structures complètes, une méthode de calcul numérique telle que celle du programme «CEFICOSS» permet de prédire le comportement au feu. Dans cet article sont décrites les possibilités de ce programme ainsi que des simulations de cadres mixtes acier-béton.

ZUSAMMENFASSUNG

Das Verhalten von Gebäuden im Brandfall stellt ein komplexes Problem dar. Für einzelne Tragelemente wie z.B. eine Stütze oder ein Träger, können vereinfachte Rechenmethoden oder Brandversuche im Massstab 1:1 zur Bestimmung des Feuerwiderstandes benutzt werden. Zur Berechnung des Feuerverhaltens einer vollständigen Struktur kann nur ein numerisches Rechenmodell wie das jenige des Programms „CEFICOSS" dienen. In diesem Artikel werden die Möglichkeiten dieses Programms sowie die Simulation von Verbundrahmen beschrieben.

1. INTRODUCTION

The probability of coming across fire in residential buildings, hotels, schools, hospitals or industrial plants depends on many factors, amongst which the age of the buildings and the level of confidence of the safety precautions are capital.
However that probability can never be reduced to zero, because it is impossible to completely avoid the presence of all burning materials as well as it is impossible to imagine a world free of any defects and of any spiteful act. That's why it is necessary to give a sufficient fire resistance to buildings.
There are various approaches to study the fire resistance of structures. The first approach, which still remains the most common approach up to now, is the use of full scale tests in furnace in which ISO-fire conditions are simulated. Another approach is given by the simplified calculation methods. But these methods, including the fire tests, can only be used for single elements like one beam or one column [1].
Thus it results that a satisfactory knowledge of the behaviour of a structure as a whole during fire and of its way to collapse can only be obtained by an accurate numerical computation method. Such a method is included in the computer program "CEFICOSS" [2,3].

2. NUMERICAL COMPUTER MODEL

CEFICOSS stands for Computer Engineering of the FIre resistance of COmposite and Steel Structures. This numerical program performs a step-by-step simulation of the behaviour of columns, beams or plane frames submitted to the fire [4,5,6].
The first part of the program calculates the temperature distribution in the cross-sections of the structure. In order to make the step-by-step simulation of the static behaviour, the temperature distribution is calculated at different instants (f.i. every minute) defined by the user. The problem is considered to be two dimensional. The cross sections are discretized by a rectangular mesh. By indicating which material (steel, concrete or insulating material) is present in each mesh, it is possible to analyse various shapes of pure steel, reinforced concrete or composite steel-concrete sections. The transient conductive equations are solved by an explicite finite difference scheme, the time step of which being automatically calculated in order to ensure convergence with the shortest computing time. As thermal conductivity and specific heat of the building materials are temperature dependent, this time step varies during the calculation.
The boundary conditions are convection and radiation or symmetry. The outside world is represented by the temperature of the gases with various possibilities; ambient temperature, ISO curve or any other curve including a cooling down phase. Evaporation and transportation of the moisture in wet materials is considered. Though it is possible to perform the thermal and the static calculations simultaneously, it is more convenient to store the temperatures on a file that can be read for different static calculations with the same cross-section.
Instead of an ultimate state design (which load can be sustained by a structure after 60 minutes of ISO fire?), CEFICOSS performs the realistic continuous simulation of a structure in a fire (how long will a structure be able to sustain the applied load). That means that the load is first applied in successive steps on the structure at ambient temperature. If collapse has not occured, stresses, strains and displacements are stored on a file. From this moment, keeping the loads generally unchanged, the temperatures are increased in the sections and the new values of

stresses, strains and displacements are computed. This is done up to the time when equilibrium can no more be obtained, which indicates that collapse has occured.
A finite beam element is used with two nodes and six degrees of freedom. The equations are written in an updated lagrangian formulation. The two hypothesis of Bernoulli and Von Karmann are made as well as the one of small incremental displacements ($\sin \Delta\theta \simeq \Delta\theta$). In order to prevent axial locking, the mean value of the non-linear term of the axial strain is considered. Large displacements are taken into account.
Stress-strain relationships in building materials are non-linear and temperature dependent. Different possibilities are offered as the quadro-linear or elastic-elliptic relationships for steel, and the descending branches for concrete. Thermal elongations as well as residual strains are explicitely considered, while creep is implicitely introduced in the stress strain relationships.
In order to have the shortest possible computing time with a simultaneous sufficient accuracy when the failure time is approached, the time step of the static calculation is controlled by the minimum proper value of the stiffness matrix.

3. SIMULATIONS PERFORMED BY CEFICOSS

Numerous practical fire resistance calculations have been performed which allow to consider this numerical computer model as a quite general and most credible engineering tool. Moreover very recently N-M interaction failure diagrams buckling included, have been established for composite construction elements and for unprotected heavy steel columns [7,8]. Besides the effect of local fire on a two level frame has been analysed for the first time [9]. In this contribution it will be shown that it is quite possible to analyse the effect of a local fire on a six level composite frame.

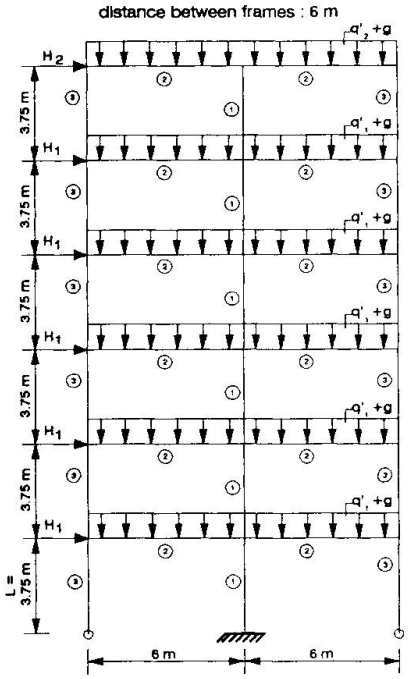

Fig. 1 Static System of the sway frame

3.1.Frame definition

The chosen composite frame has 6 levels and 2 spans. The geometrical configuration is shown on figures 1,2 and 3.

- The mechanical properties of the materials are defined by the standardized qualities: St 37 for steel profiles, BST 500/550 for rebars and B 40 for concrete.
- Three static systems are considered: braced frames with rigid or hinged beam-column connections and a sway frame. For the braced frame with hinged connections, the columns are continuous. For the sway frame the ground end condition is fixed for the central column and hinged for the other ones. For the braced

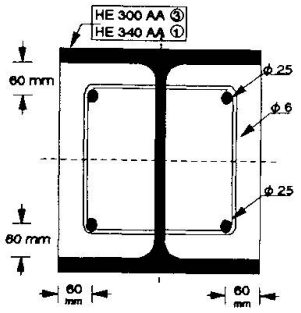

Fig. 2 Column cross section (number ① and ③)

frames the three columns have hinged ground end conditions and the horizontal stability is supposed fulfilled by a central core (see figure 10).

- For each static system the structure has been designed and optimized for service conditions with just the minimum required safety.
- The loads are divided into proper weight g, service load q', and horizontal wind load H. The basic load combination called B.L. is equal to 1,35*g + 1,5*q' + 1,12*H.
- For each static system three ISO-fire scenarios have been studied which affect either

1)the lower left column and beam or
2)the same but also the lower central column or
3)the whole lower frame.

- For each fire scenario two loadings are considered: B.L/3.5 or B.L/2.3.
- The 18 frames described hereabove have been calculated by "CEFICOSS" so that their global behaviour under fire and therefore their fire resistance time is known.

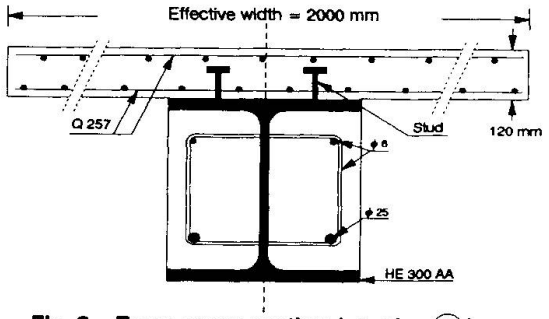

Fig. 3 Beam cross section (number ②)

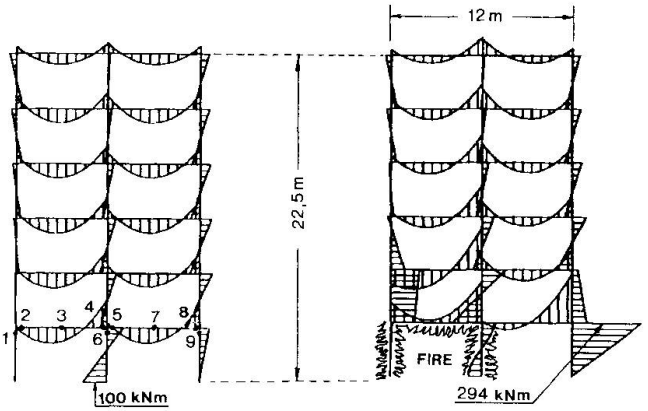

Fig. 4 Bending moments before heating

Fig. 5 Bending moments just before failure at 123'

3.2. Comparison between global system simulation and calculation of single element

For each case the critical element in the structure under hot condition was considered. This element was analysed by CEFICOSS under fire conditions as a single element submitted to the internal forces existing before fire. The column buckling length was adapted to take into account the proper end conditions. The fire resistance times found by this simplified method and by the global system calculation are noted in the figure 10. It shows that both methods give similar results for braced frames. But this is not true for sway frames. That's why we are going now to have a look at the simulation of a sway frame with f.i. the fire scenario 2 and the loading B.L./2.3 (figures 1 and 10). In this case the cross sections of the construction elements can be seen in figures 2 and 3.

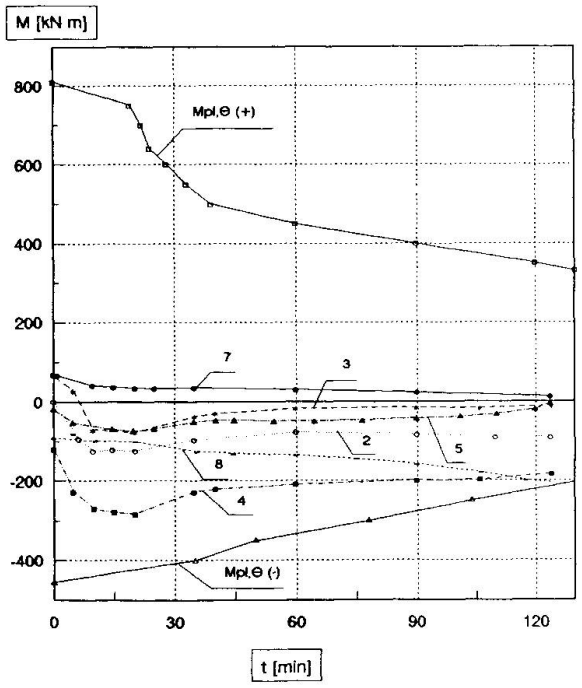

Fig. 6 Variation of bending moments in the beams during fire

3.3. Sway frame

The diagram of bending moments before heating and just before the failure are shown on figures 4 and 5. It can be seen that the bending moment distribution changes strongly during the fire.

- For the beams the variation of the bending moments can be drawn in a diagram where the ultimate positive bending moment Mpl,θ (+) and the negative one Mpl,θ(-) are represented in function of the time. This diagram shows that no plastic hinge occurs in the beams (figure 6).
- For the columns the situation is more complex because the axial force, the bending moment distribution along the column, the buckling length and the second order effect play a part. Moreover all these parameters change differently in function of the fire evolution.
- But the horizontal displacement curves in function of the time of the top of the lower columns enable to conclude that the failure is produced by the buckling of the whole lower frame. (figure 7). In fact the buckling of the central column occurs first but is followed a few seconds later by the simultaneous buckling of the left and right columns. This phenomenon also appears in the figure 8 showing the vertical displacements of the top of the lower columns.

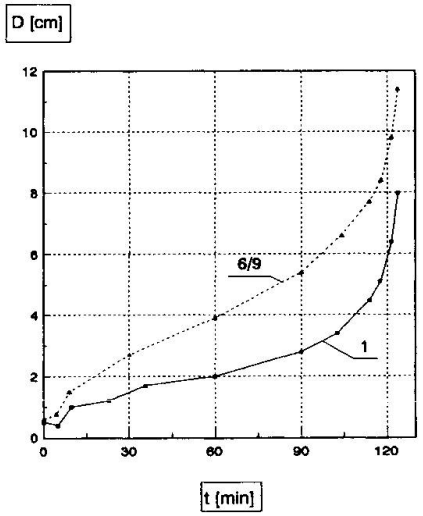

Fig. 7 Horizontal displacements of the top of the lower columns

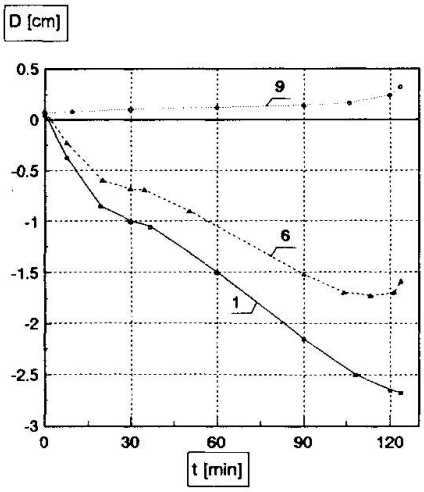

Fig. 8 Vertical diplacements of the top of the lower columns

3.4. Conclusions

- The opposite figure 9 shows the deformed structure just before the failure. It can be seen that the whole structure is submitted to important displacements. So it is not possible to calculate only a single element in order to obtain the fire resistance time of the whole frame as it is the case for braced frames. This is noted in figure 10 where the results of numerous global system simulations are recorded as well for the braced frames I and II as for the here more detailed sway frame III.
- This numerical procedure is fully in line with Part 10 "Structural Fire Design" of Eurocodes 2, 3 and 4 [10].

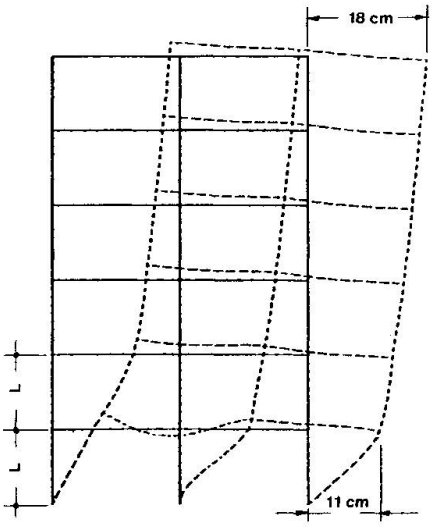

Fig. 9 Total displacement of the structure just before failure at 123'

Basic Load (B.L.) : 1.35*g + 1.5*q' + 1.12*H — CALCULATED BY CEFICOSS

Global system calculation					Single column analysis					
System	Fire Scenario	Loading	t (min)	Failure type : Buckling of	Loading N	Loading M1	Choosen column element	t (min)	dt (%)	System
I	1	B.L./3.5	75'	Lower left column	303	8.8	Lower left column	77'	2.6	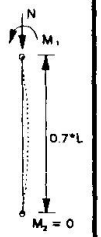
		B.L./2.3	53'	Lower left column	461	13.4	Lower left column	49'	-8.2	
	2	B.L./3.5	82'	Lower left column	303	8.8	Lower left column	77'	-6.5	
		B.L./2.3	57'	Lower left column	461	13.4	Lower left column	49'	-16.3	
	3	B.L./3.5	77'	Lower left column	303	8.8	Lower left column	77'	±0.0	
		B.L./2.3	48'	Lower left column	461	13.4	Lower left column	49'	2.2	
II	1	B.L./3.5	88'	Lower left column	319	1.7	Lower left column	94'	6.4	
		B.L./2.3	65'	Lower left column	485	2.6	Lower left column	68'	4.4	
	2	B.L./3.5	88'	Lower left column	319	1.7	Lower left column	94'	6.4	
		B.L./2.3	65'	Lower left column	485	2.6	Lower left column	68'	4.4	
	3	B.L./3.5	79'	Lower left column	626	2.7	Lower left column	94'	16	
		B.L./2.3	50'	Lower central column	956	4.1	Lower central column	49'	-2.0	
III	1	B.L./3.5	197'	Global failure of the whole frame	No equivalent single element analysis available					
		B.L./2.3	168'							
	2	B.L./3.5	206'							
		B.L./2.3	123'							
	3	B.L./3.5	110'							
		B.L./2.3	68'							

Fig. 10 Comparison between global system calculation and the simplified approach given by a single column analysis

BIBLIOGRAPHY

1. ECCS-TC3, Calculation of the Fire Resistance of Centrally Loaded Composite Steel-Concrete Columns Exposed to the Standard Fire. Technical Note N° 55, Brussels, 1988.

2. SCHLEICH J.B., Computer Assisted Analysis of the Fire Resistance of Steel and Composite Concrete-Steel Structures. Final Report EUR 10828, Luxembourg 1987.

3. FRANSSEN J.M., Etude du comportement au feu des structures mixtes acier-béton. Thèse de doctorat N° 111, Université de Liège 1987.

4. SCHLEICH J.B., Numerical Simulations, the Forth Coming Approach in Fire Engineering Design of Steel Structures. Revue Technique N°2, Luxembourg 1987.

5. BAUS R., SCHLEICH J.B., Prédétermination de la Résistance au Feu des Constructions Mixtes. Annales de l'Institut Technique du Bâtiment et des Travaux Publics N° 457, Paris 1987.

6. SCHLEICH J.B., Numerische Simulation: zukunftsorientierte Vorgehensweise zur Feuersicherheitsbeurteilung von Stahlbauten. Bauingenieur 63, Berlin 1988.

7. MATHIEU J., SCHLEICH J.B., Practical Design Tools for Composite Steel Concrete Construction Elements Submitted to ISO-Fire Considering the Interaction Between Axial Load N and Bending Moment M. Project of Final Report for C.E.C. Agreement N° 7210-SA/504, Luxembourg 1989.

8. MATHIEU J., SCHLEICH J.B., Practical Design Tools for Unprotected Steel Columns submitted to ISO-Fire. Project of Final Report for C.E.C. Agreement N° 7210-SA/505, Luxembourg 1989.

9. SCHLEICH J.B., Global Behaviour of Steel Structures in Fire. ECCS International Symposium "Building in Steel-The Way Ahead", Stratford upon Avon, 1989.

10. COMMISSION OF THE EUROPEAN COMMUNITY, Eurocodes-Part 10, Structural Fire Design. First Draft, Brussels-Luxembourg 1990.

Mixed Structural Systems of Precast Concrete Columns and Steel Beams

Systèmes structuraux mixtes de poteaux en béton prémoulé et poutres en acier

Mischbausysteme aus Betonfertigteilstützen und Stahlträgern

T. YOSHINO
Civil Engineer
Fujita Corporation
Yokohama, Japan

His research interests include design and development of composite precast concrete structures. He is a member of JCI and AIJ.

Y. KANOH
Prof. of Struct. Eng.
Meiji University
Tokyo, Japan

His research interests center around strengths and restoring force characteristics of reinforced concrete structures. He is a member of IABSE, RILEM, ACI, JCI and AIJ.

A. MIKAME
Civil Engineer
Fujita Corporation
Yokohama, Japan

His research interests include design and development of mixed structures. He is a member of JCI and AIJ.

H. SASAKI
Civil Engineer
Fujita Corporation
Yokohama, Japan

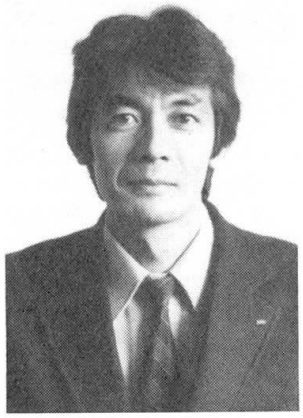

His research interests include aseismic behavior of reinforced ultra high strength concrete members. He is a member of JCI and AIJ.

SUMMARY

In this paper, mixed structural systems which consist of composite precast concrete columns and steel beams are examined through the results of an experimental research program in which interior beam-column joint specimens were tested under reversed cyclic loading.

RÉSUMÉ

Les systèmes structuraux mixtes, consistant en poteaux de béton prémoulé et poutres en acier, sont étudiés dans le présent document au moyen des résultats obtenus lors de l'exécution d'un programme de recherche expérimental, au cours duquel spécimens de joint intérieur poutre-poteau ont été soumis à des essais sous une charge cyclique inversée.

ZUSAMMENFASSUNG

Diese Abhandlung befaßt sich mit der Untersuchung von baulichen Mischsystemen, die aus vorgefertigten Verbundstützen und Stahlträgern zusammengesetzt sind. In eine experimentellen Forschungsprogramms wurden Rahmenknoten unter Wechselbeanspruchung untersucht.

1. INTRODUCTION

In Japan, a type of composite structural system called the steel reinforced concrete (SRC) structural system has been popular for many years. Since the early 1980s, mixed structural systems composed of steel reinforced concrete (SRC) columns and steel beams have been studied. Recently, new mixed structural systems composed of reinforced concrete (RC) columns and steel beams were developed.

In addition, development of precast concrete frame systems, which simplify the assembly of reinforced concrete structures, has long been a major issue in the advancement of construction methods. Due to severe conditions caused by earthquakes in Japan, precast units have been joined together at the center of the beams and columns where a minimal degree of stress and deformation is expected. However, this leads to several disadvantages including complicated configuration, high transportation costs for the large units, and limited applicability. Therefore, we developed a more simplified precast concrete frame system, as shown in Fig. 1. In this system, which was first implemented in Japan in 1978, the basic units consist of precast concrete columns and beams. The column units are separated from the beam units. The column and beam units are joined at the beam-column joint by cast-in-place concrete. This system has since been applied to many types of large-scale buildings, such as shopping centers, schools and hospitals.

Further development of new mixed structural systems which consist of composite precast concrete columns and steel beams has been carried out along the same line as that of the first system, as shown in Fig. 2. Aspects which must continue to be improved include the stress transfer mechanism at the beam-column joint and the seismic capacity of the joint between precast concrete units. To clarify the stress transfer mechanism, and to verify the effectiveness of our systems, we carried out experimental tests of the interior beam-column joint subject to reversed cyclic loads similar to the effect of an earthquake. Six specimens consisting of approximately two-thirds-scale models, whose failure modes were of the beam collapse and joint collapse types, were adopted. From the experimental results, a stress transfer mechanism between the composite precast concrete columns and steel beams in the present systems, and the ductility of the beam-column joint, were studied.

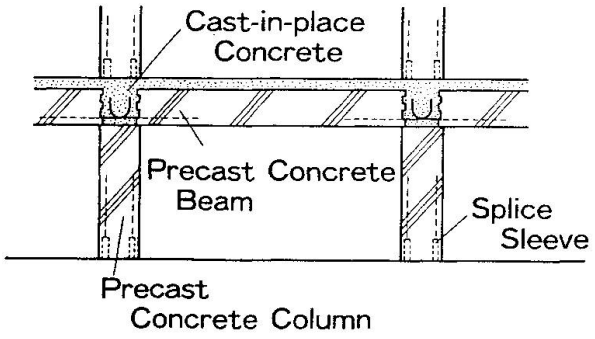

Fig. 1 Precast Concrete Frame System

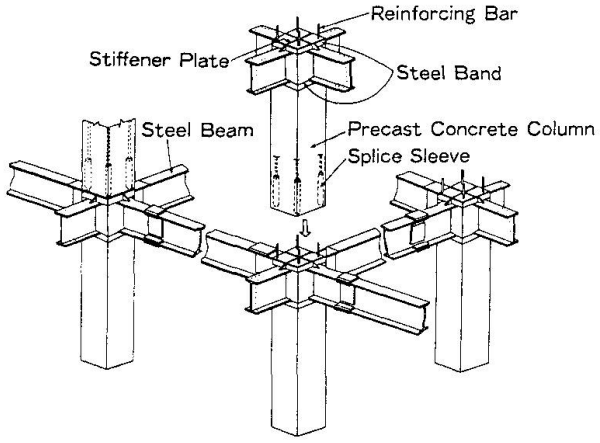

Fig. 2 New Mixed Structural system

2. JOINT DETAILS

The present systems are classified into two systems in terms of the details of beam-column joints and precast concrete columns. In the first system, as shown in Fig. 2 and Fig. 3 (specimen NO. 2), the column consists of reinforced precast concrete enclosed by steel bands which are arranged at the top and

the bottom of the column. The steel bands, whose width is equal to the thickness of the slab, are welded to the flanges of H-shaped steel beams. The steel bands are thought to be available for confining the concrete at the top and the bottom of the column. In the second system, the column consists of the reinforced precast concrete and tubular or H-shaped steel as shown in Fig. 3 (specimens NO. 3 and NO. 6). The steel, which is embedded in a reinforced concrete column, is welded to the steel beam. The embedded length of the steel is two times greater than the depth of the H-shaped steel or the diameter of the tubular steel. In both systems, mechanical joints of reinforcing bars, called splice sleeves, are embedded at the bottom of the columns.

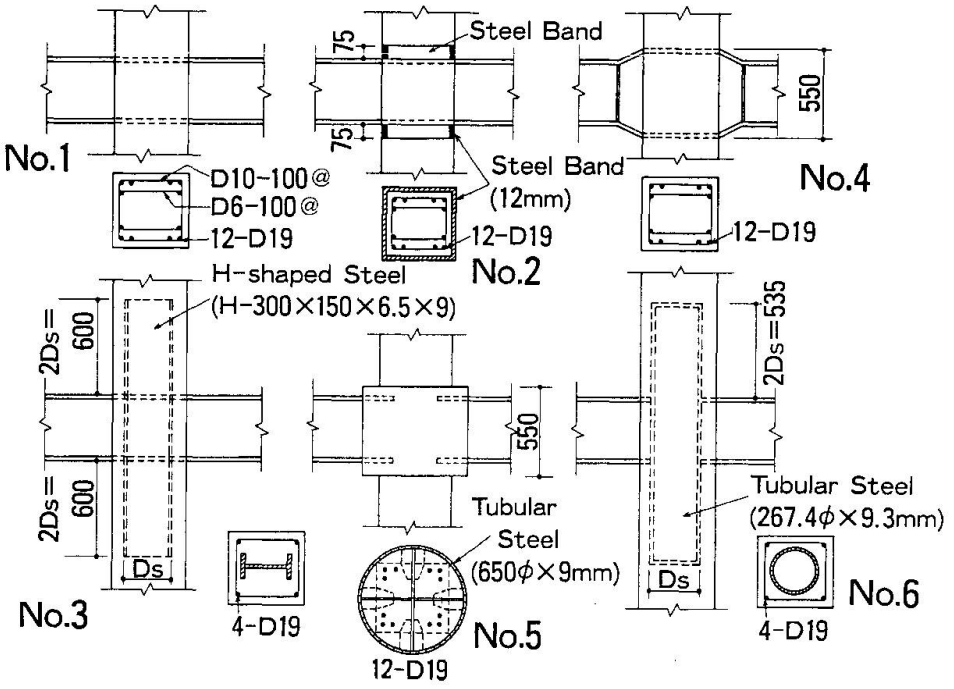

Fig. 3 Joint Details of Specimens

3. EXPERIMENTAL TESTS

3.1 Test Specimens

Six specimens consisting of approximately two-thirds-scale models were tested under reversed cyclic loads. A typical cruciform-shaped specimen geometry is shown in Fig. 4. Applied loads at the ends of the beams were so controlled as to give simultaneously the same magnitude but opposite sign displacement at loading points to these beams. A vertical load, which is kept constant ($\sigma_0 \fallingdotseq$ 4.0 MPa), is applied to the column in all specimens. In all specimens, the vertical column reinforcement was designed to exceed the anticipated beam strength. In addition to monitoring the applied beam loads, story drift and deformation of each beam, column and joint, we measured steel and concrete strains. The dimensions and material properties of the column and beam in each specimen are listed in Table 1 and Table 2. The H-shaped steel beam, which is common to all specimens, is used in the tests. The plate dimensions used in the beams are as follows: web plate 9 × 400 mm; flange plate 12 × 150 mm. The dimensions of the column section, which is common to all specimens, are 450 × 450 mm.

Specimens NO. 1, NO. 2, NO. 4 and NO. 5 are composed of reinforced precast concrete columns and steel beams. Specimens NO. 3 and NO. 6 are composed of tubular or H-shaped steel and reinforced precast concrete columns and steel

Table 1 List of Specimens

Specimen	Column				Beam	Panel
	Section	Steel Portion	Reinforcement		Section	Steel
			Vertical	Hoop		Hoop
NO.1	450x450		12-D19	D10-@100 D6- @100	H-400x150 x9x 12	Web Plate 12mm Hoop D10- @80
NO.2		Steel Band (75x12mm)				
NO.3		H-300x150x6.5x9	4-D19	D10-@100		
NO.4			12-D19	D10-@100 D6- @100		Web plate 12x550 mm Hoop D10- @80
NO.5						Tubular steel(650 ϕ) No Hoop
NO.6		Tubular Steel (267.4ϕ x9.3mm)	4-D19	D10-@100		Tubular steel(267.4 ϕ) Hoop D10- @80

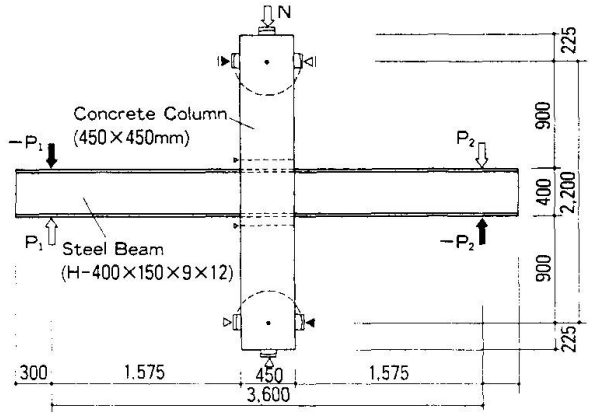

Fig. 4 Typical Test Specimen

Table 2 Properties of Materials

Material		σ_y (MPa)	σ max. (MPa)	E_s (MPa)	Elong.
Steel	6.5mm	312.6	489.0	1.92×10^5	.335
	9 m	285.7	462.0	1.95×10^5	.383
	12 mm	295.0	428.0	1.97×10^5	.360
Re-Bar	D10	364.6	522.0	1.77×10^5	.270
	D19	365.0	532.5	1.73×10^5	.208

Material		F_c (MPa)	f_t (MPa)	E_c (MPa)
Concrete	Panel	24.3	2.2	2.09×10^4
	Column	25.2	2.5	1.94×10^4

beams. In specimen NO. 1, the steel beam is continuous through the joint without special contrivances to increase the ductility of the beam-column joint. The dimensions of steel bands arranged at the top and the bottom of the column in specimen NO. 2 are 1.2 × 75 mm. In specimen NO. 5, the beam-column joint, the shape of which is cylindrical, as shown in Fig. 3 (NO. 5), is solid concrete enclosed by tubular steel. The dimensions of the tubular steel are as follows: diameter 650 mm; thickness 9 mm; height 550 mm. In specimen NO. 4, the field of the beam-column joint is extended. In specimens NO. 5 and NO. 6, the dimensions of H-shaped and tubular steel embedded in the reinforced concrete column are as follows: web plate 6.5 × 300 mm; flange plate 9 × 150 mm; tubular steel 267.4ϕ × 9.3 mm. The concrete is not solid inside the tubular steel in specimen NO. 6.

3.2 Test Results

3.2.1 Development of Test

The test results of all specimens are listed in Table 3. All specimens developed flexural yielding at the flange of the steel beam adjacent to the beam-column joint at the story drift angle of 0.7/100 ~ 1/100 rad. In specimens NO. 1 and NO. 4, which failed in panel shear, the deterioration of concrete at the joint and column adjacent to the joint was observed to be marked after the maximum load. In specimens NO. 2, 3 and 5, the decrease of bearing capacity was not observed until the story drift angle reached 5/100 rad. Specimen NO. 6 exhibited rupture of the steel beam flange at the story drift angle of 3/100 rad.

3.2.2 Concrete Cracking

In all specimens, flexural cracks in the column and diagonal shear cracks in

Table 3 Summary of the Test Results

Specimen	Flexural Strength of Beam (kN)			Shear Strength of Panel (MPa)			Mode of Failure
	Exp.(P)	Cal.(P_c)	P/P_c	τ exp.	τ cal.	τ exp./τ cal.	
NO. 1	211(207)	190	1.11(1.09)	18.8(18.5)	18.6	1.01(0.99)	Beam yielding → Panel shear
NO. 2	253(255)		1.33(1.34)	23.4(23.8)		1.26(1.28)	Beam yielding
NO. 3	228(229)		1.20(1.21)	18.3(18.2)		1.11(1.10)	Beam yielding
NO. 4	245(251)	211	1.16(1.19)	14.7(14.3)		0.97(0.95)	Beam yielding → Panel shear
NO. 5	277(286)	203	1.36(1.41)	10.2(10.4)	12.0	0.84(0.86)	Beam yielding → Local Buckling of Flange → Flange Rupture
NO. 6	260(242)	190	1.37(1.27)	20.3(19.7)	23.8	0.85(0.83)	

( ); Negative Loading

the joint occurred at a story drift angle of 3/1000 ~ 5/1000 rad. Specimens NO. 5 and NO. 6 developed very few additional diagonal shear cracks in the joints after a story drift angle of 2/100 rad. In specimens NO. 1 and NO. 4, the shell concrete spalled in the four corners near and within the beam-column joint at a story drift angle of 4/100 rad.

3.2.3 Load-Deformation Response

The load-deformation curves of all specimens are shown in Fig. 5. The vertical axis indicates the applied beam load, which is proportional to beam moments adjacent to the beam-column joint. The horizontal axis indicates the story drift angle, which is a measure of the total relative angular rotation between the steel beam and precast concrete column. Specimens NO. 2, NO. 3, NO. 5 and NO. 6 showed a favorable spindle-shape hysteresis, but specimens NO. 1 and NO. 4 showed a pinching hysteresis shape under cyclic load reversals.

The contribution of the parts of each specimen to the story drift was estimated and is shown in Fig. 6. In specimens NO. 1 and NO. 4, the deformation of the beam-column connection markedly increased after a story drift angle of 3/100 rad. In specimen NO. 6, most of the deformation was contributed by steel beam deformation which led to the beam failure. In specimens NO. 5 and NO. 6, the connection deformation is very small. The connection deformation of specimen NO. 2 is slightly smaller than that of specimen NO. 3.

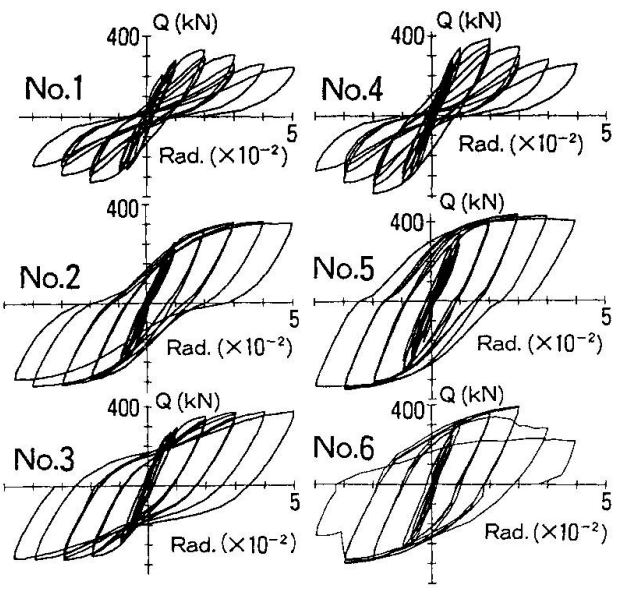

Fig. 5 Load-Deformation Curves

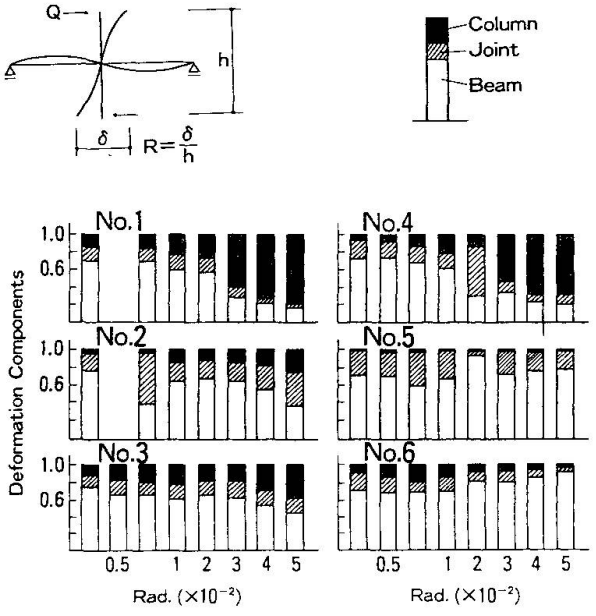

Fig. 6 Deformation Components

4. Stress Transfer Mechanism

Two hypothetic mechanisms for the stress transfer from the steel beam to the composite concrete column through a beam-column joint are shown in Fig. 7. Beam moments are shown as equivalent horizontal force couples acting in the beam flanges, and column moments are shown as vertical force couples. In mechanism TYPE Ⅰ, the joint details of which are shown in Fig. 3 (Specimen NO. 2), the concrete compression field outside the steel beam is formed by a lever action of the beam flange and confinement effects of the steel bands. Steel bands are effective in preventing the spalling of the concrete in the four corners near and within the beam-column joint. In mechanism TYPE Ⅱ, the joint details of which are shown in Fig. 3 (Specimens NO. 3 and NO. 6), the concrete compression field outside the steel beam is formed by the lever actions of the beam flange and the steel embedded in the concrete column. The test results indicate that it is impossible to transfer the stress by only a lever action of the beam flange, as in specimens NO. 1 and NO. 4.

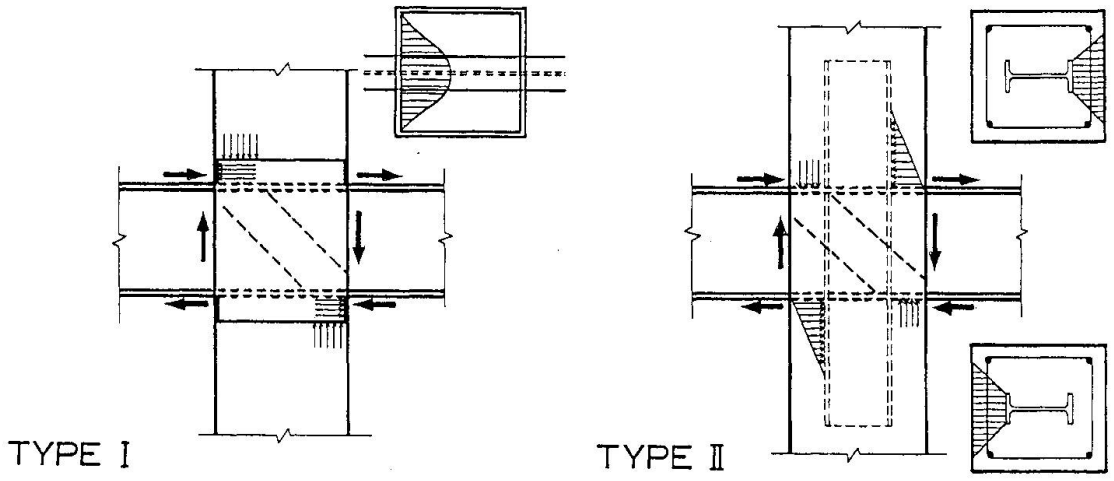

Fig. 7 Stress Transfer Mechanism

4. CONCLUSIONS

From the experimental results, the following conclusions can be stated.

1) A stress transfer mechanism between the precast concrete columns and steel beams in the present systems was studied.
2) The details of columns with steel bands or with tubular steel were very favorable for seismic design.
3) The beam-collapse-type specimens, which were designed for seismic loading, exhibited very satisfactory strength and ductility characteristics.

On the basis of these results, we refined the feasibility of these systems and their application to practical construction.

REFERENCES

1. Wakabayashi, M., "Recent Development for Composite Buildings in Japan", Composite and Mixed Construction, C. Roeder, ASCE, New York, N.Y., 1985
2. Kanoh, Y., "Review of Japanese Precast Concrete Frame Systems Used as Building Structures", Proc. of Seminar on Precast Concrete Construction in Seismic Zones, Vol. 2, JCI, Tokyo, Oct. 1986
3. Sheikh, T.M. et al., "Beam-Column Moment Connections for Composite Frames: Part 1", J. Struct. Engrg., ASCE, Vol. 115, No. ST11, Nov. 1989

Experimental and Theoretical Study of Composite Connections

Étude expérimentale et théorique d'assemblages mixtes

Untersuchung über Verbindungen bei Verbundbauweise

J.P. JASPART
Assistant
Université de Liège
Liège, Belgique

R. MAQUOI
Professeur
Université de Liège
Liège, Belgique

R. ALTMANN
Ingénieur Diplômé
Arbed-Recherches
Esch, Luxembourg

J.B. SCHLEICH
Chef de Service
Arbed-Recherches
Esch, Luxembourg

SUMMARY

This paper presents the main results of experimental research aimed at analysing the behaviour, up to collapse, of beam-to-column steel and concrete composite connections commonly used in practice. A simplified structural model for the prediction of the actual flexural behaviour is described and validated by comparison with experimental results. In addition, a non-linear finite element program for the analysis of composite frames with semi-rigid joints is presented.

RÉSUMÉ

Cet article présente les principaux résultats d'une recherche expérimentale dont le but était l'analyse, jusqu'à la ruine, d'assemblages mixtes acier-béton couramment utilisés dans la pratique. Un modèle structural de calcul destiné à prédire le comportement réel de ces assemblages soumis à flexion y est décrit; sa validité est démontrée au travers de comparaisons avec des résultats expérimentaux. Un programme de calcul non linéaire aux éléments finis pour l'analyse des structures mixtes à nœuds semi-rigides est enfin présenté.

ZUSAMMENFASSUNG

Dieser Bericht zeigt die wesentlichen Ergebnisse experimenteller Untersuchungen auf, die das Ziel hatten, das Verhalten von üblichen Riegel-Stützen-Verbindungen aus Stahl und in Verbundbauweise bis zum Grenzstand zu analysieren. Ein strukturell vereinfachtes Modell zur Vorhersage des Verformungsverhaltens wird beschrieben und die Gültigkeit durch Vergleich mit experimentellen Ergebnissen belegt. Schliesslich wird ein Finite-Elemente-Programm zur nicht-linearen Berechnung von Verbundkonstruktionen mit verformbaren Ausschlüssen vorgestellt.

1. SCOPE OF THE RESEARCH WORK

Economy in steel construction results much more from savings of labour cost than from savings of material. There is thus a trend in simplifying the detailing of joints with the consequence of a non-linear response of these joints in moment-relative rotation curves. In a beam-to-column semi-rigid joint, the relative rotation between beam and column axis is due to two contributions mainly. The first one deals with the *connection* properly (deformation of the fasteners and assembling accessories and of the column flange(s), possible slips because of hole clearances, local deformation of column web due to load introduction by the beam(s),...); the *shear deformation* of the column web panel in the vicinity of the joint is the second source of flexibility.

Much research work was conducted on bare steel framed joints with the result of a largely improved knowledge of the actual behaviour of such joints up to collapse. In contrast few information is available regarding composite joints. Therefore a recent research was launched in the Department MSM of the University of Liège with the financial help and guidance of ARBED Recherches (ECSC Research-agreement N° 7210-SA/507); it is first aimed at studying experimentally the behaviour and ultimate strength of joints between a bare steel column and composite girder(s) (steel beam section associated to a reinforced concrete slab by shear connectors) by means of web- and flange cleat(s) and 8.8 quality bolts, which were preloaded at a specified level corresponding to hand tightening (Fig. 1).

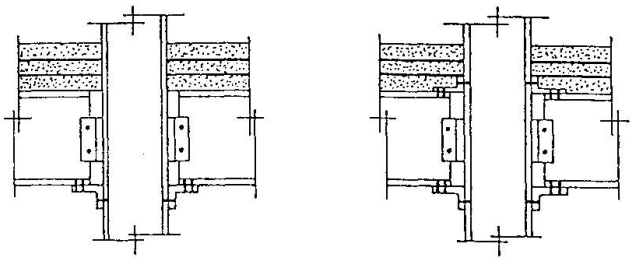

Figure 1 : Types composite joints tested in laboratory

Amongst the series of possible parameters, the following were selected because of paramount importance:

a) the relative beam-to-column flexural stiffness: a HEB 200 section column is connected successively to an IPE 240 - 300 - 360 section beam associated to a 12 cm thick RC slab ;
b) the rigidity of the assembling cleats: 150 x 90 mm angles are used with a thickness of 10 mm and 13 mm respectively ;
c) the presence or not of an upper flange cleat ;
d) the geometric proportion of reinforcements in the RC slab : 0.67 % (ϕ 10mm) - 1,3 % (ϕ 14 mm) - 2,1 % (ϕ 18 mm).

The symmetrical cruciform testing arrangement used to load the joints until collapse does not produce shear in the column web ; so the recorded experimental curves characterize only the deformability and the resistance of the composite connections.

All the test specimens were fully instrumed so that the individual components of the connection flexibility can be identified and measured, on the one hand, and that the force distribution in the assemblage be determined. Some tests were performed on full steel bare joints - i.e. without RC slabs - for sake of comparison.

The benefical influence of the stiffness and bending resistance of the joints on the performance of steel or composite frames requires the development of reliable methods for the prediction of the non-linear response of the joints and for the analysis of the frames. Present paper is only aimed at drawing the main conclusions and the critical appraisal of the acquired knowledge. The reader interested in knowing more about the test programme is begged to refer

to [1, 2].

2. EXPERIMENTAL RESULTS

The experimental results were analysed and conclusions drawn regarding the interpretation of the test results in general terms, on the one hand, and the influence of the selected parameters, on the other hand.

2.1. General interpretation of the test results

General conclusions are dealing with the nature of collapse and the level of carrying capacity exhibited by the connections :

i) All the joints used partial-strength connections; the maximum moment is however an appreciable proportion - 65 to 100 % - of the plastic moment of the composite beam section.

ii) Collapse occurs either because of buckling of the lower beam flange (for IPE 240 sections), or because of buckling of the column web or yielding of the reinforcements in the RC slab according to the proportion of such reinforcements (for IPE 300 and 360 sections).

iii) Slip between the beam lower flange and the relevant cleat due to hole clearance contributes predominantly to the connection flexibility.

iv) There are two other possible sources of connection flexibility : the compressive strains in the column web in front of the beam lower flange and the axial deformation of the RC slab between the facing ends of the beams. Their respective contributions to the connection flexibility is highly dependent on the proportion of reinforcements.

2.2. Influence of the parameters

How the parameters are liable to influence both stiffness and resistance is reflected in comparative load-displacement plots (fig. 2, 3, 4 and 5) and can be summarized as follows :

i) The individual influences of the cleat thickness, of the number of flange cleats - 1 or 2 -, and of the proportion of reinforcements respectively, are qualitatively similar, whatever the beam section used.

ii) Any increase in the proportion of steel reinforcements for a specified steel connection configuration results in larger initial rotational stiffness and maximum bending capacity (fig. 2).

iii) The rotation capacity of the connections is linked to their collapse mode - yielding of rebars (fig. 3) or column web buckling (fig. 4 and 5) - which is highly dependent on the proportion of steel reinforcements in the slab (fig. 2).

iv) An increase of the cleat thickness - in the range of sizes available on the market - does not provide with a significative increase of both rotational stiffness and maximum bending capacity (fig. 3, 4 and 5).

v) An additional upper flange cleat is not liable to change appreciably the global behaviour of the connection (fig. 4 and 5), as far as collapse is not initiated by yielding of the reinforcements.
When collapse of joints is initiated by plastic deformations of the reinforcements(fig. 3), the upper flange cleat contributes to the transmission of the tensile force through the connection, with the result of an increased bending capacity, as far as there is some strength reserve in the part of the connection aimed at transmitting compressive forces.

3. MATHEMATICAL PREDICTION OF THE COMPOSITE CONNECTION BEHAVIOUR

The shear stud connectors, that are welded on the upper flanges of the steel beams in the experimentally tested composite joints, have been designed in order to obtain a full interaction between the steel members and the RC slabs. The resulting absence of slips allows to assume the in-plane indeformability of the end sections of the composite girders (fig. 6.a). The simplified structural model (fig. 6.b) which has been developed to predict theoretically the non-linear response of the connections is based on this assumption. This model consists in an infinitely rigid beam (the end section of the girders)

lying on an elastic-plastic foundation materialized by axial springs simulating respectively the deformation and the resistance :
- of the reinforcement bars ;
- of the concrete ;
- in the zone of the upper flange cleat, of the web cleat and of the lower flange cleat: bolts in shear, in tension and in bearing, column flange, column web, cleat, slips between cleat and steel beam, ovalization of bolt holes.

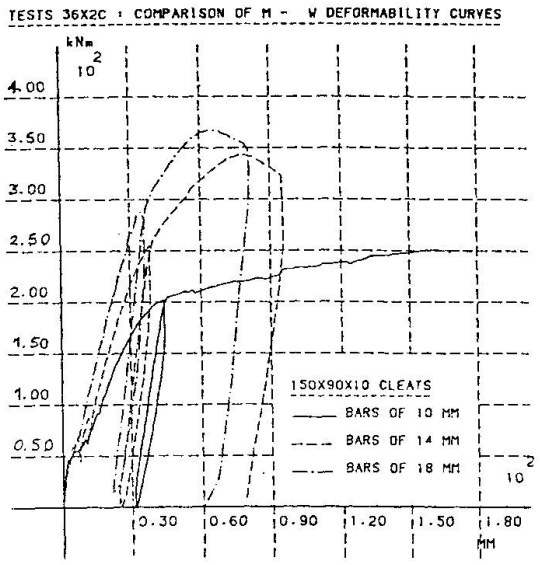

Figure 2 - Influence of the percentage of reinforcement in the concrete slab (connections with IPE 360 beams - no upper flange cleat)

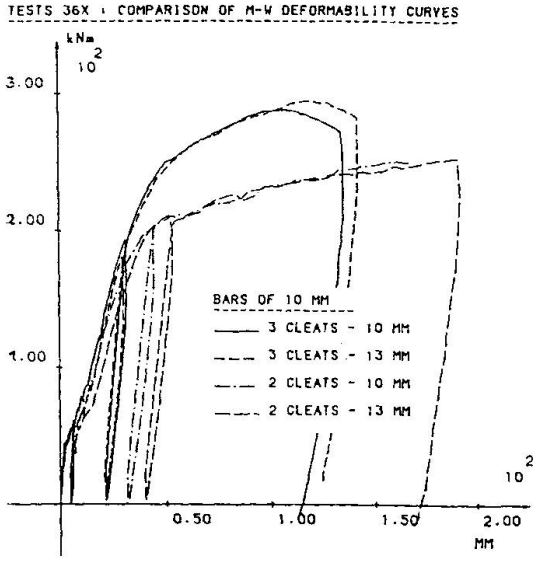

Figure 3 - Influence of cleat thickness and number of cleats-rebars of 10 mm (connections with IPE 360 beams)

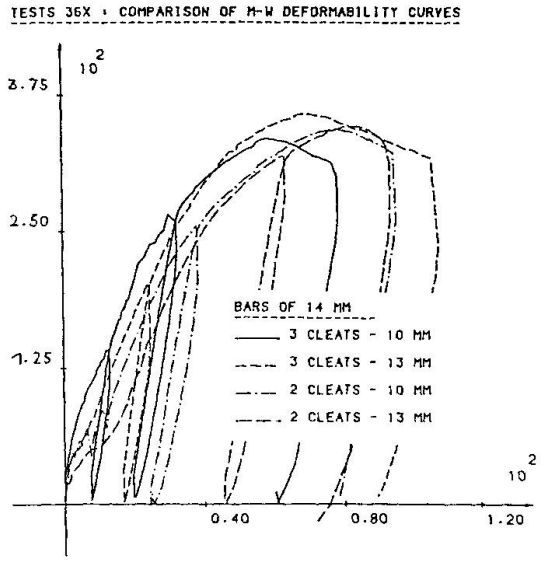

Figure 4 - ibidem - rebars of 14 mm.

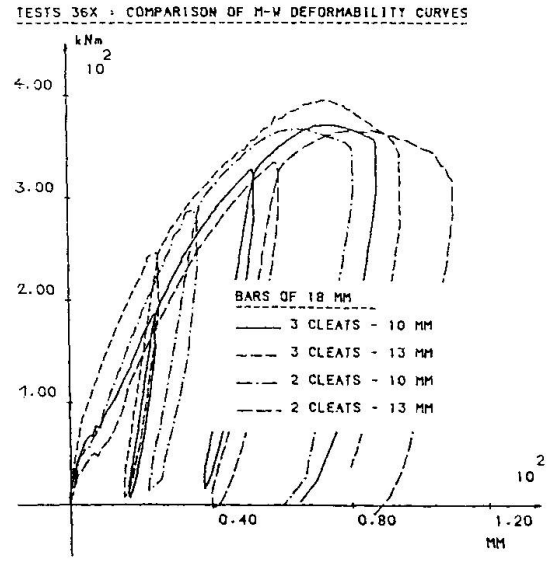

Figure 5 - ibidem - rebars of 18 mm.

Each of these springs is characterized by a specified non-linear force-displacements curve which has to be predicted as reliably as possible. Methods of modelling have been proposed for each source of deformability [2]. The introduction of concentrated loads into a column web has been particularly studied in [3].

The moment-rotation curve corresponding to a particular composite connection is built up step by step by distributing, at each level of bending moment, the loads between the springs according to their actual relative stiffness and by evaluating the associated rotation of the infinitely rigid beam.

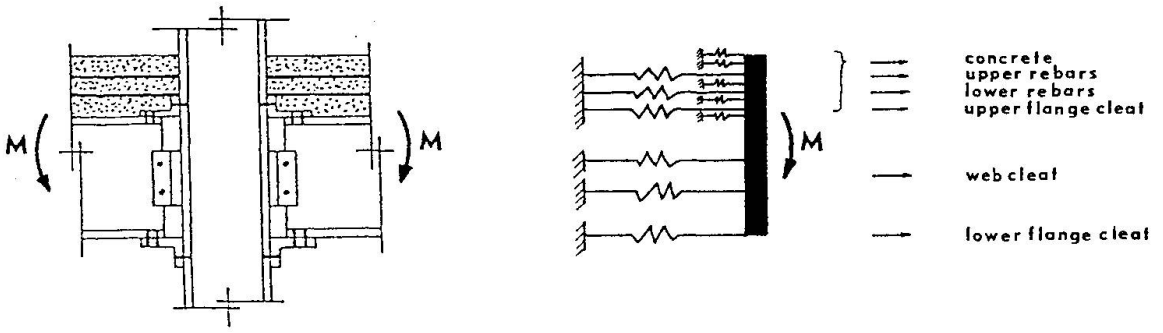

a) actual composite connection b) equivalent structural model

Figure 6 - Definition of the theoretical model for connection behaviour prediction.

This procedure has been applied in figure 7 to two composite connections only differentiated by the percentage of reinforcement.
According to the initial relative position of the bolts in their holes, the slip between the cleats and the beam may or not occur during the connection loading, what justifies the necessity to report two different theoretical curves corresponding respectively to the development of the maximum permissible slip (which depends to the hole clearances) and to the absence of slip. The influence of this parameter on the connection deformability is seen to be relatively significant.

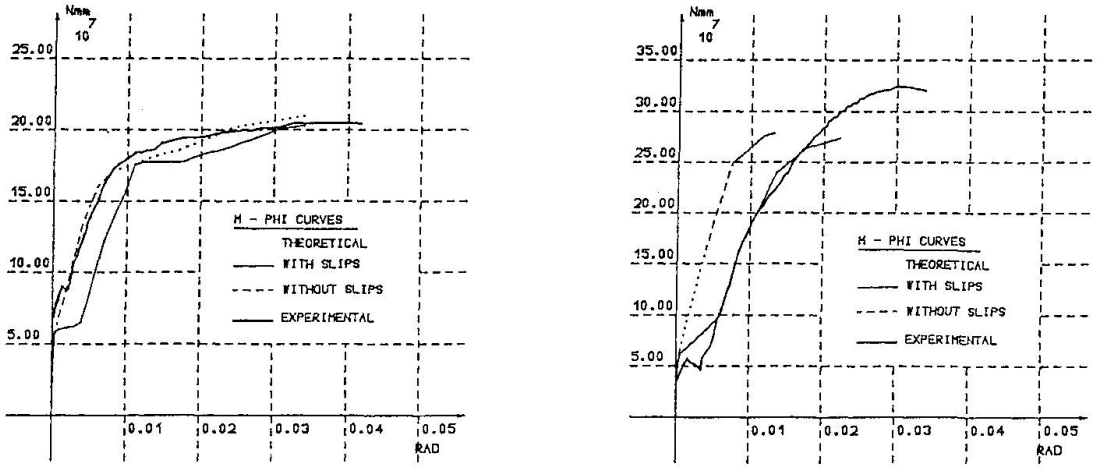

a) rebars of 10 mm b) rebars of 18 mm

Figure 7 - Comparison between experimental results and the response of the equivalent structural model (composite girders with IPE 300 beams - no upper cleat - 150 x 90 x 13 cleats).

A close agreement between the experimental curve and the response of the theoretical model is obtained in the first example where the collapse corresponds to the yielding of the rebars, as well in the second one, except for what concerns the prediction of the ultimate resistance associated, in this case, to the buckling of the column web.
This safe but important divergence may be explained (see reference [3]) by the very low out-of-plane initial imperfection of the column web measured on the specimens tested in laboratory in comparison with that, choosen on base of rolling tolerances [4], which has been considered for the assessment of the theoretical buckling load of the web.

The interest of such an equivalent structural model is threefold :
- to validate the individual mathematical models developed for each source of flexibility of the composite connections : cleats, introduction of loads in column webs,...;
- to represent a valuable tool in view of intensive parametric studies ;
- to constitute a foundation for further developments of a more simplified and practical approach for the evaluation of the deformability and resistance characteristics of the composite connections.

4. ANALYSIS OF FRAMES WITH COMPOSITE JOINTS

The finite element program FINELG which is being developed at the University of Liège and at the Polytechnical Federal School of Lausanne gives the possibility of solving two types of problems. The former consists of the calculation of the critical loads and also of the associated buckling modes. The latter consists of following the non-linear evolution of a structure under increasing external loading up to collapse or instability, and even beyond. This program allows one to take account of great displacements, ,instability phenomena, non-linear constitutive laws of materials (steel, concrete,...), initial deformations, residual stresses,... The main finite elements of the FINELG program are the following : truss elements, plane or spatial beam elements, plane composite steel elements [5], plate-membrane elements, shell elements, linear constraint elements, non-linear spring elements.
The FINELG program has been modified so as to simulate the behaviour of semi-rigid connections [6] and of sheared column web panels [3]. The moment-rotation curves, characteristics of the actual behaviour of the joints, may be modelled by using more or less complicated mathematical laws (linear, bilinear and multilinear laws, power law, extended Richard's law, Ramberg-Osgood law,...).

5. REFERENCES

1. ALTMANN, R., MAQUOI, R. and JASPART, J-P., Experimental study of the non-linear behaviour of beam-to-column composite joints. Proc. Intern. Colloquium on Stability of Steel Structures, Hungary, Budapest, 1990.
2. Semi-rigid action in steel frame structures. C.E.C. Agreement n° 7210-SA/507. Final Report. ECSC, Brussels, 1990 (to be published).
3. ATAMAZ SIBAI, W. and JASPART, J-P., Etude du comportement jusqu'à la ruine des noeuds complètement soudés. Internal report N° 194 (MSM - University of Liège)/ N° 89/7 (IREM - Polytechnic Federal School of Lausanne), October 1989.
4. ALPSTEN, G.A., Variations in mechanical and cross-sectional properties of steel. ASCE-IABSE International Conference on Planning and Design of Tall Buildings. Vol. Ib-9, 1972.
5. BOERAEVE, P., Présentation de l'élément PPCAA-BB (poutre plane en béton armé) dans le FINELG. Rapport interne MSM, Université de Liège, N° 201, Novembre 1988.
6. JASPART, J-P. and de VILLE de GOYET, V., Calcul numérique de structures composées de poutres à assemblages semi-rigides. Construction Métallique, 2 (1988), 31-49.

Inelastic Bridge Rating for Steel Beam and Girder Bridges

Evaluation inélastique de ponts à poutres d'acier

Inelastische Auswertung von Stahl Balkenbrücken

M. BARKER
Ph. D. Cand.
Univ. of Minnesota
Minneapolis, MN, USA

B. DISHONGH
Assoc. Prof.
Rose-Hulman Univ.
Terre Haute, IN, USA

R. LEON
Assoc. Prof.
Univ. of Minnesota
Minneapolis, MN, USA

C. FRENCH
Assist. Prof.
Univ. of Minnesota
Minneapolis, MN, USA

T. GALAMBOS
Professor
Univ. of Minnesota
Minneapolis, MN, USA

SUMMARY

This paper outlines the results of a study aimed at utilizing some of the inelastic reserve capacity for regular periodic rating of beam and girder bridges. Two methods are presented: one applies to multi-beam bridges with compact sections, while the other method can also be used to rate non-compact plate-girder bridges. The factored live loads will produce moderate inelastic deformations at the limit state.

RÉSUMÉ

Cet article présente les résultats d'une étude visant à profiter de la surcapacité inélastique en vue de l'évaluation périodique routinière de ponts d'acier composés de profilés laminés ou de poutres assemblées. Deux méthodes sont exposées. La première concerne les ponts à poutres multiples à sections laminées compactes. La seconde peut aussi évaluer des ponts à poutres assemblées à sections non compactes. Les surcharges pondérées produiront des déformations inélastiques modérées à l'état limite.

ZUSAMMENFASSUNG

Die Ergebnisse einer Forschung über die mögliche Ausnutzung der inelastischen Reserve von Balkenbrücken während der periodischen Bewertung werden hier zusammengefasst. Zwei Methoden werden beschrieben: eine davon gilt für Balkensysteme mit kompakten Querschnitten, die andere erfasst auch nicht-kompakte Balken. Die faktorisierten Nutzlasten bewirken nur kleine, fast unmerkliche Dauerverformungen.

1. INTRODUCTION

Many older steel beam and girder bridges have been judged to be structurally deficient based on rating methods using conservative elastic analysis techniques and current design procedures[1]. However, slab-on-steel girder bridges are highly redundant structures and show, like most steel structures, a significant redistribution of moments and a large reserve capacity in the post-elastic range. To more realistically asses the capacity of a bridge, this reserve strength should be considered. This paper summarizes development of an inelastic bridge rating procedure which considers this reserve capacity.

Two ultimate limit states are presented: (1) the shakedown limit of compact bridge systems and (2) residual damage deflection limits. The techniques are applicable to simple and continuous, straight steel beam and girder bridges.

2. SHAKEDOWN LIMIT STATE OF BRIDGE SYSTEMS[2]

The shakedown limit is defined as the maximum load cyclically applied to the system for which deflections stabilize. The two major developments for the shakedown limit state models are (1) a direct method to find the global shakedown limit load of a bridge system and (2) inelastic models to analyze bridge systems in the post-elastic range. The global shakedown limit method is derived from the shakedown theorem, the bridge deck system behavior, and global equilibrium equations. The method involves condensing the system responses and strengths into a global kinematic incremental collapse mechanism. The grillage analogy is used for the elastic and inelastic analyses. The shakedown upper bound mechanism method can be employed to find the critical shakedown limit state for an assumed global incremental mechanism shown in Figure 1:

$$\Gamma\sum_i (M_{el}^+)_i\theta_i+\Gamma\sum_j (M_{el}^-)_j\theta_j+\sum_i (M_d^+)_i\theta_i+\sum_j (M_d^-)_j\theta_j = \sum_{i,j} (M_p)_{i,j}\theta_{i,j}$$

where:

Γ	=	shakedown load factor
$(M_{el})_{i,j}$	=	maximum positive or negative girder moment at section i or j from an elastic analysis of the grillage
$(M_d)_{i,j}$	=	dead load moment at section i or j
$\theta_{i,j}$	=	global kinematic mechanism rotation at section i or j
$(M_p)_{i,j}$	=	member capacity at section i or j
i,j	=	section with rotation in the kinematic collapse mechanism

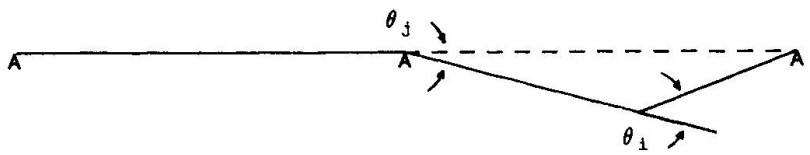

Figure 1 Global Incremental Collapse Mechanism

The result is that the bridge system can be reduced to an equivalent single girder analysis where the elastic moment envelope is the summation of all the individual grillage girder

elastic moment envelopes across the global section. Likewise, the dead load moments and moment capacities of the equivalent single girder are the respective sums of the individual girder values.

The models were used to rate three noncomposite, compact one- (13.7m), two- (16.8,16.8m), and three-span (16.8,19.8,16.8m) bridges. All had five W27X102 (US) girders spaced at 2.1m with a 180mm concrete deck. The loading consisted of the critical of the standard factored AASHTO[3] rating vehicles. Four limits were investigated: the current AASHTO method[3] using lateral distribution factors and a first hinge limit, first hinge of the system, shakedown of the system, and the system collapse limit.

Limit State Type	AASHTO Method	Grid 1st Hinge	Grid Shakedown	Grid Collapse
Single-Span	0.961	1.042	1.124	1.529
Two-Span	0.944	1.013	1.127	1.631
Three-Span	0.957	1.027	1.125	1.631
Avg Incr. over AASHTO Method	-	7.7%	18.0%	67.4%
Avg Incr. over Grid 1st Hinge	-	-	9.6%	45.5%

Table 1 Example Bridge Rating Factors

Table 1 presents the results. The shakedown limit state showed an average of 18.0% reserve capacity over that of AASHTO and 9.6% reserve capacity over that of the first hinge of the grid system. This inelastic reserve capacity is ignored in the current ultimate first hinge formation limit states. The average shakedown limit load, however, is only 70.4% of the collapse limit load. Figure 2 shows the effect on structural behavior when a load of 1% over shakedown is applied to the two-span example bridge. The bridge exhibits incremental collapse (non-stabilizing deflections). Incremental damage occurs at a rate so as to render the bridge useless after relatively few cycles. Therefore, it is reasonable to assume the shakedown load as the ultimate limit state. Shakedown better represents the ultimate strength of the bridge and still ensures an adequate margin of safety against incremental collapse.

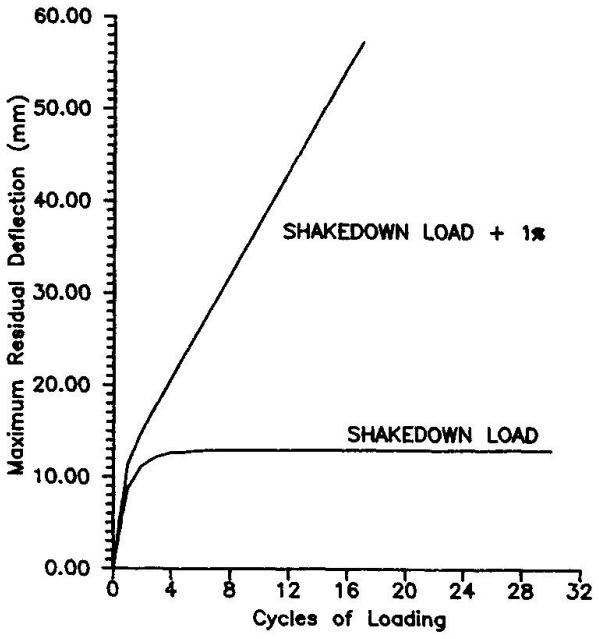

Figure 2 Residual Deflection

3. RESIDUAL DAMAGE DEFLECTION LIMITS[4]

Residual Damage Analysis (RDA) provides a new way of rating against an inelastic deflection limit state, defined as the ratio of the span to midspan inelastic deflection, or C = L/D. RDA utilizes the conjugate beam method beyond the elastic range and into the inelastic range of the structural load-deformation response. The moment-rotation model developed for RDA is based on the results of recent research into the inelastic behavior of steel composite and non-composite girders[5,6].

Current elastic bridge rating methods [1,3] restrict factored truck loads to the maximum level at which all load-induced deflections will vanish once the load is removed, i.e., the elastic load limit. Using RDA, more liberal load allowances can be achieved by allowing a modest amount of permanent deflection to remain after the factored loads are removed. Because load factors are used, we are assured that we will seldom, if ever, actually realize this residual damage. While AASHTO contains an inelastic steel bridge design method known as Autostress Design [5], it currently provides no inelastic rating method. RDA was developed to meet this need.

Residual Damage Analysis performs a single girder analysis of a bridge subjected to moving truck loads. Where inelastic rotations may form, the moment versus inelastic rotation, M-θi, relationship shown in Figure 3 is invoked to solve for the additional unknown on the conjugate beam - the inelastic rotation, θi.

A computer program was developed to accommodate the case of multiple hinges forming as the result of the moving rating truck load. In this situation, the interplay between increments of inelastic rotation and their associated residual moment field must be allowed to run its course with multiple truck passes, i.e., the bridge must be allowed to shake down. When only one inelastic hinge rotation occurs, RDA can be used to manually rate a steel girder bridge, because, in this instance, shakedown occurs with a single pass of the load.

When manually rating against a specific level of residual damage, defined as the ratio of the length of span to the midspan permanent deflection, C=L/D, the following steps are followed:

1) Determine the required value of inelastic rotation, θi, to achieve the inelastic deflection limit, C=L/D. With this value of θi, determine the accompanying residual moment, Mr. (This relationship is easily obtained using the conjugate beam "loaded" with the inelastic rotation "force," θi.
2) Determine the parameters necessary to define the moment versus inelastic rotation, M-θi, model.
3) Determine the dead load moments, Md, and the live load elastic moment envelope, Ml.
4) Equate θi of Step 1 with the expression obtained in Step 2. Solve for the hinge resisting moment, Mi.
5) Determine the inelastic rating factor, IRF, by applying the following formula at the hinge point:

$$(IRF) * Ml + Md + Mr = Mi$$

Figure 3 shows a symmetrical two-span (L=18.3m), noncomposite bridge girder subjected to a moving HS-20 truck and a uniform load

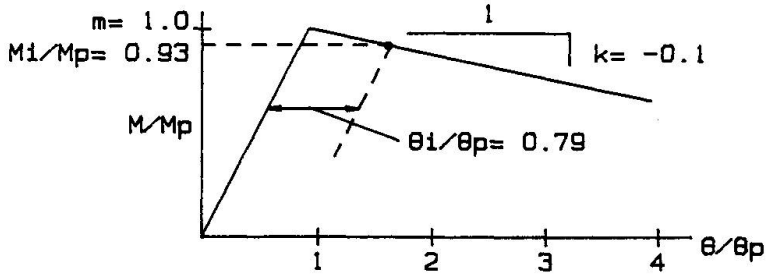

$\theta i = \theta p/Mp * (1/k - 1) * Mi + \theta p * (m - m/k)$
$\theta i = -0.0000928 * Mi - 0.206$

MOMENT ROTATION MODEL FOR RDA

Cross Section Data
tf= 25.4 mm; bf= 356 mm; tw= 9 mm; Dw= 787 mm
Fy= 345 MPa; Mp= 3006 kN m
EI= 668,644 Kn m

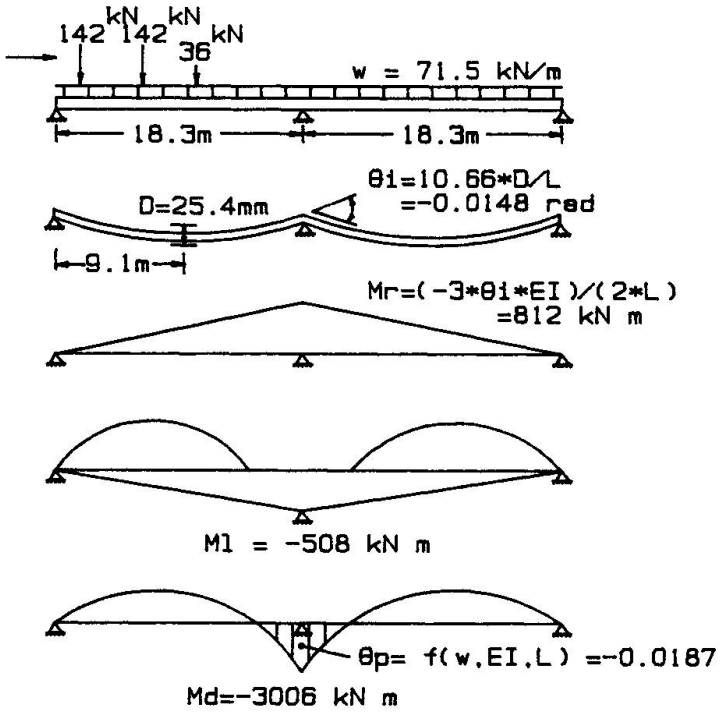

(IRF) * Ml + Mr = Mi; Mi = (θi+0.206)/(-0.0000928)
(IRF) * (-508) + (-3006) + (812) =-2793 ⟶ IRF = 1.17

Figure 3 Example of Manual Rating Using RDA

which causes the elastic bending limit, Mp, to be reached at the interior support. For purposes of clarity, the load and resistance rating factors are taken as unity. The inelastic load rating factor, IRF, is to be computed for an inelastic midspan deflection limit of 25.4mm (C=L/D=720) due to an inelastic hinge rotation at the interior support.

Based on an elastic load limit, the elastic rating factor applied to the concentrated load would be RF=0 (dead load alone is the elastic limit). However, an inelastic rating factor of IRF=1.17 is realized by allowing the 25.4mm of residual damage. This represents an overall load increase of (1.17*320)/(36.6*71.5), or 14% above the elastic limit.

4. SUMMARY

Many of the bridges classified as deficient using current methods may be reclassified as sufficient if a true representation of the ultimate strength were considered. The incorporation of the post-elastic strength of redundant structures is more rational than the current elastic limits and the system shakedown limit state or deflection limit is a more meaningful ultimate limit state for bridge rating. The new procedures, with appropriate load and resistance factors, ensure an adequate margin of safety, while utilizing the inelastic reserve capacity of the bridge structure.

ACKNOWLEDGEMENT

This research was sponsored under the auspices of the National Cooperative Highway Research Program (NCHRP 12-28(12)). The findings and conclusions herein are those of the authors and do not necessarily reflect the views of the sponsors.

REFERENCES

1. AMERICAN ASSOCIATION OF STATE HIGHWAY AND TRANSPORTATION OFFICIALS, Manual for Maintenance Inspection of Bridges, AASHTO, Washington, D.C., 1983.
2. BARKER, Michael G., The Shakedown Limit State of Slab-on-Girder Bridges, PhD Thesis Submitted to the Faculty of the University of Minnesota, March, 1990.
3. AMERICAN ASSOCIATION OF STATE HIGHWAY AND TRANSPORTATION OFFICIALS, Guide Specification for Strength Evaluation of Existing Steel and Concrete Bridges,AASHTO, Washington, D.C., 1989.
4. DISHONGH, B.E., Residual Damage Analysis: A Method for the Inelastic Rating of Steel Girder Bridges, PhD Thesis Submitted to the Faculty of the University of Minnesota, January, 1990.
5. AMERICAN ASSOCIATION OF STATE HIGHWAY AND TRANSPORTATION OFFICIALS, Guide Specification for Alternate Load-Factor Design Procedures for Steel Beam Bridges Using Braced Compact Sections, AASHTO, Washington, D.C., 1986.
6. ANSOURIAN, P., Plastic Rotation of Composite Beams, Journal of the Structural Division, ASCE, Vol 108, No ST3, March, 1982.

Semi-Rigid Composite Connections

Assemblages mixtes à rigidité partielle

Verschiebliche Verbindungen in Rahmentragwerken mit Verbundträgern

Roberto T. LEON
Assoc. Prof.
Univ. of Minnesota
Minneapolis, MN, USA

Roberto T. Leon, born 1955, received his Ph.D. degree from the University of Texas at Austin in 1983. He ia an Associate Professor of structural engineering at the University of Minnesota in Minneapolis.

SUMMARY

Semi-rigid composite connections are traditional steel frame connections in which the additional strength and stiffness provided by the floor slab has been incorporated by adding shear studs and slab reinforcement in the negative moment regions adjacent to the column. Ten full-scale semi-rigid connection subassemblies were recently tested under both monotonic and reverse cyclic loads. The results of those tests indicate that these connections can provide adequate lateral stiffness for buildings of up to ten stories in areas of low to moderate winds.

RÉSUMÉ

La présence de connecteurs à cisaillement et d'armature dans les zones de moments négatifs dans les dalles de planchers en béton à proximité des poteaux augmente la résistance et la rigidité dans les assemblages simples d'ossatures métalliques. Récemment dix assemblages mixtes à rigidité partielle de grandeur nature ont été mis à l'épreuve en les soumettant à des charges monotones croissantes et à des charges cycliques. Les résultats de ces expériences démontrent que de tels assemblages peuvent être utilisés dans des édifices jusqu'à dix étages situés dans des zones de vents d'intensité modérée.

ZUSAMMENFASSUNG

Verschiebliche Verbindungen in Rahmentragwerken mit Verbundträgern sind gewöhnliche Stahlverbindungen welche weiter mit geschweissten Dübeln und Betonarmierung verstärkt und versteift werden, so dass die Deckenplatten und die Stahlkonstruktion im Verbund wirken. Zehn Versuche an Verbindungskörpern mit verschieblichen Verbindungen wurden mit monotoner und wiederholter Belastung durchgeführt. Die Ergebnisse dieser Versuche wurden dann in einer parametrischen Studie von Rahmentragwerken angewandt, und es wurde gezeigt, dass diese Verbindungen für bis zu zehnstöckige Rahmen in Gegenden moderater Windkräfte genügend biegesteif sind.

1. INTRODUCTION

The strength, ductility and stiffness of ordinary steel frames can be significantly improved by composite action. This can be achieved by providing a few continuous reinforcing bars across the column lines and insuring full composite action through the use of sufficient shear studs in the beams. The connections can range from very weak to almost rigid, and represent variations of typical steel connections used in the U.S.A. The data generated in this study indicates that unbraced frames up to 10 stories can be erected in zones of low to moderate seismicity , and that significant economies in steel can be achieved by utilizing this structural system.

2. SEMI-RIGID COMPOSITE CONNECTIONS

Ten full-scale semi-rigid composite connection subassemblies have been tested under both monotonic and reverse cyclic loads. Semi-rigid composite connections are traditional steel frame connections in which the additional strength and stiffness provided by the floor slab has been incorporated by adding shear studs and slab reinforcement in the negative moment regions adjacent to the columns. Four different types of connections have been tested (Figure 1):

(1) Seat and web angles (Type I): These consists of a typical seat angle connection, where significant moments can be transmitted at the column face by the slab reinforcement as the tension part of the couple and the angle as the compression member. Under reversed cyclic loading this type of connection is weak if positive moments are present because the angle will pullout at relatively low loads. The strength of the connection is controlled in negative moment by the amount of slab steel and in positive moment by the size (primarily thickness) of the angle. Very stiff connections can be obtained by using large friction bolts and thick angles in the web and seat. Figure 2 shows a typical moment-rotation curve for one such connection under reversed cyclic loads.

(2) Bottom welded plate plus web angles (Type II): This represents the stiffest economical semi-rigid connection possible. The bottom angle, which in Type I connections was the weak link, has been substituted with a welded plate. This plate carries the tensile and compressive forces basically as axial loads, resulting in a very stiff and non-degrading connection. The same results can be achieved by welding the plate to the column in the shop and bolting it to the beam with high strength friction bolts in the field. The welds must be detailed to insure full transfer of moment and to eliminate the possibility of weld fracture. This connection offers very large initial stiffnesses and symmetrical behavior under cyclic loading.

(3) Seat angle (Type III): This connection is similar to Type I, except that the web angles are missing. This results is a connection with a much flatter inelastic region, because there are no web angle to provide additional restraint once the seat has yielded. In addition careful attention must be paid to the stability of the bottom angle and the beam web. As for Type I, the thickness of the seat angle is the controlling parameter.

(4) Web angles (Type IV): This connection is a variation on the simplest shear connection used in all-steel frames. Although the angles are relatively weak, the moment capacity of the composite connection can be substantially improved by increasing the thickness of the angle and lowering its position towards the bottom of the beam web. Since the web angles are carrying both

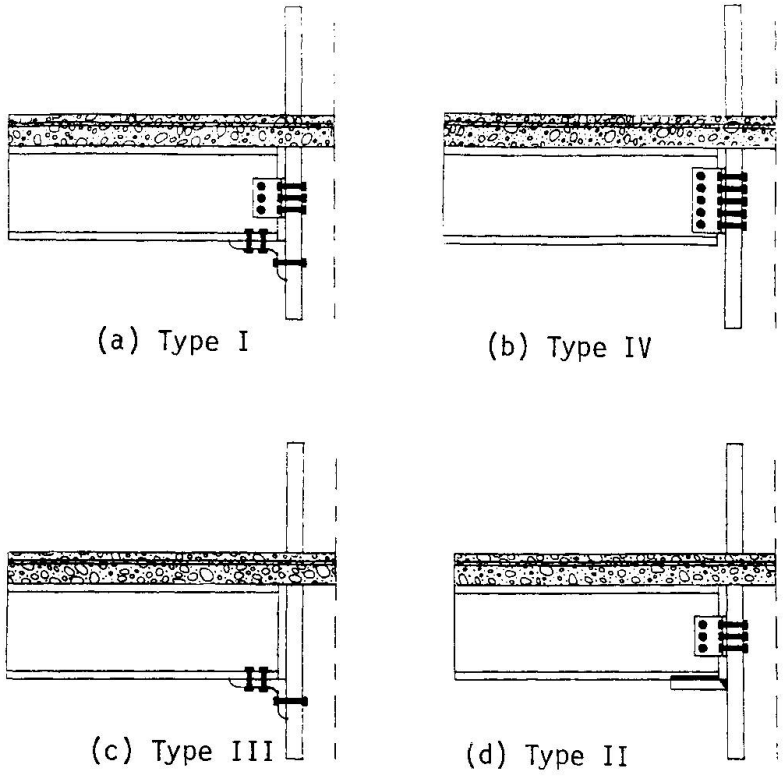

Figure 1 - Different semi-rigid composite connections.

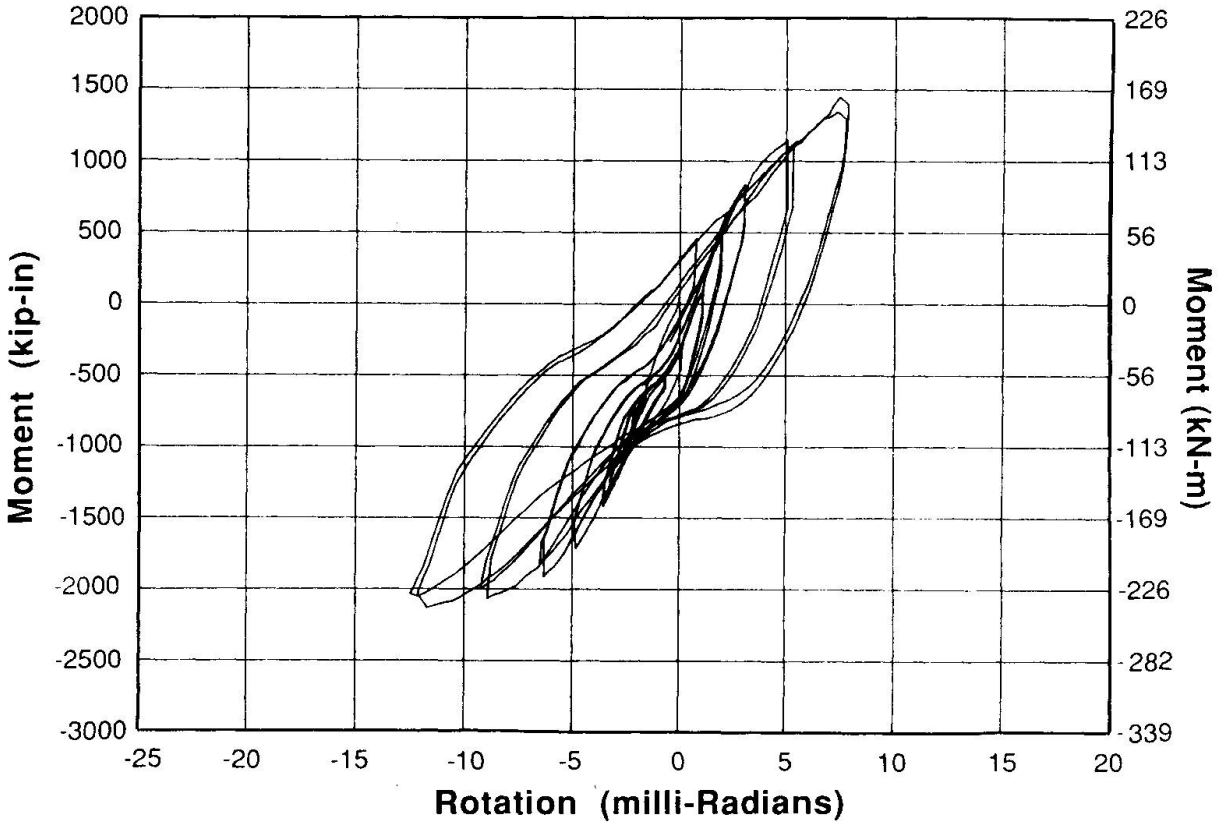

Figure 2 - Typical cyclic response for a Type I connection.

shear and moment care must be taken to prevent any type of block shear failure.

3. ANALYTICAL STUDIES

For analysis and design purposes, it is imperative to have a good knowledge of the moment-rotation characteristics of the connection. This is not a simple task, since the non-linear behavior of the connection must be carefully modelled. In order to obtain a parametric equation for Type I connections, relating the size of the angle, amount of slab steel, beam depth, and web angle size, a large number of non-linear finite element models of semi-rigid composite connections were run. These computational studies led to the development of a complete moment- rotation equation, and for the ultimate and yield moments. For the case of Type I connections the equations for the yield and ultimate moment take the form:

$$M_y = 0.170 \; [\; (4 \times A_{rb} \times F_{yrb}) + (A_{sL} \times F_{ysL}) \;] \; (d + y_3)$$

$$M_u = 0.245 \; [\; (4 \times A_{rb} \times F_{yrb}) + (A_{sL} \times F_{ysL}) \;] \; (d + y_3)$$

where M_y is the yield moment, M_u is the ultimate moment, A_{rb} is the area of the slab reinforcement, F_{yrb} is the yield stress fro the slab reinforcement, A_{sL} is the area of the seat angle, F_{ysL} is the yirld stress for the seat angle, d is the depth of the beam and y_3 is the height of the shear studs. All units in these equations are in kips and inches. These two equations allow the use of a bilinear approximation to the exact curve, considerably simplifying the computational task of analyzing a large frame.

4. DESIGN EXAMPLES

To show the potential of the semi-rigid composite system and to illustrate extremes of behavior, two frames were designed as both rigid and semi-rigid. The first frame was a four-story, three-bay frame with 9.60 m bays and 4.27 m story heights. The second frame was an eight-story, three-bay frame with 8.53 m bays and 4.27 m story heights. The frames were designed for ultimate strength, and checked under live loads for lateral deflection. Figure 3 shows the entire load-deflection curves to collapse, normalized to a load factor of 1.00 (full wind load = 1.00) and a lateral deflection of L/400 (maximum commonly allowed in the U.S.). Figure 4 shows the sequence of plastic hinge formation for both frames.

For the case of the four-story frame, the beams for both the rigid and semi-rigid frames were the same. Thus the only differences are the rigidity of the connection and the composite action. For these frames the behavior is very similar up to collapse, with the semi-rigid frame being slightly more flexible. This demonstrates that semi-rigid composite frames possess good stiffness and strength characteristics.

For the case of the eight-story frame, the beams in the semi-rigid composite frame were proportioned to be about 2/3 of the weight of those in the rigid frame. For this case the rigid frame can attain a load factor of over 3.5, while the semi-rigid composite frame only attains about 2.0. Moreover the deflections in the semi-rigid composite frame are much bigger, and it barely meets the L/400 drift criteria. From inspection of Figure 4, it is clear that as soon as the first level hinges in the semi-rigid composite frame the lateral deformations become very large and P-Δ take over.

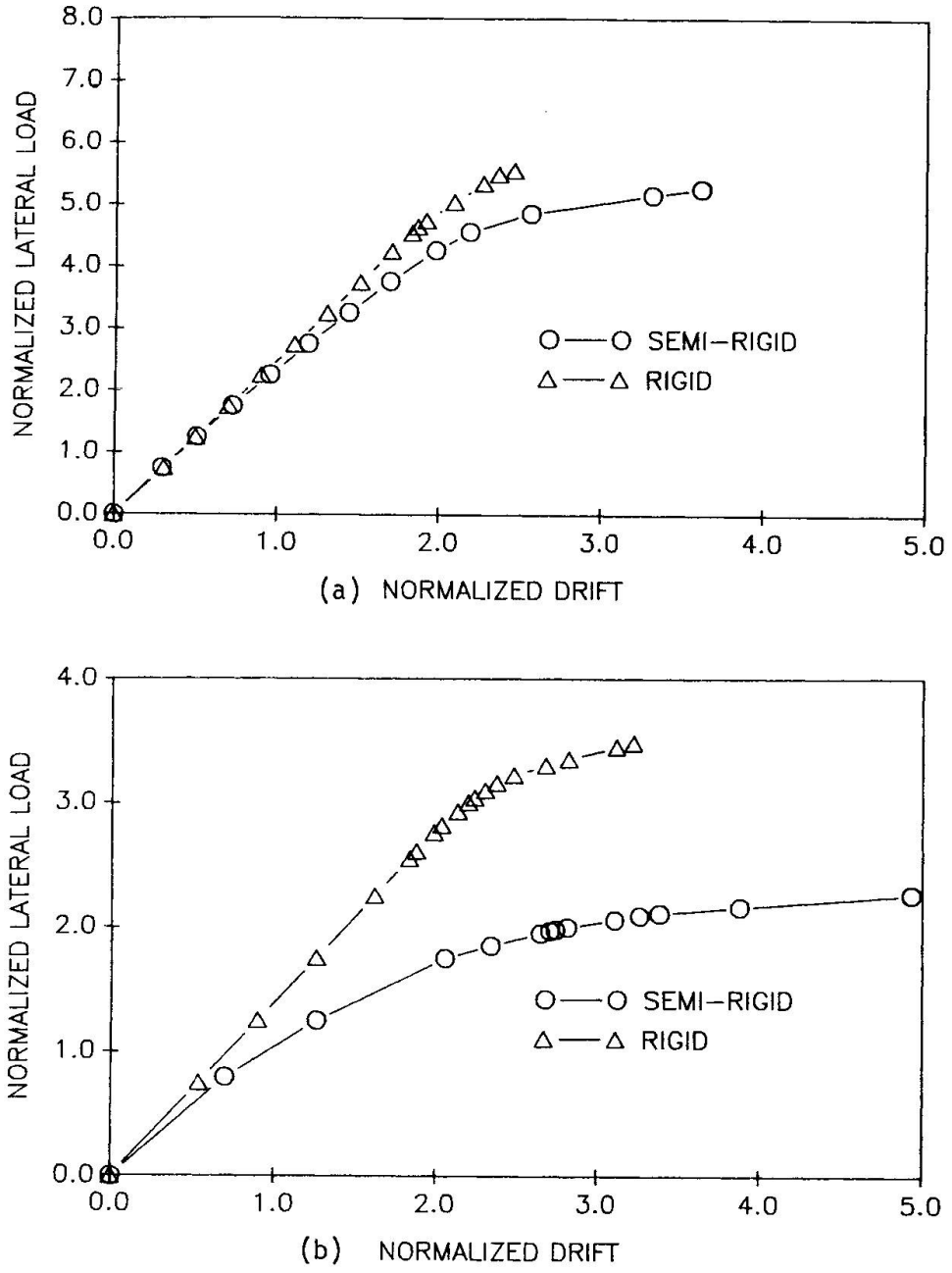

Figure 3 - Normalized drift vs. lateral load for (a) four-story and (b) eight story structures.

5. SUMMARY

The work reported here indicates that :

[1] Significant increases in strength and stiffness of simple connections can be achieved by providing some continuous slab reinforcement over the column lines. The added cost is only that of a few supplementary slab bars, since no additional shear studs or bolts are required.

[2] Semi-rigid composite connections provide a large amount of ductility and extra reserve capacity. A structure designed as semi-rigid composite would provide a very high degree of protection against progressive collapse failures.

[3] The failure mechanisms for these connections are well understood and design procedures to prevent them have already been developed.

[4] A semi-rigid composite system can be very economical in braced frame construction if the design live loads exceed the dead loads by a factor of at least two.

6. ACKNOWLEDGEMENTS

The work described in this paper was carried out under the generous sponsorship of the American Institute of Steel Construction and the National Center for Earthquake Engineering Research at the State University of New York at Buffalo.

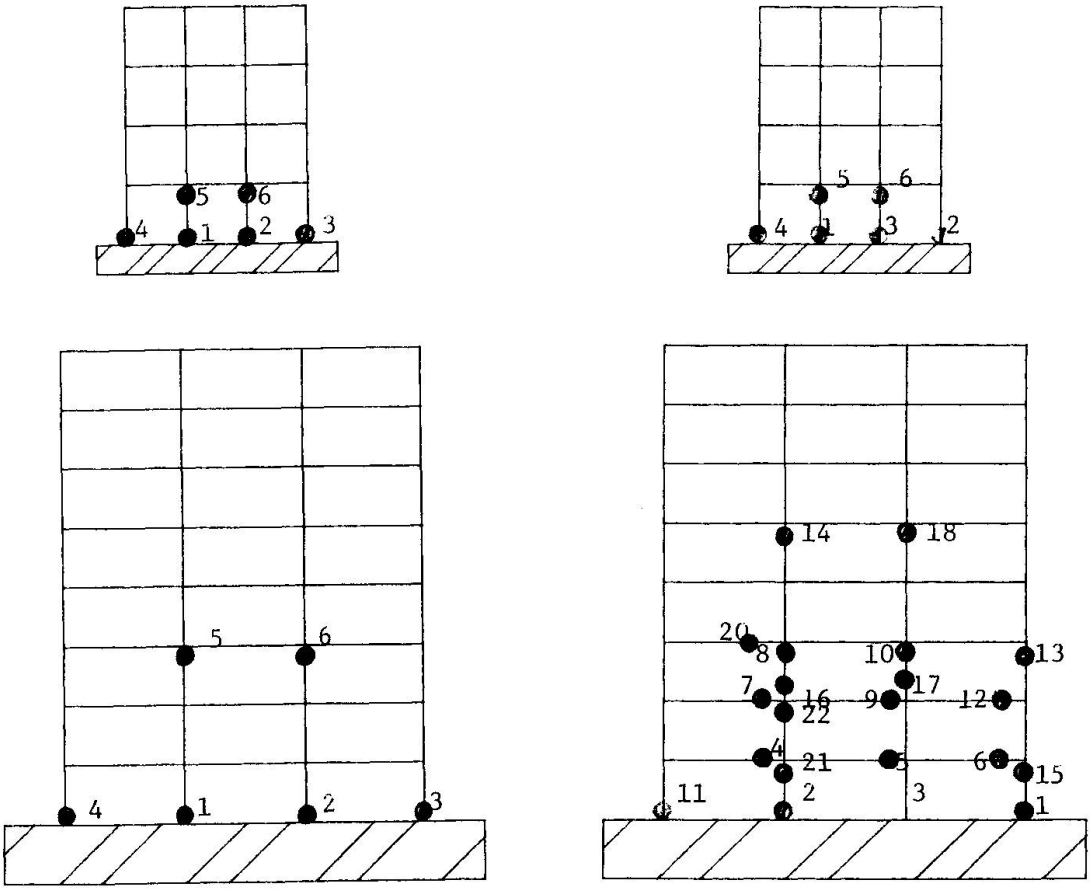

(a) Semi-rigid composite (b) Rigid

Figure 4 - Sequence of plastic hinge formation for example frames.

Joints in Hybrid Bridge of Steel Girder and Concrete Pier

Liaison entre poutre métallique et pile en béton armé dans un pont hybride

Anschlüsse in aus Stahlträgern und Betonstützen bestehenden Verbundbrücken

Jiro TAJIMA
Professor
Saitama Univ.
Urawa, Japan

Jiro Tajima, born in 1925, obtained his doctorate degree at the University of Tokyo, Tokyo, Japan. For ten years he was the Manager of the Design Department at Honshu-Shikoku Bridge Authority. He joined Saitama University in 1980.

Yoshinori ITO
Manager
Japan Highw. Publ. Corp.
Tokyo, Japan

Yoshinori Ito, born in 1943, obtained his M.S. degree at Nagoya University, Nagoya, Japan, in 1967, bridges design and construction. He is working at head office of JHPC as a manager of structural engineering division, he has a full responsibility for all expressway bridge design and construction.

A. MACHIDA
Professor
Saitama Univ.
Urawa, Japan

Atsuhiko Machida, born in 1940, obtained his doctorate degree at the University of Tokyo, Tokyo, Japan. For 21 years, he has been working for Saitama University. His research interests are seismic resistant design of reinforced concrete structures and steel concrete composite structures.

SUMMARY
Studies were carried out on joints in hybrid bridge in which steel girders are rigidly connected to reinforced concrete piers with prestressing bars. The fundamental behavior of such joints including stress transfer mechanisms and load carrying capacity was clarified through experiments and analysis. In this paper, the results of the studies are presented with the general features of a highway bridge which was designed based on the results and is now under construction.

RÉSUMÉ
On a réalisé des études sur les liaisons dans un pont hybride, dont la poutre est connectée rigidement à la pile en béton armé par des barres précontraintes. On a mis en évidence, par l'expérience et l'analyse, le comportement fondamental de cette liaison qui implique le mécanisme de transmission de contraintes et de force portante. Dans ce rapport, les résultats d'étude sont présentés avec les caractéristiques générales d'un pont d'autoroute au Japon. Ce pont a été calculé sur la base de ces résultats et est en cours de construction.

ZUSAMMENFASSUNG
Untersuchungen über die Anschlüsse einer Verbundbrücke, in der Stahlträger mittels Spanngliedern fest mit dem Stahlbetonpfeiler verbunden sind, wurden durchgeführt. Das Verhalten des Anschlusses bezüglich des Mechanismus der Kraftübertragung als auch der Traglast wurden durch Versuche und Analysen geklärt. In diesem Beitrag sind die Ergebnisse der Untersuchungen zusammen mit der generellen Darstellung einer Autobahn-Brücke, die auf Grund dieser Untersuchungsergebnisse entworfen wurde und zur Zeit im Bau ist, dargestellt.

1. INTRODUCTION

Rigid frame type bridge, in which steel girders are rigidly connected to reinforced concrete piers, has many merits as compared with the ordinary steel girder, shoe and pier system, because damages originated from local damages in shoes and expansion joints in super structure can be eliminated and smooth riding qualities can be achieved by reducing the number of expansion joints. Though such merits do exist, very few studies have been carried out on design methods for rigid joint in such hybrid bridges. Accordingly, studies on rigid joint in hybrid bridge in which steel girder is connected to reinforced concrete pier with prestressing bars were carried out experimentally and analytically to make clear fundamental behavior of such joint.

This paper describes the results of the experiments and analysis, and discusses stress distribution in such joint, stress transfer mechanism between steel girder and concrete pier, load carrying capacity of such structure and so on, based on the results. Also, the Sasaya Bridge, which was designed based on the results, and is under construction, is introduced as an example of hybrid bridges which have joints of this kind.

2. OUTLINE OF THE EXPERIMENT AND ANALYSIS

2.1 Specimens

Four specimens were prepared. They are classified into A, B, C and D type according to details of the joints and the dimension of the cross sections. All of them were such ones that a pair of steel plate girders was connected to a reinforced concrete column with four prestressing bars at the center of the girders and the bottom of the column, as shown in Fig.1. At the center of the girders, there is a space surrounded by the webs of the girders, the diaghrams and the bottom plate. This space was filled with concrete, and the prestressing bars were anchored through the filled concrete. Difference among the four specimens is also shown in Fig.1 Stud shear connectors in the A and B type specimens were welded to the diaghrams.In the B type specimen, the outer fibers of the concrete column were cut off at the contact face to the steel girders.

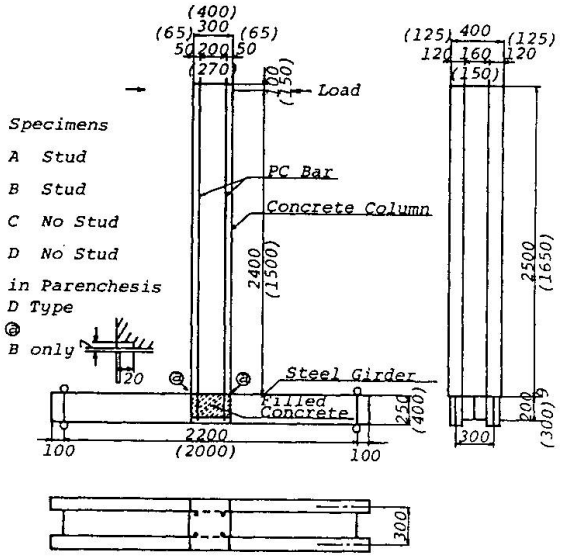

Fig.1 Specimens

2.2 Loading program

In the experiments, both ends of the steel girders were fastened to a loading bed through rollers. Horizontal loads were applied at the top free end of the concrete column with an actuator. The applied loads were 10^6 cycles of reversed load of maximum intensity that did not cause any opening at the contact face between the concrete column and the steel girders (14 kN for the A, B and C type specimens and 30 kN for the D type specimen. Hereinafter the load just causes opening will be referred as the no-opening load), 10^4 cycles of reversed load that caused opening (38 kN and 70 kN respectively) and monotonously increased load upto the collapse of the joint.

2.3 Analysis

The stresses and the deflections at each part of the specimens were analyzed based on the elementary beam theory and two dimensional FEM, and compared with the experimental results. In the analysis, it was assumed that entire section of the concrete column is effective and contribution of the prestressing bars can be neglected. At the joint, section of the filled concrete was transformed to the steel's one using the Young's modulus ratio and the effect of the stud shear connectors was neglected. In the FEM analysis, the prestressing force was considered to be an external load.

3. RESULTS AND DISCUSSION

3.1 Distribution of vertical stress in the joint under the no-opening load and stress transfer mechanism

Distribution of vertical stress in the joint was as shown in Fig.2 and 3. As shown in these figures, compressive stress takes the maximum value at the point where the compression fiber of the concrete column contacts to the flanges of the steel girders, decreasing in downward direction and being almost uniform in transverse direction. This fact shows the compressive force carried by the concrete column is transferred to the joint directly across the contact face and distributed in the longitudinal direction. As the result, the webs of the steel girders carries a part of the compressive force even the portion out of the joint.

Tensile stress, also as shown in the figures, distributes in longitudinal direction symmetrically to compressive stress, but in transverse direction, it decreases towards the outer portion. This is probably due to the fact that the tensile force carried by the concrete column is transferred at first to the bottom of the filled concrete through the prestressing bars and then transferred to the webs and diaghrams.

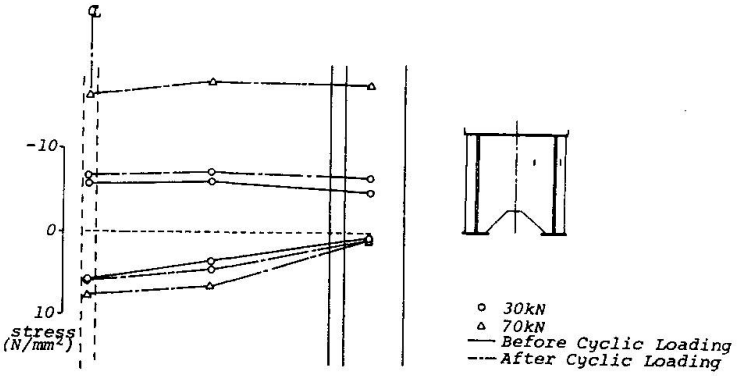

Fig.2 Vertical stress in transverse direction

The stress shown in Fig.3 was nearly equal to the one calculated assuming bending moment transferred from the concrete column is carried by the section which consists of the filled concrete, webs and diaghrams. This fact shows that vertical stress near contact face in joint can be roughly predicted based on the same assumption.

The vertical stress distribution in the type A specimen was almost exactly equal to the one in the type C specimen.

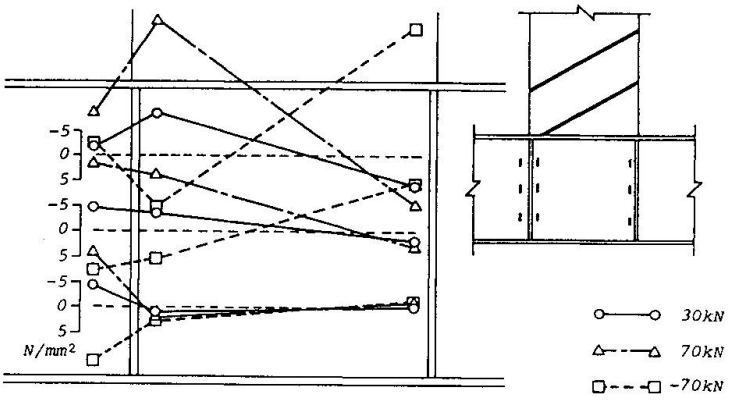

Fig.3 Vertical stress in longitudinal direction

This results suggests that the stud shear connectors did not play any significant role in stress transfer. However, it does not mean stud shear connectors are not needed in actual structures, because the experimental result was more or less owing to relatively high rigidity of the joint as compared with the one in actual joint.

3.2 Distribution of flexural stress under the no-opening load

Flexural stress was distributed along the upper and lower flanges of the steel girders, as shown in Fig.4. It can be recognized from this figure that the measured stresses agree well with the values obtained from the elementary beam theory as well as FEM analysis except the point adjacent to the joint, where the values obtained from FEM are higher a little than the others. This result shows that the elementary beam theory is very useful to predict flexural stress along flange of steel girder. A little high stress obtained from FEM shows some stress concentration could occur at outermost corners of joint, but in actual situation, it is considered to be reduced owing to creep of concrete.

Flexural stress within the joint was as shown in Fig. 5, and good agreement was observed among the measured and analyzed values except the type B specimen, again showing the usefulness of the elementary beam theory. In the type B specimen, the effect of cut off at the contact face of the concrete column was reflected, and a little higher stress was observed at inner portion of the joint and a little lower stress at outer portion.

3.3 Effect of reversed cyclic loading

Even after 10^6 cycles of reversed load below the no-opening load were applied, no significant change was observed in the stress distribution shown in Figs. 2 to 5 nor any fatigue cracks occurred in the steel girders. Furthermore, stress range in prestressing bar is considered to be very small, if load is below the no-opening load. Consequently, there is no fear of fatigue in joint of this kind if opening does not occur under service load.

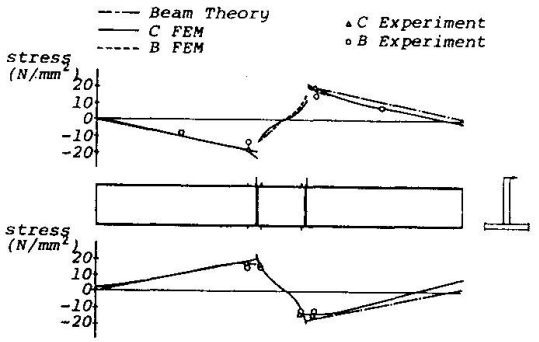

Fig.4 Flexural stress

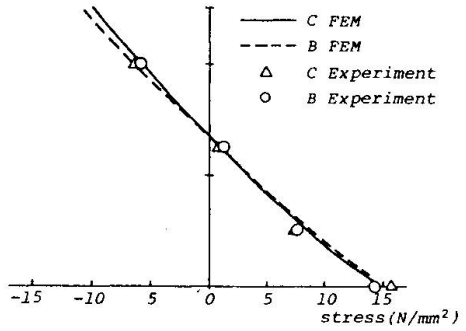

Fig.5 Flexural stress within joint

3.4 Effect of opening at the joint

Some change in the stress distribution described in 3.2 and 3.3 was observed when load exceeded the no-opening load and opening was occurred at the contact face. Firstly, the symmetry observed in the distribution of vertical stress in longitudinal direction became no longer observed, and compressive stress became larger than tensile stress, as the dotted lines shown in Fig.3. This is simply because the area of compression zone was decreased due to opening. Secondly, decrease of vertical tensile stress in transverse direction became more severe, as shown in Fig.2, and at the outermost portion near the contact face, the stress became even compressive. This is because the tensile force, which was transferred to the bottom of the filled concrete, forced the filled concrete to

move upward direction and the flanges at the contact face to deform in a convex shape. To analyze these phenomena accurately, three dimensional FEM which can simulate opening should be used instead of two dimensional one.

Even load is lower than the no-opening load, opening could occur if complete contact between the flanges of the steel girders and the end face of the concrete column can not be attained due to, for example, some irregularity, and it was recognized that opening of this kind caused the same phenomena as above, though the degree was less significant. Consequently, if joint of this kind is so designed that opening is not allowed under service load, special precaution is needed in construction to achieve complete contact.

The stress distribution described at the beginning of this section was not changed significantly even after 10^4 cycles of reversed load higher than the no-opening load was applied. This fact shows that joint of this kind can tolerate several times repetition of severe load such as earthquakes.

3.5 Behavior of the joint at failure

All specimens reached their ultimate states due to crushing, initiated by yielding of the prestressing bars, of concrete in the compression zone adjacent to the joint, and the ultimate moments at the joints coincided well with the ones of the concrete columns. At the ultimate states, no significant change was observed in the joints. This shows that hybrid structure of this kind is good enough in practical use.

4. A PRACTICAL EXAMPLE -THE SASAYA BRIDGE-

On the basis of the results described in 3, the Sasaya Bridge, a rigid frame bridge where steel girder is connected to bridge piers rigidly with prestressing bars, is under construction on the Sakata route of Tohoku Transverse express way. This bridge is the first prototype bridge, to which such a structure is applied, in Japan. The super structure of the Sasaya bridge is a three span continuous girder which is connected rigidly to the two middle supports (see Fig.6). The difference from ordinary steel plate girder is that box type cross girders are arranged at the middle supports.

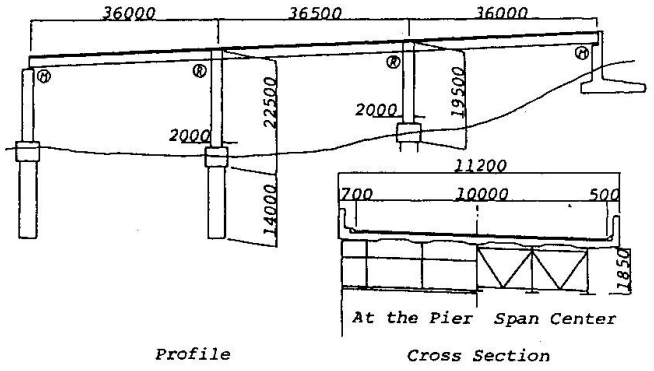

Fig.6 The Sasaya Bridge

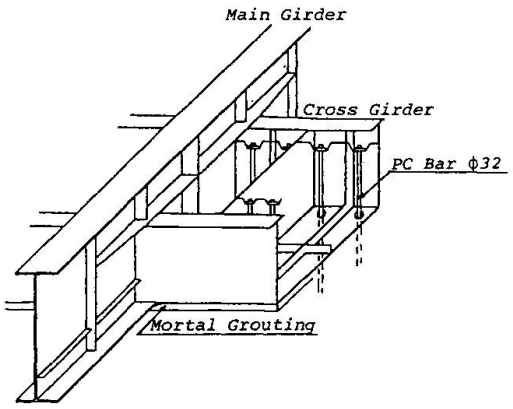

Fig.7 Structure of joint

4.1 structural analysis

Since the elementary beam theory was found to be useful for predicting flexural behavior, the main structure of the Sasaya bridge was analyzed as a two dimensional rigid frame, and then, since load distributing action of each girder can not be treated by frame analysis,

two dimensional grid girder theory was applied to analyze this action. After that, three dimensional frame analysis was carried out to check the results of two dimensional frame and grid analysis. It was confirmed from the analysis that the results given by the two dimensional analysis were satisfactorily accurate.

4.2 Structure of the joints

Structure of the joints is as shown in Fig 7. In order to achieve rigid connection between the main girders and the piers, the prestressing bars embedded in the piers are tensioned and anchored to the concrete placed in the box-like spaces in the cross girders. The magnitude of the prestress is such that no tensile stress is caused at the contact face under ordinary service load.

4.3 Test on non-shrinkage mortar grouting

In order to assure reliability of the entire structure, it was considered to be important to obtain complete contact between the piers and the cross girders, because the joints were designed as described in 4.2. Accordingly, it was planned to grout no-shrinkage mortar into the spaces between the piers and the cross girders, and the experiment was carried out using a high quality no-shrinkage agent with nonmetal aggregate to confirm the reliability of the grouting and establish grouting method.

Excellent grouting efficiency of the mean filling rate of 99% was obtained when rather soft mortar, whose consistency measured with the funnel specified by Japan Society of Civil Engineers was 7 s, was grouted through head difference, and strength test on cored specimens showed average strength of 63.2 N/mm^2, which was much higher than the design strength of concrete of the piers, 35.0 N/mm^2.

As for the construction, the election of the main girders will begin in April, 1990, and complete in October, 1990. The construction works will be reported in the Symposium accordingly.

5. CONCLUSION

The followings may be concluded from the results of the experiments and analysis reported herein.

(1) The tested joints have practically satisfactory performance and can resist reversed cyclic loads of 10^6 cycles below the load which just causes opening and of 10^4 cycles over the load.

(2) The elementary beam theory is very useful to predict stress in entire structure including joints.

(3) In compressive stress, stress transfer mechanism is very simple and can be analyzed by two dimensional FEM even after opening occurs. However, in tensile stress, it is rather complicated and three dimensional FEM is needed to analyze the mechanism, particularly after opening occurs.

(4) Opening could occur even below the load which does not cause tensile stress at the contact face if some irregularity exists. Opening of this kind also causes the same phenomena as opening due to higher load does.

(5) The Sasaya Bridge, a hybrid bridge designed based on the results described above and under construction, is introduced.

New Idea for Safe Structures in Seismic Zones

Idée nouvelle pour la sécurité des structures en zone sismique

Neue Idee für erdbebenbeanspruchte Bauwerke

André PLUMIER
Dr. Eng.
Université de Liège
Liège, Belgium

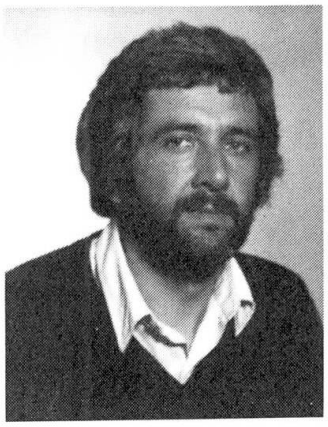

André Plumier, born in 1947, obtained his engineer degree in 1970 at the University of Liège. He was then in charge of research on fatigue, stability and welding residual stresses. He obtained his Ph.D. in 1980. He then worked in the earthquake engineering field as a member of ECCS as a researcher and as a lecturer.

SUMMARY

Ductile structures are known to be interesting in earthquake areas, but the design criteria for the connections can be difficult and expensive to comply with. A new concept, involving creating cheap specific ductile zone close to the connections can solve this problem.

RÉSUMÉ

On connaît l'intérêt de réaliser des structures ductiles en zone sismique. Mais les critères à respecter à cette fin peuvent entraîner des difficultés technologiques et des coûts élevés des assemblages. Une idée nouvelle, consistant en la création de zones ductiles spécifiques à bon marché à proximité des assemblages, peut résoudre le problème.

ZUSAMMENFASSUNG

Die Vorteile duktiler Tragwerken in Erdbebengebieten sind bekannt. Diese Anforderungen können jedoch zu technologischen Schwierigkeiten und kostspieligen Verbindungen führen. Eine neue Idee, um dieses Problem zu lösen, besteht im Einbau kostengünstiger duktiler Bauteile nahe bei den Verbindungen.

1. INTRODUCTION

Earthquake resistant structures may be designed to resist an earthquake elastically or not.

In the latter case, the structure is designed in such a way that, during an earthquake, some parts move out of the elastic range in order to dissipate energy by means of ductile hysteretic behaviour. These parts are called dissipative zones.

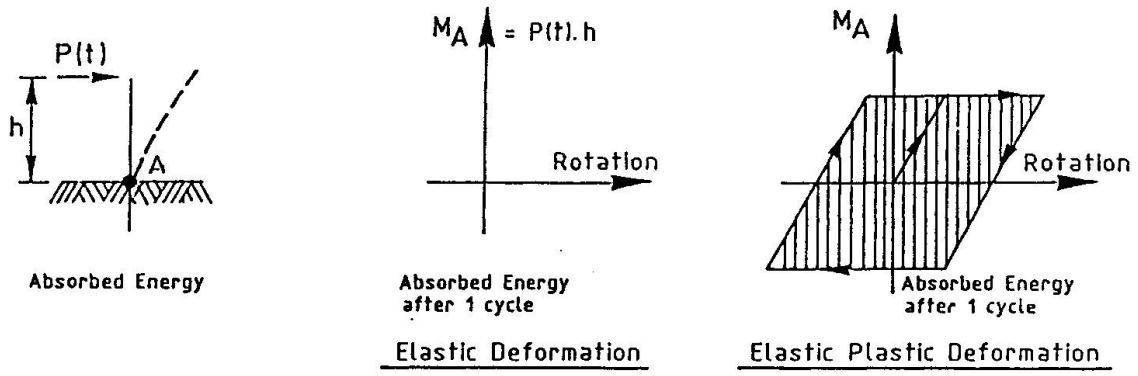

Figure 1

Figure 1 expresses the difference in absorption of energy according to the 2 concepts. As the energy input E of the earthquake is a data and as the following sum of terms

$$E_e + E_d + E_y + E_{cin}$$ with E_e : energy of elastic strain

E_d : energy dissipated in a visco elastic way.

E_y : energy dissipated by yielding

E_{cin} : Kinetic energy

is the only possibility to express how E is counterbalanced inside the structure, it is obvious that getting E_y as high as possible is an interesting way to absorb E. This is recognized by the fact that dissipative structures can be designed by means of a conventional elastic approach under forces reduced by a factor up to 6 when compared to non dissipative structures. This allows substantial economy on the size of the elements of the structure, but one has to pay for this economy in the form of a compliance to a certain amount of rules : rules on local behaviour are such that, locally, safe dissipative zones can exist ; rules on the shape of the structures intend to avoid local failure mechanism and to create the conditions for the formation of many dissipative zone in a structure.

2. SAFE LOCAL ENERGY DISSIPATIVE MECHANISMS AVAILABLE IN COMPOSITE STEEL CONCRETE ELEMENTS

The local energy dissipation mechanisms available to the designer in composite steel concrete elements are yielding in tension or compression ; yielding in shear and yielding in bending.

Yielding in tension is of practical interest in diagonal elements of truss bracings. Yielding in compression should there be avoided or not be relied on and replaced by means of a substitute safe mechanism based on tension diagonals only. - Figure 2 a.
Yielding in shear practically concerns the beam-colums cross zone of frames, generally called panel zone - Figure 2 b.

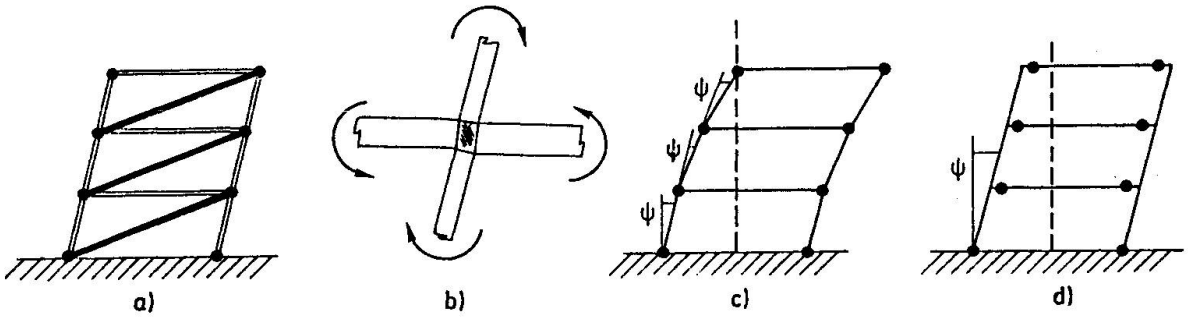

Figure 2

Yielding in bending may concern beams and columns of a frame - Figures 2 c and d. Rules on the slenderness of the compressed walls of the sections have to be complied with.
All these mechanisms may take place in composite steel-concrete elemens but concrete either in compression or in tension cannot be the place for yielding, which should be located in tension reinforcements only.
All these mechanisms should lie outside the assemblies of the elements, as the assemblies are normally not able to develop plastic mechanisms which are stable and ductile. In Eurocode 8 and in many codes around the world, this latter aim is attained by prescribing for the assemblies a resistance R_d which is superior to 120 % of the plastic resistance R_{fy} of the assembled bars according to the formula :

$$R_d \geq 1{,}2\ R_{fy}.$$

In the frames R_{fy} represents the plastic moments M_p of the bars. In the trusses R_{fy} is the normal plastic effort N_p of the bars.
This condition is very stringent , the assemblies resulting out of such calculations are very expensive and difficult, if not impossible, to realize, so that common practice cannot easily comply with safety requirement. The idea developed at paragraph 4 can solve this problem.

3. FACTORS FAVOURABLE TO THE PRESENCE OF MANY DISSIPATIVE ZONES

The regularity in stiffness distribution along the heigth of a structure is one classical condition to obtain many dissipative zones in a structure. But this concept is still improved if a mechanism is found which forces yielding to occur in chosen places of the deformed structure, for geometrical compatibility reasons. This is the case of the "weak beam-strong columns"

concept - Figure 2 d in which columns act as spreaders of yielding through the many beams of the structure. The same concept can be applied to truss bracings : the "weak diagonals-strong columns" of Figure 3a correspond to a concept aimed at by specific requirements in Eurocode 8, for instance.

It must be pointed out that the wished regularity will only be obtained if the distribution of the real yield strengths inside the real structure does not differ too much from the distribution assumed during design. For instance, if beams delivered on site have a real yield strength f_y = 320 N/mm² instead for 235 N/mm², while in the columns f_y = 235 N/mm² as assumed in design, the plastic hinges might be located in the columns instead of the beams, changing the distribution of plastic hinges from pattern c to pattern d of Figure 2. Similarly, if some elements of the connecting parts, such as butt end plates, have the assumed yield strength while the beams or diagonals have a higher yield strength than presumed, the condition (1) is not fulfilled in reality and a brittle or little ductile failure of the connection may replace the expected good ductility of the connected elements.

These discrepancies raise practical problems : new calculations will not always be enough to avoid rejecting steel ; rejecting steel causes delay and contractual problems. The idea developed here under can again solve this problem.

4. A NEW IDEA FOR SAFE STRUCTURES IN SEISMIC ZONE

The idea developped to obtain safe structures in seismic zone is the following : dissipative zones can be "prefabricated" as such, outside the connections but close to them, by creating specific weakened zones in which yielding may take place in a safe and ductile way. This zone is formed by a reduction of the actual cross section of the profile. Examples of various possible embodiments are sketched at Figure 3. The advantage resulting from this idea, now patented, lies in the fact that condition (1) is applicable while considering the value R_{fy} of the reduced cross section of the profile.

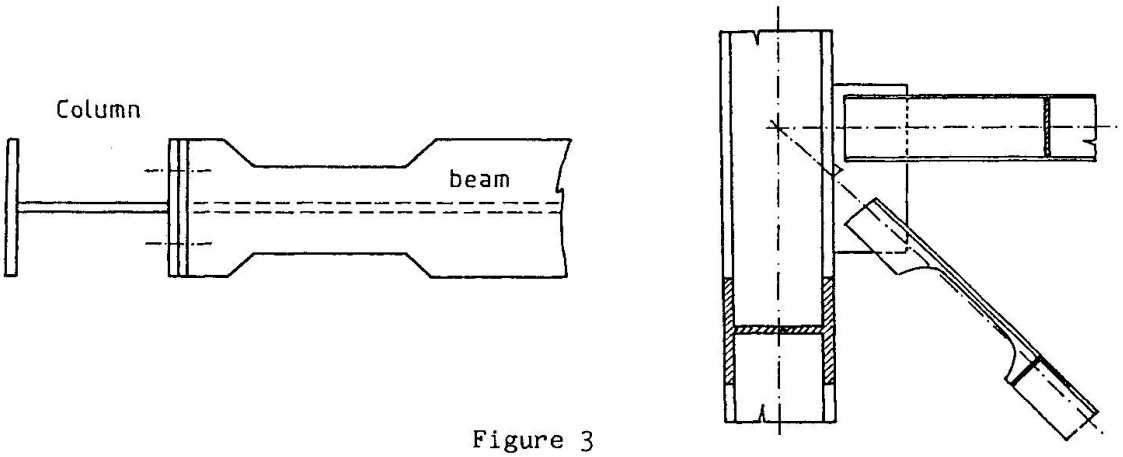

Figure 3

This allows to bring the assemblies back to dimensions comparable to those of classical projects by means of a low cost workshop operation : oxy cutting or drilling. At the same time the presence of a dissipative zone is guaranteed and it is permissible to take fully benefit from the reduction of the design loads corresponding to the seismic action, reduction which spare much more material than the eventual supplement in section resulting from a loss in rigidity. The idea can also prove its effeciency in case of troubles of the

kind explained at paragraph 3 with the steel delivered on site : taking the plastic moment $M_{p\ site}$ of an overresistant element down to the design value $M_{p\ design}$ or $N_{p\ design}$ can easily be realized by oxycutting or drilling on site . The idea thus allows a strict correspondance between the intended regular structure of the design stage and the real structure achieved.

5. TEST RESULTS AND DESIGN IMPLICATIONS

Taking material out of some sections may be beneficial on the energy dissipation side and on the connection cost side. It affects the design negatively in requiring a change in the section required to make the beam or the diagonal.
A width reduction by a factor of 1,2 of the flanges results in an increase by one section (Example : HEA 260 to HEA 280) or less, depending upon the type of section and the span. For spans less than 7 m in composite steel concrete structure, some computations show that no change in section is necessary. When taking a bigger section is required, this increase in weight is compensated by a reduction by a factor of 1,2 or more of the size of the connecting elements (plates, bolts, weld).
This necessary increase in size of the element is however theoretical and related to permissible stress philosophy, for several reasons :

- consideration of the deflections does not require a higher section ;
- the real behaviour of the elements with flange width reduction by a factor of 1,20 does not give decrease in design resistance under earthquake loading ; test results given hereafter indicate a reduction by a 1,15 factor.

On Figure 4 are reported envelope curves of Moment M Rotation R diagrammes obtained under cyclic loading of exterior column connection zone of H steel sections with concrete encased between the flanges (ARBED AF system) [2][3].
It can be seen that, in spite of the width reduction in beam F2, its M-R curve is practically similar to that of the original section E3. The design resistance M_{yd} and ultimate resistance derived form the test according to ECCS testing procedure [2] are for this HEA 260 section :

	Full section E3	Reduced flanges F2
M_{yd} (kN x m)	375	325
M_{v} (kN x m)	420	410

Also on figure 4, it can be seen that the sheared panel mechanism in the column is locked by the concrete, inforcing all yielding to take place in the beam. This positive effect of composite construction towars composite encased column combined with flange width reduction of the beam avoids the welding of a stiffening plate on the web of the column.

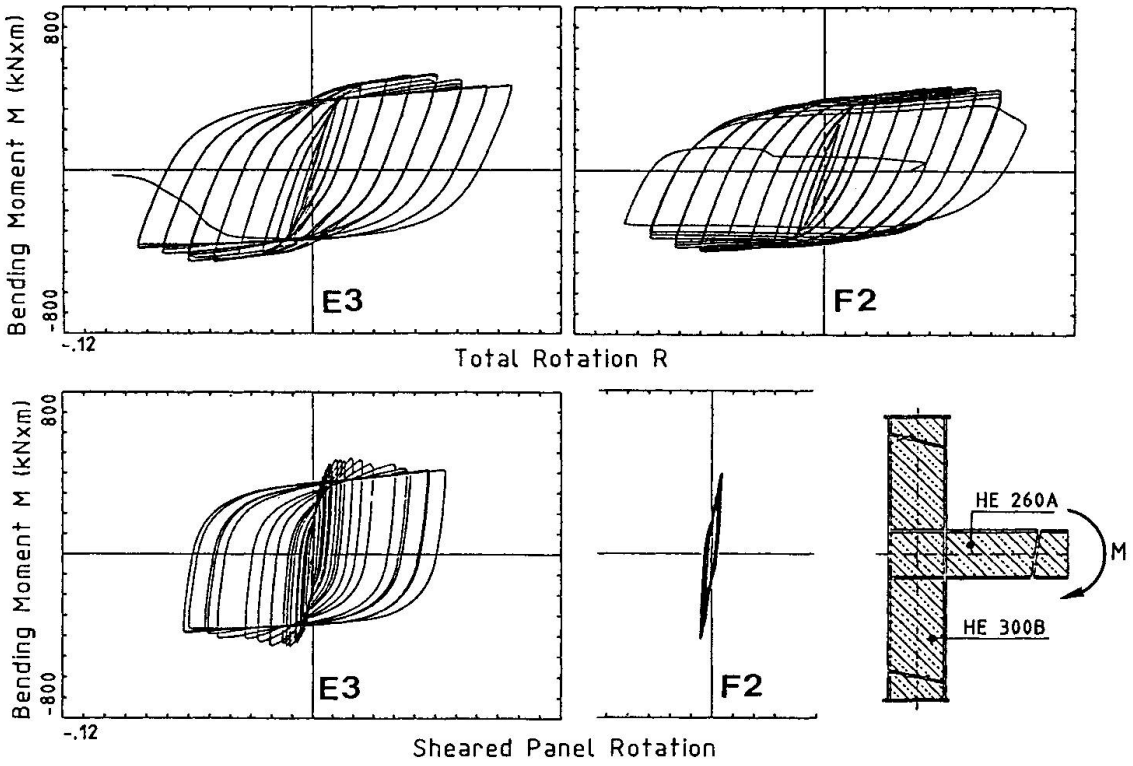

Figure 4

Test results obtained on interior columns (one column - two beams) including the presence of a slab give globally the same conclusion, with a further advantage for the application of the locally weakened section : in that case, yielding of the steel on the lower (tension) flange takes place before the crushing of the concrete of the slab against the flange of the column. It means that this new idea does not only bring more safety against collapse but also less sensitivity to damage.

7. CONCLUSION

The weakening of specific sections of a structure to change them into reliable dissipative zones in case of an earthquake is a new and simple idea. Conceptual explanations, design considerations and experimental data settle its general valididty. This now patented idea gains even more advantages in the field of composite steel-concrete structures where the concrete slab integrity can be maintained and where a steel stiffener in the web of the column can be avoided in the sheared panel zone.

BIBLIOGRAPHY

[1] Eurocode 8 - Structures in seismic regions - Design - Part 1 - May 1988. Report EUR 12266 EN - Office for official publication of the European Communities - L 2985 Luxembourg.

[2] Recommanded testing procedure for assessing the behaviour of structural steel elements under cyclic loads. European Convention for Constructional Steel work n°45 - 1986.

[3] Seismic resistance of Composite structures - ARBED - CEC Research 7210 - SA/506 Technical Report 3 - ARBED Recherches RPS. BP141 - L 4002 ESCH/ALZETTE.

Development of Mixed Structures in Japan

Développement des structures mixtes au Japon

Entwicklung von Verbundtragwerken in Japan

Koichirou OGURA
Professor
Meiji University
Kawasaki, Japan

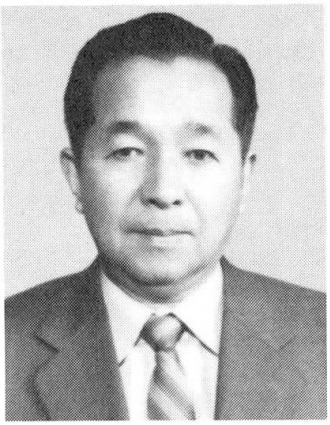

Koichirou Ogura, born 1924, received D.Eng. from the Univ. of Tokyo in 1954. His research interests include the seismic design of RC structures. He is a Chairman of JCI Committee on Mixed Structures.

Reiji TANAKA
Professor
Tohoku Inst. Techn.
Sendai, Japan

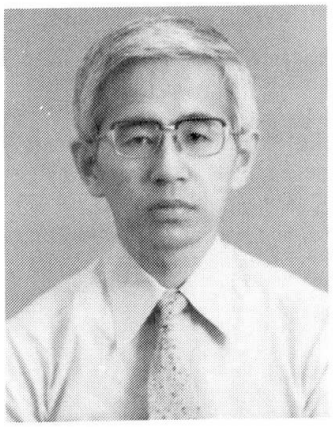

Reiji Tanaka, born 1940 received D.Eng. from Meiji Univ. in 1971. His research interests include the seismic design of RC structures. He is a Secretary of AIJ RC Committee and JCI Committee on Mixed Structures.

Hiroshi NOGUCHI
Assoc. Professor
Chiba University
Chiba, Japan

Hiroshi Noguchi, born 1946 received D.Eng. from the Univ. of Tokyo in 1976. His research interests include the seismic design of RC structures and the application of FEM. He is a member of IABSE, AIJ, JCI.

SUMMARY

This paper introduces the state-of-the art concerning research on mixed structures using concrete systems in building construction in Japan. The classifications of structures defined in building regulations, proposals for definitions of mixed structures, various structural codes defined by Architectural Institute of Japan and previous researches on mixed structures are introduced.

RÉSUMÉ

Cet article présente l'état actuel de la technique dans le domaine de la recherche sur les structures mixtes, utilisant un système pratique pour la construction des bâtiments au Japon. Ce rapport fournit les classifications des structures telles que définies par les règlements de la construction, des propositions de définition des structures mixtes, divers codes structuraux mis au point par l'Institut d'architecture du Japon, ainsi que des études antérieures sur les structures mixtes.

ZUSAMMENFASSUNG

Dieser Beitrag beschreibt den Stand der Forschung betreffend Verbundtragwerken aus Stahl und Beton in Japan. Die Klassierung der Bauwerke in den Normen und Vorschläge zur Definition von Verbund- und Mischbauwerke werden besprochen, sowie auch die bisherige Forschung zu diesem Thema in Japan.

1.INTRODUCTION

The purpose of this paper is to introduce comprehensively the state-of-the-art on the research on the mixed structures using concrete system in Japan. The mixed structure using concrete system is defined as the mixed structures of concrete members and steel members. The mixed structures using the concrete system is greatly utilized in both fields of building construction and civil engineering construction in Japan. The mixed structures in the building construction is only introduced in this paper.

2.CLASSIFICATION OF BUILDING STRUCTURES IN JAPAN

2.1 Classification of Structures Determined in Building Regulation

The buildings are constructed in accordance with the building regulation in Japan. Five kinds of building structures such as reinforced concrete (RC), steel reinforced concrete (SRC), steel (S), wood and masonry are defined in the Japanese building regulation. The mixed structures are frames which are composed of the above various kinds of structures. But there is not a present legal prescription with regard to the mixed structures. Therefore, when the mixed structure frames are constructed, it is necessary for the constructor to design in accordance with the various structural code published by Architectural Institute of Japan (AIJ) or to receive an evaluation from Building Center of Japan after the special research is carried out for the designed structures.

2.2 Various Structural Codes Defined by AIJ

Though building structures are designed in accordance with the building regulation, the detailed mechanical items necessary for the design are not defined in this regulation, Thereupon, the building structures are designed generally in accordance with various structural codes of AIJ in Japan.

The design method of each structure is shown in detail in each structural code of AIJ, but this code has no restriction imposed by law. The following code of AIJ is related to the mixed structures using concrete system.

1) Standard for Structural Calculation of Reinforced Concrete Structures (RC Code)
2) Standard for Design of Steel Structures (S Code)
3) Standard for Structural Calculation of Steel Reinforced Concrete Structures (SRC Code)
4) Standard for Design of Composite Structures
5) Standard for Design and Construction of Prestressed Concrete Structures

General examples of the section used in RC, SRC and S structural design code are shown in Fig. 1.

The strength ranges of materials used in each code are as follows; the compressive strength of concrete, Fc = 14.7 - 35.3 MPa, the yield strength of reinforcement, σy = 235 - 392MPa and the yield strength of steel, σy = 216 - 402MPa. The actual material strengths in the previous tests

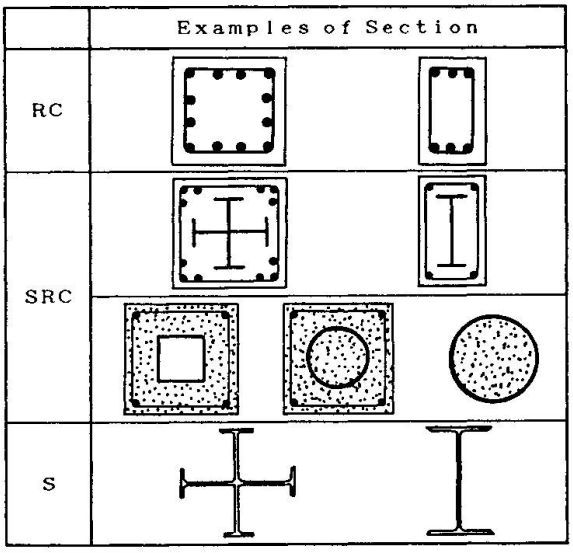

Fig.1 Examples of Sections in RC, SRC and S Structures in Japan

Table 1 Proposed Definitions on Mixed Structures

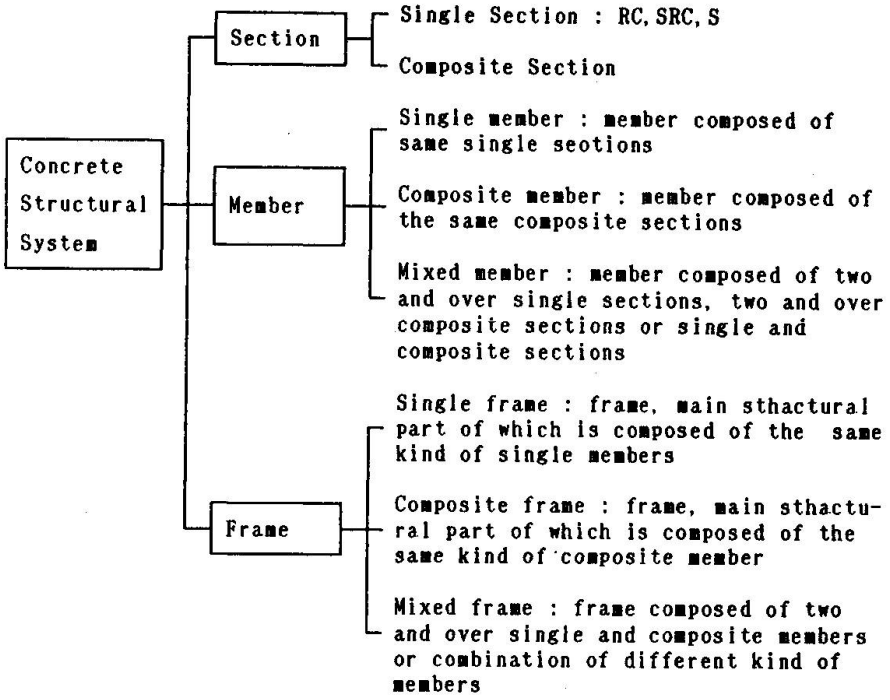

introduced in this paper are almost in this range.

3. PROPOSALS FOR DEFINITIONS OF MIXED STRUCTURES

As there is not a legal definition regarding mixed structures in Japan, it is necessary to define the mixed structures. The tentative definitions of the mixed structures have been proposed by Japan Concrete Institute (JCI) Research Committee on Mixed Structures (Chairman: Prof. K. Ogura). The proposal in Table 1 is distinguished by the definition of mixed frame using sections, members and frames.

4. PREVIOUS RESEARCHES

If mixed structures are composed of different structural members as shown in Table 1, the previous research on mixed structures in buildings in Japan are classified into the following three kinds.

1) Study on column bases on the lowest floor in steel or steel reinforced concrete structures
2) Study on connections between foundation pile and foundation slab
3) Study on superstructures

The superstructures in 3) are introduced in this paper.

The following two kinds of mixed structures using concrete system,

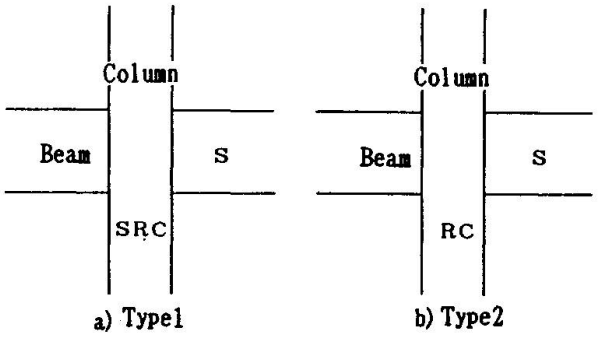

Fig.2 Typical Mixed Structures Studied in Japan

as shown in Fig. 2, have been studied popularly.

1) Type 1: column (SRC) + beams (S)

2) Type 2: column (RC) + beams (S)

There are few researches on other types such as columns (SRC) + beams (SC), columns (SC) + beams (S) or columns (SRC) + beams (composite beams).

The objects of the mixed structures in Japan are simplification of the prefabrication and the possibility of light weight design and long beam span. In the mixed structures, Type 1 and Type 2, the columns are made by concrete system. This is because of the structural merit that the axial force is contributed by RC structure and the local deformation of steel frames is restrained by concrete. The emphasis of the research on the mixed structures have been moved from on Type 1 to on Type 2. The research committees have been organized in JCI and AIJ, but the building code on mixed structures have not been proposed. Although the research on Type 1 was started from 1972 [1], the research on Type 2 has become popular in 1985 [2], and there are not so many previous researches on Type 2. The movement of the research emphasis from Type 1 to Type 2 is considered to be based mainly on the economical aspects. It is because columns made by RC is more economical than those made by SRC. The main reason why the research on mixed structures was started from Type 1 in Japan is easiness of the joint design between columns and beams. In the research on Type 1, there are many experimental works on the stress transfer mechanisms in beam-column joints. Various types of joints such as interior [1], exterior [3] and corner have been tested. For Type 1, there are also many practical design examples including a high-rise building of 36 stories [4].

It is recognized that there are no particular problems in frame behaviour, if the joint of steel between a column and beams is designed carefully for the type 1. The structure of Type 1 was defined in SRC code. The minimum value of steel in a column is restricted by Eq. (1) in SRC code as follows.

$$0.4 \leqq {}_{sc}M_A \,/\, {}_{sb}M_A \leqq 2.5 \qquad (1)$$

where ${}_{sc}M_A$ = sum of flexural strength of steel in column members

${}_{sb}M_A$ = sum of flexural strength of steel in beam members

The main problem in Type 2 is a jointing method between a RC column and steel beams. This problem has been investigated in most of the previous experimental studies. Type 2 is a structure that has lost the steel in a column of Type 1. The change of the mechanical performance from Type 1 to Type 2 was observed in the previous test by Wakabayashi, M. et al. shown in Fig.3 [5]. The beams were made of steel and same for all specimens in this test. If the amount of steel is sufficient in a column like specimen S1002N, the joint behaviour is satisfactory. But as the amount of steel in a column decreases, the hysteresis loop comes to be contrary S-typed, and the joint performance deteriorates. The joint failure occurred in a specimen S0002N in which the amount of steel was zero.

It is difficult to joint a RC column and steel beams simply as observed in the previous test shown in Fig. 3. Therefore, various methods have been considered in the viewpoint of reinforcing a joint using steel plates or frames in a part of the joint, as shown in Fig. 4 [6] - [9]. These considerations tried to transfer a part of beam stresses into a column by strengthening bearing forces of concrete in a reinforced concrete column using beam steel frames, by the confined effects of joint concrete made by steel reinforcing and through the part of steel frames.

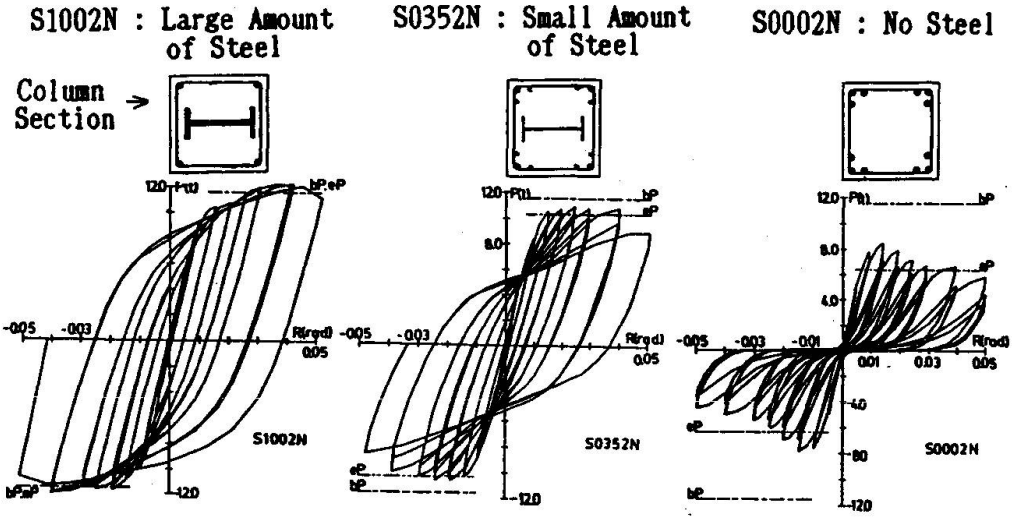

Fig.3 Test Results on Beam-Column Joints from Type 2 (RC Column) to Type 1 (SRC Column) (Wakabayashi, M. et al. [5]

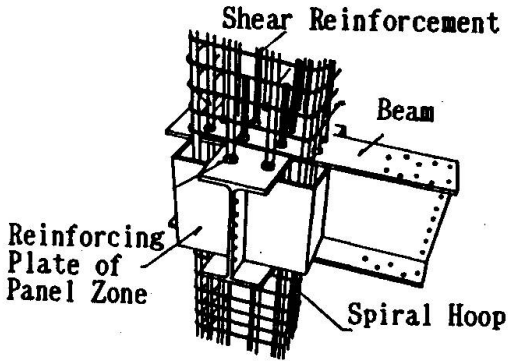

(a)Tominaga, H. et al. [6]

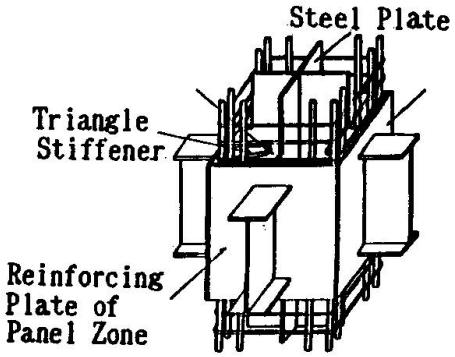

(b)Tanaka, Y. et al. [7]

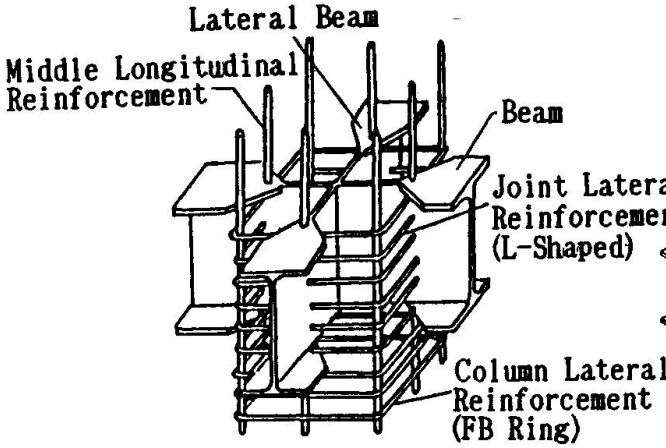

(c)Morota, M. et al. [8]

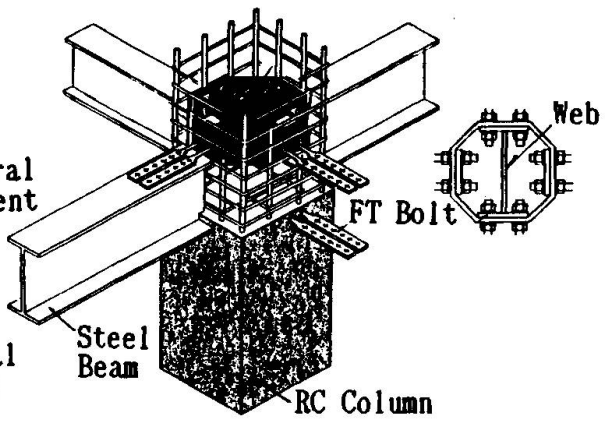

(d)Suzuki, K. et al.[9]

Fig.4 Jointing Methods between RC Column and S Beams in Previous Researches

5. CONCLUDING REMARKS

It had been a general custom to design a building structures using the same kind of structure in Japan. This is because the analysis of frames was difficult in the case that the building was composed of various kinds of structures. It is also the reason that the test data on the mechanical performances of a joint between different structural members was in sufficient.

The analytical methods of the mixed structures have been developed using macroscopic and microscopic models with the development of computers. These present situations develop a tendency to utilize the performance of each member of SRC, RC and S in the design in accordance with each aptitude. Such design philosophies are considered to be a main current in the future building structures in Japan. The studies on mixed structures will be more prosperous in cooperation with the studies on building construction.

References

1. Takeda, T. et al., Experimental Studies on Structures Using Steel and Steel R/C, Abstracts, Annual Meeting of AIJ, October 1972, pp. 1509-1510 (In Japanese).
2. K.Iwaguchi, K. et al., Stress Transferring Mechanism of Interior Joints in Mixed Structures, Abstracts, Annual Meeting of AIJ, October 1985, pp.1311-1312 (In Japanese).
3. Naka, T. et al., Experimental Studies on the Strength of Steel R/C Beam-Column Joints, Abstracts, Annual Meeting of AIJ, October 1972, pp.2283-2284 (In Japanese).
4. Yokoyama, M. et al., Study on Structure of Super High-Rise Housing with Y-Shaped Plan (Part 1-Structural System and Design Concept), Abstracts, Annual Meeting of AIJ, October 1984, pp.2805-2806 (In Japanese).
5. Wakabayashi, M. et al., Load Carrying Capacity of Composite Exterior Joints with Steel Beam (Part 3), Abstracts, Annual Meeting of AIJ, October 1984, pp.2761-2762 (In Japanese).
6. Tominaga, H. et al., Strength and Ductility of Frames Composed of RC Columns and Steel Beams, Abstracts, Annual Meeting of AIJ, August 1986, pp.1427-1428 (In Japanese).
7. Tanaka, Y., Strength and Deformability of Steel Beam-Reinforced Column Joints, Abstracts, Annual Meeting of AIJ, October 1987, pp.1331-1332 (In Japanese).
8. Morota, M. et al., Experimental Study on Reinforced Concrete Column to Steel Beam Joints of Tapered-flange-type Panels, Abstracts, Annual Meeting of AIJ, October 1988, pp.1315-1316 (In Japanese).
9 Suzuki, K. et al., Structural Behaviour of Steel Beam-to-Reinforced Concrete Column Connections Using Particular Shaped High-Strength Bolts, Abstracts, Annual Meeting of AIJ, October 1989, pp.1567-1568 (In Japanese).

Behavior of Concrete Encased Steel Frames with Reinforced Concrete Walls

Comportement des charpentes en acier enrobé de béton avec murs en béton armé

Tragverhalten von Stahl-Beton-Verbundrahmen mit Stahlbetonwänden

Tetsuro GOTO
Senior Res. Eng.
Building Res. Inst.
Tsukuba, Japan

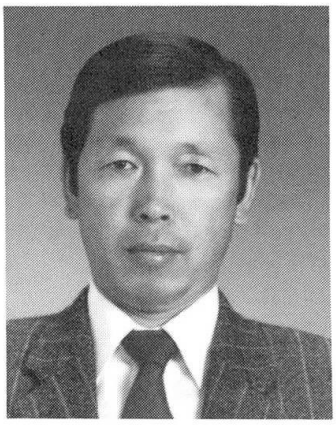

Tetsuro Goto has been actively engaged in research in concrete structures and earthquake-resistant design. In 1978, he was awarded a prize by the Japan Concrete Institute for his study.

Masaya HIROSAWA
Dep. Dir. Gen.
Building Res. Inst.
Tsukuba, Japan

Masaya Hirosawa received his doctor of engineering degree at the University of Tokyo. His research has focused on concrete structures. In 1985, he was awarded a prize by the Architectural Institute of Japan for his study.

SUMMARY

This paper describes an experimntal test of the stiffness, horizontal bearing capacity, deformation capability, and failure mechanism of Concrete Encased Steel frames containing a reinforced concrete wall. The stiffness and maximum horizontal bearing capacity are higher than those of a simple Concrete Encased Steel frame. When the frame containing a wall is deformed greatly, the wall fails and the structural behavior becomes similar to that of a simple frame.

RÉSUMÉ

Cet article décrit une série d'essais sur la rigidité, la force portante horizontale, la résistance à la déformation et les mécanismes de rupture des charpentes en acier enrobé de béton comportant un mur en béton armé. La rigidité et la force portante maximum sont supérieures à celles d'une simple charpente en acier enrobé de béton. Quand une charpente en acier enrobé de béton avec mur en béton armé se déforme de manière notable, le mur cède et le comportement structurel devient identique à celui d'une simple charpente en acier enrobé de béton.

ZUSAMMENFASSUNG

Dieser Artikel beschreibt eine Experimentalprüfung der Biegefestigkeit, der Tragfähigkeit, des Widerstandes gegen die Formveränderung und des Verhaltens bei einem Notfall bedingt durch Stahlbetonrahmen die eine Stahlbetonwand enthalten. Die Biegefestigkeit und die maximale Tragfähigkeit sind höher als jene von einem reinen Stahlbetonrahmen. Werden die Verformungen des Stahlbetonrahmens mit der Wand gross, so versagt die Wand und der Rahmen verhält sich ähnlich einem Rahmen ohne Wand.

1. INTRODUCTION

The SRC frame is suitable for various purposes because it is very ductile. This paper describes a seismic resistance test in an attempt to establish a design method for SRC frames used as part of the composite structure of medium- to high-rise apartment buildings. H-shaped steel and reinforcement are incorporated in concrete to form an SRC frame consisting of columns and beams. To use buildings as shelters, a thin concrete wall with a single reinforcing bar with openings is incorporated in the SRC frame. This composite structure has been used for many buildings in the past and will be used more often in the future. However, there are still many unsolved points concerning the lateral stiffness, maximum horizontal bearing capacity, failure mechanism, and deformation capability of frames that contain a wall with openings. In this study, we planned a frame experiment as the first step toward establishing a method by which to evaluate the unsolved points.

2. EXPERIMENTAL PROGRAM

2.1 Specimens

An 11-story apartment building with side corridors which was designed according to [1] is used as a model for specimen design. From ten spans in the longitudinal direction of the building, the central two spans of the lowest three stories are taken and reduced in half. Three specimens are used. Figures 1 to 6 show the shape and structure of the specimens. Table 1 lists the cross sectional dimensions of the columns and beams. Each specimen is 6.9 m high and 8.7 m long. Column and beam members of each specimen are incorporated in an SRC frame and has the same specifications. The depth of the column on the first floor is 42.5 cm and the width 35 cm. The depth of the column on the second floor is 37.5 cm and the width 22.5 cm.

Specimen No.1 is a pure frame without the non-seismic reinforced concrete wall, so that the difference of the deformation capability between structures with and without a wall can be analyzed. Specimen No.2 contains a reinforced concrete wing wall at the side of the SRC frame. Specimen No.3 contains a reinforced concrete wall with several large and small openings. The typical opening shape that can be seen in many apartment buildings is sampled and tested; special shapes are not considered. The wall thickness is 1/6 of the width of the column because the walls of many apartment buildings are about this thickness. Table 2 shows the results of the material test.

2.2 Loading Method

Figure 7 outlines load application. Four 686 KN actuators, producing horizontal load (Q), are set on top of the specimens. Horizontal load is applied statically in positive and negative directions for 17 cycles with small to large deflections (Figure 7). The angle of rotation of members for horizontal loading control is the value obtained by dividing the target horizontal deflection (δ_T) by the distance (H) between the base of the column on the first floor and the loading point ($R_T \fallingdotseq \delta_T/H$ rad).
Axial force of 5884 KN/m^2 equivalent to the sustained loading is applied to

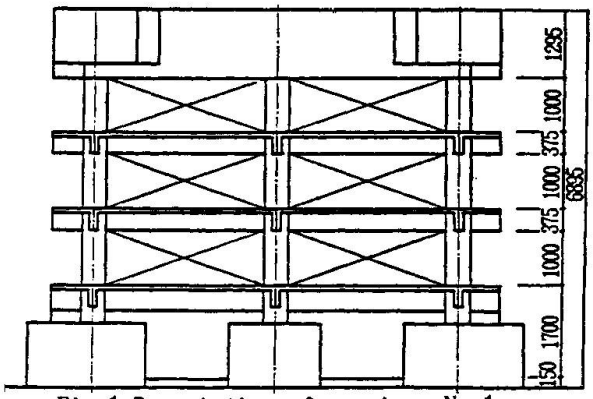

Fig 1 Description of specimen No.1

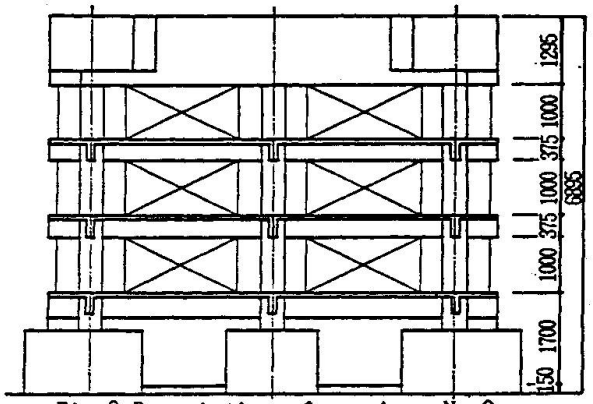

Fig 3 Description of specimen No.2

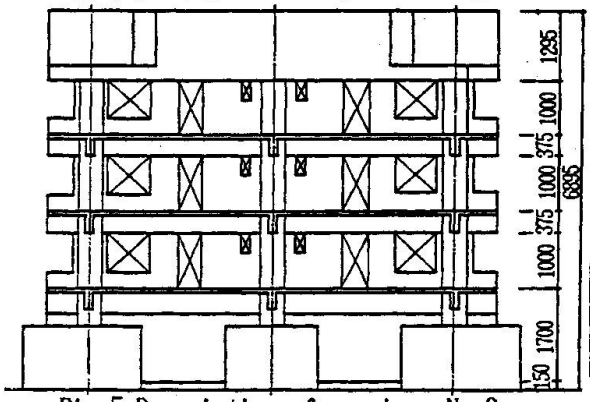

Fig 5 Description of specimen No.3

Table 2 Member list of SRC frame

			Column	Beam
			$Z_3 \sim Z_1$	end / center
Z_3	B×D	300×425	225×375	225×375
	Flg.	PL-9×100	PL-16×100	PL-16 ×100
	Web	PL-9	PL-4.5	PL-3.2
	Main bar	4-D13, 2-D10	4-D13, 2-D13	2-D13, 2-D10
Z_2	B×D	325×425	225×375	225×375
	Flg.	PL-12 ×100	PL-16×100	PL-16 ×100
	Web	PL-6	PL-4.5	PL-3.2
	Main bar	4-D13, 2-D10	3-D13, 2-D10	2-D13, 2-D10
Z_1	B×D	350×425	300×1250	300×1250
	Flg.	PL-16 ×100	——	——
	Web	PL-9	——	——
	Main bar	4-D13, 2-D10	10-D16, 10-D16	6-D16, 6-D16

Hoop[Z_3:D10-@50, $Z_2 \sim Z_1$:D6-@50] Stirrup[D6-@100]

unit : mm

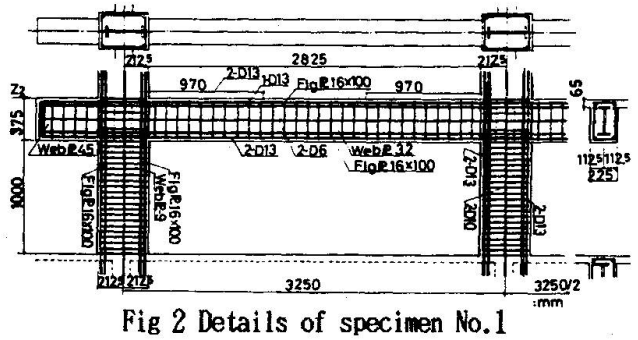

Fig 2 Details of specimen No.1

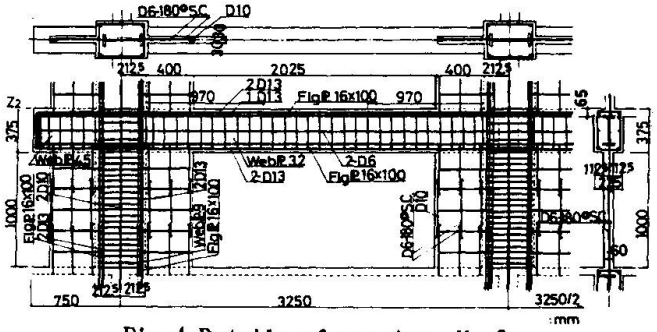

Fig 4 Details of specimen No.2

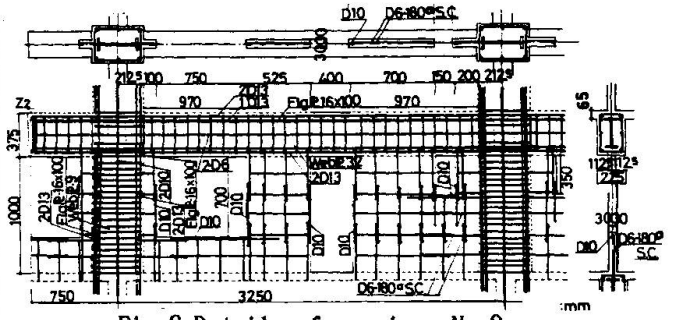

Fig 6 Details of specimen No.3

Table 1 Mechanical properties

Steel (N/mm^2)	web (3.2)	web (4.5)	web (6.0)	web (9.0)	Flange (12.0)	Flange (16.0)	D6	D10	D13
σ_y	330	249	346	334	288	280	300	427	364
σ_t	407	373	449	479	438	449	450	597	520
$E_c \times 10^3$	208	215	213	201	212	214	188	186	180

Concrete : [NO.1 σ_c =24.2 N/mm^2, σ_t =1.89 N/mm^2, Ec =2.13×10⁴ N/mm^2]
[NO.2 σ_c =24.2 N/mm^2, σ_t =1.82 N/mm^2, Ec =2.13×10⁴ N/mm^2]
[NO.3 σ_c =25.0 N/mm^2, σ_t =1.93 N/mm^2, Ec =2.16×10⁴ N/mm^2]

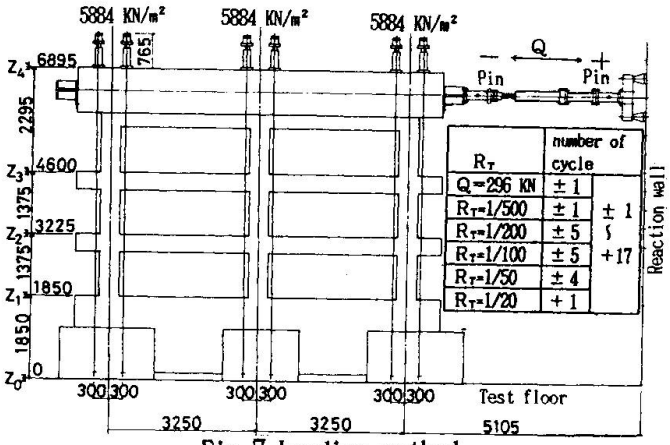

R_T	number of cycle	
Q=296 KN	±1	±1 S +17
R_T=1/500	±1	
R_T=1/200	±5	
R_T=1/100	±5	
R_T=1/50	±4	
R_T=1/20	+1	

Fig 7 Loading method

the top of the specimens. This force is kept at a constant level during horizontal loading. The total measurement items per specimen amounted to 600, including horizontal and vertical deflection, and H-shaped steel strain. The progress of failure was photographed and sketched.

3. EXPERIMENT RESULTS AND REVIEW

3.1 Relationship between failure development and horizontal loading deflection

Figure 8 shows the relationship between horizontal deflection and horizontal load measured along the center of the beam on the top of specimen No.1. Figure 9 shows the failure condition at the end of the experiment in which $R_T \fallingdotseq 1/20$ was reached. Figures 10 to 13 show the results of the same experiment for specimens No.2 and No.3.

In specimen No.1, bending crack (BC) occurred in the column bottoms on the first floor, in the beams on the second and third floors, and in the column tops on the third floor at $Q \fallingdotseq 235$ KN to 294 KN. At $R_T \fallingdotseq 1/200$, BC occurred in the columns and beams on all the floors, and bending and shear crack (BSC) and shear crack (SC) occurred in all the members. At $R_T \fallingdotseq 1/100$, the column tops on the third floor, the column bottoms on the first floor, and the beam steel of the center columns on all the floors yielded. At the cycle of the same R_T, the column tops on the third floor, the column bottoms on the first floor, and the beam ends on all the floors began to be crushed. At $R_T \fallingdotseq 1/50$, the maximum load of 1153.3 KN was measured. After repetition of $R_T \fallingdotseq 1/50$, crushing of the column tops on the third floor and the column bottoms on the first floor progressed. The final failure mode of specimen No.1 showed a flexural failure type.

In specimen No.2, at $Q \fallingdotseq 235$ KN to 294 KN, BC occurred in the column ends on all the floors. Before $R_T \fallingdotseq 1/500$ was reached, BC occurred in the column tops on the third floor, and BC and SC occurred in the wing walls on all the floors. BSC progressed before $R_T \fallingdotseq 1/200$ was reached. At the fifth cycle of the same R_T, the column tops on the third floor and the wing wall of the column bottoms on the first floor were crushed. At $R_T \fallingdotseq 1/50$, the maximum load of 1357.7 KN was measured. At the first to fifth cycles of $R_T \fallingdotseq 1/100$, crushing of the wing walls near the column tops on the first and second floors progressed. At $R_T = 1/50$, crushing of the wing wall of the column top and the beam ends on the third floor progressed. The final failure mode of specimen No.2 was almost the same as that of specimen No.1.

In specimen No.3, at $Q \fallingdotseq 392$ KN, BC occurred in the beam ends on the second floor. At 412 KN, SC occurred. When R_T reached 1/500, SC occurred in the walls on all the floors. At $R_T \fallingdotseq 1/200$, when the maximum load of 1463.6 KN was measured, shear failure occurred in some walls. At the fifth cycle of the same R_T, shear failure occurred in the walls on all the floors. At $R_T \fallingdotseq 1/100$ and $R_T \fallingdotseq 1/50$, crushing of the column tops on the third floor, the column bottoms on the first floor, and the beam ends on all the floors progressed. The final failure mode of specimen No.3 was almost the same as that of specimens No.1 and No.2.

The failure mode of the pure frame was a bending failure. The final failure

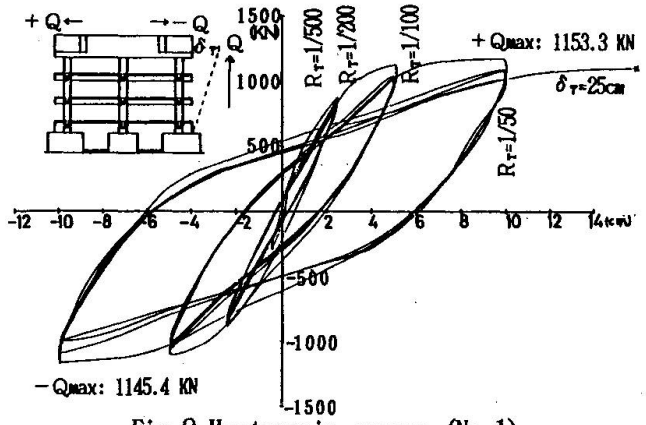

Fig 8 Hysteresis curves (No.1)

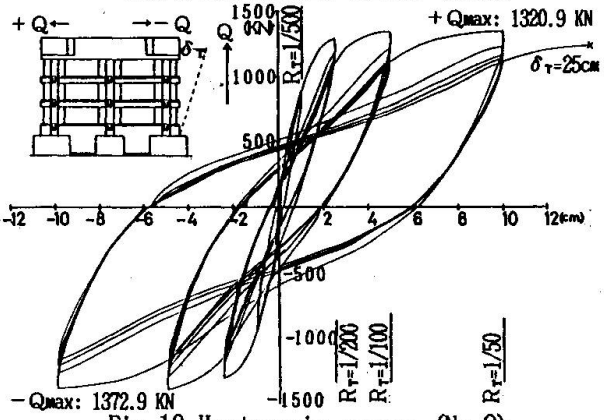

Fig 10 Hysteresis curves (No.2)

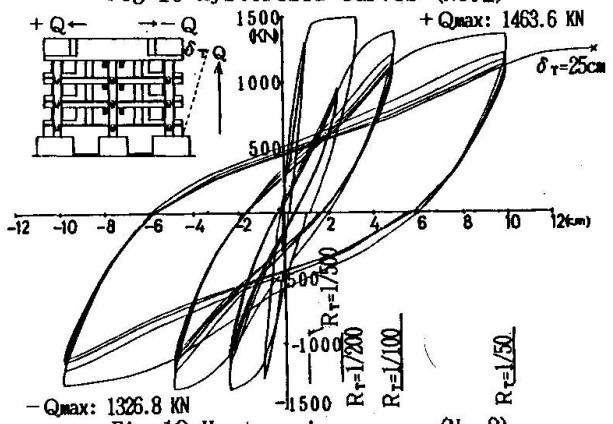

Fig 12 Hysteresis curves (No.3)

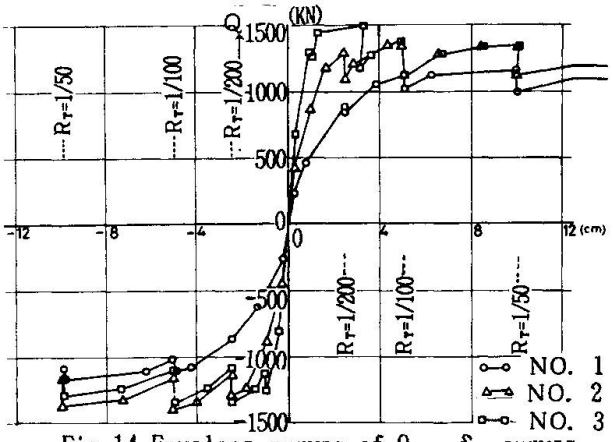

Fig 14 Envelope curves of Q - δ_T curves

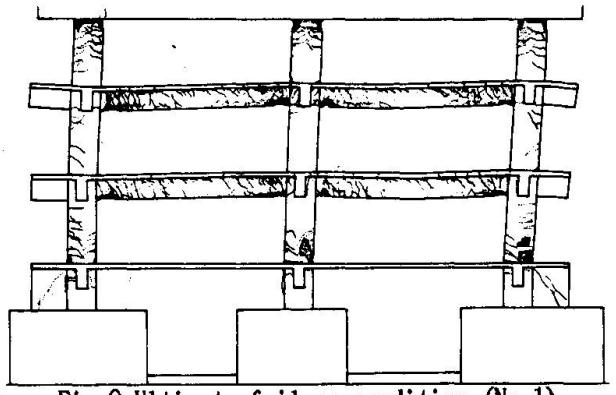

Fig 9 Ultimate failure condition (No.1)

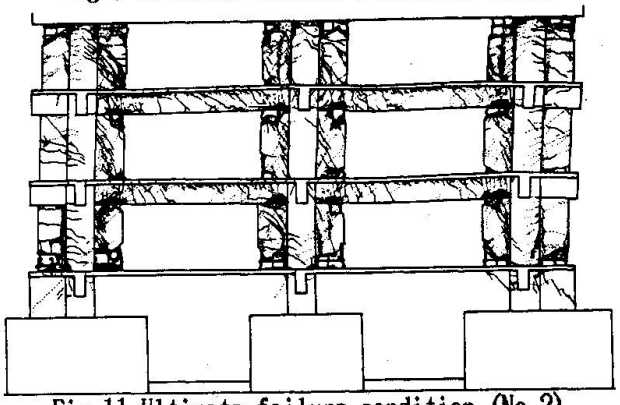

Fig 11 Ultimate failure condition (No.2)

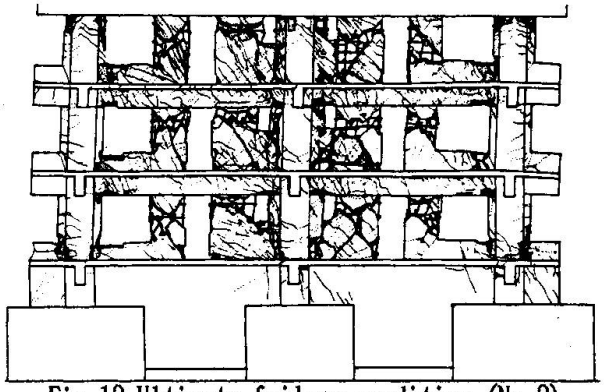

Fig 13 Ultimate failure condition (No.3)

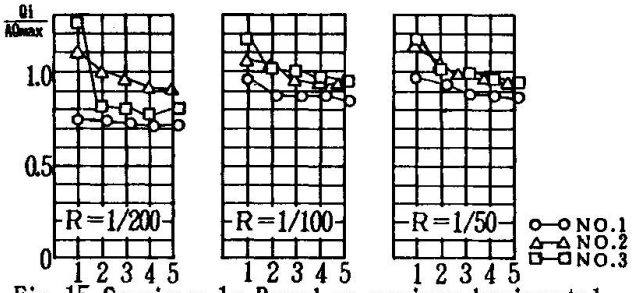

Fig 15 Specimen 1: Based on maximum horizontal load, horizontal load at each cycle

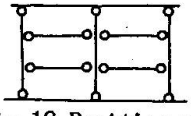

Fig 16 Position where yield hinge of SRC frame is formed

mode of the frame containing a reinforced concrete wall was the same as that of the pure frame. Although the frame contained a wall, the wall did not affect the peripheral frames much. The axial force of 5884 KN/m², applied to each column, could be kept at this level until the end of the test.

3.2 Deflection behavior and horizontal bearing capacity

Figure 14 shows an envelope of $Q - \delta_T$ curve. From this figure, we can see that the reinforced concrete wall greatly affected the lateral stiffness of the SRC frame. The measured elastic stiffness of the frame containing a wing wall was about double the elastic stiffness of the pure frame, and about five times that of the frame containing a wall with openings. A beam theory can be established to analyze the stiffness of a reinforced concrete wall if a model for the wall with openings is carefully made.

The deflection behavior of each specimen showed a stable load-deflection curve up to $R_T \fallingdotseq 1/50$. Each specimen, deformed up to $R_T \fallingdotseq 1/20$, showed a deflection curve of relatively little decrease in the bearing capacity. It can be said that each frame had sufficient ductility.

Figure 15 shows the bearing capacity ratio based on the maximum horizontal bearing capacity of specimen No.1. When deformed greatly, specimens No.2 and No.3 had the same bearing capacity as that of specimen No.1.

If the maximum horizontal bearing capacity of the pure frame is assumed to be 1, the capacity for the frame containing a wing wall was 1.19, and the capacity for the frame containing a wall with openings was 1.32. The frame containing a reinforced concrete wall improved the maximum bearing capacity. Also a virtual work method can be used to predict the maximum bearing capacity. Figure 16 shows the frame failure mode. The bearing capacity of specimen No.1, obtained by the virtual work method, was about 80% of the experiment value of the maximum horizontal bearing capacity.

4. CONCLUSIONS

From this experiment it was found that, concerning the elastic and plastic behaviors, the stiffness and horizontal bearing capacity of the SRC frame containing a reinforced concrete wall was higher than those of the pure frame. It was feared that the wall worsens the structural performance of the SRC frame. By the time the frame was deformed greatly, it showed almost the same behavior as that of the pure frame. This is because the SRC frame has sufficient structural performance. If sufficient stiffness is sustained to secure the building use and living performance, the deflection caused by an earthquake can be kept small. Even if a wall is destroyed by a big earthquake, the structure of the SRC frame is safe against collapse. If a shear failure occurs, it may be impossible to open or close doors. One way to avoid this problem is to install doors away from the columns and beams.

REFERENCE

[1] SRC Design Standard, Architectural Institute of Japan, 1987.

Poutres mixtes acier-béton avec un système de précontrainte extérieure

Stahl-Beton-Verbundträger mit einem von Aussen angebrachten Vorspannungssystem

Steel-Concrete Composite Girders with External Prestressing

J.-M. ARIBERT
Prof. des Univ. INSA
Rennes, France

Jean-Marie Aribert, né en 1941, Ingénieur et Docteur es Sciences, enseigne la Mécanique des Structures à l'Institut National des Sciences Appliquées de Rennes, depuis 1970. Il dirige un laboratoire orienté principalement vers la Construction Métallique et la Construction Mixte.

Wadii HAMADEH
Ingénieur
CTICM
Paris, France

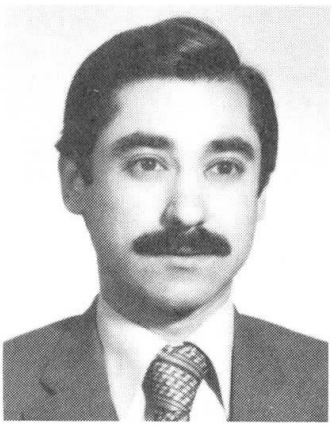

Wadii Hamadeh, né en 1953, Ingénieur en Génie Civil Université d'Alep, Syrie, poursuit ses travaux au CTICM sur la précontrainte extérieure, en vue de l'obtention du grade de Docteur en Génie Mécanique à l'Université Pierre et Marie Curie (Paris VI).

Bruno CHABROLIN
Chef de Département
CTIM
Paris, France

Bruno Chabrolin, né en 1954, Ingénieur diplomé de l'Ecole Polytechnique et de l'ENPC, dirige actuellement au CTICM les activités de recherche: développement en Construction Métallique. Son activité s'est exercée dans le domaine des ouvrages d'art et des structures en mer.

RÉSUMÉ

Cette communication concerne la présentation d'un modèle original de calcul numérique, valable jusqu'à la ruine pour des poutres continues à précontrainte extérieure avec déviation du câble. Plusieurs exemples sont traités par le modèle et comparés aux résultats d'un dimensionnement simplifié aux états-limites de résistance et stabilité.

ZUSAMMENFASSUNG

Dieser Beitrag beschreibt ein nummerisches Rechenmodell für das Verhalten von Verbundträgern mit aussenliegender Vorspannung bis zum Versagen. Mehrere Beispiele werden vorgestellt und mit den Ergebnissen einer vereinfachten Bemessung für die verschiedenen Grenzzustände verglichen.

SUMMARY

In this article a numerical model of the behaviour up to failure of continuous composite beams prestressed by deviated exterior cables is presented. Examples of model predictions are compared to the results given by simplified design for the various limit states.

1. INTRODUCTION

Dans le domaine des poutres mixtes, un intérêt particulier semble être accordé actuellement à l'utilisation de systèmes de précontrainte extérieure, en particulier en France pour les ponts où les charges permanentes sont relativement importantes rapportées à la longueur des travées [1]. Avec le système de précontrainte considéré ici [2], on améliore évidemment le comportement de la dalle de béton en réduisant les zones de béton tendu aux appuis intermédiaires, mais ce système introduit aussi, au droit des déviateurs de câbles en partie courante, des efforts verticaux ascendants qui soulagent la structure de l'action des charges permanentes.
Peu de modèles de calcul non-linéaire semblent avoir été développés dans la littérature à ce sujet, et seulement pour des configurations simples [3]. La première partie de cette communication est consacrée précisément à la présentation succincte d'un modèle numérique, applicable à des poutres isostatiques ou hyperstatiques, intégrant le comportement non-linéaire des sections et des câbles ainsi que les phénomènes de frottement et de glissement au passage des déviateurs. On illustre ensuite les possibilités du modèle sur quelques exemples de poutres isostatiques et hyperstatiques avec des travées allant de 7.50 m à 30 m. Enfin, dans la troisième partie, une comparaison au modèle est effectuée à l'aide d'une approche analytique simplifiée aux états limites, sans négliger l'aspect du voilement de l'âme qui peut réduire l'efficacité du système.

2. MODELISATION NUMERIQUE

2.1. Présentation du type de poutre étudié

La géométrie présentée sera limitée au cas d'une poutre continue à deux travées (Fig. 1), le cas isostatique n'étant qu'un cas particulier et la généralisation à plus de deux travées ne soulevant pas de difficultés.

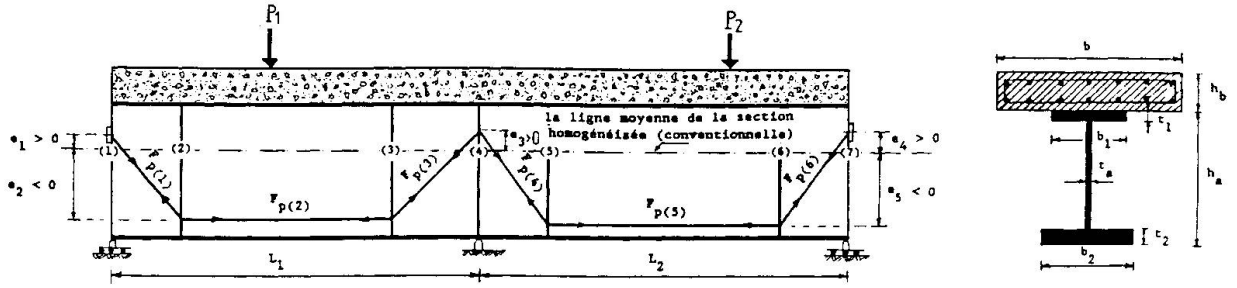

Fig. 1

Le câble de précontrainte est dévié ici deux fois par travée. Pour le chargement, on distinguera la charge permanente, supposée répartie et fixe, des surcharges concentrées et appliquées de manière croissante jusqu'à la ruine. En outre, la connexion entre acier et béton sera supposée complète [4], ce qui autorisera à négliger le phénomène de glissement à l'interface. Enfin, pour traduire le comportement des matériaux, des lois relativement élaborées seront introduites dans le modèle, comme le montrent les figures 2a pour le béton, 2b pour l'acier du profilé et 2c pour le câble.

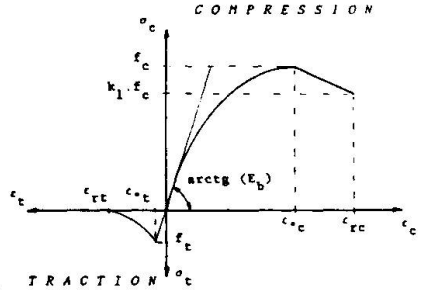

Fig. 2a

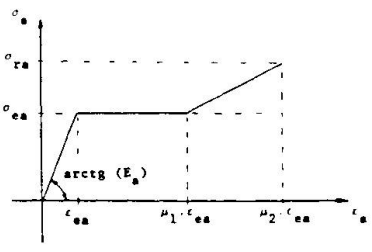

Fig. 2b

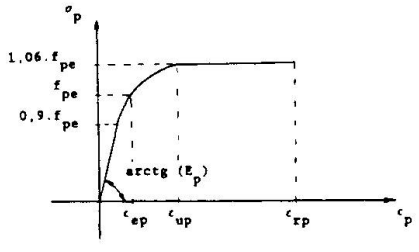

Fig. 2c

2.2 Modélisation préalable sans la présence de la précontrainte

Le module de calcul de base du programme développé se place dans l'hypothèse d'un comportement élastique linéaire et sans précontrainte, la poutre étant découpée en éléments finis de barre le long de sa ligne moyenne (définie conventionnellement comme celle du centre de gravité de la section homogénéisée pour le comportement élastique initial); évidemment, chaque élément fini a des propriétés élastiques équivalentes a priori différentes. La résolution est

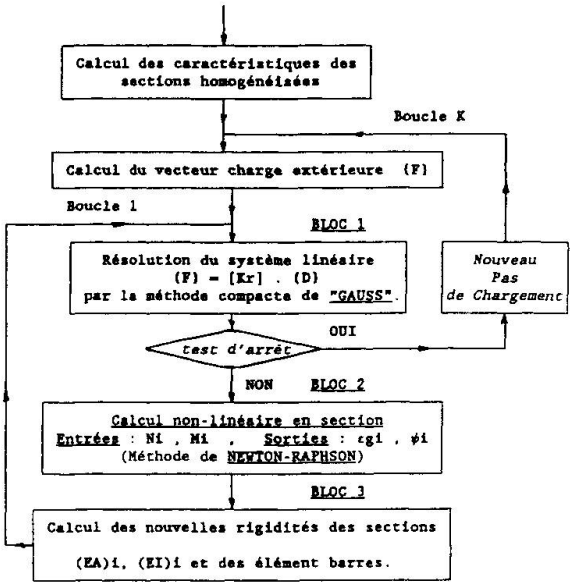

Fig. 3

effectuée par la méthode matricielle classique des déplacements. La non-linéarité de comportement de l'acier et du béton est résolue à l'aide d'un calcul itératif sécant (boucle d'indice ℓ dans l'organigramme de la figure 3), la réactualisation à chaque itération des rigidités axiale $(EA)_i$ et flexionnelle $(EI)_i$ d'une section quelconque i de la poutre étant faite à partir de l'effort normal N_i et du moment fléchissant M_i obtenus à l'itération $(\ell-1)$; en particulier, pour le calcul en section (bloc 2 sur l'organigramme), l'algorithme de calcul permettant de trouver la déformation axiale ε_i et la courbure Ψ_i en fonction de N_i et M_i a été rendu plus performant par l'utilisation d'une procédure itérative tangente de type Newton-Raphson, par comparaison à celui déjà publié [5]. On précise encore que les rigidités de chaque élément fini de barre sont obtenues par pondération de celles de plusieurs sections intermédiaires (bloc 3). L'organigramme très général de la figure 3 permet de resituer, les uns par rapport aux autres, les différents calculs précédents, le test d'arrêt de la boucle ℓ étant basé sur l'écart relatif des efforts internes entre deux itérations successives (pris ici inférieur à 10^{-4}).

2.3 Généralisation du modèle en présence de la précontrainte

Seuls sont abordés ci-après les aspects originaux de cette généralisation.

2.3.1. Réduction du torseur des efforts de chaque déviateur au niveau de la ligne moyenne de la poutre.

Aux charges extérieures déjà mentionnées viennent s'ajouter les efforts exercés par le câble sur les déviateurs ; ces efforts peuvent être réduits sur la ligne moyenne de la poutre, au droit de chaque déviateur, comme le montre la figure 4 pour le cas des 7 déviateurs de la figure 1.

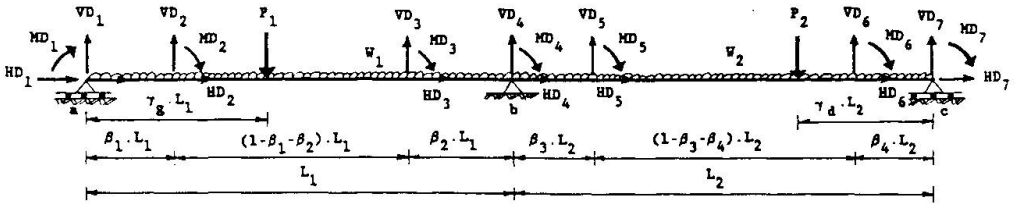

Fig. 4

Il est facile de calculer ces efforts réduits à partir des efforts dans le câble $F_{p(1)}$, $F_{p(2)}$, ... $F_{p(6)}$ supposés connus; par exemple, pour le déviateur 2, on a :

$HD_2 = F_{p(2)} - F_{p(1)} \cos\alpha_1$; $VD_2 = F_{p(1)} \sin\alpha_1$; $MD_2 = HD_2\, e_2$ où α_1 désigne l'angle du segment de câble (1-2) par rapport à l'horizontale.

2.3.2. Actualisation de la position des déviateurs au cours du chargement

Les coordonnées des déviateurs, qui doivent être actualisées au cours du chargement, sont calculées par rapport à l'état de référence de la structure (état de mise en tension du cable, sans chargement). Connaissant les translations et la rotation de la section où se trouve le déviateur, il est aisé de calculer les coordonnées du déviateur à partir de l'hypothèse de Bernoulli (d'autant plus valable que la section a été nécessairement raidie). Si l'on fait l'hypothèse de non glissement du câble aux déviateurs, l'allongement de chaque segment de câble s'en déduit immédiatement, ainsi que sa variation de tension par rapport à l'état de référence.

2.3.3. Prise en compte du glissement du câble aux déviateurs

Désignant par $F^{(j,k)}_{p(d-1)}$ et $F^{(j,k)}_{p(d)}$ les tensions du câble respectivement à gauche et à droite du déviateur d, pour le stade de chargement (k) et à l'itération (j) de ré-équilibrage de ces efforts, l'absence de tout glissement relève de la condition

suivante, où f est le coefficient de frottement retenu :

$$F_{p(d)}^{(j,k)} \; e^{-f\alpha_d^{(k)}} < F_{p(d-1)}^{(j,k)} < F_{p(d)}^{(j,k)} \; e^{f\alpha_d^{(k)}} \qquad (1)$$

Si l'une des deux inégalités n'est pas satisfaite , il se produit un glissement $g_d^{(j,k)}$ que l'on peut calculer analytiquement en utilisant le module d'élasticité tangente du câble (Fig. 2c) et qui se traduit par une redistribution des efforts dans les segments de câble ; par exemple, avec un glissement vers la droite, on a :

$$F_{p(d)}^{(j+1,k)} = F_{p(d)}^{(j,k)} - \Delta F_{p(d)}^{(j,k)} \; ; \; F_{p(d-1)}^{(j+1,k)} = F_{p(d-1)}^{(j,k)} + \Delta F_{p(d)}^{(j,k)} \qquad (2)$$

Le concept précédent peut être généralisé à deux déviateurs ou plus. En fait, à cause du comportement non-linéaire du câble, un calcul itératif est nécessaire pour déterminer $g_d^{(j,k)}$ et l'on a constaté à ce sujet que l'introduction d'un coefficient d'amortissement numérique de 0.5 accélérait la convergence.

2.3.4. Résolution numérique

La résolution du problème oblige à passer maintenant par trois grande boucles itératives ; par rapport à l'organigramme de la figure 3, une boucle d'indice j vient s'intercaler entre les boucles ℓ et k afin d'effectuer l'analyse du glissement des câbles au droit des déviateurs. Par ailleurs, par suite de l'interaction entre les variation d'effort dans le câble et la distribution des rigidités le long de la poutre, la boucle ℓ devient plus complexe. Pour assurer une bonne convergence, cette boucle ℓ a été décomposée en deux séquences, la première permettant le calcul des nouveaux efforts de câble pour une distribution fixée des rigidités, et la seconde celui des rigidités à partir des nouveaux efforts de câble. Le test d'arrêt pour chaque séquence est toujours basé sur l'écart relatif des efforts internes (précision de 10^{-4}). Un contrôle au niveau global de la boucle ℓ est également nécessaire sur l'écart relatif des efforts de câble (précision de 10^{-5}). Une fois la convergence acquise avec la boucle ℓ, on entre dans la boucle j pour vérifier si l'hypothèse de non glissement utilisée était valable et éventuellement corriger cette hypothèse conformément à ce qui a été exposé en 2.3.3. Pour terminer, on précise qu'au niveau de la boucle externe k, on distingue deux phases de calcul nettement séparées: l'une correspond à la mise en tension du câble jusqu'à la valeur de précontrainte désirée, l'autre au chargement proprement dit.

3. APPLICATIONS NUMERIQUES

On illustre les possibilités du modèle sur trois poutres, dont deux isostatiques de portées 7.5 et 30 m, et la troisième hyperstatique avec deux travées égales de 30 m. Les caractéristiques adoptées pour les matériaux sont les suivantes (cf Fig. 2 pour les notations) :

- profilé : σ_{ea} = 240 MPa ; σ_{ra} = 360 MPa ; E_a = 210000 MPa ; μ_1 = 10 ; μ_2 = 30
- armatures passives : σ_{es} = 400 MPa ; E_s = 210000 MPa ; μ_1 = 10
- dalle béton : f_c = 30 MPa ; f_t = 2.4 MPa ; E_b = 30000 MPa ; k_1 = 0.85
  ε_{oc} = 0.28 ‰ ; ε_{rc} = 0.4 ‰ ; ε_{rt} = 0.2 ‰
- câbles : f_{pe} = 1623 MPa ; E_p = 190000 MPa ; ε_{up} = 2 ‰ ; ε_{rp} = 4 ‰

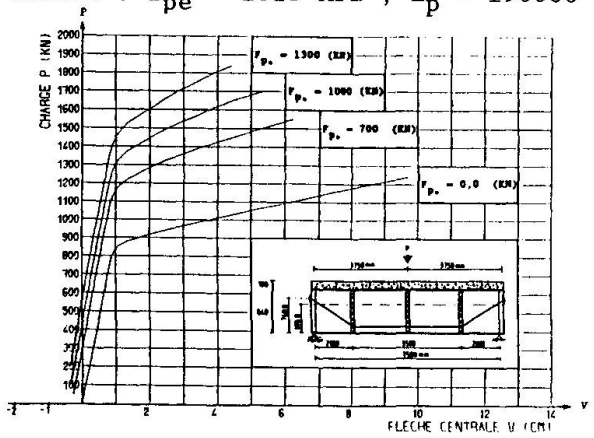

Fig. 5 : Influence de la valeur initiale de précontrainte sur l'évolution de la flèche centrale en fonction du chargement

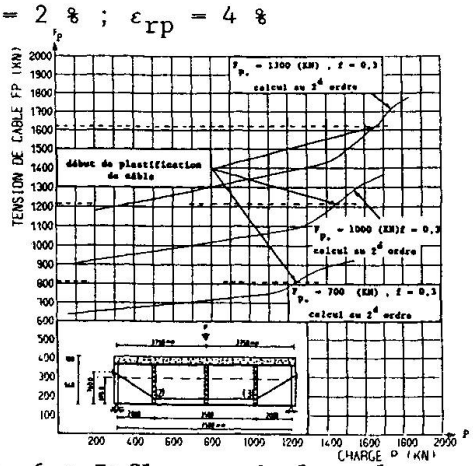

Fig. 6 : Influence de la valeur initiale de précontrainte sur l'évolution de la tension du câble (2-3) avec le chargement

La première poutre isostatique étudiée, de portée 7.50 m, a les dimensions de sections suivantes (en cm) : b = 120, h_b = 10, h_a = 80, t_a = 0.4, $b_1 = b_2$ = 30, $t_1 = t_2$ = 2.
Les résultats présentés aux figures 5 et 6 supposent une possibilité de glissement (f = 0.3) et tiennent compte d'un effet de 2ème ordre géométrique (moment fléchissant secondaire dû à la déformée de la poutre). L'évolution de la courbe "charge-flèche" est montrée à la figure 5 pour divers niveaux de précontrainte initiale; on note, par exemple, que lorsque F_{po} passe de 0 à 1000 kN, la charge ultime passe de 1240 kN à 1700 kN. Parallèlement, le câble est amené à subir des surtensions plus marquées vers l'état limite ultime, en moyenne de 30 %, mais qui peuvent aller au delà en partie centrale (fig. 6).
La deuxième poutre isostatique, de portée 30 m, a les dimensions de sections suivantes en cm : b = 280, h_b = 22, h_a = 130, t_a = 1, b_1 = 40, b_2 = 55, $t_1 = t_2$ = 3.

Pour une tension de câble réaliste, F_{po} = 4000 kN, l'effet de précontrainte est toujours aussi efficace sur la capacité portante qui passe de 1625 kN à 2230 kN (calcul au premier ordre), mais les effets du 2ème ordre géométrique sont ici plus importants (cf les courbes "charge-flèche" de la fig. 7), ramenant la capacité ultime de 2230 kN à 1945 kN. La poutre continue, avec deux travées égales de 30 m, a la même section que la poutre isostatique précédente. Avec la même tension de câble F_{po}, le gain de capacité est plus important (P_u passant de 1745 kN à 2670 kN); ceci s'explique par la valeur faible de P_u en l'absence de précontrainte, due à la fissuration de la dalle sur appui intermédiaire.

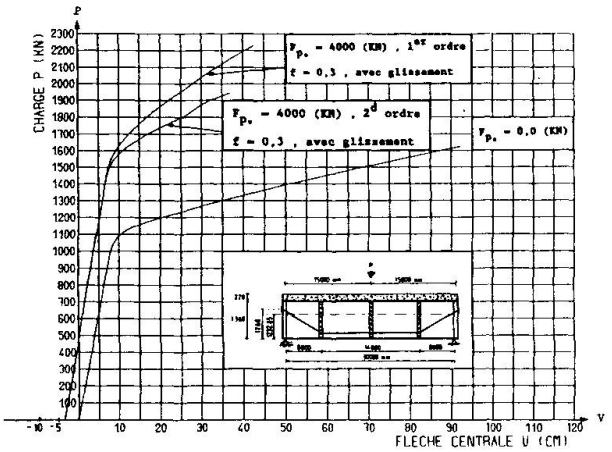

Fig. 7 : Influence des effets du 2ème ordre dans la poutre de portée 30 m

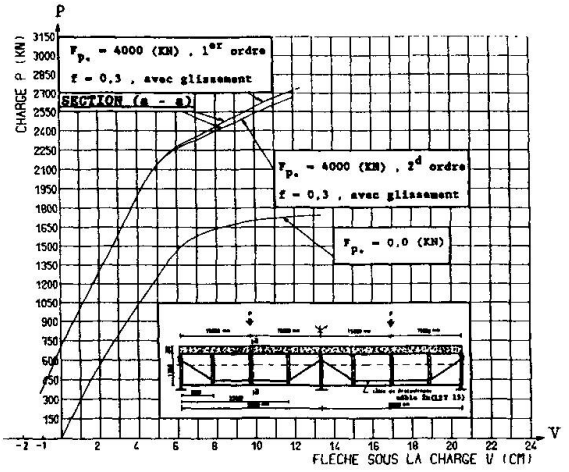

Fig. 8 : Courbes charge-flèche pour une poutre à deux travées de 30 m

Par ailleurs, les effets du 2ème ordre sont encore plus marqués, ce qui était prévisible (fig. 8). A noter encore, comme l'illustre la figure 9, que le déviateur 2 ne subit ici aucun glissement alors que le déviateur 3 se trouve soumis au glissement dès le début du chargement (toutefois avec une précharge P de 350 kN simultanément à la mise en tension); ce glissement du déviateur 3 a par ailleurs un effet favorable sur la surtension du segment de câble 2-3 qui est plus limitée (fig. 10).

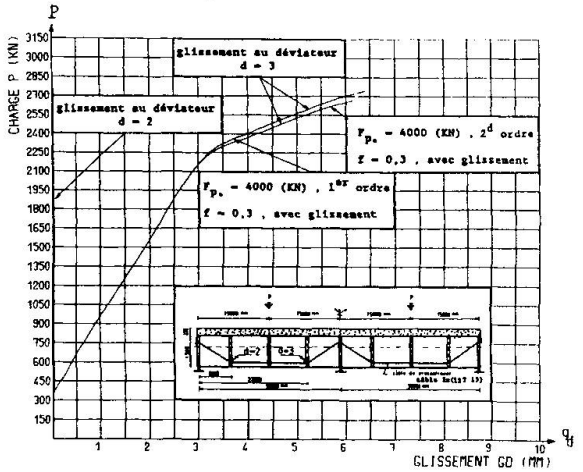

Fig. 9 : Charge-glissement aux déviateurs (D=2, D=3)

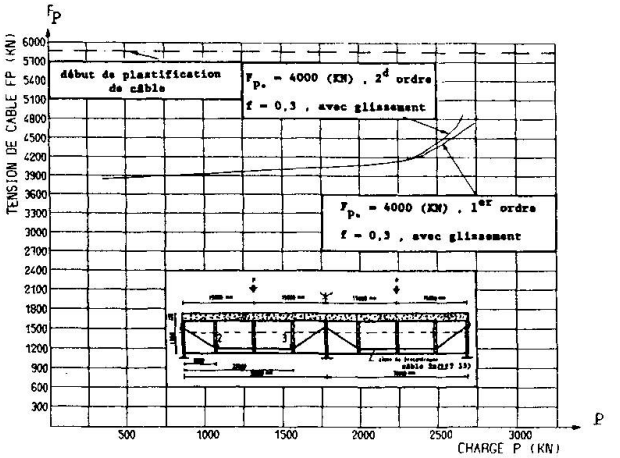

Fig. 10 : Evolution de la tension du câble 2-3

4. COMPARAISON AVEC UN DIMENSIONNNEMENT AUX ETATS LIMITES

Il a paru utile de comparer les charges limites calculées à l'aide du modèle numérique à celles que peut fournir un modèle analytique simplifié basé sur des hypothèses classiques de résistance des matériaux et sur des dispositions règlementaires (règlement français sur les ponts mixtes [6] et EUROCODE 3 [7]). Sont examinés ici l'état limite d'utilisation de résistance et les états limites ultimes de résistance et de stabilité de l'âme. Pour la résistance, on ne retient que l'évolution des contraintes en section. Le calcul des sollicitations iso- ou hyperstatiques suppose une zone de béton fissurée de 20 % de chaque côté de l'appui intermédiaire. On considère les résistances de l'acier et du béton comme suit (le béton tendu ne résiste pas) :
- aux ELS : σ_{ea} , 0.6 f_c, diagramme de déformations élastique (triangulaire),

- aux ELU : σ_{ea} , 0.85 f_c, diagramme de déformations plastique (rectangulaire)

ces valeurs, étant jugées mieux correspondre aux hypothèses du modèle numérique que les valeurs réglementaires parfois différentes. Des calculs relativement simples permettent alors d'évaluer les charges limites selon le schéma de la figure 1 (poutre à 2 travées) aux ELS et aux ELU.
En ce qui concerne l'état limite ultime d'instabilité de l'âme, on a utilisé les prescriptions de l'EC3 et retenu la méthode la plus simple dite "post-critique" (cf. EC3 - Clause 5-6-4). L'EC3 introduit, outre le calcul de l'effort tranchant ultime au voilement, une règle d'interaction effort tranchant-moment fléchissant qui a été prise en compte. Le tableau 1 regroupe les résultats comparés à ceux du modèle numérique pour les trois poutres étudiées ici :

	F_{po} (kN)	Mod. Numérique (*) sans voilement		Calcul analytique sans voilement	Résistance ultime au voilement (EC3)
1e poutre iso	1000	ELS	1195	1118	
		ELU	1700	1477	362
2e poutre iso	4000	ELS	1340	1361	
		ELU	1945	1718	1600
poutre hyperst.	4000	ELS	1685	1678	
		ELU	2670	2224	2100

(*) avec effet du 2e ordre Table 1 : Comparaison de modèles

On voit sur ce tableau, la bonne concordance en ce qui concerne la résistance pure entre le modèle numérique et le modèle analytique (qui place logiquement en sécurité à l'ELU par non prise en compte du raffermissement de l'acier). On constate aussi que la première poutre, élancée (λ = 200), est très pénalisée par le voilement de l'âme.

5. CONCLUSIONS

Le modèle numérique présenté ici semble capable de simuler correctement, en fonction de divers paramètres, le comportement de poutres mixtes précontraintes jusqu'à la ruine, d'autant que l'on y a introduit un critère de résistance ultime au voilement de l'âme. A ce sujet, nous notons que, pour les configurations étudiées, le voilement de l'âme devient très pénalisant dès que l'élancement devient important. Il y a lieu d'examiner plus avant cette question pour justifier l'intérêt économique du procédé.

BIBLIOGRAPHIE

[1]. CAUSSE G. et DUVIARS M., Ouvrage à âme plissée mis en place par poussage. Charolles, France. Symposium AIPC, Paris-Versailles, 1987.

[2]. VIRLOGEUX M., Bilan de la politique d'innovation dans le domaine des ouvrages d'art. Travaux, n°597, mars 1985.

[3]. SAADATMANESH H., ALBRECHT P. et AYYUB B.M., Guidelines for flexural design of prestressed composite beams. ASCE Journal of Structural Engineering, vol. 115, n°11, novembre 1989

[4]. Commission des Communautés Européennes. Eurocode n°4, chapitre 6, EUR 9886FR 1985

[5]. ARIBERT J.M. et ABDEL AZIZ K., Calcul des poutres mixtes jusqu'à l'état ultime avec un effet de soulèvement à l'interface acier-béton. Revue Construction Métallique n°4-1985

[6]. Circulaire n°81-63 du 28 juillet 1981 relative au règlement de calcul des ponts mixtes acier-béton. Ministère des Transports, Fascicule spécial n°81-31 bis

[7]. Eurocode n°3 Design of Steel Structures, Part. 1, General Rules and Rules for Buildings. Edited draft, issue 2, novembre 1989

Le viaduc de l'Eau Rouge

Eau Rouge Viadukt

Eau Rouge Viaduct

Jean-Marie CRÉMER
Ingénieur Civil
Bureau d'Études Greisch
Liège, Belgique

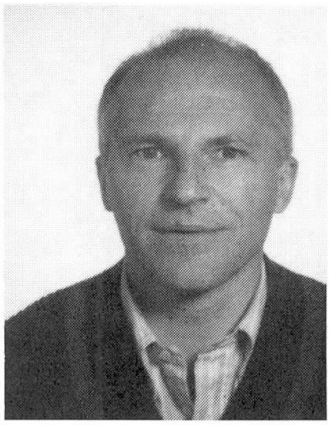

Jean-Marie Crémer, né en 1945, a obtenu son diplôme d'ingénieur civil des constructions à l'ULG Liège en 1968. Pendant 4 ans, il dirige des chantiers de génie civil. En 1973, il entre au bureau Greisch où il est actuellement responsable des études des ouvrages d'art.

RÉSUMÉ

Le viaduc de l'Eau Rouge est un ouvrage mixte dont la partie principale est un arc de 270 m d'ouverture composé de 2 petits caissons métalliques supportant le tablier par l'intermédiaire de montants et de diagonales. Cette portée centrale place cet ouvrage parmi les dix plus grands arcs du monde. Le dimensionnement aux états ultimes est basé sur l'Eurocode 4.

ZUSAMMENFASSUNG

Der Viadukt von „Eau Rouge" ist eine Verbundkonstruktion. Die Hauptöffnung wird von einem Bogen von 270 m Spannweite überbrückt, welcher aus zwei kleinen, stählernen Hohlkästen besteht, die die Brückenfahrbahn mittels Stützen und Diagonalen aufnehmen. Mit dieser Spannweite ist der Bogen einer der zehn größten der Welt. Die Bemessung nach der Grenzzustandsphilosophie erfolgte auf der Grundlage des Eurocode 4.

SUMMARY

The Eau Rouge viaduct is a composite structure, the main part of which is a 270 m span length arch made of two steel boxbeams supporting the deck by means of columns and diagonals. This central span places this structure among the ten longest arches existing in the world. The structural design using ultimate limit state is based on the Eurocode 4.

SITUATION GENERALE

L'ouvrage se situe entre Francorchamps et Malmédy sur l'autoroute E 42 (ex A 27) Verviers - Saint-Vith - Prüm - Francfort.

C'est pour permettre le développement industriel et touristique de la région des Hautes Fagnes et de l'Eifel que les états belges et allemands ont décidé simultanément en 1972 de construire une autoroute entre Verviers en Belgique et Prüm en Allemagne pour relier entre elles des autoroutes déjà existantes. La longueur du tronçon à réaliser en Belgique est de 52,5 km comprenant 9 viaducs dont celui de l'Eau Rouge qui est le dernier ouvrage à réaliser à l'heure actuelle.

PRESENTATION GENERALE DE L'OUVRAGE

L'autoroute traverse la vallée de l'Eau Rouge en la surplombant à une hauteur de 45,0 m. Ce site bien connu des promeneurs, fagnards et naturalistes, l'est également par sa source ferrugineuse et carbo-gazeuse : le Pouhon de Bernister.

L'agressivité du sol de fond de vallée, spécialement au Sud du ruisseau, a nécessité une portée centrale de 270,0 m pour éviter la zone de terrain décomposé, siège d'eau carbogazeuse où l'acidité est telle que le ph est inférieur à 3.

Cette portée centrale est franchie grâce à deux arcs en caissons métalliques entredistants de 14,0 m sur lesquels vient s'appuyer le tablier mixte par l'intermédiaire de montants et diagonales. De part et d'autre de cette travée centrale, les travées d'approche sont de 33,75 m et 5 fois 45,0 m au Nord, 2 fois 45,0 m et 33,75 m au Sud. Le viaduc a une longueur totale de 652,50 m.

Le tablier mixte acier-béton a une largeur de 27,0 m avec deux chaussées, chacune comportant deux bandes de circulation de 3,75 m et une bande d'arrêt d'urgence.

INFRASTRUCTURE

La qualité du sol a permis de s'appuyer en fondation directe sur le rocher. La pression maximale admissible a été prise égale à 10 kg/cm^2 sauf pour l'appui de l'arc en rive gauche (Sud) où la pression admissible a été réduite à 5 kg/cm^2 en raison de la forte tectonisation.

Le viaduc comporte deux culées d'extrémité C1 et C2, sept piles intermédiaires des travées d'approche P1 à P5, P8 et P9, et deux appuis d'arcs avec piles renforcées P6 et P7.

Les culées en béton armé sont composées d'une poutre chevêtre creuse avec murs en retour et mur garde-grève posés sur deux voiles verticaux de 1,80 m d'épaisseur, ceux-ci encastrés chacun dans une semelle de fondation. La hauteur de C1 est de 21,80 m, celle de C2 13,60 m.
Les piles intermédiaires sont constituées de deux colonnes de 3,60 m de diamètre extérieur et 3,0 m intérieur posées sur des semelles indépendantes dont la surface d'appui varie de 6,50x7,00 à 7,50x8,50 m^2.

Les colonnes sont renforcées en tête pour recevoir l'appui de la superstructure.
La hauteur des piles varie de 18,30 à 42,0 m.

Les fondations d'arcs sont des massifs en béton armé de 13,0 m x 20,0 m par 4,0 m d'épaisseur en P6 (rive droite) et de 20,0 m x 26,0 m par 4,0 m d'épaisseur en P7 (rive gauche), inclinés sur l'horizontale de 20 à 25°.
Chacun de ces massifs compte deux fourreaux en béton armé destinés à recevoir les naissances d'arc en acier et à les protéger des eaux agressives. Les arcs métalliques prennent appui sur la semelle de fondation par l'intermédaire d'un bloc intermédaire en béton comportant des niches à vèrins et permettant un règlage ultérieur éventuel des pieds d'arc.

Sur chacune des semelles d'arc sont encastrées deux colonnes de 4,20 m de diamètre extérieur et 3,0 m de diamètre intérieur, renforcées en tête, et dont la hauteur hors tout est de 51,30 m en P6 (rive droite) et 44,60 m en P7 (rive gauche).

Les semelles de fondation et les pieds de colonnes situés dans les zones d'eaux agressives sont protégés pour éviter la désagrégation du béton.
Ce béton, de qualité 40, est composé de granulats et sables quartzeux et siliceux et doit avoir un rapport E/C < 0,4. Il est entouré d'une enveloppe protectrice en PEHD.

SUPERSTRUCTURE

Les deux arcs métalliques dont l'ouverture est 270,0 m ont une forme parabolique de rayon minimum 150,0 m et d'une flèche d'environ 50,0 m.
Les deux caissons, entredistants de 14,0 m, ne sont reliés entre eux par aucun contreventement, sauf pendant les phases de montage.
Les arcs supportent le tablier par l'intermédiaire de montants et diagonales entredistants de 33,75 m.
Sur 67,0 m en clé, l'arc et le tablier se confondent pour ne plus former qu'un caisson unique de hauteur variable.

Chacun des arcs est formé d'un petit caisson métallique dont les dimensions extérieures sont 2,70 m x 2,70 m.
Ce caisson est formé de quatre tôles (de 30 à 60 mm d'épaisseur), chacune raidie longitudinalement par 1/2 HEB 500 qui s'appuie tous les 4,0 m sur un diaphragme transversal.
Les noeuds de liaison des arcs avec les montants et diagonales sont évidemment renforcés de même qu'à la naissance des arcs, la transmission des efforts au béton se fait par une plaque d'assise raidie.

Le tablier est du type poutre continue mixte.
Il est constitué de deux petits caissons métalliques à âmes verticales associés à une dalle de plattelage en béton armé.

La dalle de plattelage de 26,70 m de large et dont l'épaisseur varie de 18 à 50 cm, porte sur les quatre âmes des caissons. Elle est fixée aux semelles supérieures par des goujons connecteurs.
Le porte-à-faux extérieur est de 5,0 m et la portée intérieure de 11,30 m.

Les caissons de tablier sont de hauteur constante 2,0 m, sur 80 % de la longueur de l'ouvrage. Cette hauteur est variable de 2,0 à 7,0 m dans la zone commune arc-tablier et sur 33,75 m de part et d'autre.

Les caissons sont constitués d'âmes non raidies (de 15 à 25 mm d'épaisseur), de semelles supérieures de 60 cm de large (épaisseur variable de 20 à 80mm), d'un fond de caisson raidi par trois raidisseurs longitudinaux 1/2 IPE 360 ou 1/2 IPE 500 (épaisseur variable de 12 à 90 mm).
Les cadres d'entretoisement sont entredistants de 5,625 m. Ils sont renforcés au droit des piles et aux jonctions du tablier avec les montants et diagonales.
Dans la zone commune arc-tablier, les âmes sont raidies longitudinalement pour éviter le voilement sous l'effet de la compression importante de l'arc.

FABRICATION ET MONTAGE

Les colonnes sont bétonnées dans des coffrages grimpants voligés par levées de 4,0m.

Les caissons d'arc et de tablier sont fabriqués en usine par tronçons dont le poids est inférieur à 65 tonnes.
Les travées d'approche sont assemblées sur terre ferme par boulons HR et lancées en place par poussage.
La travée d'arc est montée en encorbellement par un portique à partir des naissances jusqu'à la clé. L'équilibrage se fait par des tirants ancrés dans le rocher.

Le bétonnage de la dalle nécessite un coffrage sur équipage mobile s'appuyant sur la structure métallique et avançant par pas de 15,0 m en respectant des phases qui permettent de limiter les tractions dans le béton.

ETUDES

Les études de stabilité du viaduc sont basées sur le concept des ETATS LIMITES et s'inspirent principalement des EUROCODES 3 et 4. L'absence, au moment de l'étude du projet, de directives précises relatives aux sections mixtes acier-béton en présence d'efforts normaux importants, a conduit au développement d'une étude théorique dont le but fut la définition de critères spécifiques d'interaction M,N,T à l'état limite ultime.

La méthode tient compte de la réserve post-critique de l'âme, due à l'apparition d'une bande de traction diagonale, telle que proposée par CARDIFF. Cette bande de traction s'ancre partiellement dans la semelle supérieure constituée par la dalle de béton et le patin métallique. La longueur de cet ancrage décroit avec la réserve de la semelle vis-à-vis de l'écoulement plastique.

La vérification d'une section mixte suit le schéma suivant:
- détermination de la section équivalente plastique, où l'équivalence est basée sur le rapport de résistance des matériaux;
- classification de cette section en fonction des sollicitations ELU, on distinguera les sections compactes (classe 2), des sections élancées (classe 4).

- Les sections compactes, essentiellement celles soumises à un moment positif, peuvent développer totalement leurs caractéristiques plastiques (diagramme bi-rectangulaire des contraintes normales).
  La stabilité de la section est assurée si le point représentatif d'un état de calcul ELU est intérieur au tracé ABC.

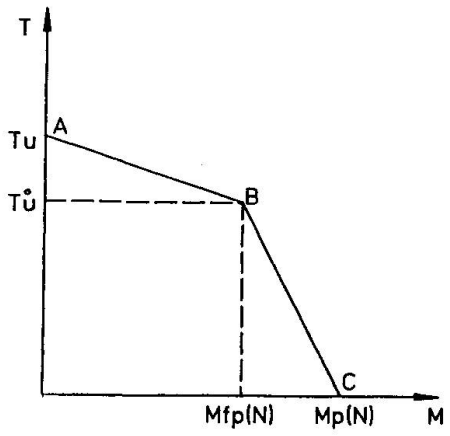

Mfp(N): moment plastique, en présence de l'effort normal de calcul, de la section limitée aux 2 semelles.

Mp (N): moment plastique, en présence de l'effort normal de calcul, de la section complète.

Tu : effort tranchant ultime tenant compte de l'ancrage maximum de la bielle de traction dans la semelle supérieure.

Tu° : effort tranchant ultime sans cet ancrage.

- Les sections élancées, essentiellement celles soumises à un moment négatif, respectant une distribution linéaire des contraintes normales.

  Le critère de stabilité se présente de la façon suivante:

  Dans le fonctionnement en treillis, la section se limite aux deux semelles.

  Dans le fonctionnement en poutre, l'âme est prise en compte, compte-tenu d'une éventuelle perte d'efficassité.

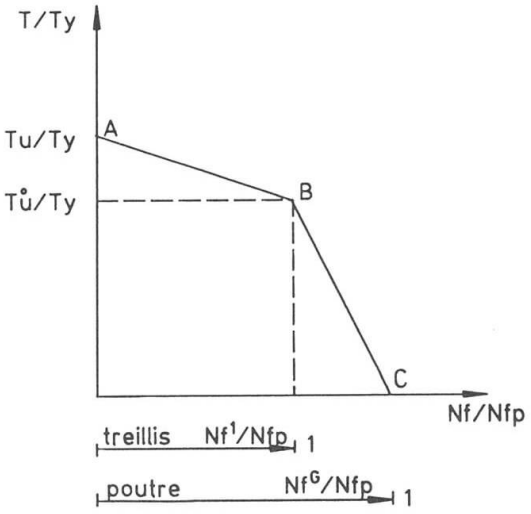

Nfp est l'effort normal ultime dans la semelle la plus sollicitée;

Nf^1 et Nf^G l'effort normal dans cette semelle respectivement dans l'hypothèse du fonctionnement en treillis et dans celle du fonctionnement en poutre;

Ty est l'effort tranchant plastique de l'âme;

T est l'effort tranchant de calcul;

Tu et Tu° définis précédemment

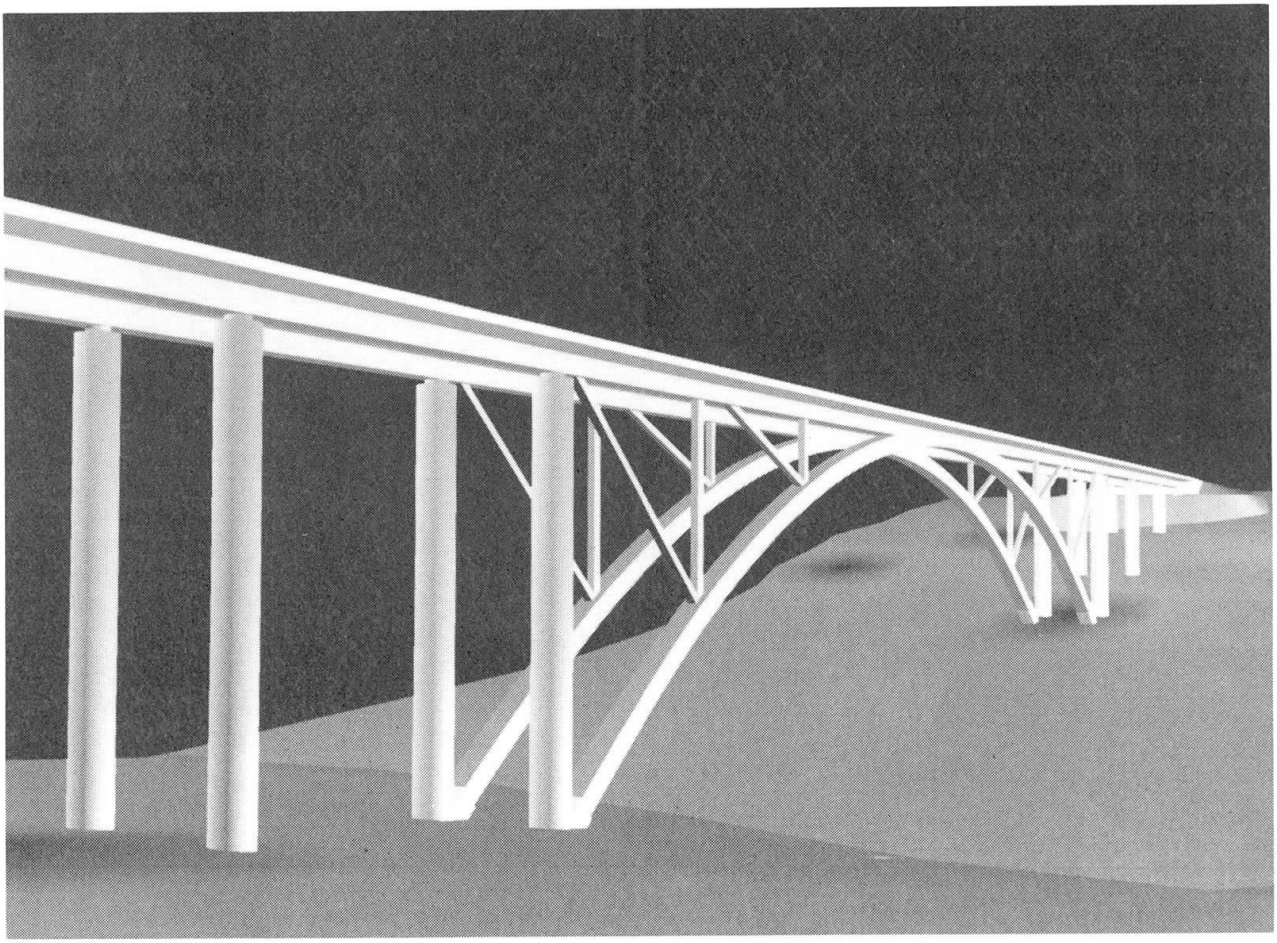

CALCULS SPECIAUX

La structure a fait l'objet de plusieurs calculs spéciaux entrepris avec le programme de calcul non linéaire, FINELG.
Ce logiciel écrit sur la base de la théorie des éléments finis, permet d'obtenir 3 types de résultats:
- des fréquences propres et les modes de vibration de la structure avec ou sans prise en compte de ses efforts internes;
- les charges critiques et les modes d'instabilité de la structure;
- comportement pas à pas de la structure en cours de chargement, avec la prise en compte des phénomènes d'instabilité des lois constitutives élasto-plastiques du matériau, des contraintes résiduelles, etc...

Dans un premier temps, l'ensemble du viaduc a été discrétisé avec des éléments de poutres spatiales afin de vérifier son comportement global. Les études réalisées ont permis d'obtenir:
- ses fréquences propres de vibration;
- ses premiers niveaux de charges critiques sous un chargement vertical;
- grâce à un calcul non linéaire pas à pas la quantification des effets du second ordre lors du chargement simultané du viaduc par le vent et les charges verticales.

Dans un second temps, les diaphragmes des caissons au droit des piles ont fait l'objet d'une étude détaillée. Trois géométries ont été traitées et discrétisées avec des éléments de coques. Les simulations numériques ont permis d'obtenir:
- leurs charges critiques;
- leur charge et leur mode de ruine après avoir pris en compte tous les phénomènes d'instabilité et la loi élasto-plastique de l'acier.

VUE EN ELEVATION

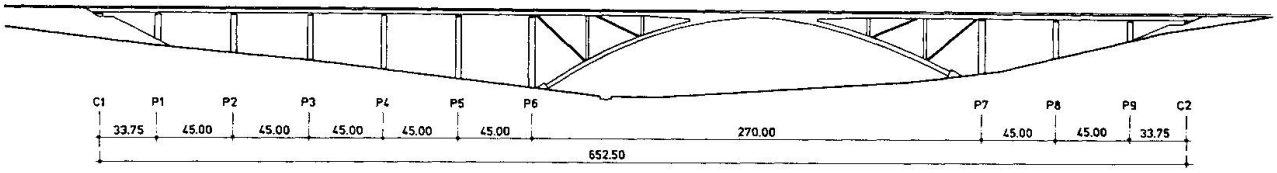

COUPE TRANSVERSALE

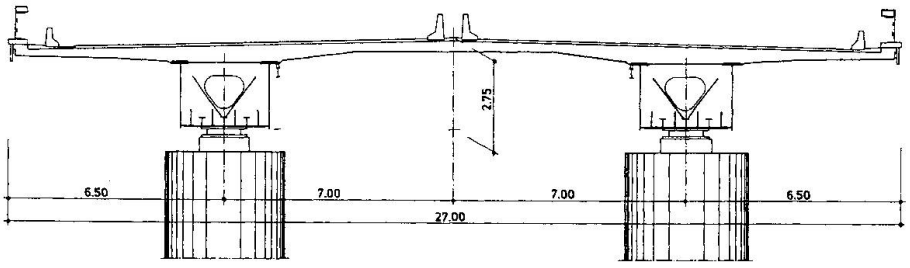

VIADUC DE L'EAU ROUGE

The Tampico Bridge in Mexico

Le pont Tampico au Mexique

Die Tampicobrücke in Mexiko

H. ZAMBRANO RAMOS
Dir. Gen. of Fed. Roads
Mexico, DF, Mexico

M. ARMIJO MEJIA
Pres.
COMEC Engineering
Mexico, DF, Mexico

Alain CHAUVIN
Head of Bridge Division
SOGELERG Engineering
Paris, France

SUMMARY

The Tampico bridge in Mexico represents an innovative example of mixing concrete sections and orthotropic steel sections in cable-stayed bridge decks. This paper sets out the various advantages of this concept which will most likely be frequently used in future projects.

RÉSUMÉ

Le pont de Tampico au Mexique est un exemple original d'association des matériaux béton et acier orthotrope dans les tabliers de ponts haubanés. L'article présente les nombreux avantages de ce concept qui devrait devenir d'usage fréquent dans le futur.

ZUSAMMENFASSUNG

Die Tampicobrücke ist ein Beispiel für die neuartige Verwendung von Beton und orthotropen Stahlquerschnitten für Brückenträger bei Schrägseilbrücken. Der Beitrag zeigt die Vorteile dieses zukunftsträchtigen Konzeptes auf.

1. GENERAL DESCRIPTION OF THE PROJECT

1.1 Main characteristics : (see fig 1 to 3)

- Location : bridge across the Panuco river in Tampico City (Gulf of Mexico).
- Clearance of main span above water : 50m.
- Total length of the bridge, including approach viaducts : 1543m.
- Length of the cable-stayed section between expansion joints : 878m.
- Main span : 360m. Short side spans : 70m.

- Structure of the deck :
  . Orthotropic steel girder for a 293.50m long central section of the main span,
  . Prestressed concrete girder for the remaining sections of main span, and lateral short spans.

  This concept which is the purpose of this paper, will be discussed in further details.

- Deck width : 18.10m, providing four lanes of traffic.
- Pylon : inverted Y shaped, 123.50m high. Rigid deck / pylon connection.
- Suspension : semi-fan shaped axial suspension composed of 4*11 stay cables.
- Foundations : undercut concrete cylinders up to 60m deep (North pylon).

Comec established the basic design around 1980.
The bridge has been in use and carrying traffic since October 1988.

1.2 New Stay technology :

Apart from the innovative deck structure design, mention has to be made of unique cable stay technology which has been specifically developped for this project: (see ref [1]).

The stays are composed of 30 to 60 galvanized T15 strands, housed within a petroleum wax injected HDP duct. The stays were prefabricated on the deck before erection.
This technology provides a 3 barrier protection against corrosion.

Moreover, the wax injection also provides the stay strands with a high performance fatigue behaviour, and overall damping of the stay is increased.
No vibration of the stays has been observed.

Lastly, contrary to classical cement grouting, wax injection can be carried out before erection, under high quality control conditions, which brings about a reduction in the overall construction time.

1.3 Special tests and studies :

The following tests and design studies were performed :

- Fatigue tests on stay samples at Empa laboratory (Zurich-Switzerland).

- Wind tunnel non-stationary tests of deck section model at Onera (Paris-France) and mathematical study of aeroelastic stability of the bridge using these tests.

- Study of hurricane behavior of the bridge when in operation and under construction, using Sogelerg "RAFALES" software.

- Non-linear step by step analysis of the construction stages of the main span, using Civilsoft "SCANNER" software.

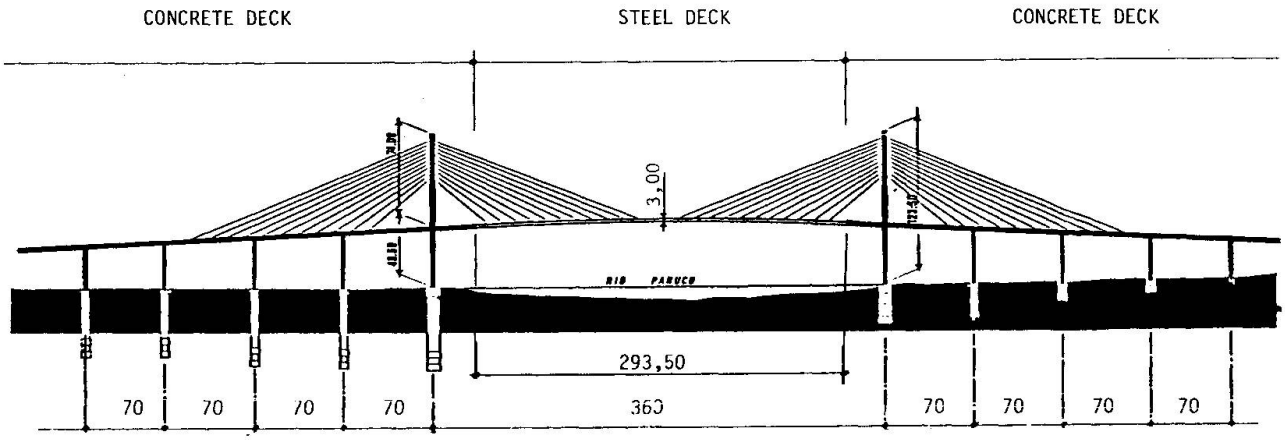

Fig. 1 Elevation of the Bridge

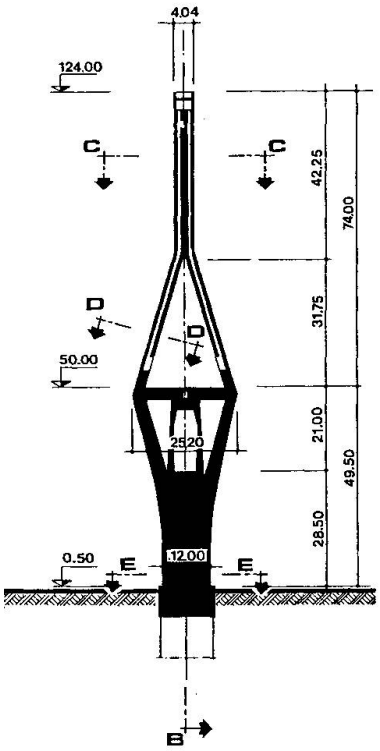

Fig. 2 - Elevation of the pylon

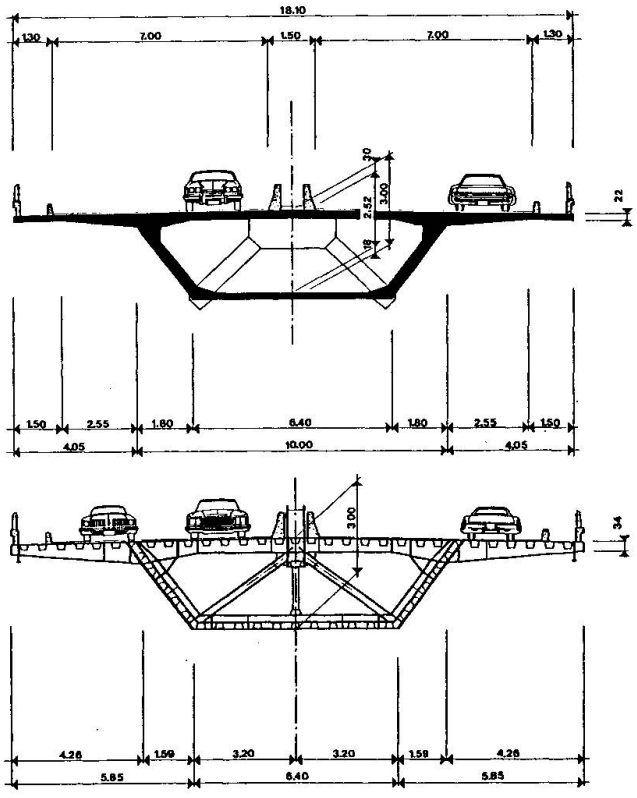

Fig. 3 Concrete and steel cross-sections of the deck

1.4 Construction of main span :

The length of the steel segments of the main span is 12m , which corresponds to the distance between stays. Due to the high risk of hurricane at the location of the bridge, it was finally decided to erect 24m long double segments in order to reduce the construction time of the main span.

These double segments, weighing 160 tons, produced large deflections of the flexible deck during its construction , so the above mentionned SCANNER non-linear analysis became nesessary, so as to ensure good geometrical control of the process, as well as an effective control of stresses in the structure during its construction.

The construction of the steel section of main the span was carried out within 4 months.

The facts confirmed our doubts, since the very powerfull hurricane "GILBERTO" passed within 100km of the bridge, only one month after the completion of the main span...!

2. BASIS OF THE MIXED DECK DESIGN OF THE TAMPICO BRIDGE. (see fig 1)

At an early stage of the project, the very poor soil conditions were considered.
For reasons of economy, it was decided to design the lateral deck short spans with a prestressed concrete girder, while using an orthotropic steel deck girder in the central part of main span.
This allowed both a drastic reduction of vertical forces on the pylons foundations, and a reduction in the cost of the imported steel for the stays.

The length of the main span concrete girder sections was set at 35m, which corresponds to half the length of the lateral spans. The construction of the whole of the concrete deck section was then carried out by the segmental cantilever method.

The external shapes of the concrete and steel deck cross-sections were designed to be compatible (see fig 3). These two sections are linked together using 60 12T13 prestressing tendons.

The following gives an overview of the benefits one can find from such mixed concrete/steel deck design.

3. ADVANTAGES OF THE CONCEPT FOR LARGE CABLE-STAYED BRIDGES.

Let us analyze the advantages of this structural design from the following points of view :

- Static equilibrium,
- Dynamic and wind behavior,
- Construction method,
- Cost.

3.1 Static equilibrium : (see fig 4).

Assuming steel being material 1 and concrete being material 2, we define :

- DW1 : lineal dead weight in orthotropic steel deck section,
- DW2 : lineal dead weight in concrete deck section,
- LL : lineal live load on main span

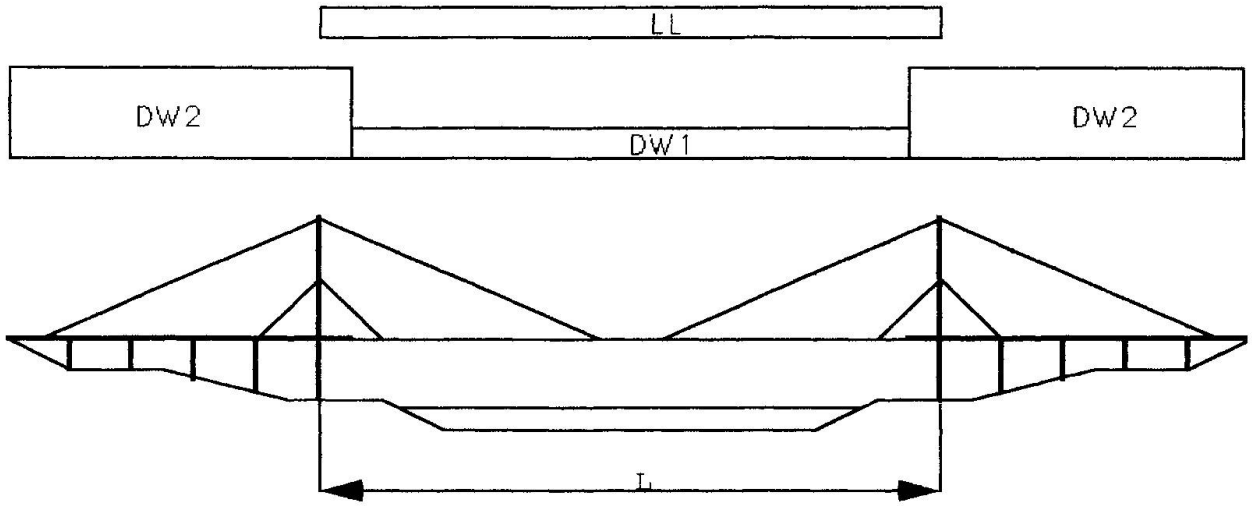

Fig 4 Static equilibrium of the bridge

- Positive contact of the deck on its side piers is ensured since :
  DW2 > (DW1 + LL) (29.50 >> (11.50 + 4.78 = 16.28))

- Max vertical force on pylon is proportional to (DW1 + LL), so, in comparison with the case of concrete main span, it is reduced by (DW1 +LL)/(DW2 +LL) = 0.475 , and longitudinal compression of the deck is reduced by the same ratio.

3.2 Dynamic and wind behavior :

Compared to conventional cable-stayed bridges with long steel side spans , static and dynamic vertical deflections of the main span are reduced. Lateral deflections of the main span under wind effects are also significantly reduced for the bridge during construction and also when in service.

3.3 Construction method :

The concrete section of the deck by being built first, gives a permanent access during the construction of the central span.

3.4 Cost:

- This design allows the construction of the concrete side spans with the same advantageous economic conditions as for ordinary short concrete spans viaducts.
- In comparison with conventional cable-stayed bridges, the points mentioned in 3.2 and 3.3 above also provide savings on both material and construction costs.
- The cost of whole the suspension (pylon+stays), and foundations of the pylons is reduced proportionally to the (DW1 + LL)/(DW2 + LL) ratio.

4. MULTI-MIXED DECK STRUCTURE CONCEPT APPLIED TO LARGER SPANS.

A good economic criteria for main span, is actually based on the total **(suspension + deck)** cost per unit length of deck. For deck structure type i , this unit cost can be expressed as follows, versus abscissa x :

$$Ci = a*(DWi + LL)*x + Cdi \qquad \text{(case of Harp suspension)}$$

where **a** = constant value, depending upon the geometrical shape of the suspension, and on the cost of the stays per unit weight.
Cdi = cost of the deck per linear meter including construction costs.

The upper graphic of fig 5 shows the linear variation of C for 3 different deck structures, for instance : i = 1 : prestressed concrete deck, i = 2 : composite concrete/steel deck, i = 3 : orthotropic steel deck.
It is interesting to note that lighter deck structures have an higher Cdi deck cost, but a lower a* (DWi + LL) slope of their suspension cost.

From these 3 curves, the x1 and x2 limits of the economical area for every deck structure type, in a large multi-mixed deck span can be obtained. Note that the deck structure types with the best resistance to longitudinal compression are also, from an economic point of view, placed in the areas close to the pylon.

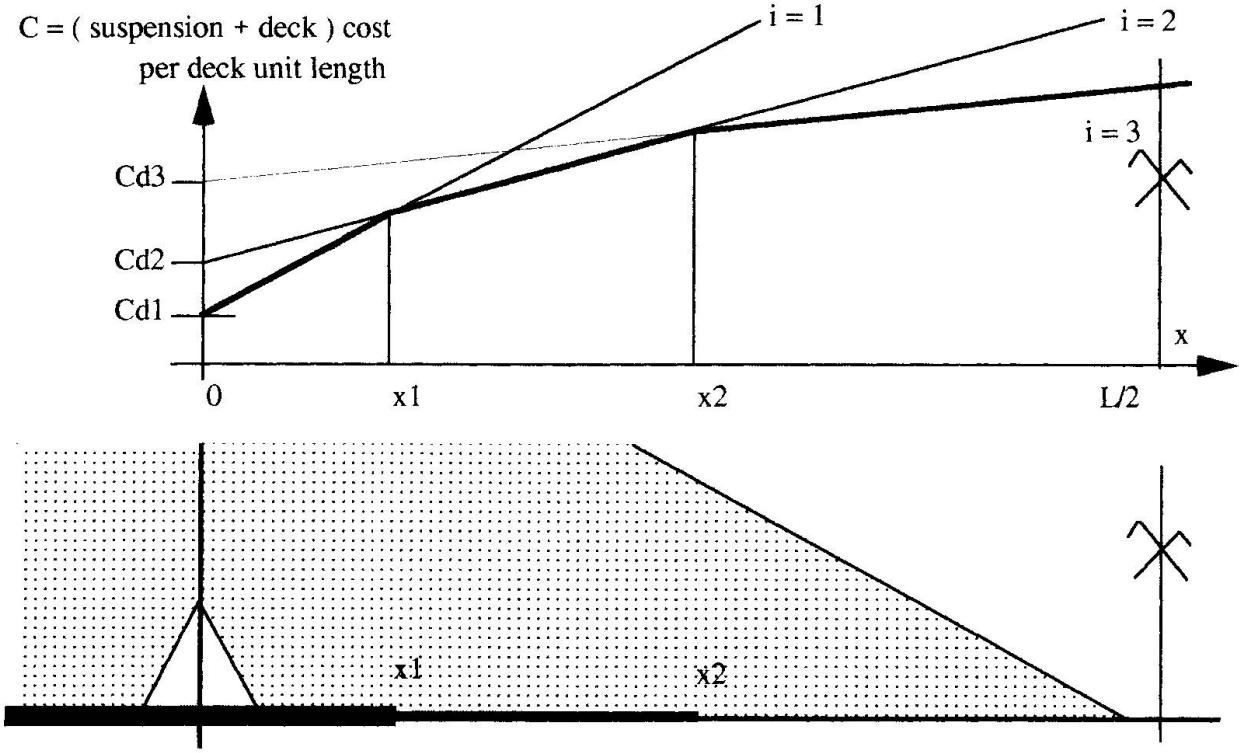

Fig 5 Multi-mixed deck structure for larger spans.

The above example which is a theoretical extension of the Tampico bridge concept would obviously need at least 1000m span to be of interest.

5 CONCLUSION :

We have presented the various innovative aspects of the Tampico bridge, in terms of stay-cables technology, construction process, and principally in terms of its original structural concept.
We sincerely hope that this second large cable-stayed bridge designed and built by Mexico, will greatly contribute to the development of cable-stayed bridges , generally.

Ref [1] : Alain CHAUVIN - Developments in the technology of bridge stays .
FIP Congress New Delhi, Feb 1986.

Entwurf vonVerbundbauten in Erdbebengebieten

Design of Composite Structuresin Seismic Regions

Projet de structures mixtesen zones sismiques

G. SEDLACEK
Prof. Dr.-Ing.
RWTH
Aachen, BRD

Gerhard Sedlacek, geboren 1939, promovierte an der TU Berlin. Acht Jahre arbeitete er in der Stahlbauindustrie, zuletzt als Leiter einer Brückenbauabteilung, seit 1976 ist er Professor für Stahlbau an der RWTH Aachen.

Jürgen KUCK
Dipl.-Ing.
RWTH
Aachen, BRD

Jürgen Kuck, geboren 1960, ist seit 1987 an der RWTH Aachen am Lehrstuhl für Stahlbau als wiss. Angestellter tätig.

B. HOFFMEISTER
Dipl.-Ing.
RWTH
Aachen, BRD

Benno Hoffmeister, geboren 1961, ist seit 1989 an der RWTH Aachen am Lehrstuhl für Stahlbau als wiss. Angestellter tätig.

ZUSAMMENFASSUNG

Für die Interpretation von Testergebnissen, die aus Versuchen an zyklisch belasteten Träger-Stützen-Verbindungen mit unterschiedlichen Anschlußkonstruktionen gewonnen wurden, ist eine Methode entwickelt worden, die sowohl die Verbundwirkung von Stahlträgern und bewehrtem Beton als auch das lokale Verhalten der nachgiebigen Knotenverbindungen numerisch erfaßt. Diese Methode erlaubt die Simulation des nicht-linearen Verhaltens von Stahl- und Verbundkonstruktionen unter monotoner, zyklischer und zeitabhängiger Belastung einschließlich des überkritischen Bereiches und berücksichtigt die Steifkeits- und Festigkeitsdegradation als Folge der zyklischen Dehnungen. Das entwickelte Programm ist u.a. zur Herleitung von Bemessungsregeln im Eurocode 8 und zur Überprüfung von Gebäuden unter vorgegebenen Akzellerogrammen benutzt worden.

SUMMARY

For the interpretation of the test results of cyclic tests that were conducted with beam-to-column-connections with different structural detailing, a numerical calculation method was developed that takes into account the composite action of the steel parts and the reinforced concrete parts as well as the local semirigidity of the joints. The method allows to simulate the non-linear behaviour of steel and composite structures with such beam-to-column-connections under time dependent monotonic or non-monotonic loading in the ultimate range and considers the stiffness and strength degradation due to cyclic straining. The program has been used for deriving design rules in Eurocode 8 and for the verification of buildings with given accelerograms.

RÉSUMÉ

Pour l'interprétation de résultats d'essais, obtenus lors des essais sur différents types d'assemblages poutre-poteau chargés cycliquement, une méthode de calcul a été développée saisissant numériquement l'effet combiné des poutres métalliques et du béton armé, ainsi que le comportement local des assemblages semi-rigides. Cette méthode permet la simulation du comportement non linéaire des structures métalliques et des constructions mixtes sous des charges monotones, cycliques et périodiques, au delà de la charge ultime prenant en compte la dégradation de la rigidité et de la résistance due aux élongations cycliques. Le logiciel a été utilisé pour la dérivation de règles de dimensionnement dans l'Eurocode 8 ainsi que pour la vérification de bâtiments soumis à des accélérogrammes donnés.

1. KURZE VORSTELLUNG DER VERSUCHE (ARBED-SRCS)

Um das Verhalten von Stahl- und Stahlverbundkonstruktionen in erdbebengefährdeten Gebieten sicher abschätzen zu können und um aus der Vielfalt möglicher Träger-Stützen-Verbindungen diejenigen auszuwählen, welche unter zyklischer Belastung hinsichtlich ihres duktilen Verhaltens die besten Eigenschaften aufweisen, wurden im Rahmen des ARBED-SRCS-Projektes eine Reihe verschiedener Träger-Stützen-Verbindungen untersucht, die ein günstiges Verhalten erwarten ließen.

Es wurden drei Versuchsserien durchgeführt (vgl. Bild 1), zunächst Untersuchungen an einzelnen Träger-Stützen-Verbindungen in Form von T-Verbindungen (Serie 1) und Kreuzverbindungen (Serie 2) und anschließend Versuche mit ausgewählten Träger-Stützen-Verbindungen an kompletten Rahmensystemen (Serie 3).

Variiert wurden bei den Versuchen außer den Anschlußausbildungen auch die Träger und Stützen, indem sie als reine Stahlträger oder Stahlverbundträger mit oder ohne Betonplatte ausgebildet wurden.

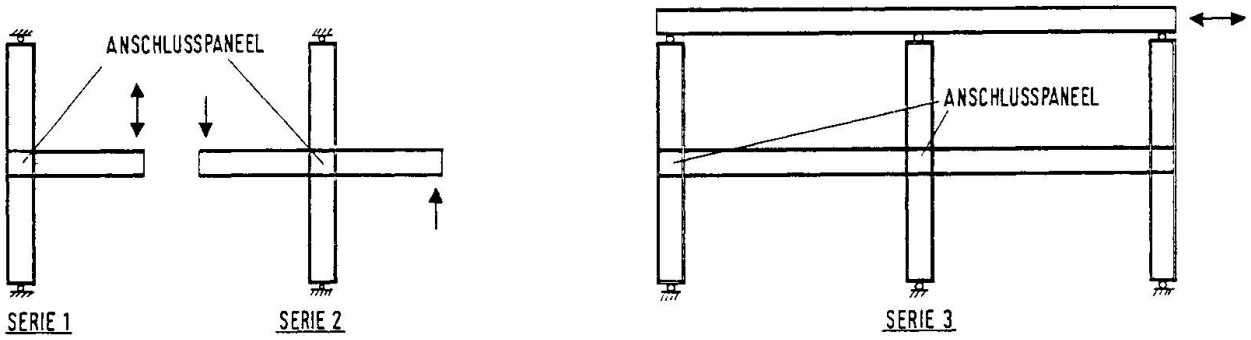

Bild 1 Versuchsserien des ARBED-SRCS-Programms mit Träger-Stützen-Verbindungen

Die Ergebnisse der Verformungshysteresen, die in Serie 1 und Serie 2 ermittelt wurden, siehe Bild 2, haben gezeigt, daß die Ausbildung eines plastischen Schubmechanismus im Anschlußpaneel von Träger und Stütze von maßgebendem Einfluß auf das Verformungs- und Dissipationsverhalten der untersuchten Konstruktionen war. Dieses Verhalten mußte bei der numerischen Simulation berücksichtigt werden (vgl. Abs. 2.3).

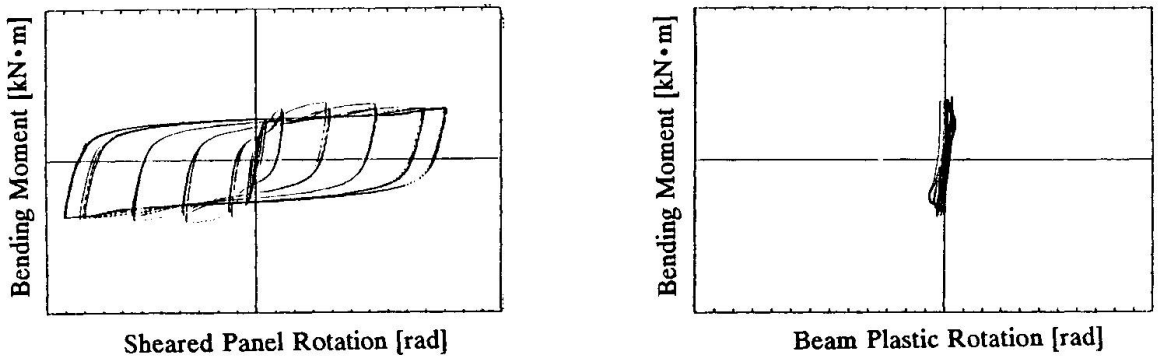

Bild 2 Momenten-Rotationskurven des Versuchs J3

2. ALLGEMEINES ZU DEM VERWENDETEN SIMULATIONSPROGRAMM

Als Simulationsprogramm wurde das an der RWTH Aachen entwickelte Programm PLANT [3] benutzt. Dieses ist ein räumliches Stabwerksprogramm, das zunächst für den Stahlbau entwickelt wurde und folgende Leistungsmerkmale aufweist:

- Berücksichtigung großer, räumlicher Verformungen und beliebig vorgegebener Werkstoffgesetze für monotone und zyklische Belastung [4,5]

- Erfassung beliebiger Momenten-Rotations-Kurven für die Träger-Stützen-Verbindungen [6,7]
- Berechnung mit monotoner Last- oder Verformungssteigerung für statische Fragestellungen
- Zeitverlaufsberechnungen für beliebig vorgegebene Akzellerogramme [8]
- Anwendbarkeit auf Stab-, Seil- und Trägerkonstruktionen

2.1 Berücksichtigung der Nichtlinearität

- Last-Verformungs-Zustände

Eine besonders effektive Berechnung wird durch die Verwendung des Verfahrens der orthogonalisierten Last-Verformungszustände [9] erreicht, bei dem die Steifigkeitsmatrix des Gesamtsystems nur am Anfang der Berechnung für den elastischen Ausgangszustand aufgestellt wird, um Last-Verformungszustände für die iterative Bestimmung der Gleichgewichtslagen zu generieren. Die Gleichgewichtslagen auf der nichtlinearen Last-Verformungskurve des Systems werden mittels der Orthogonalisierung dieser Last-Verformungs-Zustände iterativ ermittelt.

- Belastungsgeschichte

Bei auftretenden Plastizierungen der Querschnitte unter zyklischer oder dynamischer Belastung (z.B. Erdbeben) ist es notwendig, die Belastungsgeschichte zu erfassen. Es wurde ein Verfahren zur Integration der Spannungen zu Schnittgrößen entwickelt, das mit der geringstmöglichen Zahl von Integrationspunkten für die Spannungen im Querschnitt beginnt und bei komplizierter werdender Belastungsgeschichte zusätzliche Punkte auf den Eckpunkten des Spannungspolygons einsetzt und eventuell auch wieder löscht [8]. Damit ist erstens eine exakte Integration der Spannungen möglich und zweitens ist an jedem Querschnitt nur das benötigte Minimum an Integrationspunkten vorhanden (vgl. Bild 3).

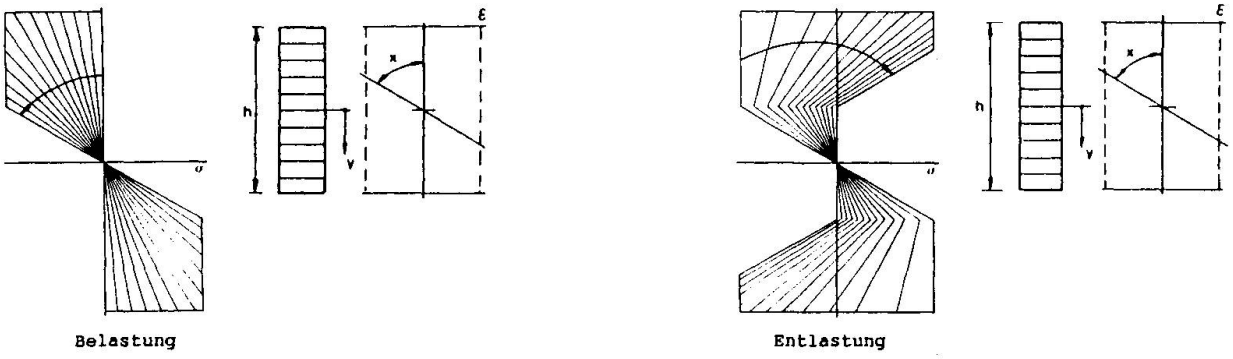

Bild 3 Berücksichtigung von Eigenspannungen und der Belastungsgeschichte

- Zeitschrittverfahren

Die Erweiterung der Berechnungsmöglichkeiten auf dynamische Belastung erfolgt in der Weise, daß die für die statische Belastung entwickelten Verfahren mit Hilfe der Newmarkschen Gleichungen in kleinen Zeitschritten angewendet werden.

2.2 Berechnungsmethoden

- Die Berechnung unter monotoner Last kann sowohl belastungs- als auch verformungsgesteuert durchgeführt werden. Die verformungsgesteuerte Berechnung ermöglicht, das Systemverhalten auch an der Traglast und im überkritischen Bereich zu simulieren.
- Zur Simulation von Low-Cycle-Fatigue-Versuchen, wie sie im Rahmen des SRCS-Projektes durchgeführt wurden, verfügt das Programm über die Möglichkeit einer verformungsgesteuerten zyklischen Berechnung.
- Das Verhalten von Systemen unter Erdbebenbelastung kann mit gegebenen Akzellerogrammen untersucht werden.

2.3 Werkstoffgesetze und mechanische Modelle

- Querschnittsbeschreibung

Der Querschnitt setzt sich aus dünnen, plattenartigen Lamellen zusammen, so daß die Spannungen genügend genau durch die Spannungen in der jeweiligen Lamellenachse beschrieben werden. Der Verlauf der Spannungen in einer Lamelle wird durch die Dehnungen der Lamellenendpunkte bestimmt und hängt von der Art des Materials ab, aus dem die Lamelle besteht und, wenn erforderlich, von der Belastungsgeschichte.

- Materialgesetze

Der Querschnitt kann sich aus folgenden Materialkomponenten zusammensetzen: Baustahl, Bewehrungsstahl und Beton.

Das Verhalten von Baustahl unter Druck- oder Zugspannung wird durch ein idealisiertes bilineares σ-ϵ-Gesetz beschrieben, in dem die Verfestigung des Stahls nach Erreichen der Fließgrenze berücksichtigt wird.

Die Bewehrungsstäbe werden im Druckbereich des Querschnittes mit ihrer wirklichen Querschnittfläche zusätzlich zum Betonanteil berücksichtigt. Im Bereich von Zugspannung wird die noch vorhandene Zugfestigkeit des Betons zwischen den Rissen durch den Ansatz einer vergrößerten ideellen Querschnittfläche des Betonstahls erfaßt.

Das Materialverhalten des Betons im Druckbereich wird durch eine Parabel 2. Grades abgebildet.

- Kennlinie mit Belastungsgeschichte und Schädigung

Die Erfassung und Abbildung komplexer Träger-Stützen-Verbindungen wird mittels vereinfachender Ersatzmodelle unter Verwendung von Stäben, die durch Normalkraftkennlinien beschrieben werden, ermöglicht [10] (vgl. Bild 4).

Für Berechnungen unter zyklischer Belastung wird die Belastungsgeschichte und die Schädigung [11] berücksichtigt. Mittels Variation verschiedener innerer Parameter ist es möglich, das aus Versuchen gewonnene Anschlußverhalten sehr genau abzubilden.

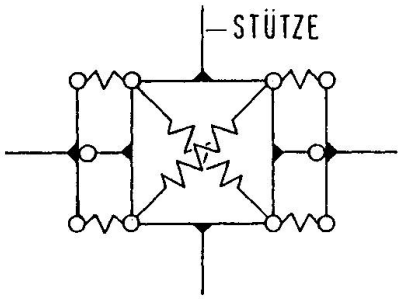

Bild 4 Modell der Träger-Stützenverbindung

Der plastische Schubmechanismus in den Anschlußpaneelen wird durch das in Bild 5 abgebildete Modell simuliert. Die Anpassung der Momenten-Rotationsbeziehungen des Mechanismus an die Versuchsergebnisse erfolgt durch die Vorgabe der Kennlinien der Diagonalstäbe in dem Anschlußpaneel.

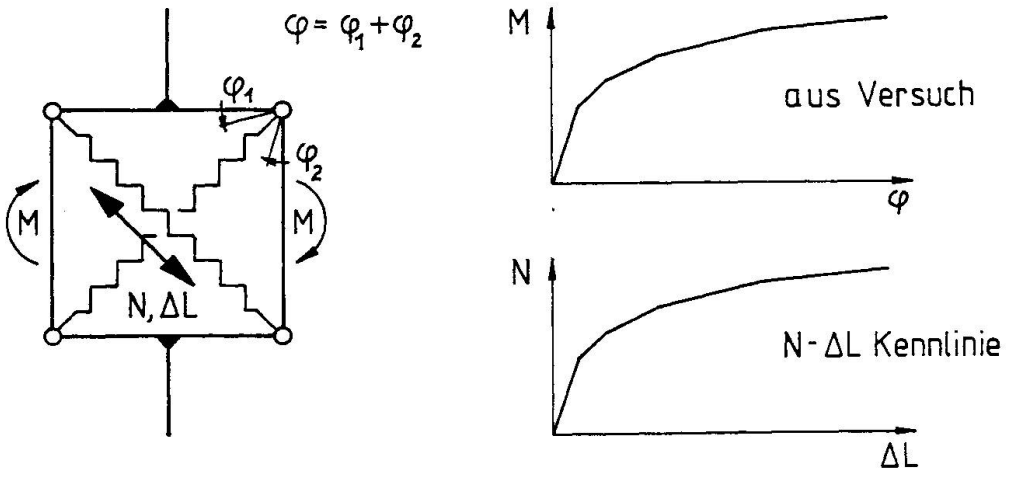

Bild 5 Modell für die Anschlußpaneele der Träger-Stützen-Verbindungen mit zugehöriger Kennlinie

3. BERECHNUNGSBEISPIELE

3.1 Rahmen, verformungsgesteuert

Der unten abgebildete Rahmen wird an der Universität in Lüttich auf das Verhalten unter zyklischer Belastung getestet. Die vorgestellte Berechnung stellt eine mögliche Prognose auf Grundlage der Versuche aus Serie 1 und Serie 2, wie sie zu erwarten sind, dar (Bild 6).

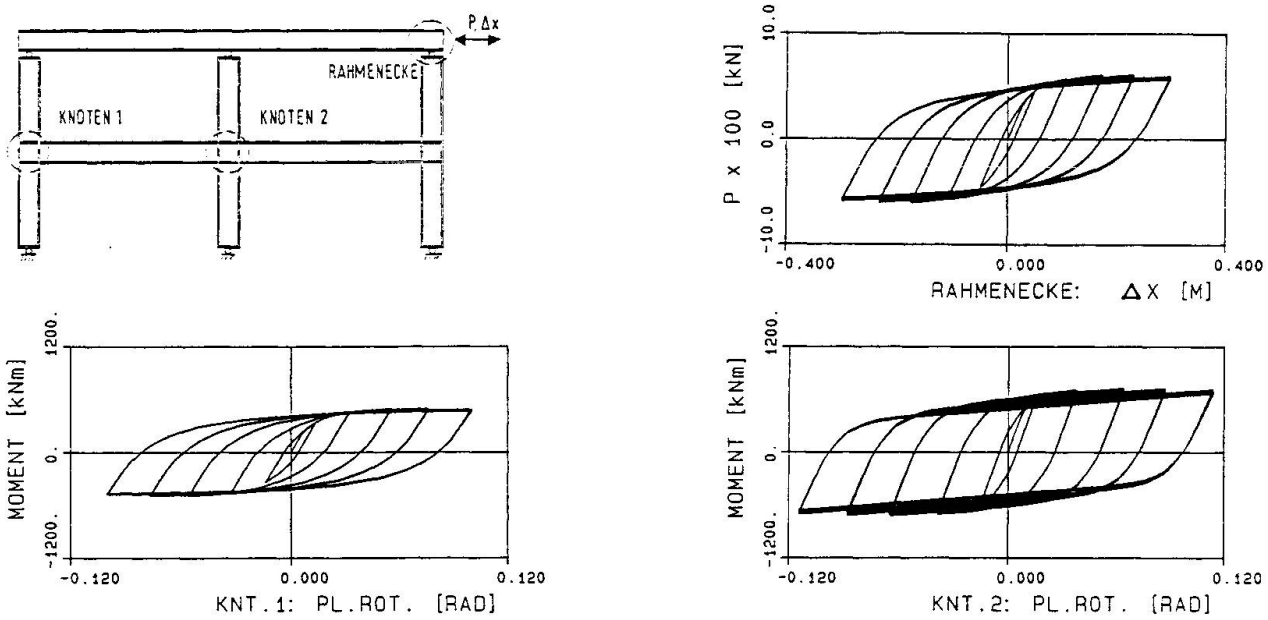

Bild 6 Ergebnisse der verformungsgesteuerten Berechnung

3.2 Rahmen unter Erdbebenbelastung

Es wurde das Verhalten eines fünfstöckigen Rahmens unter Einwirkung des El-Centro Erdbebens untersucht. Die Momenten-Rotationsbeziehungen der Träger-Stützen-Verbindungen wurden aus den Versuchsergebnissen entnommen (Bild 7).

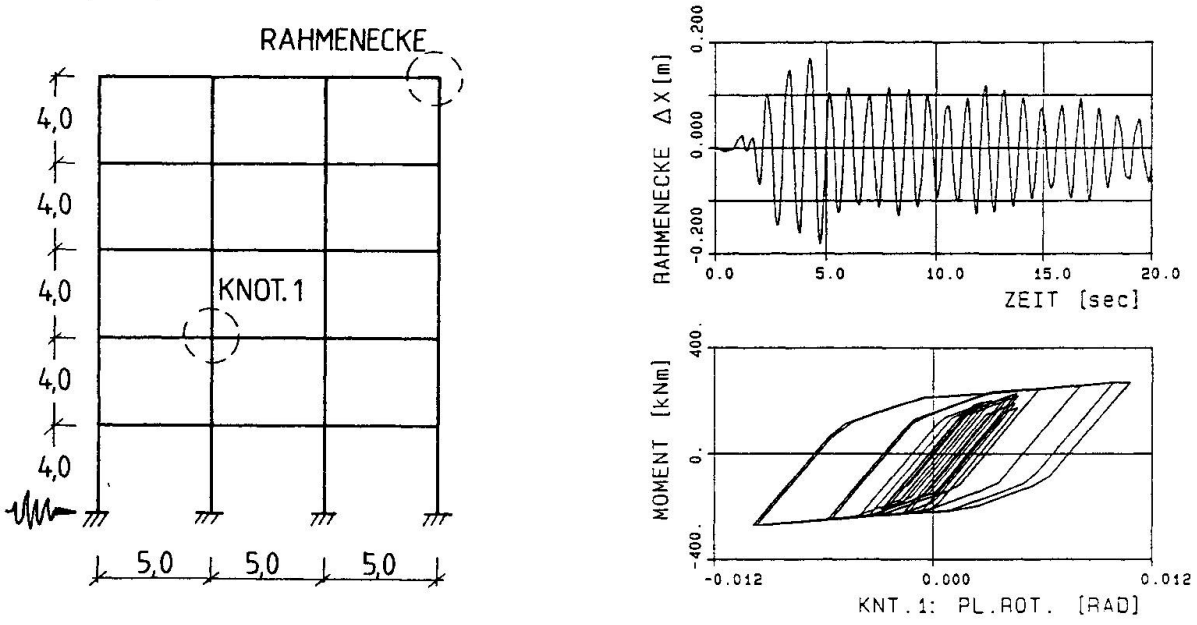

Bild 7 Ergebnisse der Berechnung unter Erdbebenlast

4. SCHLUSSFOLGERUNG

Es hat sich gezeigt, daß mit dem vorgestellten Simulationsprogramm die vorhandenen Versuchsergebnisse auf numerischem Wege sehr gut wiedergegeben werden können. Es ist damit möglich, das Verhalten komplexerer Strukturen, mit ähnlichen Anschlüssen, wie sie experimentell untersucht wurden, vorherzusagen. Außerdem lassen sich die Sicherheitsreserven solcher Strukturen unter Erdbebenlast zuverlässig abschätzen.

Anerkennung

Für die freundliche Übersendung von Unterlagen und Versuchsergebnissen des ARBED-SRCS-Projektes und die fruchtbaren Diskussionen sei der Firma ARBED, insbesondere Herrn Schleich und Herrn Pepin sowie den Herren Prof. Ballio, Prof. Bouwkamp, Prof Klingsch und Dr. Plumier herzlich gedankt.

Literatur

1. EGKS-Projekt Nº 7210-SA/506 - Seismic Resistance of Composite Structures

2. EUROCODE NR. 8, Bauten in Erdbebengebieten. Kommission der Europäischen Gemeinschaften, Ausgabe Mai 1988

3. LOPETEGUI J.; SALEH A.; STUZKI CH., Benutzerhandbuch zu PLANT. Aachen 1987

4. SEDLACEK G.; LOPETEGUI J.; SPANGEMACHER R.; STUTZKI CH., Nichtlineare Berechnungen von Stabwerken aus Stahl. Nichtlineare Berechnungen im konstruktiven Ingenieurbau; Springer-Verlag Berlin, Heidelberg, New York, Tokyo, 1989

5. SEDLACEK G.; LOPETEGUI J.; STUTZKI CH.; SALEH A., Ein Computerorientiertes Verfahren zur statischen Berechnung räumlicher Stabwerke unter Berücksichtigung nichtlinearer Effekte. Der Bauing. 60 (1985) 297-305.

6. STUTZKI CH; LOPETEGUI J.; SEDLACEK G., Semi-rigid Connections in Frames, Trusses and Grids. State of the Art Workshop: Connections and the Behaviour, Strength and Design of Steel Structures, Ecole Normal Superieur, Cachan-France, May 25-27. 1987

7. STUTZKI CH., Traglastberechnung räumlicher Stabwerke unter Berücksichtigung verformbarer Anschlüsse. Heft 3 der Schriftenreihe des Lehrstuhls für Stahlbau der RWTH Aachen, 1982

8. SEDLACEK G.; KOOK S.; KUCK J.; LOPETEGUI J.; NGUYEN B.T., Entwicklung eines Verfahrens zur Ermittlung der Bauwerksantwort räumlicher Stahlbauten auf Erdbeben. Nichtlineare Berechnungen im konstruktiven Ingenieurbau, Springer-Verlag Berlin Heidelberg New York Tokyo, 1989

9. LOPETEGUI J., Verfahren der orthogonalisierten Last-Verformungszustände zur Lösung nichtlinearer Probleme der Stabstatik. Heft 2 der Schriftenreihe des Lehrstuhls für Stahlbau der RWTH Aachen, 1983

10. TSCHEMMERNEGG F. et al., Rahmentragwerke in Stahl. Österreichischer Stahlbauverband (ÖSTV); Schweizerische Zentralstelle für Stahlbau (SZS), 1987

11. DORKA U.E., Ein Beitrag zur Beurteilung und vereinfachten Berechnung von Bauwerken unter Berücksichtigung der Hystereseevolution. Tech.-wiss. Mitteilungen des Instituts für konstruktiven Ingenieurbau, Ruhr-Univ. Bochum, Mitteilung Nr. 88-10

Composite Cable-Stayed Bridge: the Lumberjack's Candle

Pont mixte haubané de Lumberjack Candle

Die Schrägkabel-Verbundbrücke in Lumberjack's Candle

Esko JÄRVENPÄÄ
Techn.Lic.
Suunnittelukortes Oy
Oulu, Finland

Esko Järvenpää, born 1946, received his Civil Eng. and Techn. Lic. degree at the University of Oulu. He is technical manager of Suunnittelukortes Oy and is also responsible for the birdge design.

SUMMARY

This paper deals with the composite cable-stayed bridge design and construction procedure. The construction has followed the process defined in the design calculations. The standard calculation method seems to give reasonably good results for the behaviour of the bridge. The beauty of the bridge has caused a great deal of interest.

RÉSUMÉ

Cet article traite du projet, du calcul et de la construction d'un pont à haubans avec poutre mixte. Le procédé de construction a suivi les directives définies par les hypothèses de base. Les méthodes de calcul usuelles semblent donner des résultats suffisamment bons pour le comportement du pont. La beauté du pont a suscité un intérêt considérable.

ZUSAMMENFASSUNG

Es wird über den Entwurf, die Berechnung und den Bau einer Schrägkabelbrücke mit Verbundträgern berichtet. Der Bauvorgang folgte den Vorgaben der Entwurfsberechnung. Die üblichen Berechnungsmethoden scheinen ausreichend gute Ergebnisse für das Verhalten der Brücke zu geben. Die Schönheit der Brücke hat beträchliches Interesse geweckt.

A COMPOSITE CABLE STAYED BRIDGE, THE LUMBERJACK'S CANDLE

1.GENERAL

In Autumn 1989 at the Artic Circle town of Rovaniemi Finland's first cable stayed bridge for motor traffic was opened. The composite beam bridge has been, for many years, competitive compaired with concrete bridges. The reason has been the optimal construction timing between the cold winter period and the warm summer. The manufacturing of steel structures in Finland is also a highly automated industry.

The bridge design was selected as the result of the result of the invitation design competition. The aim was to provide an attractive bridge, which would enhance the image of Rovaniemi town. The bridge was not selected on the basis of the lowest price. The tender contract was for two deck alternatives. A concrete,prestresed box carried out by the incremental launching method and a composite box beam bridge. The contract itself was awarded on the basis of the lowest tender.

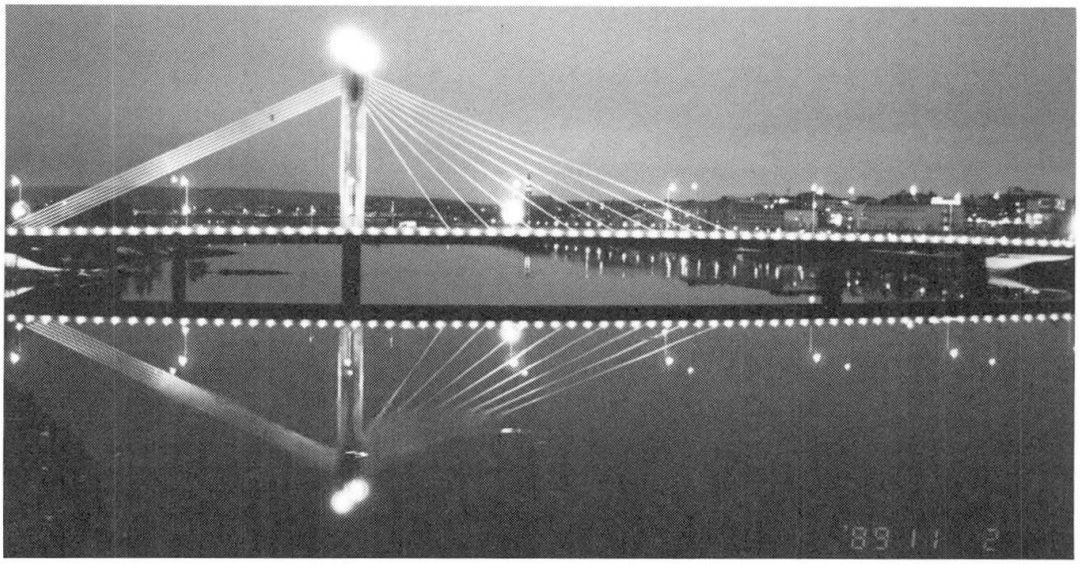

Picture 1. The bridge illuminated at night, complete reflection

2.EXTERNAL APPEARANCE

An assymetrical cable arrangement was selected for the bridge to balance the construction mass of the town and the high opposite bank. At the top of the pylon a "Lumberjack's Candle" was designed to symbolize the locking tradition. The pylon was split into twin round pillars, which are combined to one joint wall at the cable fixing position.

The subructures were designed to be narrow so that the river landscape, as seemed from the bank, would be as free as possible. The edge cantilevers of the bridge were supported with diagonal elements.

The edge beams of the bridge which have a side surface height of 700 mm were inclined. The inclined position lightenes the side surface. The bridge and its reflection in the water present an increadibly beautiful and impressive spectical.

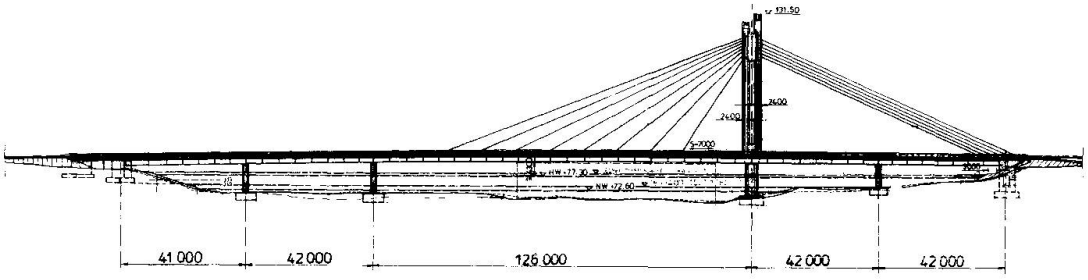

Picture 2. The Lumberjack's Candle

3. BRIDGE TECHNICAL DETAILS

The main span of the bridge is 126 m long and the side spans 42 m. The effective width of the bridge is 25,5 m. Box width is 8,8 m.

The cables are located along the center line of the bridge. At the main span the cables arranged in eight pairs with a fan shape. The back stay cables are arranged parallel and the cable group is formed of six cable pairs. The abutment operates as a counterweight due to its own mass and is not anchored to the rock bed. The deck structure is fixed to the abutment without bearings or expansion joints.

The diameter of the twin pillars of the pylon is 2,3 m and the free space width between the pylons is 1,5 m. The pylon pearcers the deck.

4. DESIGN OF COMPOSITE STRUCTURE

The bridge was designed so that the steel girders, without the deck slab, was launched over the river. Temporary auxilliary supports were constructed for the main span. During the construction phase, the bridge was a seven span beam bridge and each span length was 42 m

The bottom plate stiffners of the steel beam are trapetsidal in shape. The intermediate trusses are formed of tubular steel structures and are at intervals of about 5,6 m.

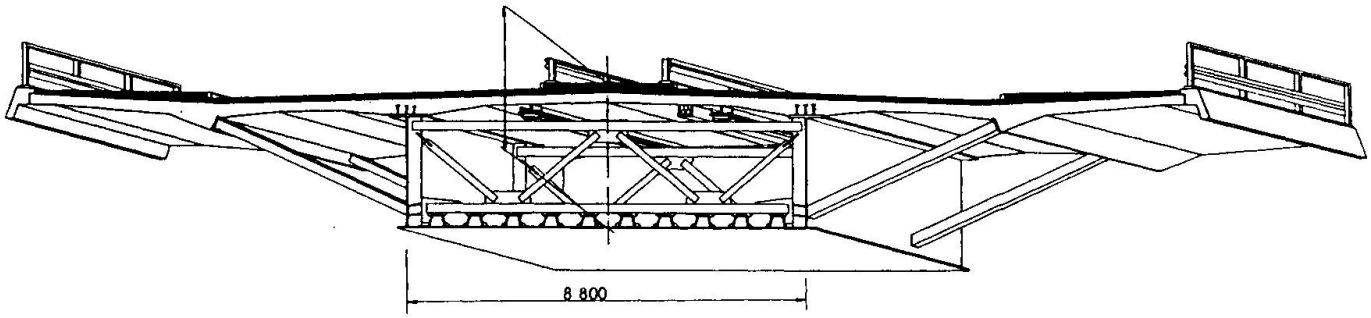

Picture 3. Cross sections of bridge

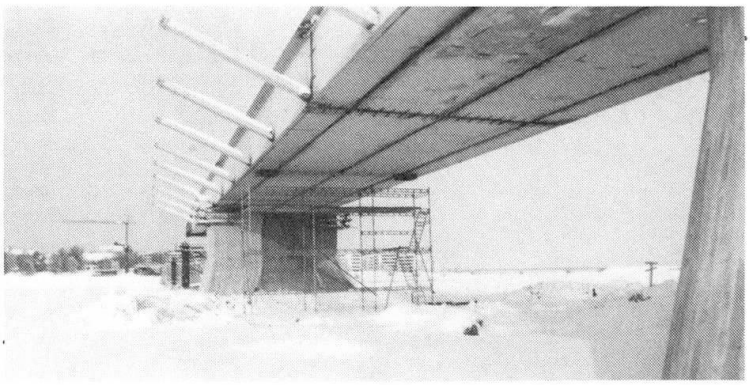

Picture 4. Launching work in progress

In the main direction the box was analyzed with a grid model describing the box structure. The torque loads were also analyzed in accordance with source /1/ to solve the truss forces.

The superposing of the stresses was done by following the various static phases of the structure. The following list describes the calculation chain in the main direction:

- A simple steel structure supported on auxilliary supports with a span interval of 7 x 42 m.
- Casting of the deck slab in sections, a total of 23 different structures supported on temporary supports. A separate computer programme was made for this casting stage which took into account shrinking and creep in accordance with source /2/.
- Calculation of the magnitudes of the stresses caused by post-tensioning in the longitudinal direction over the support areas.
- Removal of temporary supports and cable stressing. The magnitude of the forces in the cable stressing were calculated by bridecing the complete structure in reverse order to the cable stressing programme. Stressing was done in principle with two stressing cycles.
- The loading of the surface layers on the asymmetric cable structure.
- The fixing cast of the deck structure to the abutment and inclusion of the creep caused by this structural change.
- Calculation of traffic loads and other natural loads on the entire structural system.

5. DECK SLAB CONSTRUCTION AND DESIGN

In the structure an effort was made to have as cracked-free structure as possible. In the construction phase the schedule was also aimed at this.

The composite structure was casted so that in areas in which prestressing was not used in the longitudinal direction, the cast in the support region was done only after the middle span area had been casted. Thus it was necessary to move the forms frequency. This succeeded very well in the work arrangements. The area built in this way is that between the bridge cables. The compressive force from the cables caused a compressive force of about 60 MN on the composite structure. In the support areas outside the cable areas, prestressing in the longitudinal direction was used

to prevent cracking. Approximately 0,5 MN tendon units were used. Transversal prestressing in the deck slab was approximately 0,5 m intervals.

The superelevation of the steel structure was defined also in accordance with the development of the composite action according the casting order of the deck slab.

After the deck cast it could be confirmed that work had succeeded in producing almost totally uncracked concrete. No water ligide has been, up till now, observed in the deck slab.

Cracks were eliminated at the cable anchoring locations by distributing the anchoring horizontal force of the cable both trough the steel structure and concrete clab. Bult studs were used.

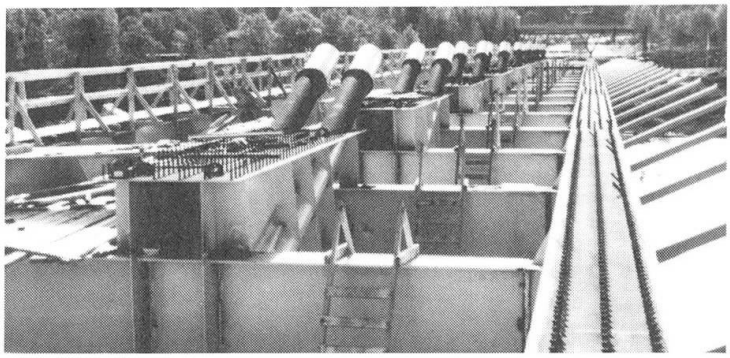

Picture 5. Cable anchoring structures, studs

6. CABLES AND PYLON

The cables were formed of unbonded, greased and coated strands. The anchoring area was injected with grease and other cable parts were injected with a cement grout. The cable grease was tested to ± 50 ^{o} C. The behaviour of the grease made it necessary to arrange separate expansion cylinders in the anchors due to the pressure changes caused by the changes in temperature /3/.

The cables were wrapped with white tape to minimize temperature differencies and make possible /4/. The lower regions of the cables were protected against mechanical damage by white painted steel tubes. At the head of the pylon there is the anchoring chamber designed as composite structure. The steel structure was analyzed as plate elements with a FEM programme.

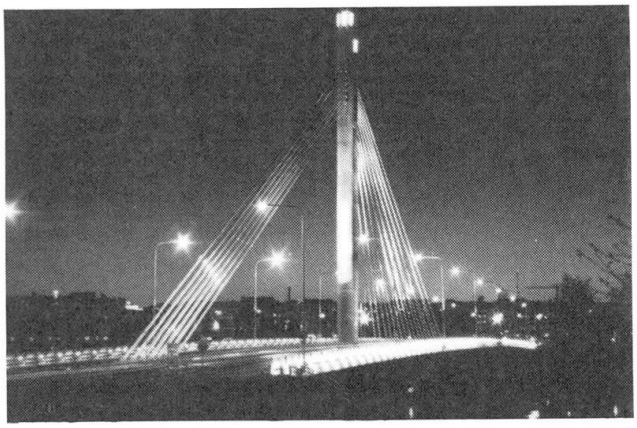

Picture 6. The tower and the cables

7. MEASUREMENT OF STRUCTURAL BEHAVIOUR

The behaviour of the structure was measured with trial loads in autumn 1989. The main interest was to confirm the difference between the calculated and actual magnitudes in the stiffness of the bridge both in bending and twisting and also in the dynamic behaviour.

In the design phase the lowest nominal frequency was achieved with a sideways movement of the pylon and cable system 0.45 Hz.

In longitudional bending the first frequency was 0.67 Hz. The same value was registred during tests. The displace of the girder during testloading was 45 mm and calculated value was 48 mm.

The position of the bridge deck in the completed bridge and the cable forces correspond well to the theoretically calculated values.

On the basis of this project, it can been assumed that the functioning of composite structures can be handled with normal calculation assumption for practical design.

/1/ ISOKSELA ERKKI:
Torsional moment in Thin-Walled Box Girder
(not publiced)

/2/ GHALI A. AND FAVRE R.
Concrete Structures: Stresses and deformations
1986 London

/3/ VSL INTERNATIONAL, BUERGI P. AND SCHNEITER T.
Method statement for the stay cable injection
1989

/4/ LEONHARDT FRITZ
Cable stayed bridges, FIB-congress 1986,
New delhi 16. February

/5/ WALTHER RENE
Ponts Haubanes
1985 Lausanne

Composite Bridges with Corrugated Steel Webs — Achievements and Prospects

Ponts mixtes à âmes plissées — Réalisations et perspectives

Brücken in Verbundbauweise mit Wellstahlstegen — Durchführungen und Perspektiven

Marcel CHEYREZY
Scientific Director
Campenon Bernard
Clichy, France

Jacques COMBAULT
Bridge Design Director
Campenon Bernard
Clichy, France

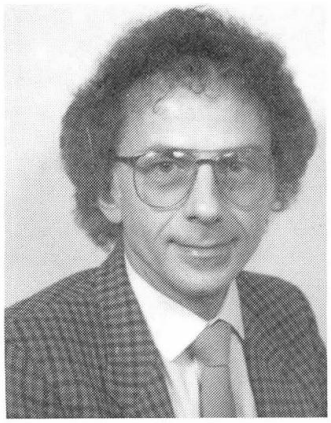

SUMMARY

This paper presents a description of the design studies and the projects that have led to the construction of composite bridge superstructures with corrugated steel webs. Bridges of this type already completed are briefly reviewed and the prospects for further development of this major innovation are discussed.

RÉSUMÉ

Le présent article fait le point sur les études et les travaux qui ont conduit à la réalisation de tabliers de ponts mixtes à âmes plissées. On rappelle quels sont les ouvrages de ce type déjà réalisés et quelles sont les perspectives de développement de cette innovation majeure.

ZUSAMMENFASSUNG

Dieser Artikel berichtet über den Stand der Studien und Arbeiten, die zur Konstruktion von Brückenträgern in Verbundbauweise mit Wellstahlstegen führten. Es werden bereits ausgeführte Brücken dieser Art angesprochen und die Entwicklungsperspektiven dieser bedeutenden Innovation erörtert.

I - INTRODUCTION

More than ten years ago Pierre Thivans (CAMPENON BERNARD) thought to use webs made of corrugated steel plates for prestressed concrete bridge superstructures with box girdered cross sections. After considerable theoritical analysis and model testing several bridges using corrugated webs have been constructed. Through the experience acquired the field of competitivity of corrugated webs has been investigated and more clearly defined.

II - PRINCIPAL ADVANTAGES OF CORRUGATED STEEL WEBS

Corrugated steel webs have been used for prestressed composite bridges with upper and lower slabs in concrete, as well as for conventional composite bridges with steel bottom flanges. Consequently their advantages have to be evaluated either using concrete webs or using flat steel webs with traditional stiffeners.

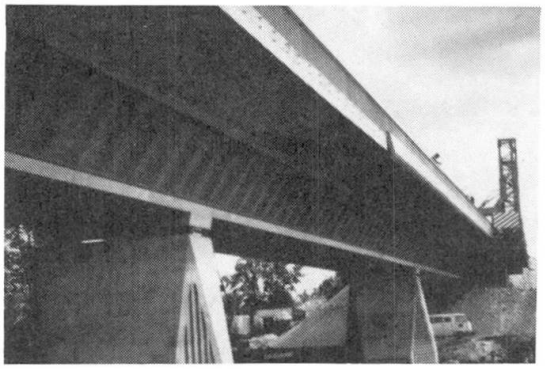

Fig 1 : Cognac Bridge

Compared to concrete webs, the advantages of corrugated steel webs are :

- *Self weight is decreased* thus allowing a lengthening of the feasable maximum span length and savings on piers when they are founded on poor soil or when earthquake is a design criterion.
- *The right material is at the right place* ie concrete to sustain bending moments and steel to carry shear.
- *The elastic lever arm is increased* to its maximum value .
- *The difficulties linked with the casting of deep concrete webs are avoided.*
- *Construction equipment is simplified.* For instance, in segmental construction, the weight of freshly poured concrete for bottom and top slabs can be supported by the already placed web element.
- *Construction pace is faster.* For instance in segmental construction, the cast-in-place box element is approximately three times longer.

Compared to plane steel webs the advantages of corrugated webs are :

- *An important decrease of the web thickness.*
- *Elimination of all the web stiffeners.*
- *Reduction in the number of intermediate diaphragms.* Transverse loads, due to wind pressure for instance, are directly transmitted to the top slab owing to the high inertia of the webs.
- *A much lower sensitivity to premature buckling* because of geometrical defects.
- *Longitudinal prestressing forces are not dissipated into the webs.*
- *Incremental launching of composite bridge deck is possible.*
- *Steel top flanges are considerably reduced.*
- *Three dimensional flexibility* facilitates the construction of curved bridges, it also makes tight tolerances unnecessary for assembling web panels.

III - MAIN PROPERTIES OF CORRUGATED WEBS

A considerable research program has been accomplished since 1980. It has included theoritical analysis, computer analysis and model testing. Part of this program has been sponsored by French Authorities : MRT, ANVAR ,SETRA and LCPC. The outcome of this research work has been that in many respects girders with a corrugated web behave like tradionnal composite structures with orthotropic plates. However the three following specific behaviours have been identified and analysed :

- *Diffusion of concentrated forces* (for instance vertical reaction at an intermediate support of a continuous girder).
  In order to render compatible strains in the steel web and in the concrete slabs , local bending appears in the top and bottom slabs together with vertical forces applying at the slab to web connections.
- *Torsional behaviour* [Ref.1]
  The lack of longitudinal stiffness of corrugated webs induces a torsional behaviour quite different to that observed in traditional box girders (concrete or composite). An external torsional bending moment applied to a box girder with corrugated webs generates horizontal transverse forces applying in one direction to the top slab and in the opposite direction to the bottom slab. Practical effets are the appearance of in-plane bending moment in the slabs, and additionnal torsional shear stress in the webs.
- *Buckling under shear stress* [Ref.3]
  Most of the advantage in corrugated webs comes from their excellent buckling behaviour.
  It is easy to obtain high safety coefficients against buckling at negligible extra costs by increasing the amplitudes of the folds. However for deep webs it has been necessary to investigate buckling conditions more thoroughly.
  The different buckling modes have been identified by computer analysis. Knowing the mode shapes it has been possible to develop analytical formulas giving the critical shear stress for each mode. Finally, tests performed on corrugated panels gave results in agreement with the theoritical analyses.
  Three different types of buckling modes have been identified and calculated :

. the *local buckling* mode corresponding to the stability of a steel strip simply supported between two folds.
. the *intermediate buckling mode* characterised by a sudden snap and a non-reversible steel plastification along the folds.
. the *general buckling mode* similar to the one observed in an orthotropic plane plate .

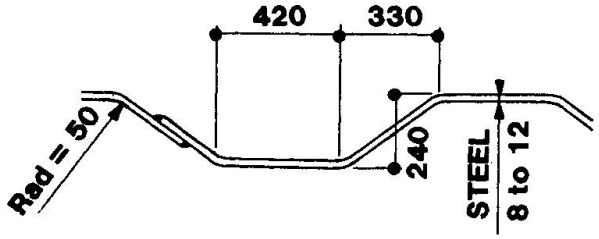

Fig 2 : Typical cross section of corrugated web

IV - EXAMPLES OF BRIDGES WITH CORRUGATED WEBS (Fig.5)

Three bridges with corrugated webs, all designed according different concepts, have been completed. Two others are at the preliminary design stage. A brief description of these projects is given hereunder :

Completed bridges

- Cognac bridge (Fig.1).
The bridge deck is a composite trapezoidal box girder. The longitudinal prestressing external to the concrete is deviated at the diaphragms. The concrete upper and lower slabs have been cast in place on falsework.

- Maupré viaduct at Charolles.
The bridge deck is a triangular box girder. The corrugated webs, which slope at 45°, are welded on a steel tube acting as a bottom flange. This tube is grouted with concrete. Longitudinal prestressing tendons are external to concrete.
The construction method was by incremental launching.

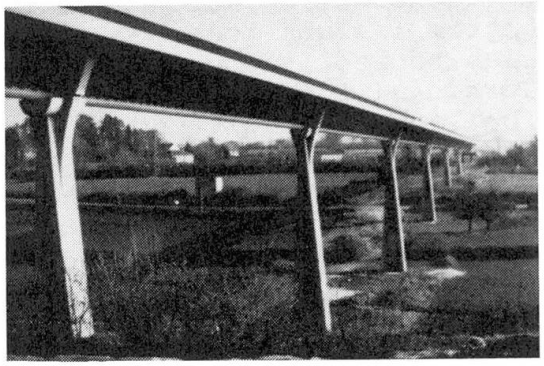

Fig.3 : Maupré Viaduct

- Asterix bridge.

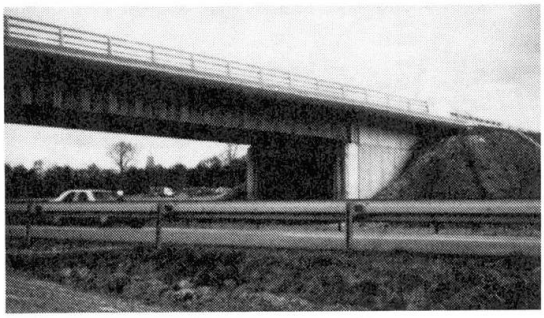

Fig 4 : Asterix Bridge.

The upper slab is stiffened by prestressed transverse girders. The corrugated webs are vertical. Bottom flanges are traditional steel plates. There is no intermediate diaphragm or bracing. The bridge was constructed at the abutment and launched accross the freeway. There was no welding done in situ.

Proposed Bridges

- Tronko bridge - Norway.
The bridge will have two cantilevered side spans with longitudinal prestressing in the top slab, and a simply supported central span. The corrugated steel webs, variable in depths, will be welded on steel bottom flanges. The three spans will be prefabricated. They will be put in place with a large size marine crane. The only works to be done in situ are the casting of the concrete counterweights and the second phase prestressing.

- Caracas bridge - Venezuela.
The bridge will be a composite trapezoidal box girder with a variable depth. The upper slab will bear upon prestressed transverse girders. Longitudinal prestressing will be external to the concrete.
The construction method will be the cast-in-place cantilever method. The bridge is designed against earthquake.

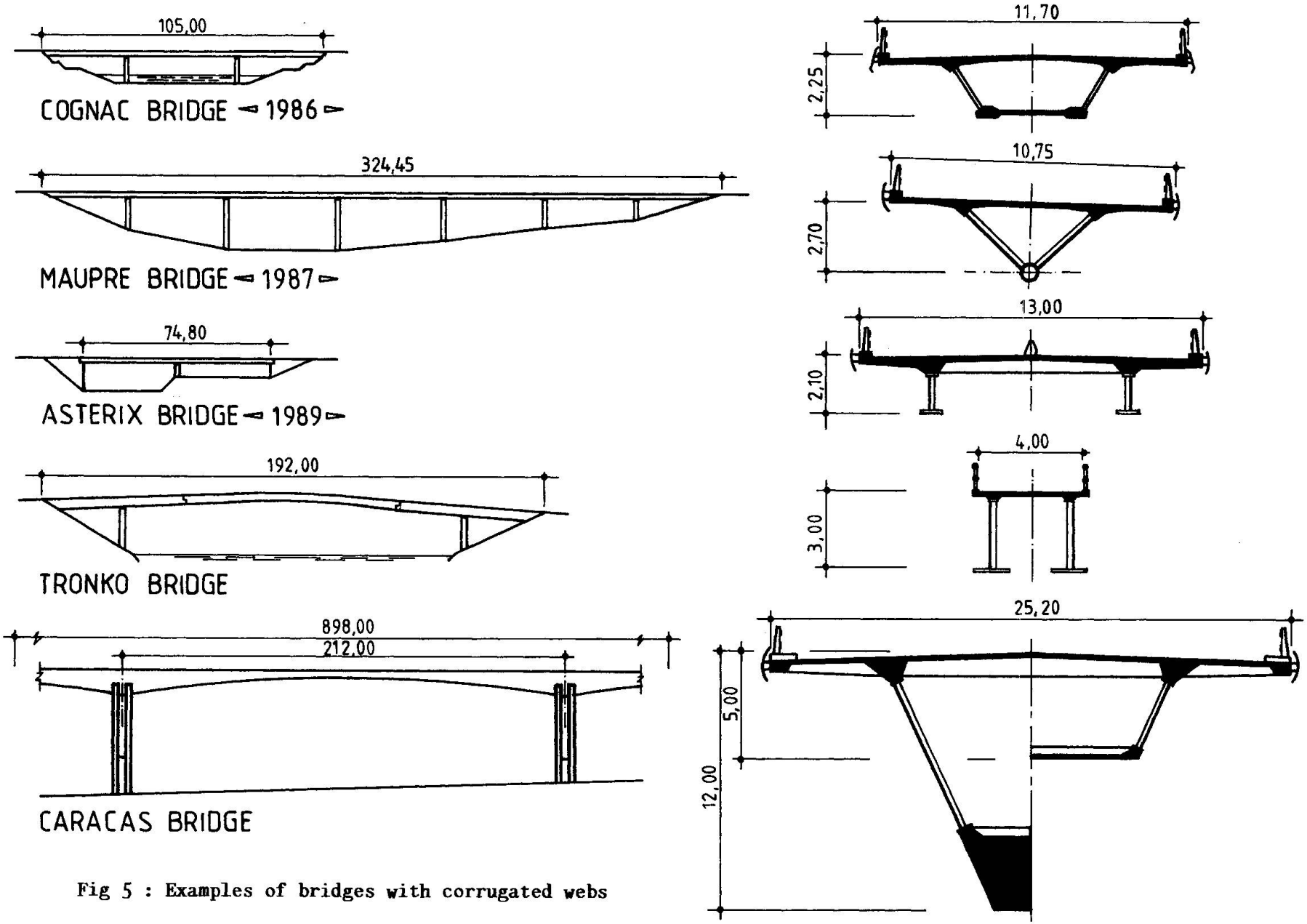

Fig 5 : Examples of bridges with corrugated webs

V - CONCLUSION

The three bridges now opened to trafic were built without any major technical problem, they have been successfully tested and they give full satisfaction to the Owners.

Technical problems regarding design and construction have been overcome and from now on, the change from a conventional design to a corrugated web design should no longer be considered a risky operation.

Concerning the competitivity of such a technique one must consider several aspects : construction cost, construction time, maintenance, aesthetics etc...It seems that two types of corrugated web bridges can successfully compete with traditional designs.

Caracas bridge gives a good illustration of the first type. That is, a bridge with a very long main span, a minimum number of spans and a wide deck. Existence of seismic loads and poor soil conditions for the pier foundations are also factors treated more favorably.

Asterix bridge and Tronko bridge illustrate the other type of competitive solutions for corrugated webs. These are composite bridges with steel lower flanges. For continuous spans the deck may be prestressed. Welding on site must be limited to a minimum. This can be obtained by launching the bridge or by setting it up with heavy handling equipment.

VI BIBLIOGRAPHY

1- Journée d'étude AFPC-ITBTP -CESDA du 28 novembre 1985 : Innovation dans le domaine des structures mixtes. M. VIRLOGEUX, P. THIVANS, B. GODART, J.A CALGARO, M. CHEYREZY, J.COMBAULT, G. CAUSSE - Annales de l'ITBTP - Octobre et Novembre 1987.

2 - IABSE symposium Paris-Versailles - September 2-4, 1987 - Maupré Viaduct near Charolles - G. CAUSSE, M. DUVIARD.

3 - 3ème colloque Génie Civil et Recherche Paris - Juin 1987 - Ponts mixtes - Analyse des conditions de flambage des âmes plissées - M. CHEYREZY

4 - AISC 1988 National Steel Construction Conference - Miami Beach - Florida
The Maupré Viaduct near Charolles - France - J. COMBAULT.

5 - Journées d'études AFPC - ITBTP des 15 et 22 mars 1989 : Le pont d'Asterix, M. CHEYREZY, M. GUICHARD, B. LECROQ, D. DUVAUT.

Rehabilitation of the Beauharnois Suspension Bridge

Remise en état du pont suspendu de Beauharnois

Instandsetzung der Hängerbrücke von Beauharnois

Yvon D.J. DELISLE
Head of Struct. Dep.
DESSAU Inc.
Laval, PQ, Canada

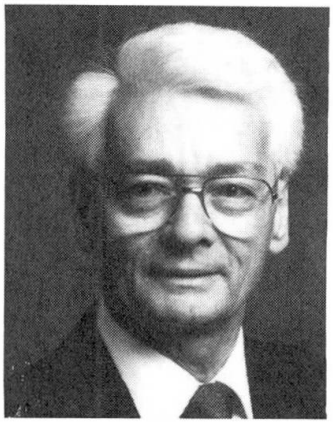

Graduate Civil Engineer McGill 1956 (Montreal), 16 years bridge engineer with local construction and consulting firms, in private practice for 15 years and partner in DESSAU since 1988.

SUMMARY

Under certain constraints, the rehabilitation of a structure may leave the Engineer with no alternative but to resort to rarely-used mixed repair techniques. Provided that a thorough scrutiny of the whole design procedure is conducted, the born-again structure may become a perfectly safe and viable solution. Not only will the exercise always be beneficial to the designer but such a structure will often provide unexpected additional bonuses.

RÉSUMÉ

En raison de certaines contraintes, la remise en état d'une structure force souvent l'ingénieur à recourir à des principes structuraux mixtes, peu usuels. La remise en question de chaque phase de la conception et de chaque détail de construction s'impose pour que la viabilité et la sécurité de l'ouvrage soient assurées. Non seulement l'exercice est-il enrichissant pour le concepteur mais le résultat technique offre souvent pour l'ouvrage, des avantages additionnels inattendus.

ZUSAMMENFASSUNG

In gewissen Zwangslagen muss der Ingenieur bei der Instandsetzung von Brückenbauten auf verschiedene selten benützte Verfahren zurückgreifen. Bei äusserst genauer Überprüfung jeder Konstruktionphase und jedes technischen Details kann die Widerstandsfähigkeit und Sicherheit des erneuerten Bauwerks garantiert werden. Diese Aufgabe stellt für den Konstruktionsingenieur nicht nur eine bereichernde Erfahrung dar, das technische Resultat selbst kann auch oft unerwartete Vorteile bringen.

1. INTRODUCTION

Ladies and gentlemen, I am pleased to report this experience in the rehabilitation of a bridge. As happens in most projects, one element often becomes a determining factor in the solution that is to be chosen. Here, had a larger amount of reinforcement or all of the suspension cables required replacement, then a totally different approach would have had to be adopted, leading to certain increases in costs and in delays.

The Beauharnois suspension bridge spans one of the numerous spillways of the HYDRO-QUEBEC power plant, which is located on the St. Lawrence river, 40 km South-West of Montreal. This facility is a modest 2-lane, 177 m conventional suspended structure. The deck is composed of 2 built-up I-beam stiffening girders, supporting transverse floor beams and longitudinal stringers. The roadway is concrete-filled grating, with an asphalt overlay.

Designed and built by a local bridge construction company in 1947, the bridge structure was submitted to ever increasing heavy traffic loading and to chemical attack by polluted air and generous salt sprayings over the roadway during periods of up to 6 months, every year. As all too often, insufficient maintenance budgets allowed the structure to deteriorate - in spite of some occasional strengthening efforts -, to a point where in 1987, traffic had to be reduced to one lane only and lower speed limits had to be posted.

2. INVESTIGATIONS

A number of condition surveys had shown the extent of the deterioration that prevailed and recommendations were made that appropriate corrective measures be taken to prevent further damage or to allow a protentially dangerous situation to develop. DESSAU was mandated to draw up complete rehabilitation documents, based on retrofitting the suspension system and on replacing the entire deck structure, while the original foundations and anchor blocks should remain.

The main cables had already suffered some corrosion and a number of wires were known to be broken. Thus, the main load-carrying members were in a deficient condition. Additionally, recent highway codes were calling for higher truck loadings, so that coming up with a solution to compensate for an overall cable deficit estimated to be about 20%, could prove to be quite difficult.

The road profile was to be maintained and the existing suspenders were to be reused, as required by the Client. Various deck configurations were analysed and checked for stiffness, weight and cost. The increased live loads led to larger deck weights and therefore, to still larger cable strenght deficits.

3. SOLUTION

For a viable solution to be implemented, major changes had to be considered. The task was to find a way to increase the carring capacity of the catenary cables and at the same time, to provide a deck that is stronger and lighter.

DECK STRUCTURE: it is well known that a torsionally rigid ORTHOTROPIC deck can be designed to be both stronger and lighter than conventional structures. By adding extensions to the suspenders, the entire structure could then be built under the deck level, allowing full torsion capacity to be developed. Still, the stiffening trusses had to be made more resistant to satisfy the controlling quarter-point moments.

SUSPENSION SYSTEM: no ready-made example could be found, despite a long search through printed records and theoretical publications on suspension bridges. Supplementing catenary cable deficit by the addition of diagonal cable stays seemed to provide a logical solution, but to our knowledge, the two systems have not been used on the same structure on many occasions. Very few accounts of actual applications were available to provide guidelines.

Numerous computer runs where all indicative of the perfect compatibility of the two systems applied to the same structure. Therefore, diagonal stays were dimensioned to compensate for the load-carrying deficit that was found in the catenary cables.

Since the two systems were found to behave similarly, not much horizontal resistance could be developed to reduce cable-to-deck displacements, which occur under unbalanced loadings. The critical quarter-point moments were not substantially reduced either. If anything could be done to reduce the large reversals of stress and geometry in the main cables, at the clamp level, it would help in preventing the condition of distress that was found to exist at that location, to develop further.

HORIZONTAL ANCHOR: by transferring the longitudinal force, which is generated by unbalanced loading on the bridge, directly into the abutment instead of into the main cables, an attempt was made to eliminate the mid-span cable clamp. This might be possible because of shallow foundations which are resting on competent bedrock. Indeed, this single feature would achieve more than expected. The reduction in the horizontal displacements between the deck and the cables allows dispensing completely with the mid-span deck-to-cable clamp. Moreover, calculations show a considerable reduction in the quarter-points moments.

Thus, the overall solution to the deficient suspension system was possible by providing à TORSIONALLY RIGID ORTHOTROPIC DECK, by incorporating DIAGONAL CABLE STAYS and by ANCHORING the deck to the foundation at one end of the bridge. These three features also favor greater lateral distribution of eccentric loads, thereby reducing values in the design moments and forces. Very real reductions in the weight of structural steel were possible, which in turn, further reduced cable reinforcement requirements.

4. DESIGN CONSIDERATIONS

After a feasible solution was found, the creation of a mathematical model was undertaken. The sizing of the diagonal cables was done by basic, preliminary calculations - the cables having been assumed to carry about 15% of the total uniform loads -. A house-developed computer program was used, first, to calculate stresses and moments in a two-dimension beam-elements model. The same program was used to treat a two-dimension truss-elements model and, finally to analyse the far more complicated three-dimension truss-elements structure.

Envelopes for stresses were generated for each individual member, by developing influence lines to determine the exact maximum loading conditions, and then by running a complete computer analysis to determine the resulting loads in the member under observation. The model was then revised according to the final construction details and, new computer runs where made to verify that the maximum stresses were not exceeded.

For fatigue evaluations, the magnitude of stress reversals needed to be evaluated. The Canadian National Building Code sets very rigid rules to determine the maximum allowable stresses in welded bridges. For the expected life of this structure,the 500 000 cycle category was used.

5. CONSTRUCTION

In the summer of 1988, rehabilitation work was undertaken by the owner, on the concrete anchor blocks, where drilled anchors and surface treatment has been specified, as part of the program.

Rehabilitation of the catenary cables started in the fall of the same year, by THE JANIN CONSTRUCTION COMPANY, with the assistance of STEINMAN of New York.

Fabrication of the steel deck structure was sub-contracted to LES ATELIERS PONCIN of Belgium who provided top notch workmanship, in complete agreement the very demanding specification clauses. SECO of Brussels, lent assistance with Quality Assurance in shop practices.

LES LABORATOIRES VILLE MARIE (DESSAU-owned), conducted all shop and field inspections for the project.

Welded sub-assemblies of deck and truss components were prepared in Belgium and shipped to the Beauharnois dock site. Larger, full-width assemblies, corresponding to bridge sections between field splices, were erected on a construction barge, and then floated into position. The first section was raised on June 15th 1989. As each section of the old bridge was dimantled and towed to shore heading for the scrap yard, its newly-assembled replacement was erected in the vacant space. Working progressively from the center of the river towards the abutments, nine such sections were floated in, raised on hydraulic jacks and connected to the existing bridge suspenders.

The Contractor, under the very able guidance provided by its own Consultant, managed to pre-measure all suspender links and to erect the whole bridge to a near-perfect match of the theoretically specified geometry. The results were excellent considering that the old bridge showed all kinds of imperfections, ranging from uneven oblique towers, erratic cable profiles, a twisting distorted road deck, etc. After all sections of the bridge had been erected and assembled into a rigid continuous structure, the cable stays were tensioned to pre-set values which were adjusted to the prevailing temperature.

With less than half of the underside of the bridge left without its final coat of paint, the job was stopped in November 1989, to be completed in the following spring.

OWNER and CONSULTANT were proud to point out that the completed bridge was opened to traffic, in October 1989, as scheduled.

6. NOTICE

This paper (conference) is presented for information and discussion purposes only and its content should not be construed as giving guidance for application to any other structure, without express written consent.

Innovative Method Concrete Arch Construction

Méthode innovatrice de construction d'un arc en béton

Neuartige Baumethode für Stahlbetonbögen

Yasushi SATO
Chief Engineer
Niigata Prefectural Office
Niigata, Japan

Ryuichiro TOHYAMA
Chief Civil Engineer
P.S. Concrete Co. Ltd
Tokyo, Japan

Introduction

The "CLCA method"--a new method of construction for arch bridges, was developed in Japan. In this method the steel and concrete composite column structure is applied to the arch rib construction. CLCA stands for Concrete Lapping method with pre-erected Composite Arch.

The common feature of the method presented can be summerized as following:

* Using the steel tube, the equipment required for erection is light, simple, and economical.
* Filling concrete in the tubes at the early stage of construction, the tubes become very rigid arch components and it is very effective for safety during construction and have many merits for wind force, earthquake and accuracy of dimension.

From the cost of Joushi bridge by this method, the total cost can be predicted to fall within 90% of other methods (such as centre or Melan), making steel weight about 1/2 - 1/3 of them.

This method is useful for the arch bridges of 50m to 150m span.

Brief Description of Arch Construction

Fig.1 shows the construction sequence of concrete arch bridges by CLCA method.

1. After construction of abutment, the steel tubes are assembled in vertical direction and then tubes are lowered and connected in arch axis.
2. Steel tubes are concreted and then arch rib is concreted by form travellers from each springings.
3. Piers and superstructure are completed.

Fig.2 show the dimensions of Joushi bridge constructed by this methods, and Table-1 shows the design load of Joushi bridge.

Table-1 Design Load

		In service	Under construction
Live load		TL-20	
Snow load		100kg/m²	
Shrinkage		15×10^{-5}	
Support movement	Horizontal Vertical	5mm 3mm	
Temperature change	Arch rib Slab girder Steel tube	±10℃ ±15℃	±10℃ ±30℃
Wind load		55m/s	25m/s
Seismic coefficient	In plane Out of plane	0.15 0.15	0.1 0.1
Traveller weight	Traveller Form		25t 15t
Lateral pressure of conc.			ACI standard
Tolerance of axial line		±5cm	

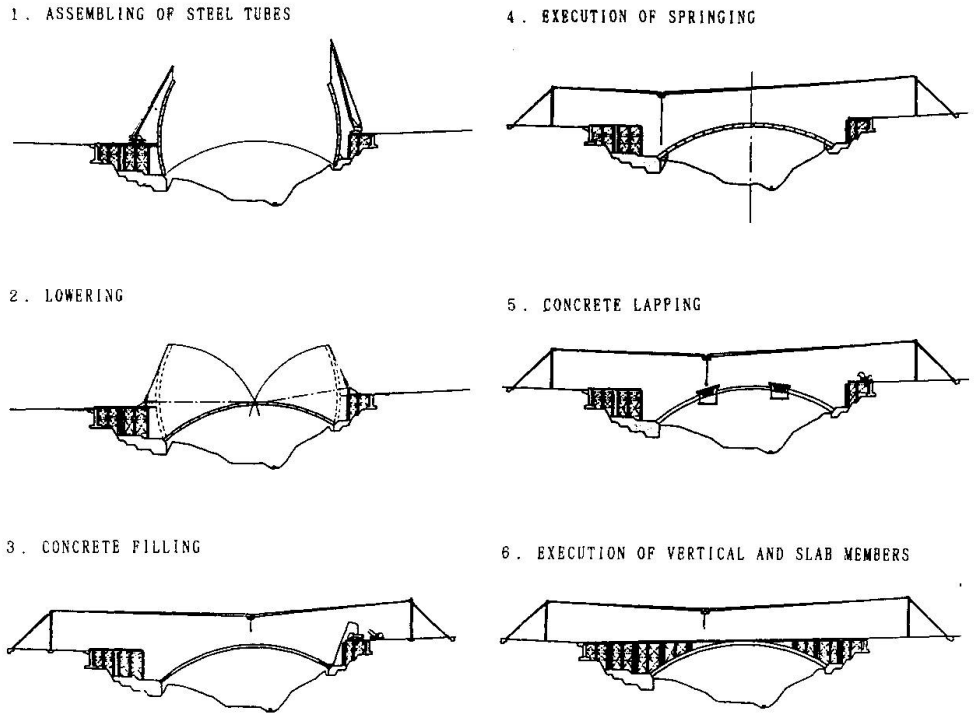

Fig.1 Construction Sequence of CLCA method

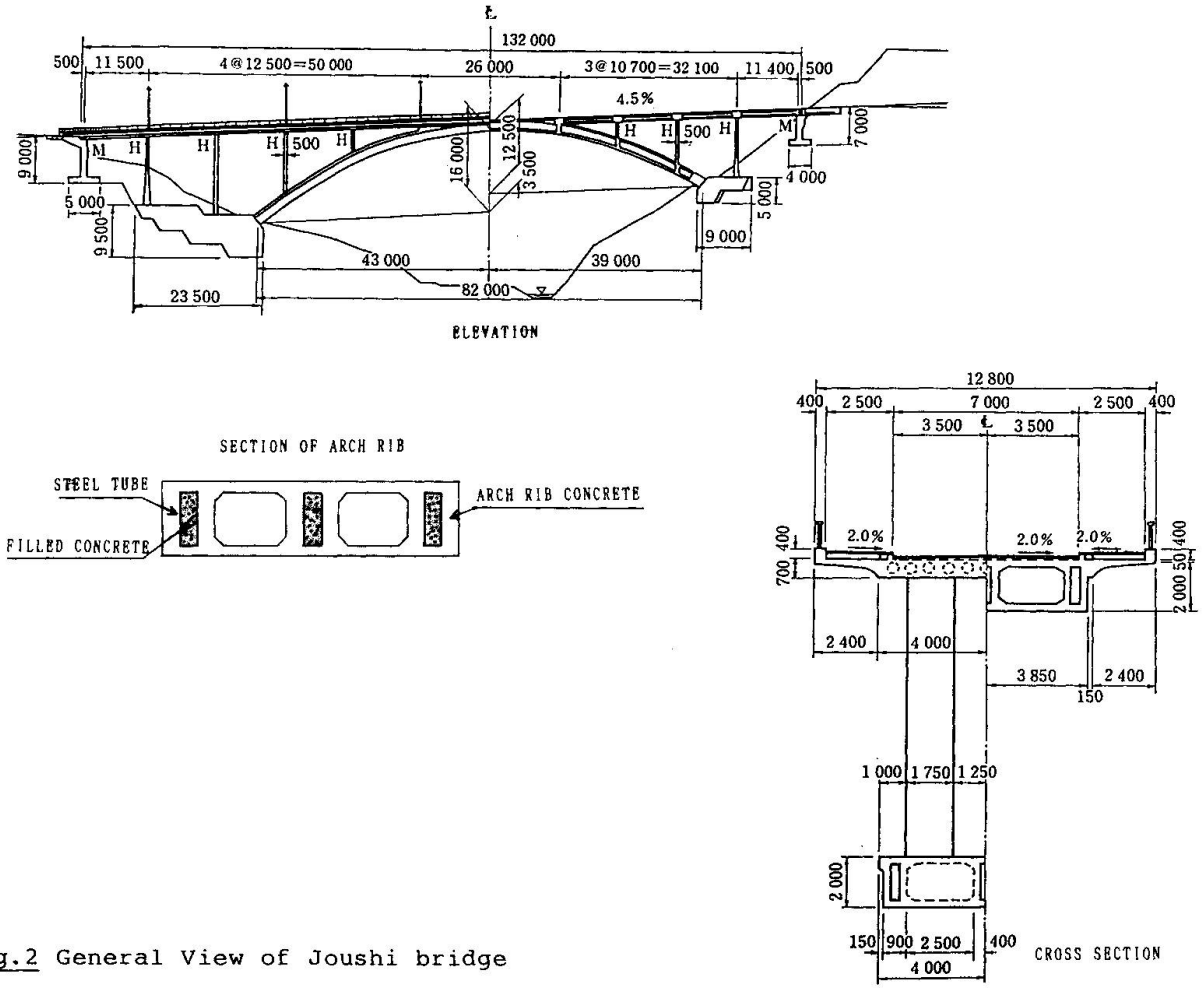

Fig.2 General View of Joushi bridge

Design of Large Span Composite Floor

Dimensionnement d'un plancher mixte de grande portée

Bemessung von Verbunddecken grosser Spannweite

Fa-Kun YAO
Researcher
Guanzhou Inst.
Guanzhou, China

INTRODUCTION

The large span composite floor is a composite space truss structure which steel upper chords are replaced with r.c. rib-slab. It's a space structure that the members act as a whole with the beams and the slabs throgh appropriate connections. It could make the most of the mechanical properties of the two materials and could strengthen whole rigidity of the structure. In China built several multistory and tall buildings and the results are very satisfied. Those are the Changsha Texile Building (column distance 12m, Fig. 1) and the Xinxiang Department Store (span 35m, Fig. 2) and the Rehearsal Hall of Changsha Opear and Dance Drame House (span 21m, Fig. 3) etc.

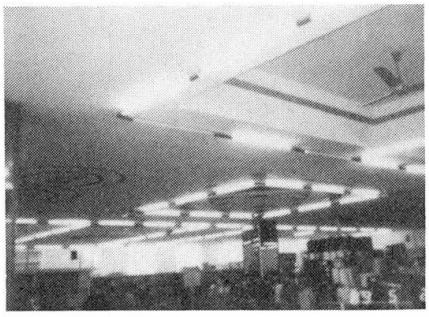

Fig. 1

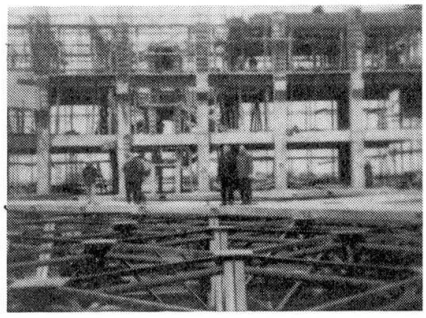

Fig. 2

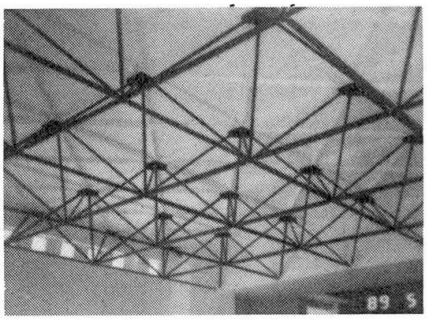

Fig. 3

STRUCTURAL ANALYSIS

The composite space truss can be analyzed in three mechanical models:

1) Finite Element Method The discrete rib-slab in the structure into beam elements and plate elements which carried the axial force and the plane force and the bending moment. But the web members and the lower chords remain carrying axial force.

2) Equivalent Sandwich Plate Method The rib-slabs are regarded as the upper layer and the web members and the lower chords are regarded as the sandwich layer and the lower layer respectively. The differential equation on the above basis is seted, the solution is obtained with the Analytic Method.

3) Equivalent Space Truss Method According as energy principl, the rib-slab is idealized as a three-way or four-way planar truss system. The complex composite structure may be assumed as an equivalent space truss system which can be solved by the Matrix Displacement Method.

STRUCTURAL DESIGN

Basic Assumption for Design and Calculation:

1) The plane rigidity of the composite floor is limitless.
2) The connections between the floor with the columns (or the walls) are hinged joints.
3) The floor trasmit axial force only in the horizontal direction.

Structural Shape Various kinds of the space truss are applicable to composite floor. But the space truss of orthogonal and ortholaid types and the ortholaid square pyramid space grids are better.

Upper Joints The axial force and the shearing force and the bending moment are transmited tegether in the upper joints. The joints must have enorgh regidity.

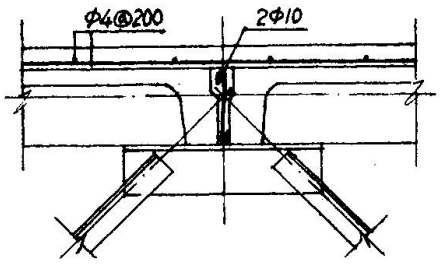

Fig.4

STRUCTURE MEASUREMENT

The measurements of the stress and the deflection on the composite floor has proved: (Fig.5,6,7)

1) Within the calculated loads, the structural members are working in the elastic stage.
2) The largest deflection of the joints is 1/600-1/800 that of the floor's span.
3) The rib-slab is a compression-bending members and the lower chords and the webs remain carrying axial force.
4) The rigidity of the upper joints will affect the space rigidity of whole structure and the internal force of the members.
5) The measure is to 70-90 per cent that of the calculation.

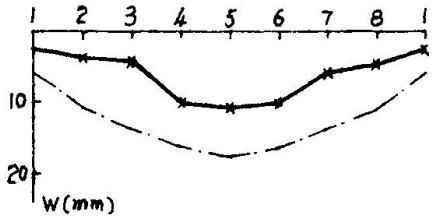

Fig.5 Max-defleetion of the joints

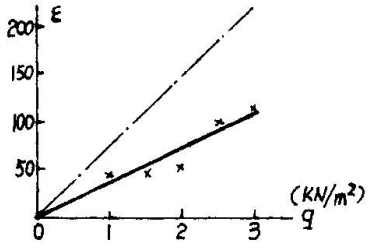

Fig.6 Lood-strain of the slab

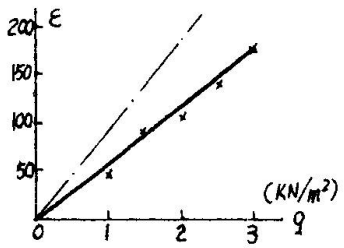

Fig.7 Lood-strain of the member

——The measurment —·— The calculation

ECONOMICAL ANALYSIS

The economic indexes of the composite floor and the r.c. floors are comparable in folowing Table..

Floor'stype	Deadweight	Concrete	Steel	Timber	Cost (¥ yuan/m²)			
	(kN/m²)	(m³/m²)	(kg/m²)	(m³/m²)	Floor	Column	Fundation	Total
Mushroom-slab	9.25	0.37	43.6	0.025	70.50	67.55	104.8	242
Groined-slab	8.25	0.33	43.6	0.024	75.33	46.60	92.2	214
Beam-slab	7.50	0.30	35.4	0.018	52.20	51.20	87.3	196
Rib-slab	6.25	0.25	31.6	0.016	50.80	37.40	75.4	166
Com-sp-truss	1.80	0.06	26.6	0.003	58.40	31.50	63.0	153

Properties of Brace Encased in Concrete-Filled Steel Tube

Propriétés d'une entretoise de contreventement encastrée dans un profil tubulaire rempli de béton

Eigenschaften betonumhüllter Fachwerkdiagonalen

Akira WADA
Professor
Tokyo Inst.
Tokyo, Japan

Mamoru IWATA
Doctor of Eng.
Nippon Steel Corp.
Tokyo, Japan

A. WATANABE
Structural Eng.
Nippon Steel Corp.
Tokyo, Japan

H. KURIBAYASHI
Structural Eng.
NTT Corp.
Tokyo, Japan

1. PREFACE

Steel has high strength and deformation resistance (see Fig. 1). Braces are extremely effective in increasing the horizontal stiffness and strength of steel frame structures. But braces buckle and rapidly lose strength when subjected to compression force (see Fig. 2). This makes it difficult in plastic design depending on stable plasticity and braces cannot be expected to absorb energy.

Therefore, particularly in earthquake-prone countries, designs of structure are considerably limited when braces are adopted for high-rise buildings.

The authors considered that, if brace buckling could be prevented and the energy absorption capacity increased, damage by earthquakes to columns and beams which support permanent loads would be reduced. The authors developed a bracing system having stable restoration property (see Fig. 3) and in which buckling was prevented by using core plate encased in concrete-filled steel tubes. This paper reports on an experiment conducted on a scale model to study the application of such braces to an actual 24-storied building.

2. EXPERIMENT

2.1 Experiment models

As shown in Fig. 4, the experiment models are 1/2.5 scale and consist of braces, columns and beams. Model A has braces whose core steel yield point is 260.7 N/mm^2, and model B 477.3 N/mm^2, while model C has no braces. Figure 5 shows the cross section of the brace used in Models A and B. Core steel is bound by mortar and steel tube to prevent buckling. The coating material isolates the core plate from mortar to prevent an axial force from traveling from core steel to mortar and steel tube.

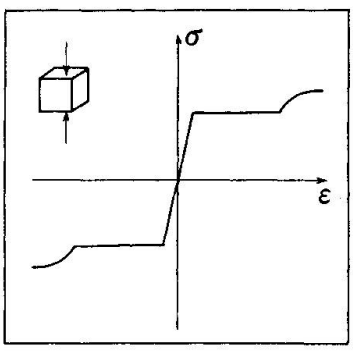

Fig. 1

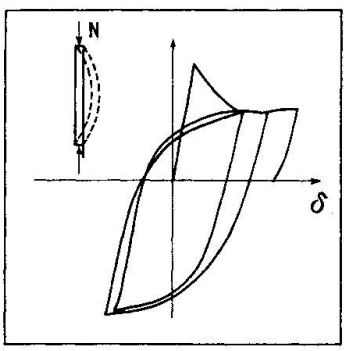

Fig. 2

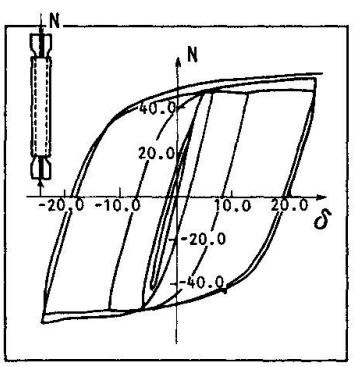

Fig. 3

2.2 Experiment methods

To simulate the behavior of an actual structure under a horizontal force, horizontal rollers were attached to the underside of the columns. And to bear the horizontal force, a vertical roller was attached to the center of the lower beam (see Fig. 4). The horizontal force was applied to the column tops, the direction of application being alternated from left to right. Measurements were made regarding relative storey deformation, axial deformation, strain of braces, etc.

2.3 Results of experiment

All models were confirmed to possess stable restoration property up to a relative storey deformation angle of 1/100. And braces did not buckle under compressive forces. Figure 7 shows the hysteresis curve of Model A and envelop curves of Models B and C. Models A and B show that the bracing system markedly increases the horizontal stiffness and strength of frame keeping deformation capacity.

3. CONCLUSION

The above results confirm that frames with high energy absorption and earthquake resistance can be made by incorporating braces whose buckling is prevented by concrete-filled steel tube. The authors are confident that by adjusting the cross-sectional area and yield point of the brace core steel, the strength and stiffness of structures can be freely designed.

REFERENCE

1. M. FUJIMOTO, A. WADA, E. SAEKI, Y. HITOMI, A. WATANABE : Properties of Brace Encased in Buckling-Restraining Concrete and Steel Tube, Ninth World Conference on Earthquake Engineering, August 1988, Tokyo-Kyoto, Vol. IV, pp. 719-723.

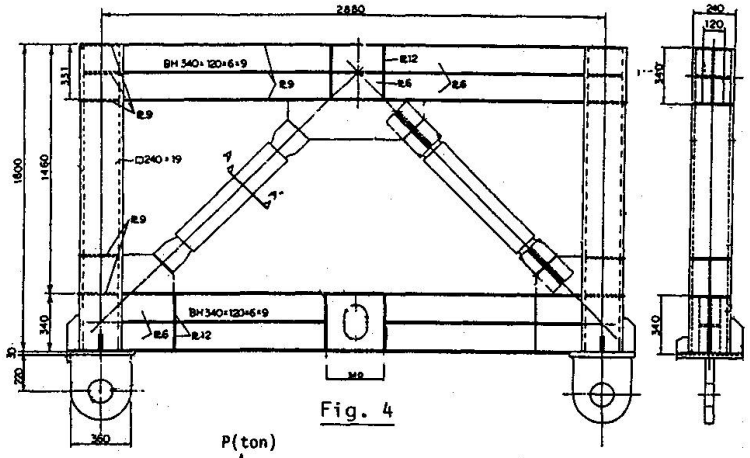

Fig. 4

Table 1 List of Experiment Models

Name	Core Plate			Steel Tube
	Cross-sectional Area(cm²)	Yield Stress (N/mm²)	Yield Load (kN)	
Model A	24.64	260.7	642.3	□-150x150x4.5
Model B	14.44	477.3	689.2	□-150x150x4.5
Model C	-	-	-	-

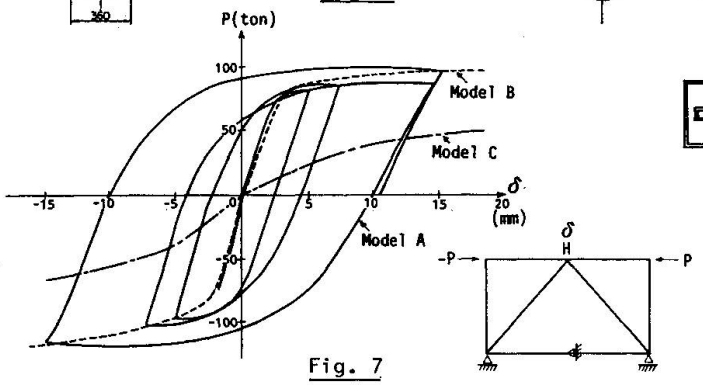

Fig. 7

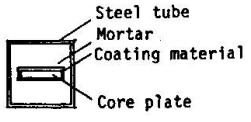

Section A-A'

Fig. 5

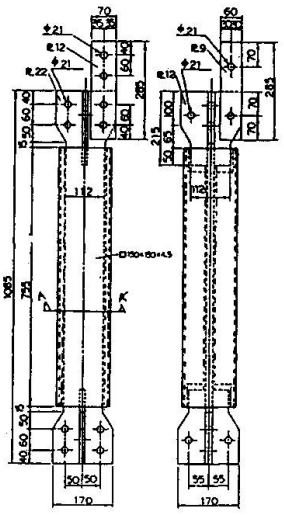

Model A

Fig. 6

Ultimate Strength of Bonding of Composite Beams

Résistance des assemblages de poutres en acier et béton

Tragwiderstand des Verbundes in Verbundträgern

Tatsuro SAKIMOTO
Prof. Dr.
Kumamoto Univ.
Kumamoto, Japan

Yasuharu KAJIKAWA
Dr.
Kawada Constr.
Osaka, Japan

A total of 14 specimens of steel-concrete jointed beams was tested to investigate the ultimate strength of the joint which connects a steel beam with a concrete beam longitudinally. The aim of this study is to clarify the basic behavior of the jointed beam and to find simple conceptual models by which the ultimate strength of the joint can be evaluated. For this purpose the joint was designed as simple as possible as shown in Fig.1. A steel plate welded to the end of a steel H-beam is jointed to a reinforced concrete beam of rectangular cross-section by two prestressing bars.

Five specimens were tested under pure bending (4 points loading), six specimens under bending with shear (3 points loading) and three specimens under pure shear. All the results are summarized in Table 1.

The ultimate bending strength of all the bending test specimens were governed by crushing of the concrete at the upper fiber adjacent to the end plate where the normal compressive stresses transmitted from the upper flange plate of the steel beam concentrate(see Fig.2). It was found that increase in the end plate thickness and installation of connecting bars contribute to decrease the stress concentration at the end plate surface and increase the ultimate bending strength of the jointed beam.

It was also shown that the ultimate bending strength of the jointed beam with an end plate of sufficient thickness (36 mm for our tests) can be predicted fairly well by the formula based on the usual stress block models shown in Fig.3.

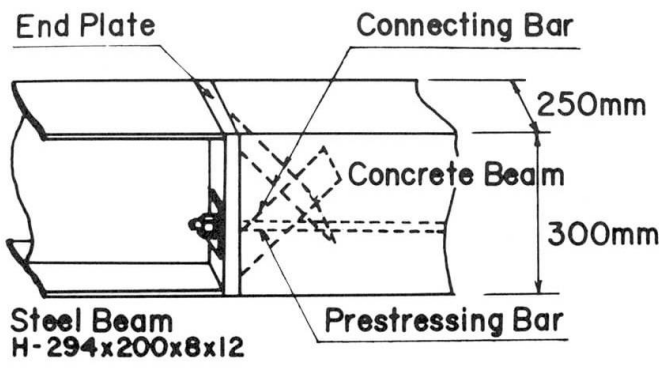

Fig.1 Steel-concrete jointed beam

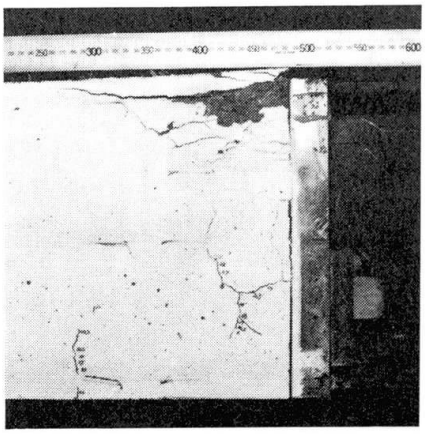

Fig.2 Ultimate state of the bending test specimen

Table 1 Test Results

Loading Condition	Name of Specimen	Span a (m)	Thickness of End Plate(mm)	Diameter of Connection Bar(mm)	$M_{u,test}$ (kN·m)	$M_{u,theory}$ (kN·m)	Test Theory	Remarks
Pure Bending	JB-8	1.0	8	None	90.8	152.5	0.60	Full Prestressing
	JB-8-16	1.0	8	16	107.9	174.4	0.62	〃
	JB-36	1.0	36	None	137.3	147.9	0.93	〃
	JB-36-16	1.0	36	16	161.9	170.9	0.95	〃
	CB	1.0	Reference PC Beam		161.3	151.9	1.06	〃
Bending with Shear	JSB-2	0.6	36	None	150.1	138.4	1.08	〃
	JSB-2-6	0.6	36	6	148.6	141.4	1.05	〃
	CSB-2	0.6	Reference PC Beam		167.8	133.1	1.26	〃
	JSB-3	0.9	36	None	141.4	140.6	1.01	〃
	JSB-3-6	0.9	36	6	142.1	142.2	1.00	〃
	CSB-3	0.9	Reference PC Beam		149.2	135.1	1.10	〃
Pure Shear					$V_{u,test}$ (kN)	$V_{u,theory}$ (kN)		
	JS-6	0.6	36	6	465.8	424.3	1.10	〃
	JSR	0.6	36	None	279.6	312.7	0.89	30% Prestressing
	JSR-6	0.6	36	6	367.9	333.6	1.10	〃

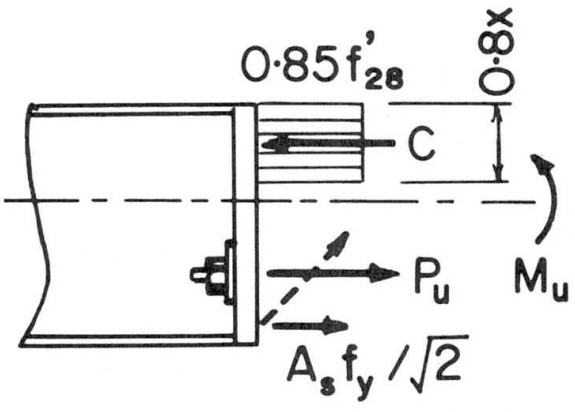

Fig.3 Theoretical model for estimating bending strength

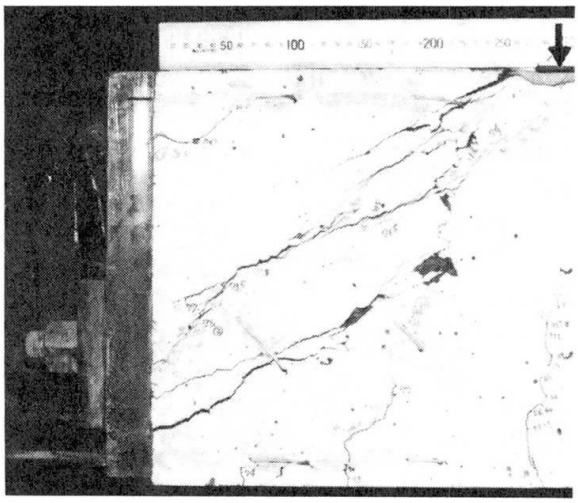

Fig.4 Ultimate state of the shear test specimen

In the tests under pure shear, the ultimate shear strength of the jointed beam was governed by the inclined shear cracks which run between the end of the prestressing bars and the loading point (see Fig.4). It was found that the experimental load for the initiation of the shear cracks can be predicted fairly well by the theoretical value which is evaluated from the criterion that the shear crack initiates when the principal tensile stress attains the tensile strength of the concrete.

The ultimate shear strength of the jointed beam is affected by the magnitude of the prestressing force. It was also found that the ultimate shear strength of the joint can be determined by the sum of the shear resistance of the concrete and the yield strength of stirrups and connecting bars. Further study is needed to clarify the mechanism of the ultimate shear resistance of the concrete, but the magnitude of the shear resistance of the concrete can be approximated by the shear force under which the principal tensile stress computed from average normal stress and average shear stress for the effective depth of the beam attains the tensile strength of the concrete.

Seismic Resistance of Composite Structures

Résistance sismique des constructions mixtes

Erdbebensicherheit von Verbundbauten

J.B. SCHLEICH
Dep. Mgr
ARBED Recherches
Esch/Alzette, Luxembourg

R. PEPIN
Research Manager
ARBED Recherches
Esch/Alzette, Luxembourg

Introduction

Several times each year, earthquakes occur all over the globe, causing incalculable human and material losses. In order to reduce these dammages, a great number of research projects have been realized in the last two decades. Most of these projects were dealing with steel or steel reinforced concrete structures. Unfortunately, the structures combining the advantages of both steel and concrete, namely the composite structures, were analyzed only in some rare cases in relationship with their seismic resistance, leading thus to large gaps in different chapters of EUROCODE 8 project "Seismic Design".

Aim of the research project

The scope of the project was to show that composite structures have besides their good fire resistance properties also an inherent seismic resistance which is due to the combination of

- the steel ductility and
- the damping properties and rigidity of the concrete

This seismic resistance can even be increased by improving the beam-to-column joint design, without loosing the fire resistance.

The project was realized under the leadership of ARBED, in collaboration with the universities of Darmstadt(D), Liège(B), Milan(I) and Wuppertal(D).

Description of the tests

To reach the scope, three test series are performed:

- series 1: 18 tests on Tee-form joints
- series 2: 20 tests on cross-form joints
- series 3: 10 tests on full scale frames

The tests of series 3, which are performed on real size up to two spans and two storey frames with concrete slab, are used for the verification of the numerical code to be developped.

Results

After finishing test series 2, it can be stated that:

- composite structures show an astonishing ductility
- concrete increases the ultimate bearing capacity substantially and
- local instability phenomena are reduced

The 38 tests performed gave important data for the design of composite structures submitted to earthquakes.

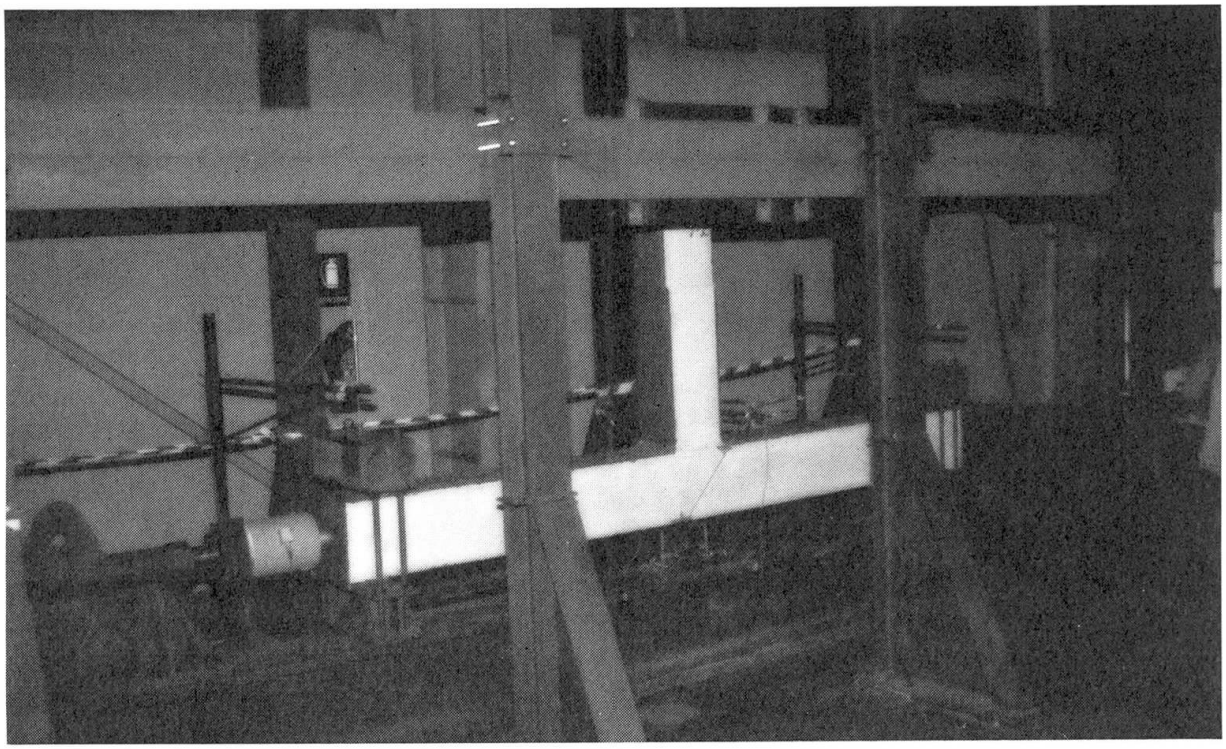

Fig. 1 Testing installation for T-joints in Milan

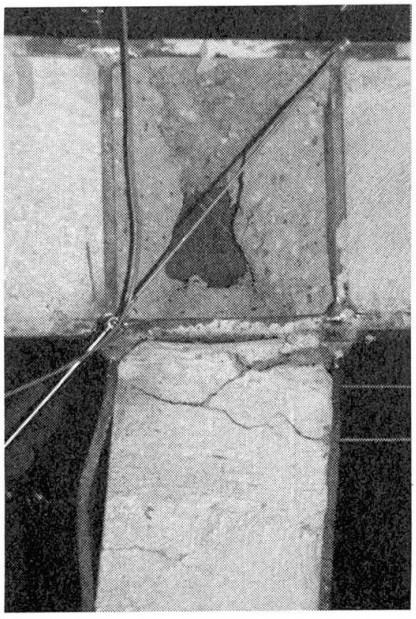

Fig. 2 Welded joint E3 after testing

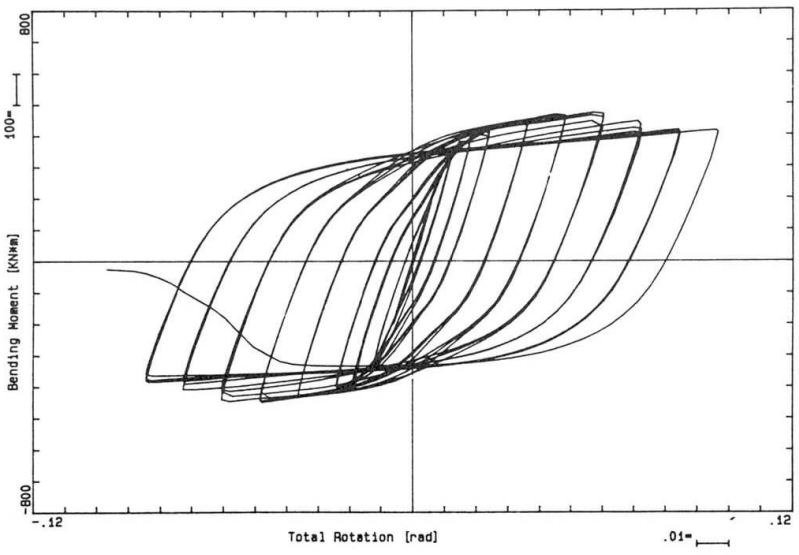

Fig. 3 M-θ hysteresis diagram of E3

Unbonded Composite Steel Tube Concrete Columns

Colonnes en béton moulées dans un tube d'acier non adhérent

Stahlrohrbetonsäulen ohne Verbund

H. TSUKAGOSHI
Research Engineer
Shimizu Corp.
Tokyo, Japan

Y. KUROSE
Structural Engineer
Shimizu Corp.
Tokyo, Japan

Y. ORITO
Structural Engineer
Shimizu Corp.
Tokyo, Japan

1. Introduction

The UTC (unbonded steel tube concrete) column has a circular RC (reinforced concrete) section encased with a steel tube. The tube is unbonded to maximize its confining effect on inside concrete. A series of column tests and beam-column assemblage tests have been conducted to study the behavior of the UTC columns under severe load conditions and to establish design criteria for RC frame structures using the UTC columns.

2. Test program

The UTC column specimens were designed varying the shear span ratio and the amount of reinforcement.The RC beam-UTC column subassemblages were designed varying the amount of joint confinement, column axial force and joint configurations.

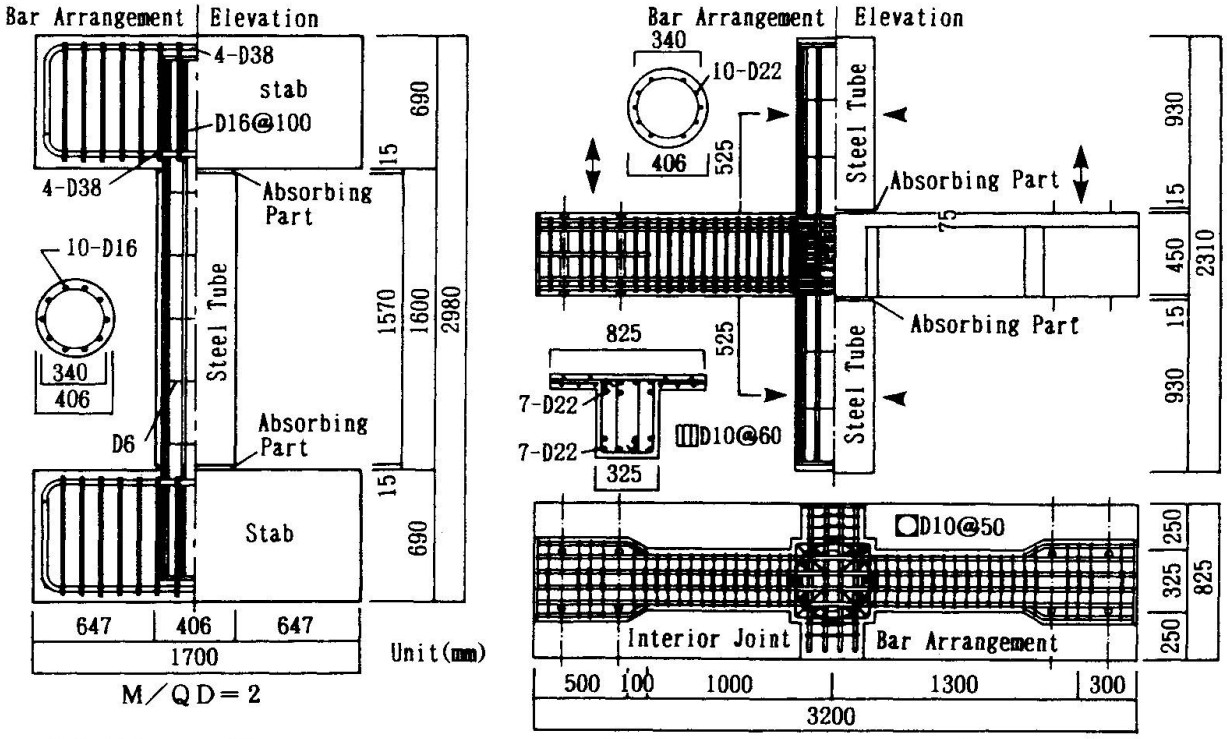

(a) Column Tests (b) Beam-Column Assemblage Tests

Fig. 1 Test Specimens

The test specimens, shown in Figure 1, were half-scale models. The steel tube was unbonded by coating a thin layer of asphalt on the inside surface. The UTC column had a slit of 15 mm at both ends to accommodate column axial deformation. The column specimens with a rigid stub at both ends were loaded to produce a contraflexural moment distribution along the height. The joint specimens were subjected to vertical force at the beam tips and axial force at the column. The joint had a square section and was reinforced with circular and rectangular ties.

3. Test results

Obserbed envelope curves of the load-deflection relations are shown in Figure 2. Major findings from the tests are summarized below:

1) All test specimens showed a ductile and stable behavior until large deformation.

2) The column specimens showed excellent load-carrying capacities becase the steel tube confined inside concrete and enhanced its strength.

3) The interior joint specimen with a lateral reinforcement ratio of 0.64% showed almost the same ductility and strength as those with 1.27% reinforcement.

4) With regard to the exterior and corner joints, a large amount of lateral reinforcement appeared to be effective in confining the joint concrete and maintaining the integrity of the joint.

4. Conclusions

A series of seismic tests on columns and joints have verified that the UTC columns have high strength and good ductility. Design of RC frames using the UTC columns has been developed based on the test results.

Figure 3. shows the UTC column in construction of a high-rise building in Tokyo.

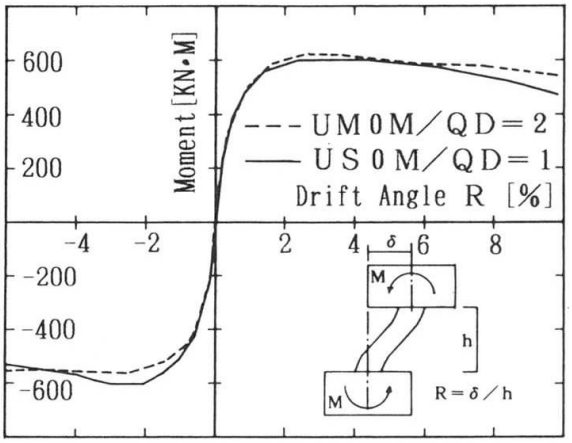

(a) Colum Tests

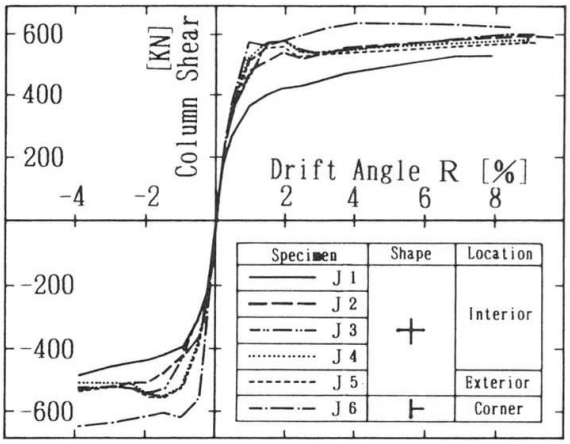

(b) Beam-Column Assemblage Tests

Fig. 2 Envelope Curves

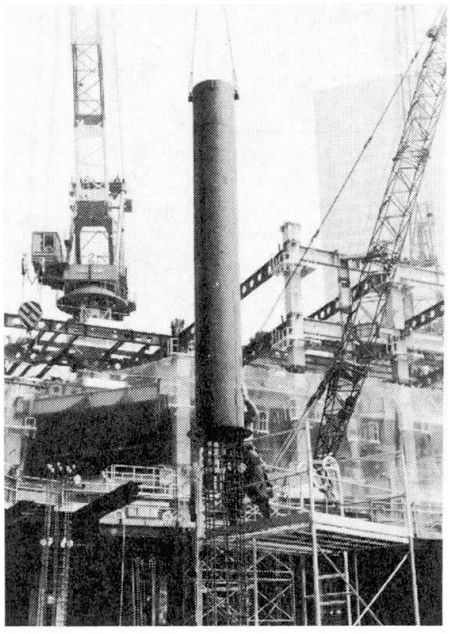

Fig. 3 Construction of UTC Column